Author:
Birnie, Matthew

Title:
The Molecular and Physiological Effects of Synthetic Glucocorticoid Treatment

The Molecular and Physiological Effects of Synthetic Glucocorticoid Treatment

By

Matthew Thomas Birnie

Bristol Medical School

UNIVERSITY OF BRISTOL

A dissertation submitted to the University of Bristol in accordance with the requirement of the degree of DOCTOR OF PHILOSOPHY in the Faculty of Health Sciences

July 2018

Word count: 48166

ABSTRACT

Glucocorticoids are one of the most frequently prescribed families of drugs. In addition to their anti-inflammatory efficacy, their use is complicated by many side effects, including sleep disturbance and memory impairment for which the underlying mechanism is unknown. In this thesis, I show that the therapeutic glucocorticoid methylprednisolone (MPL) disrupts the circadian regulation of the core clock genes *Period1*, *Period2* and *Bmal1* in the master clock, the suprachiasmatic nucleus (SCN). I also found that the Type II corticosteroid receptor mRNA is expressed in the SCN. RNAseq of whole hippocampi revealed a significant dysregulation of clock genes in the MPL treated rats. I demonstrate that locomotor activity is altered in the presence of MPL and that sleep architecture during the 6h memory consolidation period of a novel object location task is altered, leading to memory impairment. I therefore conclude that MPL acts directly on the SCN to dysregulate the central clock, leading to disrupted peripheral clocks and circadian rhythms, resulting in altered sleep and impaired hippocampal-dependent memory. These data reveal a novel role for glucocorticoids in the regulation of the master clock in the SCN and provides a potential mechanism to understand glucocorticoid related sleep disturbances and memory impairment in patients treated chronically with long acting synthetic glucocorticoids.

DEDICATIONS AND ACKNOWLEDGEMENTS

I would first and foremost like to express my sincerest gratitude to my supervisors Dr. Becky Conway-Campbell, Dr. Georgina Russell and Professor Stafford Lightman. Thank you for your ongoing support throughout my time with you and encouragement to reach this goal. I would especially like to thank Becky for her endless support and advice.

Thank you to Dr. Gavin Welsh and Dr. Gareth Barker for your advice and support during my yearly progress reviews and at other points throughout my PhD. Your comments and insight were extremely helpful.

I would also like to thank some of my work colleagues who have put up with me throughout this process. Firstly, thank you to Yvonne Kershaw and Ben Flynn for all of your help and amazing contributions to this project. Thank you to the rest of the Lightman group for being an ear when I needed to moan, but also for making this experience a pleasurable one. Thank you to Clare Sims for ASU support, and a big thank you to the animals that were used in this project, as without them, none of this could have happened.

To my family, a big thank you for your ongoing support throughout this process. You know who you all are.

Collaboration

Wavelet transform and Lomb-Scargle analysis of locomotor activity and core body temperature was done in collaboration with Dr. Amitesh Pratap. Thank you for providing the MATLAB script to interpret these data. In vivo electrophysiology was done in collaboration with Prof. Matt Jones and Dr. Alice Fodder. Thank you for help, guidance and support throughout this element of work.

Sponsorship

I would like to thank the Wellcome Trust, Medical Research Council and Neuroendocrinology Charitable Trust for supporting this project providing me with my scholarship and the costs of all materials and consumables.

DECLARATION

I declare that the work in this dissertation was carried out in accordance with the requirements of the University's *Regulations and Code of Practice for Research Degree Programmes* and that it has not been submitted for any other academic award. Except where indicated by specific reference in the text, the work is the candidate's own work. Work done in collaboration with, or with the assistance of, others, is indicated as such. Any views expressed in the dissertation are those of the author.

SIGNED: ..... DATE:.....

TABLE OF CONTENTS

LIST OF FIGURES

LIST OF TABLES

Table **Title**

LIST OF ABBREVIATIONS

24h	24 hours
ACTH	Adrenocorticotropin hormone
ADX	Adrenalectomy
AF1	Activation function domain 1
alpha-MSH	Alpha-melanocyte-stimulating hormone
AMY	Amygdala
ANOVA	Analysis of Variance
ARC	Arcuate nucleus
AVP	Vasopressin
BDX	Biotinylated dextran
bHLH-PAS	BasicHelix-Loop-Helix Per-Arntl-Single
BLA	Basolateral amygdala
BMAL1	Brain and Muscle Arntl Like 1
Bmal1$^{(-/-)}$	Bmal1 KO
BNST	Bed nucleus of the stria terminalis
BP	Base pair
CA1	Cornu Ammonis 1
CA2	Cornu Ammonis 2
CA3	Cornu Ammonis 3
Camk2δ	Calcium/Calmodulin Dependent Protein Kinase II Delta
CBP	CREB binding protein
cBT	Core body temperature
CCG	Clock controlled genes
cDNA	complimentary DNA
CeA	Central nucleus of the amygdala
CK1δ	Casein kinase 1 Delta
CK1ε	Casein kinase I Epsilon
CLOCK	Circadian Locomotor Output Cycles Kaput
Clock Δ19	Single point mutation of intron 19
CORT	Cortisol/Corticosterone
CREB	cAMP Response Element Binding Protein

CRF	Corticotropin-releasing factor
CRH	Corticotropin-releasing hormone
Cry1	Cryptochrome 1
Cry2	Cryptochrome 2
CSF	Cerebral spinal fluid
CT	Circadian Time
Ct	Cycle threshold
CUS	Chronic unpredictable stress
DBD	DNA binding domain
Dbp	D-box binding protein
DD	Dark/Dark
DEX	Dexamethasone
DG	Dentate Gyrus
DHEA	dehydroepiandrosterone
DHEA-S	DHEA-sulfate
DMH	Dorsomedial hypothalamus
DNA	Deoxyribonucleic Acid
DSPS	Delayed sleep phase syndrome
E-box	Enhancer Box
EC	Entorhinal Cortex
ECon	Endogenous control
EDTA	Ethylenediaminetetraacetic acid
EEG	Electroencephalography
FASPS	Familial advanced sleep phase syndrome
Fbxl3^{Afh}	F-box and leucine rich repeat protein 3; after hours
FDR	False discovery rate
FEO	Food-entrainable oscillator
Fkbp5	FK506 binding protein 5
FKPM	Fragments per kilobase per million mapped reads
FSH	Follicle stimulating hormone
GABA	Gamma-Aminobutyric Acid
GC	Glucocorticoid
GHT	Geniculohypothalamic tract

GILZ	Glucocorticoid Induced Leucine Zipper
GLUT4	Glucose Transporter type 4
GnRH	Gonadotropin-releasing hormone
GOI	Gene of Interest
GR	Glucocorticoid Receptor
GRE	Glucocorticoid Response Element
GRP	Gastrin-releasing peptide
H3K27	Histone 3 Lysine 27
H3K9	Histone 3 Lysine 9
HAT	Histone acetyltransferase
HC	Hippocampus
HGH	Human growth hormone
HPA	Hypothalamic-pituitary-adrenal axis
HSA	Hypothalamic-spinal-adrenal axis
HSP	Heat shock proteins
IGL	Intergeniculate leaf
Il6	Interleukin 6
IP	Intraperitoneal
ipRGC	Intrinsically photosensitive retinal ganglion cell
KO	Knockout
LA	Locomotor activity
LBD	C-terminal ligand-binding domain
LD	Light/Dark
LEC	Lateral EC
LFP	Local field potential
LH	Luteinising hormone
LL	Light/Light
LTD	Long-term depression
LTP	Long-term potentiation
MeA	Medial nucleus of the amygdala
MEC	Medial EC
min	Minute
MLL	Myeloid/Lymphoid or Mixed Lineage Leukaemia

mPFC	Medial PFC
MPL	Methylprednisolone
MPOA	Medial preoptic area
mPSPs	Monosynaptic postsynaptic potentials
MR	Midbrain raphe
MR	Mineralocorticoid Receptor
mRNA	messenger RNA
N1	Non-REM1
N2	Non-REM2
N3	Non-REM3
NAc	Nucleus accumbens
NOL	Novel object location task
NPAS2	Neuronal PAS domain 2
NPY	Neuropeptide Y-immunoreactivity
NREM	Non-REM sleep
NTD	N-terminal domain
NTS	Nucleus of the solitary tract of the brainstem
OB	Olfactory bulb
OT	Oxytocin
PCR	Polymerase Chain Reaction
pCREB	phosphorylated CREB
Per (LDC)	Per1 (Lysine Decarboxylase)
Per1	Period 1
Per2	Period 2
Per2 (brdm1)	PAS domain deletion in Per2 protein
Per3	Period 3
PFC	Prefrontal cortex
PK2	Prokineticin-2
POMC	Proopiomelanocortin
PP	Perforant path
pP90RSK	phosphorylated P90 ribosomal s6 kinase
PrhC	Perirhinal cortex
PRL	Prolactin

PrL	Prelimbic area of the prefrontal cortex
PVN	Paraventricular nucleus
PVT	Paraventricular thalamus
Q	False discovery rate
qPCR	quantitative PCR
REM	Rapid eye movement sleep
Reverbα	Nuclear Receptor 1 group D member 1
RHT	Retinohypothalamic tract
RNA	Ribonucleic Acid
RORα	RAR-related orphan receptor alpha
RORβ	RAR-related orphan receptor beta
RORe	Retinoic acid-related orphan receptor response element
RORγ	RAR-related orphan receptor gamma
RRE	Rev-erba/Ror response element
RU-486	Mifepristone
SC	Schaeffer Collateral
SCN	Suprachiasmatic nucleus
SCNx	SCN lesion
SEM	Standard error of the mean
SGK1	Serum Glucocorticoid Kinase 1
Sirt1	Silent mating type information regulation 2, homolog 1
SLC19A3	Solute Carrier family 19 member 3
SLM	Stratum moleculare
SO	Stratum oriens
SON	Supraoptic nucleus
SP	Stratum pyramidale
SPP	Skeleton photoperiod
sPVZ	subparaventricular zone
SR	Stratum radiatum
SUB	Subiculum
SuM	Supramammillary nucleus of the hypothalamus
SUMO	SUMOylation
SWA	Slow wave activity

SWS	Slow wave sleep
TGFα	Transforming growth factor-alpha
TH	Thyroid hormones
TMN	Tuberomammillary nucleus
TRH	Thyrotropin-releasing hormone
TSH	Thyroid stimulating hormone
U	Ubiquitination
vHC	ventral HC
VIP	Vasoactive intestinal peptide
VLPO	Ventrolateral preoptic area
VM	Ventral medulla
VMH	Ventral medial hypothalamus
vSUB	Ventral SUB
VTA	Ventral tegmental area
zif268	Early growth response protein 1
ZT	Zeitgeiber - Time giver

Chapter 1

Introduction

1.1 Circadian rhythms

The daily rotation of the earth, as well as its annual revolution around the sun provides daily and seasonal changes to the photoperiod, with significant changes in light intensity, temperature and the availability of food observed across this period. Most organisms, certainly mammalian, have evolved to contain an innate clock that drives behaviour to the circadian (latin *circa = around, dia = day*) period, enabling the anticipation to, and accommodation of the fluctuating environment. Hormone secretion, body temperature, behavioural activity and sleep have all been shown to have clear circadian rhythm (Weitzman 1976; Refinetti & Menaker 1992). Breeding animals, and for example sheep, exhibit differences in their behaviour, reproductive physiology, and metabolism, across seasons (Arens et al. 2007; Baldock et al. 1988). Rodents show altered patterns of behavioural activity when exposed to changing day lengths and light patterns (Edmonds & Adler 1977). Daily fluctuations have influence on almost all aspects of physiology and behaviour, as the rest-wake cycle i.e. behavioural activity, cardiovascular activity and metabolism all exhibit circadian rhythmicity (Huikuri et al. 1992; Huang et al. 2011). The hippocampus, a brain region important for the consolidation of memory and processing of sleep, changes volume with circadian and seasonal timing (Miller et al. 2015), as does the size and shape of the pupil of the eye (Loving et al. 1996). These systems are driven by the molecular clock, through changes in light intensity, hormone levels, and metabolic processes to name a few.

1.1.2. Organisation of the suprachiasmatic nucleus

The suprachiasmatic nucleus (SCN) of the hypothalamus is the master regulator of the mammalian circadian clock. Circadian rhythmicity of the SCN persists not only within the animal, but also in vitro in both hypothalamic slice and cell culture preparation (Inouye & Kawamura 1982; Yamaguchi et al. 2003). In the hypothalamic slice, SCN neurons fire at rates of approximately 24 hours, with peak firing occurring during the animal's subjective activity period (Welsh et al. 1995). In cell culture, vasopressin (AVP) and vasoactive intestinal peptide (VIP) are secreted in a circadian oscillation, although this period ranged from between 22 to 27 hours (Murakami et al. 1991; Shinohara et al. 1994; Watanabe et al. 1993).

Lesions of the SCN abolish circadian rhythmicity of locomotor activity, neuroendocrine secretion and core body temperature. However, locomotor activity and body temperature rhythms were restored when SCN transplants were placed into the third ventricle (Silver et al. 1996). The period of the restored rhythm was set to the timing of the transplanted SCN, demonstrating that its periodicity is an intrinsic phenomenon that is not, in part, driven by inputs from other brain areas or external cues.

The SCN has been described in many mammalian species, including the rat, human and guinea pig. In the rat, the SCN is the cluster of densely packed neurons in both cerebral hemispheres separated by the periventricular stratum and third ventricle, located in the rostral, ventral hypothalamus, which is bordered by the optic chiasm and supraoptic commissures. Bregma level -0.92-1.44mm (Paxinos & Watson 2007).

1.1.2.1 Input

The retina, midbrain raphe (MR) and intergeniculate leaf (IGL) drive the regulation of the core clock within the SCN via dense projections, predominantly to the core (Levine et al. 1986; Dudley et al. 1999; Moore et al. 2002). The retinal input to the SCN has been extensively studied. Varying light cycles, light intensity and applying different wavelengths of the light spectrum have shown that the SCN is regulated by the light-dark cycle (Rea et al. 1993; Meijer & De Vries 1995). The SCN's response to light is further modulated by serotonergic input, with neurons of the midbrain raphe projecting to and innervating the core and shell of the SCN, although dominance of the core is observed (Rea et al. 1994; Moga & Moore 1997; Meyer-Bernstein & Morin 1996). Intrinsically photosensitive retinal ganglion cells (ipRGCs) transmit directly to the SCN via the retinohypothalamic tract (RHT) (Berson et al. 2002). The RHT, conveys direct input from melanopsin containing ipRGCs in the eye to the SCN, with the projections terminating predominantly at neurons in the SCN core, however some connections directly activate neurons of the shell (Hattar et al. 2002; Baver et al. 2008). Non-photic entrainment of the circadian rhythm is mediated by the IGL, which although is an area that receives input from the retina, targets the SCN via the geniculohypothalamic tract (GHT) (Harrington 1997). The RHT is crucial to driving circadian rhythms via light/dark signals and although the role of the IGL-GHT pathway in light/dark signal entrainment is not fully understood, rats with lesions of the IGL entrain normally to the light-dark cycle, but when in the presence of a

skeleton photoperiod (SPP), they exhibit free running rhythms, indicating that the IGL is important for entraining circadian rhythms (Edelstein & Amir 1999).

Axonal projections from the pretectum group along the lateral border of the SCN, terminating in both the core and shell, and can therefore innervate the whole SCN (Mikkelsen & Vrang 1994). The infralimbic cortex projects only to the SCN shell (Hurley et al. 1991), whereas afferent cell populations, including the PVN and subparaventricular zone (sPVZ) innervate the entire SCN (Watts & Swanson 1987; Moga et al. 1995).

Serotonin-containing fibres located predominantly within the core of the SCN receive dense serotonergic innervation. The median raphe nuclei are most likely responsible for this innervation as in a previous study, the SCN lacked axonal labelling after a biotinylated dextran (BDX) injection placed centrally in the dorsal raphe nucleus (Moga & Saper 1994). Serotonin significantly decreases in the SCN following midbrain median raphe lesions, however not after lesioning the dorsal raphe nucleus. The dorsal raphe nucleus innervates the SCN, although the median raphe is dominant (van de Kar & Lorens 1979).

The SCN is further innervated from retinorecipient areas including the IGL and pretectum (Mikkelsen 1990). The projection from the IGL terminates in the lateral core of the SCN, where neuropeptide Y-immunoreactivity (NPY) was reported (Card & Moore 1988). NPY-immunoreactive neurons of the IGL project directly to the SCN (Harrington et al. 1987). Free running animals infused with NPY into the SCN present with a phase shift in the circadian rhythmicity of locomotor activity (Albers & Ferris 1984).

This result was similar to that of phase shifts from non-photic stimuli that induce locomotor activity, further evidencing that the GHT mediates non-photic entrainment of the SCN (Reeth & Turek 1989).

Dense projections from the paraventricular thalamus (PVT) are sent to the SCN, innovating both the core and shell (Moga & Moore 1997). However, lesions of the PVT do not alter the free-running circadian behaviour of locomotor activity, suggesting it is not crucial for circadian rhythm generation (Ebling et al. 1992).

The hypothalamic input to the SCN arises from many nuclei. Hypothalamic cell groups project largely to the SCN shell, and therefore avoid the VIP/GRP-expressing cell population in the SCN core (Moga & Moore 1997). Tracer studies indicated that axonal labelling to the SCN shell was sparse, signifying that the hypothalamic inputs to the SCN are possibly of little importance to circadian function. However, with such a vast number of inputs terminating in the shell from these areas, indicates that the hypothalamus must play a crucial role in the regulation of the SCN (Van den Pol 1980).

Preoptic projections to the SCN originate from within the medial preoptic area (MPOA), (median and medial preoptic nuclei) and the anteroventral periventricular nucleus (Moga & Moore 1997). Gonadotropin-releasing hormone (GnRH)-immunoreactive fibres in the SCN overlap with the preoptic terminal field, providing a role for GnRH as a neuromodulator of the preoptic projection to the SCN (van der Beek et al. 1997). This is supported as the lamina terminalis and medial preoptic area, both of which project directly to the SCN, contain GnRH-immunoreactive cells (Kawano & Daikoku 1981; van der Beek 1996). The ventral medial hypothalamus (VMH), which controls feeding and thermoregulation, preferentially targets the SCN shell (Bernardis 1973), similarly to the majority of other hypothalamic afferents, however these projections are relatively minor whereas the SCN sends a reciprocal projection to the VMH, driving the circadian rhythmicity of body temperature (Krieger 1980). The dorsomedial hypothalamus (DMH), which is involved in feeding and body weight regulation projects densely to the SCN region, yet only a minor input was shown to the SCN shell (Thompson et al. 1996).

Whereas most hypothalamic nuclei project to the SCN shell, the sPVZ and tuberomammillary nucleus (TMN) both innervate the core and shell of the SCN (Watts & Swanson 1987; Moga & Moore 1997). The sPVZ can be further subdivided into the dorsal and ventral subdivisions and relays signals to the SCN to drive body temperature and locomotor activity and sleep regulation, respectively, whereas the TMN controls arousal, memory and sleep (Blandina et al. 2012). The TMN is the neuronal source of histamine in the mammalian brain and histaminergic terminals are evident in the SCN and appear evenly distributed across the core and shell (Inagaki et al. 1988; Panula et al. 1989). The histaminergic input may be involved in circadian timing and rhythms. Free-running rats exhibit a pronounced phase delay in locomotor activity and drinking behaviour following histamine administration at the onset of the active period (Itowi et al. 1990). Interestingly,

histamine administration didn't cause a phase advance in these animals if given during the late subjective night.

1.1.2.2 Cell types and neurotransmission

The rat SCN can be divided into two major subdivisions, the ventral 'core' and dorsal 'shell', characterised based on cytoarchitecture and neuropeptide immunoreactivity (Antle & Silver 2005; Gamble et al. 2007; Ibata et al. 1989; Kiss et al. 2008). The core expresses vasoactive intestinal peptide (VIP) and gastrin-releasing peptide (GRP) immunoreactive cells (Abrahamson & Moore 2001; Antle & Silver 2005), whereas the shell expresses vasopressin (AVP) immunoreactive cells (Moore et al. 2002). VIP-expressing neurons release VIP and GABA in the SCN to critically regulate the circadian cycle and the synchrony of other SCN neurons and their synapses, controlling the firing rate of target neurons (Castel & Morris 2000).

VIP expression has been assessed in different areas, and a clear circadian rhythm of expression is evident in the cerebral spinal fluid (CSF), characterising it as a humoral output of the SCN (Kruisbrink et al. 1987). However, it was confirmed to act as a humoral factor as infusion of VIP into the ventricular system didn't alter daily sleep/wake cycles (Kruisbrink et al. 1987). It is however the only SCN output shown to be secreted this way *in vivo*, primarily as a result of the circadian firing rate of VIP-expressing neurons of the SCN core. Further evidence indicating the importance of the humoral output of the SCN was shown when Silver et al. 1996**,** transplanted a SCN with a semi-permeable membrane into the third ventricle of SCN lesioned rats, restoring circadian rhythm to locomotor activity, implying that diffusible factors emanate from the SCN to control peripheral clock driven systems as well as via neural connectivity. Other factors, including prokineticin-2 (PK2) (Zhou & Cheng 2005) and transforming growth factor-alpha (TGFα) (Kramer et al. 2005) have been identified as humoral outputs of the SCN that inhibit locomotor activity, however there are currently no SCN factors shown to promote arousal or feeding activity, as instead the SCN appears to drive other nuclei to induce these behaviours.

AVP-expressing neurons, confined mainly in the shell of the SCN, are critical for interneuronal coupling between the core and shell to regulate circadian behavioural

rhythms (Mieda et al. 2015). A targeted *Bmal1* deletion of AVP-expressing neurons showed a marked increase in the free-running period as well as a significant increase in the total activity period. When these mice were subjected to a jet-lag paradigm, exposing them to an abrupt 8-hour phase advance, the *Bmal1*$^{(-/-)}$ mice reentrained to the light cycle faster than their controls, indicating that *Bmal1*-dependent oscillations in AVP-expressing neurons are vital to modulate the coupling of the SCN network. A functional lesion of AVP in the SCN using a cytotoxic antibody altered AVP expression in the parvocellular region of the PVN, a major site of SCN hypothalamic efference, which lead to the conclusion that the SCN and AVP were able to disrupt corticosterone release (Gomez et al. 1997).

GRP-expressing neurons, located predominantly in the core of the SCN with VIP-expressing neurons, are able to phase reset SCN neurons via spike-dependent and independent mechanisms, however *Per1* localisation was key to mediating these downstream events in the neurons of the SCN (Gamble et al. 2007). Treatment with GRP to rat and hamster SCN slices during the subjective day did not alter the peak time of SCN firing, however when GRP was applied to these cultures during the subjective night, it phase delayed the SCN firing peak, with this result being completely blocked using the GRP specific receptor antagonist (Mcarthur et al. 2000), indicating the importance of GRP in a time of day specific manner.

The SCN transplantation work of Silver et al. 1996 demonstrated that as well as humoral activation of circadian driven systems, intact neural projections from the SCN are required for full circadian control of biological systems, as although this study reinstated locomotor activity circadian rhythm, it did not reinstate neuroendocrine rhythms, such as the circadian release of corticosterone, with this system requiring the activation of VIP-projecting neurons to the paraventricular nucleus, enabling the release of corticotropin-releasing hormone (CRH) to be secreted, activating the hypothalamic-pituitary-adrenal axis (HPA) (Waite et al. 2012).

1.1.2.3 Circuitry and projections

Projections from the SCN show that the outflow control is predominantly limited to the medial hypothalamus (Berk & Finkelstein 1981) as most SCN projections target areas containing interneurons, such as the medial preoptic area (MPOA), the dorsomedial

hypothalamus (DMH), and the paraventricular nucleus (PVN) (Saper et al. 2005; Watts & Swanson 1987). Direct connections have also been observed in neurons containing corticotropin-releasing hormone (CRH), thyrotropin-releasing hormone (TRH), thyroid hormones (TH) and GnRH neurons (Kalsbeek & Buijs 2002; de la Iglesia et al. 2003).

The first description of circadian timing involved in SCN and neuroendocrine control, showed that VIP-expressing neurons of the SCN project to the PVN/DMH area, controlling the secretion of corticosterone from the adrenal cortex, in the later well-described hypothalamus-pituitary-adrenal (HPA) axis (Lightman & Conway-Campbell 2010). This daily rhythm of corticosterone release is controlled by at least two SCN transmitters, as VIP released in the DMH is able to inhibit the activity of the HPA axis at the beginning of the inactive period (Smith & Vale 2006). However, VIP and GRP also stimulate adrenocorticotropin hormone (ACTH) and corticosterone release prior to the onset of the active period (Oliva et al. 1982; Olsen et al. 1992). The circadian release of corticosterone is also regulated by the polysynaptic projection from the SCN to the adrenal gland, via preautonomic neurons in the PVN and spinal cord that act on the splanchnic nerve, allowing the SCN to directly influence the sensitivity of the adrenal cortex to ACTH (Ulrich-Lai et al. 2006).

The SCN relies on hormones binding to their specific receptors and for neurons to deliver their message to drive rhythmicity on targeted tissues (Reul & Kloet 1985). The circadian secretion of corticosterone provides evidence for this, as the SCN utilises hormones and neurons to precisely drive the secretion of CORT via direct input to neuroendocrine neurons to control the release of ACTH from the anterior pituitary, as well as maintaining the control of adrenal sensitivity for ACTH via the autonomic nervous system (Herman & Cullinan 1997). This is not limited to the HPA axis, as the SCN also increases the sensitivity of insulin prior to wakening, causing an increase in glucose intake in muscle, whilst also increasing glucose production in the liver to ensure sufficient glucose availability for the active period ahead (Coomans et al. 2013).

The neuroendocrine rhythms driven by the SCN, are further connected to the circadian release of melatonin from the pineal gland via sympathetic innervation (Moore 1995). The pineal gland sends multisynaptic projections to the SCN and PVN. Projections were also observed in preganglionic sympathetic neurons of the spinal cord, as well as noradrenalin-

containing neurons of the superior cervical ganglion (Moore & Klein 1974). The release of melatonin from the pineal gland can be altered by manipulating the GABAergic transmission in the PVN, and GABAergic neurons in the SCN mediate direct inhibitory effects of light on melatonin release (Kalsbeek et al. 1999). SCN lesions significantly blunt the circadian rhythmicity of melatonin secretion in the pineal gland (Perreau-Lenz et al. 2003).

The daily rhythms of body temperature and cardiovascular activity are under the control of the autonomic nervous system located in the brain stem, however they are under the circadian control of the SCN (Honma et al. 1988; Schroeder et al. 2011). A balance of GABA and glutamate in the PVN, DMH and the MPOA are necessary for cardiovascular and body temperature to function in circadian cycling (De Novellis et al. 1995; Chen et al. 2003). The GABA/glutamate balance is important for regulating the sleep/wake regulatory system (Sherin et al. 1996), driven primarily by the VLPO.

1.1.3 Molecular mechanism

Whole transcriptomic sequencing has showed that the circadian clock drives rhythmic expression of almost half of the protein coding transcriptome (43%) (Zhang et al. 2014). The molecular clock has been extensively studied, with the 2017 Nobel Prize for Physiology or Medicine going to Michael W. Young, Michael Rosbash and Jeffrey C. Hall for their early studies on the molecular clock (Hall 1983; Young et al. 1985; Rosbash & Hall 1985) and its importance in *Drosophila* and has now been studied further in other animals. Further characterisation of the molecular clock has been carried out since its discovery, with a striking result indicating that it remains robust and consistent across different cell types and importantly, across different species (Ko & Takahashi 2006).

A set of core clock genes generate circadian gene expression. In mammalian physiology, these core genes interact in two major transcriptional feedback loops (Reppert & Weaver 2002; Witkovsky et al. 2003; Kriegsfeld et al. 2003; Goto & Denlinger 2002; Kume et al. 1999; Gekakis et al. 1998; Rudic et al. 2004; Cho et al. 2012; Sato et al. 2004; Etchegaray et al. 2009; DeBruyne et al. 2006).

The primary transcriptional feedback loop (Figure 1.1) includes two master heterodimer transcription factors, Circadian Locomotor Output Cycles Kaput (CLOCK) and Brain and Muscle ARNT-Like 1 (BMAL1). This basic helix-loop-helix Per-Arnt-Single-minded (bHLH-PAS) transcription factor rhythmically activates the expression of its transcriptional repressors PERIOD (*Per1*, *Per2* and *Per3*) and CRYPTOCHROME (*Cry1* and *Cry2*) by binding at the enhancer box (E-box) cis-regulatory sequences of these target genes. CLOCK and BMAL1 drive rhythmic gene expression regulating biological functions. Rhythmic binding of the CLOCK:BMAL1 dimer on the DNA promotes rhythmic chromatin opening and remodelling allowing for further transcription factors to bind, contributing to genome-wide effects of transcriptional output of the heterodimer. Following the accumulation of PER and CRY proteins, these dimerise and translocate into the nucleus and act as the negative arm of the molecular clock, blocking the activity of the CLOCK:BMAL1 dimer by binding to the complex, inhibiting transcription of its own, and all other clock-controlled genes (CCGs).

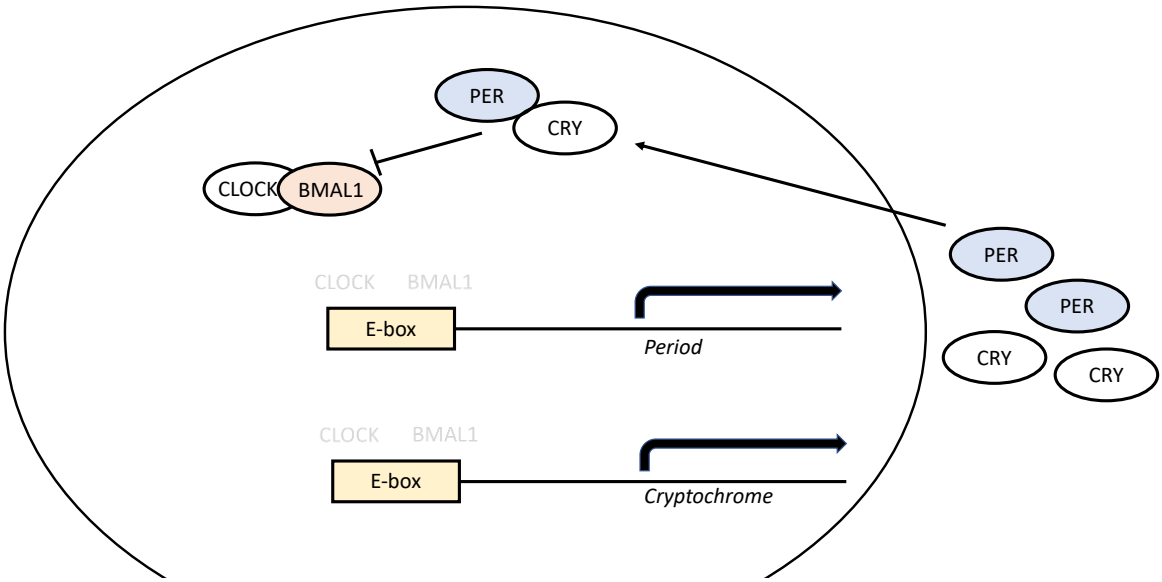

Figure 1.1 The primary loop of the molecular clock. CLOCK:BMAL1 heterodimers bind to E-box elements facilitating the transcription of PER and CRY genes. The translated proteins translocate into the nucleus and target the CLOCK:BMAL1 heterodimers, downregulating further transcription of their own gene. Adapted from Udoh et al. 2015**.**

The second transcriptional feedback loop (Figure 1.2), the accessory loop, similarly induced by CLOCK:BMAL1 heterodimers, activates the transcription of the retinoic acid-related orphan nuclear receptors, REV-ERBα and RORα. Subsequently, these REV-ERBα and RORα proteins translocate into the nucleus and competitively bind to the retinoic acid-related orphan receptor response elements (ROREs) which are present on the *Bmal1* promoter. RORα, β and γ, as well as REV-ERBα and β regulate the transcription of *Bmal1* through ROREs; RORs promote the expression of *Bmal1*, whereas REV-ERB repress the expression of *Bmal1*.

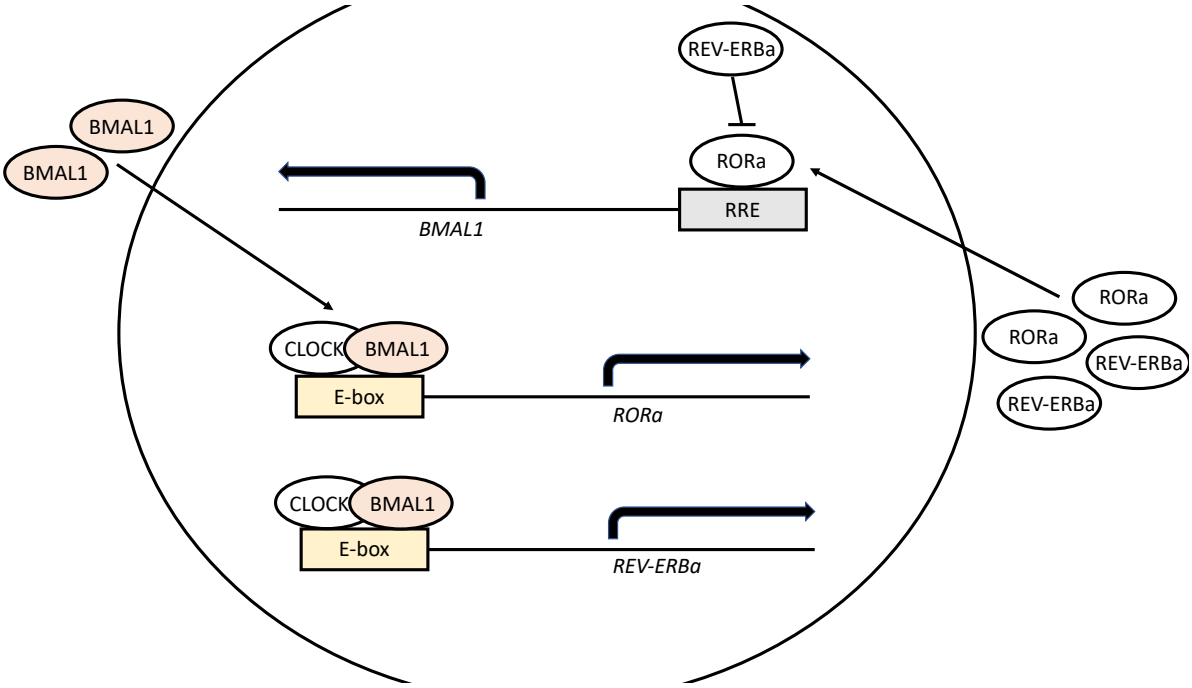

Figure 1.2 The accessory loop of the molecular clock. CLOCK:BMAL1 heterodimers bind to E-box elements facilitating the transcription of *Ror* and *Rev-erb*. The translated proteins translocate into the nucleus where ROR bind at RRE sites to facilitate *Bmal1* transcription, whereas REV-ERB bind to suppress the transcription of *Bmal1*. Adapted from Udoh et al. 2015.

This complex autoregulatory system takes ~24h to complete a cycle and therefore constitutes the circadian molecular clock. The precise timing of this system is governed by post-translational modifications including phosphorylation and ubiquitination (Yoshitane et al. 2009; Stojkovic et al. 2014), affecting the stability and nuclear translocation accessibility of the core clock components to regulate their own activity. In mammals, Casein kinase Iε and 1δ (*CK1ε* and *CK1*δ) are critical in regulating core circadian clock

protein turnover (Zheng et al. 2014; Lee et al. 2011). A mutation to both *CK1ε* and *CK1δ* proved this, as the circadian period was significantly altered, with a decrease in total time detected (Etchegaray et al. 2009). CK1ε and CK1δ are therapeutic targets in humans due to their activity being linked with familial advanced sleep phase syndrome (FASPS), which manifests as a daily biological clock that is phase-advanced 3-4 hours (Jones et al. 1999). The mouse *Clock* gene has histone acetyltransferase (HAT) activity driving the rhythmic expression of the core clock and its output genes, targeting specific histone subunits (Doi et al. 2006). *Clock* also acetylates *Bmal1* at Lys537 and appears to be essential for clock function, as it was shown to be rhythmic in liver and appeared to be required to inactivate *Bmal1* transcriptional activity (Hirayama et al. 2007). Deacetylation of these components also occur. *Sirtuin1* (Silent mating type information regulation 2, homolog) 1 (*Sirt1*), is a circadian deacetylase that interacts with *Clock* and is involved in the rhythmic acetylation pattern of *Bmal1*-Lys537 (Nakahata et al. 2008; Belden & Dunlap 2008). However, although rhythmic binding of SIRT1 to BMAL1:CLOCK occurs, a lack of activity was shown, however SIRT1 oscillatory acetylation of PER2 increases its stability (Asher et al. 2008). In addition to the posttranslational processes of phosphorylation and acetylation, BMAL1 is modified by SUMOylation (small ubiquitin-like modifier) to enhance transcriptional activity (Lee et al. 2008).

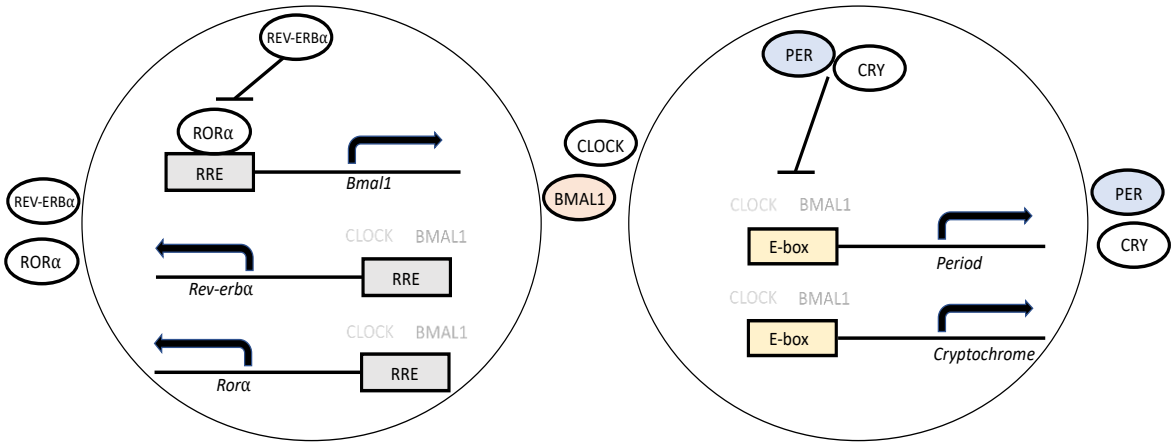

Figure 1.3 The interacting primary and accessory loop of the molecular clock. RORα binds at RREs upstream of the *Bmal1* gene to facilitate the transcription and translation of BMAL1. REV-ERBα competitively binds at RREs to block the transcription of *Bmal1*. CLOCK:BMAL1 dimers bind at E-box elements upstream of *Per*, *Cry*, *Rev-erbα* and *Rorα* to facilitate their transcription. PER and CRY proteins competitively bind at the E-box elements upstream of the *Per* and *Cry* genes to prevent their transcription.

1.1.3.1 PERIOD

The PER proteins were first isolated in 1971 by Konopka and Benzer but later sequenced by Rosbash and colleagues in 1984 are a core component of the primary loop of the circadian clock which were first identified in Drosophila. They are instrumental in signal conduction in the negative feedback involved in circadian core clock oscillations. The mammalian PER proteins bind to the CLOCK:BMAL1 dimer to suppress the transcription of its own gene and to regulate the expression of other CCGs. The *Per* genes have been extensively studied, not only because of their role within the circadian clock, but also because of their importance in other systems, including suppressing tumour proliferation and development (Yang et al. 2009), to the necessity of *Per* for the formation of long-term memory (LTM) (Sakai et al. 2004). *Per2* has been linked with preferred alcohol intake in mice (Spanagel et al. 2005), and alcohol consumption itself being shown to shorten the free running period (Hofstetter et al. 2003). *Per* targeted mice, in the case of $Per1^{ldc/ldc}$ and $Per2^{ldc/ldc}$, (lysine decarboxylase) exhibit an altered phase of locomotor activity and core body temperature rhythms relative to the light/dark cycle, as well as deficits to long term memory (Rawashdeh et al. 2014a). However, total sleep period was maintained in these animals, suggesting that only the distribution of sleep, and not the circadian period may be affected by this mutation.

Classically, *Per* gene expression is driven by the dimerization of the bHLH transcription factors CLOCK:BMAL1 or CLOCK:NPAS2 dimerising and binding to E-box enhancer elements upstream of the *Per* transcriptional start site (TSS). As PER proteins accumulate within the cytoplasm, they are regulated by phosphorylation and their association with CRY proteins encoded by the *Cry* genes. PER and CRY translocate into the nucleus where they negatively regulate their own transcriptional output, blocking the activity of the CLOCK:BMAL1 dimer at the E-box. However, more recently it has been shown that *Per* gene expression can be driven independent of the classically known mechanism, as exposure to glucocorticoids can increase *Per* transcriptional levels independent of circadian cues (Reddy et al. 2012).

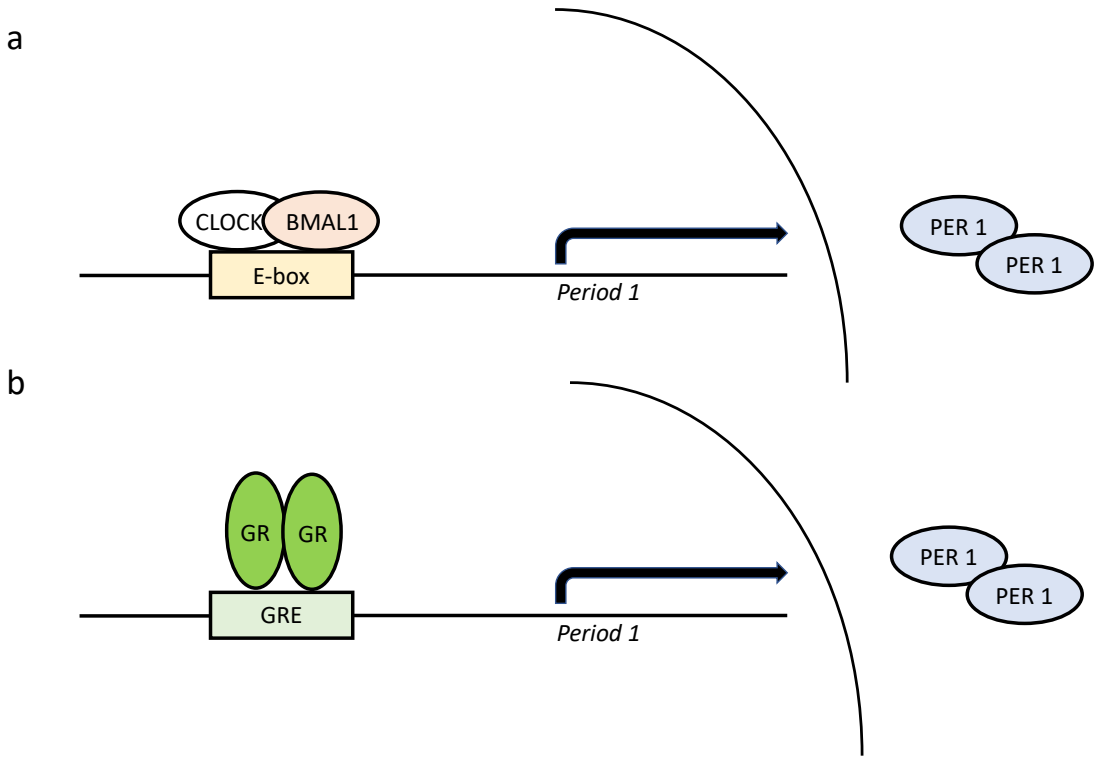

Figure 1.4 Classical pathways facilitating the transcriptional and translational output of *Per* gene. (**a**) CLOCK:BMAL1 dimers bind to E-box elements upstream of *Per* gene. (**b**) Ligand bound glucocorticoid receptors bind to GREs upstream of the *Per* gene transcriptional start site.

PER function is not only necessary for retaining clock function but is also functionally important in other biological processes. For instance, PER regulates cell growth and acts as tumour suppressors, although this hasn't yet been determined as a result of dysregulation of the master clock, known to be within the suprachiasmatic nucleus of the hypothalamus (SCN), or 'local' clock dysregulation as this was shown in breast, endometrial and pancreatic cell lines (Chen et al. 2005; Yeh et al. 2005; Relles et al. 2013).

PER is also important in facilitating long-term memory formation, in particular in the hippocampus, although in this study, dysregulation to other core clock components did not exhibit similar effects (Sakai et al. 2004). In *Per1*$^{(-/-)}$ mice, clock gene expression in peripheral tissue is delayed, and subsequently, locomotor activity and feeding rhythms were altered, with a shortened free-running period reported. However, in these *Per1*$^{(-/-)}$

animals, the oscillatory expression of the clock genes in the SCN, as well as immediate early genes in response to light remained unaffected (Cermakian et al. 2001).

Disruption to sleep and its effects on glucose homeostasis are well documented (Knutson 2007), as the molecular clock regulates metabolic processes in the liver, and disruption to this peripheral clock leads to obesity and metabolic syndrome (Turek et al. 2005; Tong & Yin 2013). In particular, *Per1/Per2*$^{(-/-)}$ mice display a blunted metabolic response to food intake, leptin levels and adipose transcription (Husse et al. 2012). Furthermore, in humans, a mutation to the *Per2* gene has been linked to FASPS (Toh et al. 2001). Whereas in contrast, delayed sleep phase syndrome (DSPS) patients, who exhibit sleep-onset insomnia has been linked with a specific haplotype of the *Per3* gene (Hida et al. 2015). These data reiterate the importance of the *Per* gene and that alterations to it can increase one's susceptibility to sleep disorders, supported further by altered sleep patterns exhibited in various *Per* deficient mice (Hasan et al. 2011; Xu et al. 2007).

1.1.3.2 BMAL1

BMAL1 was first identified in 1997 (Hogenesch et al. 1997; Ikeda & Nomura 1997). BMAL1 and CLOCK function as activators of the molecular clock, promoting the transcription of *Per*, *Cry*, *Rev-erb* and *Ror*. CLOCK:BMAL1 dimers bind at E-box sites on DNA to regulate gene expression during the initiation of transcription (Xiong et al. 2016). The CLOCK:BMAL1 dimer recruits histone modifying enzymes including acetyltransferases p300 and CBP to mediate the acetylation of H3K9 and H3K27 as well as the histone methyltransferases, Myeloid/Lymphoid Or Mixed Lineage Leukaemia (MLL1 and MLL3), to promote the tri-methylation of H3K4 to influence chromatin modification at the core clock gene promotor and enhancer regions (Koike et al. 2012; Valekunja et al. 2013; Katada & Sassone-Corsi 2010). The rhythmic binding of CLOCK:BMAL1 to DNA also promotes rhythmic nucleosomal removal, generating a chromatin landscape accessible for transcription factor binding at its enhancer region. The CLOCK:BMAL1 dimer recruits transcriptional co-activators such as RNA Polymerase II to initiate core clock transcription (Menet et al. 2014; Le Martelot et al. 2012).

BMAL1 binding to E-box elements drives the expression of *Per* and *Cry* in the primary loop of the molecular clock. However, *Bmal1* gene expression is driven primarily by the

secondary loop, or accessory loop, which consists of REV-ERBs and RORs, that act as transcriptional repressors and activators, respectively (Patel et al. 2016; Ono et al. 2015). *Bmal1*$^{(-/-)}$ disrupts the circadian rhythm of activity, whilst also accelerating aging resulting in a shortened lifespan. These animals also exhibit increases in total sleep period, yet fragmented, with an attenuated sleep-wakefulness rhythm noted (Kondratov et al. 2006; Yang et al. 2016)**.**

1.1.3.3 CLOCK

CLOCK dimerises with BMAL1 and binds to E-box elements on DNA to facilitate the transcription of *Per* and *Cry* genes. Along with *Casein kinase 1ε* (*CK1ε*), it is the only other clock mechanism gene that is not rhythmic but is instead constitutively active in the SCN, however oscillates at a circadian frequency in peripheral tissues (Patel et al. 2016). The CLOCK protein is essential in regulating the negative feedback circuitry that generates the circadian oscillations observed in the molecular clock, but also for the rhythmic transcriptional profile of the transcription factor D-box binding protein (DBP) (Ripperger et al. 2000). CLOCK binds to an E-box motif within the enhancer regions of the first and second intron of the *Db*p gene (Yamaguchi et al. 2000). This same E-box motif has been identified in the promoter region of the *Per1* gene, however CLOCK binding to this element has not yet been described (Ripperger & Schibler 2006). *Clock*$^{\Delta 19/\Delta 19}$ mice, produce a dominant-negative CLOCK protein which is therefore defective in transcriptional activation activity (King et al. 1997), exhibit a decrease in total sleep period whilst also presenting with small increases in rapid eye movement (REM) sleep (Naylor et al. 2000).

1.1.3.4 CRYPTOCHROME

CRYTOCHROME (CRY), a major component of the primary loop of the molecular clock was first identified in Arabidopsis (Ahmad & Cashmore 1993), before being described in the fly (Emery et al. 1998; Stanewsky et al. 1998). They are blue light responsive and are found to be highly expressed in the ganglion cells and inner nuclear area of the retina where they target the SCN to rhythmically cycle, and more recently shown to express across different tissues in the brain and body (Thompson et al. 2003; Sancar 2004; Levy et al.

2007). However, CRY is not a photopigment in mammals. CRY1 and CRY2 are essential clock components that along with PERIOD, inhibit the activity of the CLOCK:BMAL1 dimer to prevent their own transcription. However, following the accumulation of PER and CRY, the subsequent proteasomal degradation of CRY and PER proteins cease this inhibition, allowing the molecular cycle to restart.

The co-expression of *Cry1* and *Cry2* are required for periodic molecular and behavioural circadian rhythmicity. However, individual knockout models of *Cry1* and *Cry*2 present with opposing circadian phenotypes, where the *Cry1*$^{(-/-)}$ mice circadian period is shortened but *Cry*2$^{(-/-)}$ mice lengthened (Horst et al. 1999), eluding to the requirement of a functional *Cry1* and *Cry2*, to retain circadian oscillations to 24h. This was further examined *in vitro*, with these studies corroborating what was observed *in vivo,* and enhanced further in these cells when presented with *Fbxl3*^{Afh}, a stabiliser of CRY protein (Anand et al. 2013). Further support for its requirement was shown as *Cry1/2*$^{(-/-)}$ mice become arrhythmic (Horst et al. 1999). In the liver, CRY inhibits the P300 induced increase in CLOCK:BMAL1 driven transcription, through REV-ERBα activity, leading to a delay in *Cry1* mRNA rhythm, in relation to *Per1* rhythm (Etchegaray et al. 2003; Sato et al. 2004) Interestingly, although *Cry1*$^{(-/-)}$ and *Cry2*$^{(-/-)}$ mice exhibited differences in circadian period, both presented with increased baseline levels of NREM and consolidation of NREM sleep episodes, compared to wildtype (Wisor et al. 2002), but also lacked the compensatory response in the sleep period, which is usually evident following sleep deprivation.

1.1.3.5 NPAS2

Neuronal PAS domain 2 (NPAS2) and CLOCK have overlapping roles in the molecular clock. NPAS2 was discovered in 1997 (Zhou et al. 1997). In the SCN, CLOCK:BMAL1 or NPAS2:BMAL1 heterodimers bind to E-box elements located in the regulatory regions of *P*er and *C*ry genes to activate their transcription. Targeting this dimer, *Clock*$^{(-/-)}$/*Npas2*$^{(-/-)}$ mice become arrhythmic, however when *Clock*$^{(-/-)}$ mice were assessed, both the SCN and peripheral tissues exhibited a stable, autonomous circadian rhythm, eluding to NPAS2 compensating for the loss of CLOCK in these animals (DeBruyne et al. 2007; Landgraf et al. 2016).

1.1.3.6 Retinoic acid-related orphan receptors

Proteins of this orphan receptor family bind to REV-ERB/ROR (RRE) elements in responsive genes such as *Bmal1*. RRE binding of REV-ERBα and REV-ERBβ transcriptionally repress *Bmal1*, whereas RRE binding of RORα, RORβ and RORγ transcriptionally activate *Bmal1* (Guillaumond et al. 2005).

1.1.3.6.1 REV-ERB

REV-ERBα and β synchronise with RORα, β and γ to protect the circadian clock and regulate metabolic function. They regulate the oscillations in *Bmal1* expression by binding to the RRE at the *Bmal1* promoter region, suppressing its expression during periods when REV-ERBα is elevated (Bugge et al. 2012). Further modulation of the molecular clock occurs through REV-ERBα, as *Npas2* and *Clock* gene expression is regulated by this transcription factor. A RRE was identified in the first intron of the *Clock* gene, and suppression of *Reverb*α leads to an elevation in *Clock* mRNA production (Crumbley & Burris 2011). *Reverb*α mRNA expression is also controlled by negative feedback downregulation of its own gene, with the *Reverb*α gene promoter containing a functional RRE binding site (Raspé et al. 2002).

In the SCN and in liver tissue, the circadian expression of *Reverb*α mRNA is in antiphase to circadian *Bmal1* mRNA, potentially identifying its role as a transcriptional repressor of *Bmal1* (Ueda et al. 2002). This was further supported as *Reverb*$\alpha^{(-/-)}$ mice exhibited high levels of *Bmal1* mRNA expression, which also lacked circadian oscillations in expression (Preitner et al. 2002). The expression of *Reverb*α mRNA is regulated by CLOCK:BMAL1 dimers binding at E-box elements in its promoter region. This interconnection between the primary and accessory loops of the molecular clock indicates that *Reverb*α is a major determinate of the circadian oscillations observed in *Bmal1* mRNA expression, through its rhythmic repressive action (Guillaumond et al. 2005).

1.1.3.6.2 ROR

The retinoic acid-related orphan receptors (ROR) are closely related to REV-ERB, recognising similar response elements, however they differ by promoting opposing effects to that of REV-ERB, as they promote transcription, rather than suppress the transcription of its target genes.

RORα competes with REV-ERBα for activity on the same promoter element of *Bmal1* to drive the transcription of this target gene, defining the accessory loop of the molecular clock (Guillaumond et al. 2005). BMAL1 RREs can drive the rhythmic expression of the molecular clock alone, indicating their positive transcriptional role, and also their role to repress the clock (Ueda et al. 2002). *Rorα* and *Rorβ* gene expression is driven by CLOCK:BMAL1 regulation on the E-box element of its promoter region (Sato et al. 2004), and is robust in the SCN and remains under the control of the master clock in peripheral tissues (André et al. 1998; Kamphuis et al. 2005). *Rorγ* however is not expressed within the SCN but is robustly expressed in peripheral tissue (Hirose et al. 1994). However, it remains a vital component of the clock machinery in these tissues, as circadian oscillations of *Rorγ* have been observed in the liver (Medvedev et al. 1996). Peak mRNA levels of all three variants in the SCN and peripheral tissue coincide with the peak expression of *Bmal1* mRNA levels (Preitner et al. 2002; Ueda et al. 2002). Further stability to the molecular clock has been described, as RORα regulates *Reverbα* expression, whereas REV-ERBα is able to regulate its own transcription, providing evidence of extra regulatory processes in the molecular clock (Adelmant et al. 1996; Delerive et al. 2002).

A frame shift deletion of $Ror\alpha^{(staggerer)}$ leads to a non-functional protein and significantly shortened locomotor behaviour whilst blunting corticosterone circadian rhythmicity (Frédéric et al. 2006). However, these mice were shown to retain normal clock rhythm within peripheral tissue, indicating a role for *Rorγ* as a major *Bmal1* transactivator, as for example in the liver, all three *Ror* variants may contribute to the rhythmic activation of *Bmal1* (Sato et al. 2004). Because $Ror\alpha^{(staggerer)}$ mice only change the circadian behaviour a small amount, a redundancy transactivation function between *Rorα* and *Rorβ* could account for this small effect, at least within the SCN, as *Rorβ* is robustly expressed here, and because $Ror\beta^{(-/-)}$ mice retain a circadian phenotype, albeit significantly lengthened

(André et al. 1998). Targeting the *Ror*α or *Ror*β gene in mice impairs circadian locomotor rhythm and feeding behaviour (Billon et al. 2017). RORα positively regulates *Bmal1* expression and is therefore vital to driving circadian rhythms (Akashi & Takumi 2005). A *Ror*α/*Ror*$\beta^{(-/-)}$ mouse could further identify if redundancy does occur in the single knockout animal.

1.1.4 Targeting the molecular clock

The molecular clock has been extensively studied, in particular in the mouse to understand the role of each component within the overall functionality of the clock. Below (Table 1.1) shows the core clock components with peak gene expression and behavioural phenotype following mutation (Ripperger & Merrow 2011; Peirson et al. 2006; Cermakian et al. 2001; Oishi et al. 2003; Meng et al. 2008; Guillaumond et al. 2005; DeBruyne et al. 2007; Preitner et al. 2002; Ueda et al. 2002; Sato et al. 2004; Karolczak et al. 2004; Field et al. 2000).

Table 1.1 Effects of altering clock genes expression.

Gene	Transcript peak		Mutation	Behavioural phenotype
	SCN	Peripheral		
Bmal1	16-24	22-02	Bmal1$^{-/-}$	Arrhythmic
Clock	Constitutive	21-03	*Clock*$^{\Delta 19/\Delta 19}$	Arrhythmic
			Clock$^{-/-}$	23.5h
Per1	4-12	10-16	*Per1*$^{-/-}$, *Per1*^{brdm1}, *Per1*^{ldc}	23-23.5h
Per2	4-16	14-18	*Per2*^{brdm1}	22.5h
			Per2^{ldc}	Arrhythmic
Per3	4-16	10-14	*Per3*$^{-/-}$	23.5h
Cry1	8-16	14-18	*Cry1*$^{-/-}$	23h
Cry2	8-16	8-12	*Cry2*$^{-/-}$	23h
Reverbα	2-6	4-10	*Reverbα*$^{-/-}$	23.5/
Rorα	6-10	Arrhythmic	*staggerer*	23.5h
Rorβ	4-8	18-22	*Rorβ*$^{-/-}$	24.5h
Rorγ	Not SCN	16-20	*Rorγ*$^{-/-}$	-
Npas2	Not SCN	0-4	*Npas2*$^{-/-}$	23.8h
Ck1ε	Constitutive	Constitutive	*CK1ε*^{taud}	20hr
Ck1δ	Constitutive	Constitutive	*Csnk1δ*$^{-/+}$	23.5h

1.1.5 Tissue specific clocks

The molecular clock is a self-sustained, cell-autonomous system that is driven primarily by the master circadian regulator, the SCN, as well as in peripheral tissue and cell culture, to maintain their circadian rhythmicity (Welsh et al. 1995). There are variations in timing across different tissues, as for example, *Clock* mRNA cycles in peripheral tissue, but remains constitutively active within the SCN (Ripperger & Merrow 2011). *Rorα* displays a robust circadian rhythm within the SCN, but only a slight oscillation has been observed in peripheral tissue. On the other hand, *Rorγ*, which is not expressed in the SCN, is rhythmic in peripheral tissue and is important in regulating the peripheral clock (Sato et al. 2004).

Interestingly, *Ror$\alpha^{(staggerer)}$* mice, which should affect the transcriptional output of *Bmal1*, maintain circadian rhythm in peripheral tissue, including the *Bmal1* mRNA rhythm, suggesting that ROR proteins may contribute to the activation of the molecular clock in a tissue specific manner, as for instance, *Bmal1$^{(-/-)}$* mice display a loss of circadian rhythm, decreased body weight, infertility and a shortened lifespan (Kondratov et al. 2006). This suggests that BMAL1 and other clock components are instrumental in a variety of functions, depending on the tissue in which they are expressed. *Clock$^{(-/-)}$* mice also present with reduced lifespan and altered circadian profiles in a tissue specific manner (Dubrovsky et al. 2010). *Clock$^{(-/-)}$* mice exhibit a dampened amplitude of *Reverbα* mRNA oscillations in the SCN, whereas the amplitude of the transcript is markedly reduced in the liver. Interestingly, liver *Per1* mRNA expression in these animals was also robustly rhythmic, however a delay in peak expression was observed compared to that of wild-type liver (DeBruyne et al. 2006), indicating that the transcription factors that promote circadian gene patterns, in the absence of *Clock*, are target gene and tissue specific. Further, *Per2* mRNA rhythms also exhibit tissue specific disruption in *Clock$^{\Delta 19/\Delta 19}$* mutation. The circadian rhythmicity of *Per2* persists in *Clock* mutant liver and muscle, with only slight changes in amplitude and peak phase, when compared to wild-type, however the *Per2* transcript is severely blunted in *Clock$^{(-/-)}$* kidney and heart (Turek et al. 2005).

1.1.5.1 In the brain

The master clock, located in the suprachiasmatic nucleus (SCN), is one of many nuclei that make up the hypothalamic region of the brain. Not only does the SCN contain robust clock machinery, the other nuclei of the hypothalamus do too, in turn driving circadian regulated processes, such as metabolism (Arcuate nucleus ARC), hormone secretion (Paraventricular nucleus PVN) and the sleep-wake cycle (Ventrolateral preoptic area VLPO) (Abe et al. 2002; Lu et al. 2000; Lu et al. 2002).

The SCN disseminates, via neural and humoral activation, to other brain regions to regulate those tissues in a circadian rhythmic manner (Guo et al. 2005; Silver et al. 1996). Established areas of the brain that are known to contain the clock components, but also drive circadian rhythm of these particular areas are vast, and include, but are not limited to, the hippocampus (HC), the perirhinal cortex (PrhC), the amygdala (AMY), bed nucleus of

the stria terminalis (BNST), pineal gland, frontal cortex, and brainstem (Uz et al. 2005; Lamont et al. 2005; Segall et al. 2006; Takekida et al. 2000; Kaneko et al. 2009).

The SCN is known as the master clock in the body, regulating all tissues to remain in rhythm and controlling processes including locomotor activity, core body temperature and metabolic processes (Stephan & Zucker 1972; Ruby et al. 2002; Schwartz et al. 1983). The SCN has been extensively studied, both *in vivo* and *in vitro* to describe the components of the clock and to understand its importance on the rest of the body. The SCN's major activator is through light, where photosensitive retinal ganglion cells activate the clock machinery in the SCN to signal rhythmic processes (Berson et al. 2002; Hattar et al. 2002). However, animals in constant dark retain circadian rhythmicity, through other key activators of rhythms, including hormone secretion and feeding rhythms (Hara et al. 2001; Balsalobre et al. 2000). Rats in constant light become arrhythmic in activity (Eastman & Rechtschaffen 1983). Lesions to the SCN produce arrhythmic activity similar to what is observed in constant light (Stephan & Zucker 1972), however following transplantation of a SCN into SCNx animals, activity periods and body temperature circadian rhythmicity returned (Silver et al. 1996) confirming its role in driving the circadian oscillations in animal behavioural output (Oishi et al. 1998b; Akhtar et al. 2002; Terazono et al. 2003).

Molecular clocks peripheral to the SCN, but still within the brain have also been identified, in particular using transgenic animal models whose circadian rhythmicity can be measured in real-time (Weger et al. 2013). The olfactory bulb (OB) contains robust circadian rhythmicity (Granados-Fuentes et al. 2006), as well as the pineal gland and arcuate nucleus. *Per1* in these peripheral clocks was delayed in comparison, with peak expression occurring during the night, whereas in the SCN it occurred in the late day. Interestingly, the expression of *Per1* was assessed in the olfactory bulb following a SCN lesion, and the rhythmic activity of *Per1* was not affected, indicating further regulatory systems target the OB to remain in rhythm (Granados-Fuentes et al. 2004; Abraham et al. 2005), eluding to the possibility that the SCN acts to synchronise individual peripheral brain oscillators, rather than necessarily driving circadian rhythmicity in these tissues.

The reward system, which is composed of structures including the ventral tegmental area (VTA), the nucleus accumbens (NAc) and prefrontal cortex (PFC) can modify behaviour, learning capabilities and mood (Fields et al. 2007; Drevets et al. 1992; Mayberg et al. 2000).

Food, alcohol and cocaine all influence the reward system, with reward-related behaviours exhibiting a rhythmic period of ~24h, suggesting there is an interaction between circadian and reward systems in the brain (Abarca et al. 2002). Further to circadian effects on the reward pathway, seasonal patterns also influence addictive drug use and is often accompanied with depression (McGrath & Yahia 1993; Rosenwasser et al. 2005). People with genetically determined sleep disorders are also more prone to addiction (Shibley et al. 2008).

The mouse neocortex and cerebellar cortex display circadian oscillations of *Per1*, *Per2*, *Cry1*, *Bmal1* and *Rev-erbα*, however a 6h delay compared to the SCN was described, reflecting the known 'master-slave' relationship between SCN and peripheral clocks (Rath et al. 2014).

The hippocampus is known to contain components of the molecular clock which are vital for daily processes including sleep and memory consolidation (Rawashdeh et al. 2016), as well as regulating neurogenesis (Bouchard-Cannon et al. 2013). Ultradian glucocorticoid exposure directs *Per*1 gene pulsing in the hippocampus (Conway-Campbell et al. 2010), providing a further mechanism that regulates core clock genes irrespective of SCN signal. *Per1*$^{(-/-)}$ mice display deficits to memory in a hippocampal specific task (Rawashdeh et al. 2014b). Another area involved in memory consolidation through the action of recognition memory is the perirhinal cortex. Although unpublished, clock genes are expressed in this area, with data similar to that observed in the hippocampus, with a delay in phase compared to that of the SCN (Rozwaha 2017).

Although clock genes are expressed in different brain regions, such as the prefrontal cortex, the olfactory bulb, and hypothalamic nuclei (Chen et al. 2016; Granados-Fuentes et al. 2006), the rest of the brain has been overlooked. For instance, clock gene expression studies in the hippocampus is limited (Mure et al. 2018; Tam et al. 2017). Classically, peripheral clocks have been identified in regions outside of the brain, with an extensive publication list in organs such as the heart and liver. Further to this, skeletal muscle is also a commonly targeted area for clock gene function.

1.1.5.2 Heart

Expression of clock genes *Bmal1, Clock, Cry* and *Cry/2* and *Per1, Per2,* and *Per3* in the heart is integral in priming the heart to anticipate and subsequently adapt to physiological alterations throughout the day (Young et al. 2001). Heart rate was assessed in infants ranging from 2 months to 15 years, with a significant circadian rhythm identified and the rhythm being most pronounced between high frequency periods in day and night. A rise in heart rate was also observed during night and was associated with sleep maturation (Massin et al. 2000). *Per1* mRNA expression peaks at ZT12-16 in the heart, delayed in comparison to that of the master clock in the SCN, where *Per1* mRNA expression peaks at ZT4-12, lending to a delay in response between these tissues. This was also evident in *Cry1* mRNA expression, as in the SCN it peaked between ZT8-16, whereas in the heart it peaked at ZT14-18 (Peirson et al. 2006).

1.1.5.3 Liver

Clock gene expression and its role within the liver is well established, both *in vivo* and further characterised *in vitro* (Tong & Yin 2013; Zmrzljak et al. 2013; Peirson et al. 2006). Energy homeostasis is maintained in the liver in mammals, where glucose is broken down into smaller carbohydrates and gluconeogenesis reverses this reaction (Inoue et al. 2004). Although light is the most potent timing queue for entraining daily rhythms in the SCN and peripheral tissues, the liver is further circadian regulated by processes including feeding and hormone secretion (Davidson et al. 2003; Díaz-Muñoz et al. 2000), known as the food-entrainable oscillator (FEO) or through HPA axis steroid secretion. SCN-disrupted animals still respond to rhythmic food availability (Krieger 1980) and lesions to the SCN do not affect food-anticipatory behaviours in these animals (Stephan et al. 1979).

Glucocorticoids have been shown to alter the clock in the liver, whilst unaffecting the clock in the SCN. Dexamethasone, which binds to the glucocorticoid receptor (GR), phase shifts clock gene expression in the liver, and other peripheral tissues to the SCN, proposing the theory of differential expression of the GR across the liver and SCN accounting for this effect (Balsalobre et al. 2000; Reul & Kloet 1985; Reul & de Kloet 1986). Glucocorticoid signalling affects almost 60% of the rhythmic liver transcriptome (Reddy et al. 2007), and the importance of feeding time has been further described as having an effect on clock

rhythms, as restricted feeding induces changes to the phase of circadian gene expression of the liver and other peripheral organs, without affecting the SCN, demonstrating an uncoupling of peripheral clocks from the central clock (Damiola et al. 2000; Stokkan et al. 2001). Food metabolites and hormones secreted upon feeding and fasting further regulate the circadian clock mechanism in the liver and other peripheral tissues, indicating an additional entraining signal for circadian rhythmicity in the liver (Schmutz et al. 2012). For instance, targeting *Bmal1* in mice hepatic tissue only exhibit hypoglycaemia in their resting phase, whereas in a global knockout, the mice had normal resting blood sugar levels (Gatfield & Schibler 2008), therefore providing evidence that a failed synchrony between the SCN and hepatic clocks resulted in this hypoglycaemic state, suggesting that peripheral pacemakers in the liver, may ultimately determine metabolic function in response to environment inputs. Similarly, other peripheral clock tissues, such as the liver clock, is also delayed in comparison to the SCN with peak timing of *Per1* and *Cry1* at CT12 in the liver (Peirson et al. 2006).

1.1.5.4 Skeletal Muscle

The critical role that clock genes have in the liver and on metabolic processes, ultimately leads to the question of what peripheral and tissue-specific actions do these circadian regulators have in insulin-sensitive tissues. The skeletal muscle circadian transcriptome was described in 2007 (Miller et al. 2007), however it was previously shown that skeletal muscle activity rhythms can be reset by altering the timing of exercise/activity or by the timing of feeding, rendering it partially independent of the central clock (Maywood et al. 1999).

Bmal1$^{(-/-)}$ mice exhibit reduced activity, decreased muscle mass and accelerated aging (Laposky et al. 2005; Kondratov et al. 2006). However, a targeted *Bmal1*$^{(-/-)}$ in skeletal muscle only resulted in mice exhibiting a normal lifespan and increased muscle mass. The circadian activity of these animals was also unaltered, however an increase in the amplitude of activity during the active phase was observed (Dyar et al. 2014). Insulin-stimulated glucose uptake into skeletal muscle was substantially reduced, whereas whole-body glycemia remained unchanged. GLUT4, an insulin-regulated glucose transporter protein, was reduced to almost 50% in *Bmal1*$^{(-\backslash-)}$ muscle, although the mRNA levels remained unchanged, indicative of a post-translational event causing this alteration. Targeting the

Bmal1 gene in skeletal muscle also altered the expression of other clock genes and clock-controlled genes (Peek et al. 2017). A subtle difference is observed between the synchronicity of the SCN and skeletal muscle and may underlie the increased risk of type 2 diabetes due to an impaired glucose disposal (Marcheva et al. 2010), and therefore targeting the clock therapeutically could be a possible method to treat insulin-resistant skeletal muscle commonly observed in metabolic dysfunction (DeFronzo & Tripathy 2009).

Per mRNA expression profiling of skeletal muscle showed that similarly again to the other peripheral tissue mentioned, peak expression occurred around ZT12. Interestingly in the same study, *Cry1* had modest circadian oscillations, with a small increase in expression occurring early in the day cycle, at ZT0 (Yang et al. 2006).

1.1.6 Diseases associated with altered clock

The molecular clock drives most tissues in the body to regulate their activity to the daily period, whether it be entrainment by light, driving activity periods, to feeding, causing the release of glucose prompting gluconeogenesis to occur whilst stimulating muscle activity. The absence of a synchronised clock in animal models delivers alterations in activity, sleep, memory and metabolic processes. There are an increasing number of disease states in humans that are associated with circadian timing disruptions, however it is important to note that most studies have connected disease state with correlative evidence of gene variation which does not ultimately indicate causation. See table 1.2 (Zhao et al. 2016; Vanselow et al. 2006; Hida et al. 2015; Woon et al. 2007; Patke et al. 2017; Archer et al. 2003).

Table 1.2 Diseases associated with affected genes of the clock.

Gene	Phenotype
Per1	Abnormal apoptosis, abnormal behavioural sensitization to psychostimuli
Per2	Cancer development, Increased alcohol intake, FASPS
Per3	DSPS
Bmal1	Altered sleep and metabolic syndrome
Clock	Altered sleep and metabolic syndrome
Cry (1 and 2)	Altered sleep
Npas2	Altered sleep and impaired memory
CK1e/Ck1d	FASPS

1.2. Organisation of the HPA axis.

Glucocorticoids are secreted from the adrenal gland in a circadian pattern of ultradian pulses governed by the circadian drive of the SCN. Adrenocorticotrophic hormone releasing factor (CRF) or corticotropin releasing hormone (CRH) and vasopressin (AVP) are secreted from the PVN in response to circadian cues but also in response to stress. These hormones in turn, stimulate the secretion of adrenocorticotrophic hormone (ACTH) from the anterior pituitary, which in turn, drives the secretion of glucocorticoids from the adrenal cortex.

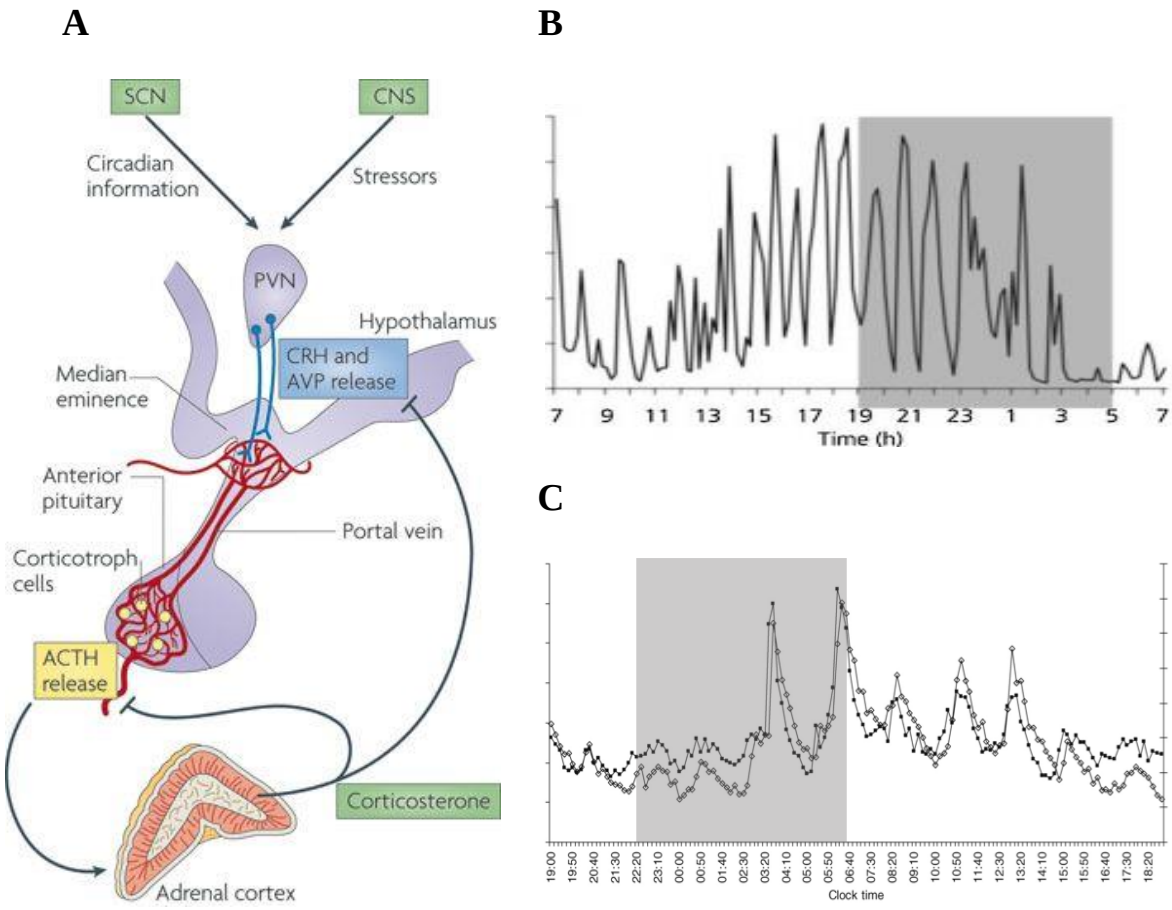

Figure 1.5 The HPA axis and its hormonal output over the day. A schematic of the HPA axis (**A**) and measurement of corticosterone in rat (**B**) and cortisol in human (**C**) over one day (Lightman & Conway-Campbell 2010; Henley et al. 2009).

1.2.1 Paraventricular nucleus

The paraventricular nucleus of the hypothalamus (PVN) is a group of densely packed neurons that are stimulated by physiological changes, such as the changing light/dark cycle and in the presence of a stress. The PVN contains CRF cell bodies which through axonal projections to the capillaries of the median eminence, secretes CRH directly into the portal system to act on the pituitary to regulate ACTH secretion. Neurons of the PVN project directly to the posterior pituitary where oxytocin is released, or to the brainstem and spinal cord, to regulate appetite and autonomic functions. The PVN is highly vascularised and is protected by the blood-brain barrier, however its neuroendocrine cells beyond it. The magnocellular neurosecretory cells' axons extend into the posterior pituitary, as well as the HPA reactivity parvocellular neurosecretory cells, which secrete CRH and project to the

median eminence. The PVN also projects to the brainstem and spinal cord via parvocellular preautonomic cells (Ter Horst et al. 1991).

The magnocellular neurons secrete oxytocin (OT) and vasopressin (AVP), which are transported down the axonal projections and released from the neurosecretory nerve terminals residing in the posterior pituitary gland. Magnocellular neurons are also found in the supraoptic nucleus (SON) and secrete vasopressin, to enhance water reabsorption in the kidney (Erkut et al. 1998).

The parvocellular neurons project to the median eminence, where they secrete CRH, AVP and TRH from nerve terminals at the primary capillary plexus of the hypophyseal portal system. The secretion of CRH and AVP from parvocellular neurons act synergistically to stimulate ACTH secretion from the anterior pituitary (Berk & Finkelstein 1981).

The PVN, in addition to neuroendocrine neurons, also contains interneurons and populations of other neurons that project centrally to other brain regions. Parvocellular oxytocin secreting cells project to the brainstem and spinal cord, to suppress nociception, promoting analgesic effects (Eliava et al. 2016). Parvocellular vasopressin secreting cells project mainly to the hypothalamus, including the SCN, and the limbic system. Parvocellular CRH secreting neurons project to the amygdala, where an overexpression of CRH in this brain region, results in increased anxiety (Kalin 2018).

1.2.2 Pituitary gland

The pituitary gland is made up of three lobes (the anterior, intermediate and posterior lobes) that sits at the base of the brain in a protective bony enclosure. The lobes differ greatly; however, the release of hormones is governed by the hypothalamus.

CRH, AVP and TRH are released by parvocellular neurosecretory cells into hypothalamic capillaries joining to infundibular blood vessels, that in turn leads to a second capillary bed in the anterior pituitary, constituting the hypothalamic-hypophyseal portal system. These hormones diffuse out of the second capillary bed and target anterior pituitary endocrine cells, regulating the release of ACTH. The anterior lobe is further subdivided into the *pars tuberalis*, *pars intermedia* and *pars distalis*. The anterior pituitary not only secretes ACTH,

it also contains cells that synthesise and secrete other hormones, such as human growth hormone (HGH), thyroid stimulating hormone (TSH), luteinising and follicle stimulating hormone (LH/FSH), as well as prolactin (PRL) (Childs et al. 1989).

The posterior lobe of the pituitary develops as an extension of the hypothalamus, with hormones secreted from here being synthesised by cell bodies within the hypothalamic area. The posterior lobe contains glia (pituicytes) that store and secrete OT and AVP and this lobe can be subdivided into the *pars nervosa* and infundibulum stalk. The infundibulum stalk bridges the hypothalamic and hypophyseal systems and connects to the median eminence. The *pars nervosa* contains OT and AVP secretory cells. The magnocellular neurosecretory cells of the SON and PVN in the hypothalamus project axons down the infundibulum to terminals in the posterior pituitary where the storage and secretion of neurohypophyseal hormones OT and AVP into the neurohypophyseal capillaries occurs, and further into the systemic circulation (Bisset et al. 1973).

The intermediate lobe is important in many animals but is not a distinctive structure in humans. In rodents, it is composed mainly of melanotrophs, endocrine cells that secrete alpha-melanocyte-stimulating hormone (alpha-MSH) and beta-endorphin. This area is poorly vascularised, and here pituitary melanotrophs are supplied by nerve fibres emanating from the hypothalamus (Lamacz et al. 1991). Pituitary melanotrophs synthesise proopiomelanocortin (POMC) and cell bodies targeted for POMC are located in the arcuate nucleus of the hypothalamus (ARC) and the nucleus of the solitary tract of the brainstem (NTS), both of which functionally drive appetite and food intake.

1.2.3 Adrenal gland

The adrenal gland is made up of three main zones (*glomerulosa*, *fasciculata* and *reticularis*) with each having a distinct function, producing mineralocorticoids, glucocorticoids and androgens, respectively. Although each zone has a specific mechanism of regulation, ACTH acts on all zones (Vinson 2016).

The *zona glomerulosa* is the most superficial layer of the adrenal cortex. The mineralocorticoid aldosterone is released from this layer in response to increased potassium and renin levels, or decreased blood flow within the renin-angiotensin system.

The *zona fasciculata*, which sits between the *glomerulosa* and *reticularis*, is the primary producer of glucocorticoids. This layer produces androgens; however, the main source of androgen is from the *zona reticularis*. Adrenal tumours and hyperplasia in this region result in excess cortisol production and present as adrenal Cushing's disease. In rodents, the *fasciculata* synthesises corticosterone instead of cortisol (humans), due to the lack of 17alpha-hydroxylase.

The *zona reticularis* is the innermost layer of the adrenal cortex and produce precursor androgens including dehydroepiandrosterone (DHEA). It is either further converted in the cortex to DHEA-S or enters the bloodstream and testis and ovaries to produce testosterone and oestrogens, respectively. ACTH partly regulates adrenal androgen secretion.

1.3. The central nervous system

The central nervous system comprises the brain and spinal cord in mammalian physiology. Decoding the chemical, electrical and genetic processes that account for brain output is one of the greatest challenges in modern biomedical research. The mammalian brain is the most developed brain of all animals, with distinct differences observed in the size of the neocortex, the area of the brain that processes higher learning, such as cognition and language (Amato et al. 2004; Benedict et al. 2006). The brain itself can be grossly simplified into four distinct regions; the cerebrum, the cerebellum, the limbic system and the brainstem.

1.3.1 Brainstem

The brainstem, which consists of the midbrain, pons and medulla oblongata, is posterior in the brain and directly connects to the spinal cord. Autonomic regulation of cardiac and respiratory function occurs here (Harper et al. 2000), as well as the maintenance of consciousness and sleep (Steriade & McCarley 1990). The midbrain can be further subdivided into the tectum, tegmentum, cerebral aqueduct, and cerebral peduncles in which the tectum comprises the inferior and superior colliculi, which receive input from auditory and visual cues, resulting in the head turning in the direction of either stimulus (Merzenich & Reid 1974; Sprague 1966). The tegmentum, which extends from the substantia nigra to

the cerebral aqueduct processes voluntary and involuntary movement, as well as arousal, self-consciousness and reward (Lammel et al. 2012; Sukhotinsky et al. 2005). The cerebral peduncles - structures at the front of the midbrain contain ascending and descending nerve tracts to assist in refining motor movements, using sensory and motor contact, respectively. Damage to this area results in unrefined motor skill, imbalance and poor proprioception (Hosp et al. 2011). The pons contains the end terminal of four cranial nerves, of which serve to regulate involuntary movements such as respiration, chewing and swallowing, and the secretion of saliva and tears (Meng et al. 2000). The medulla oblongata, the final subdivision of the brainstem is also responsible for autonomic actions, such as vomiting and sneezing (Martin et al. 1991) and it is the area of the brainstem that contains the centres for breathing, heart rate and blood pressure control (Verner et al. 2004).

In addition to the role of the HPA axis on stress, the brainstem also plays a crucial role in regulating the adaptive response to stress through brainstem noradrenergic neurons, sympathetic adrenomedullary circuits and parasympathetic systems (Herman et al. 2016; Habib et al. 2001; Whitnall et al. 1993), primarily in response to alterations in homeostatic mechanisms, such as hypovolaemia and inflammatory challenges. The nucleus of the solitary tract (NTS) and ventral medulla (VM) target the PVN through noradrenergic, adrenergic and glucagon-like peptide 1 containing neurons to affect the HPA axis response (Sawchenko et al. 1993; Smith & Vale 2006). Neurons of the brainstem receive input from the vagus and sympathetic nervous system, as well as local inflammatory signals which then target the parvocellular cells of the PVN, dictating the activity of the HPA axis (Herman et al. 2003; Ulrich-Lai & Herman 2009; Cunningham et al. 1990).

1.3.2 Cerebellum

The cerebellum, which sits at the most caudal location of the brain structure above the brainstem is well known to play an important role in motor control in humans, where it distinguishes between actual and learned movement. Damage to the cerebellum results in deficits in fine motor skill, balance and posture (Ivry et al. 1988).

However, in 1976 evidence for the importance of the cerebellum in emotion and emotional disorders, describing its importance in the Papez circuit was published, with follow up work indicating a functional role of the cerebellum in cognition and emotion (Schmahmann

1991). In cerebellar dysfunction, where motor activity is often affected, evidence for an increased risk in mental health disorders was reported, with schizophrenia and depression often observed (Schmahmann 2004).

The cerebellum projects wholly to the limbic system, with observations in the hypothalamus, hippocampus, amygdala and basal ganglia, as well as to brainstem nuclei, substantia nigra and locus coeruleus (Heath & Harper 1974). Targeted lesions to the cerebellum in the monkey resulted in reduced aggressive behaviour, and stimulation of the cerebellum in rats resulted in limbic system activation (Peters 1971; Heath et al. 1978), indicative of the importance of the cerebellum on the limbic and HPA axis systems.

1.3.3 Cerebrum

The cerebrum, the largest part of the mammalian brain is a vast structure that contains the cerebral cortex, as well as subcortical structures including the amygdala, basal ganglia and hippocampus. The cerebrum, being such a major component controls a magnitude of different functions dependent on the location but is fundamental for, and not least of all, emotion, hearing, vision, personality, voluntary action and memory storage (Grol et al. 2006; Gais et al. 2007).

The HPA axis and the release of glucocorticoids can significantly affect different areas of the cerebrum. For instance, lesions to the central nucleus of the amygdala (CeA) or medial nucleus of the amygdala (MeA) results in HPA axis attenuation and reduction of the stress response in various stimuli (Dayas et al. 1999; Buller et al. 1998). However, as the projections from the CeA and MeA are limited (Gray et al. 1989; Prewitt & Herman 1998), they must affect the PVN via an indirect pathway, possibly through the bed nucleus of the stria terminalis (BNST), as projections from the CeA and MeA are GABAergic (Swanson & Petrovich 1998), and projections from the BNST to the PVN are GABAergic, resulting in HPA axis activation. This pathway could be disinhibitory, as the CORT response to stimulation of the MeA can be attenuated by lesioning the BNST (Feldman et al. 1990).

1.3.4 Limbic system

The limbic system has been extensively studied for its role in emotional processing and is located deep within the cerebrum, consisting of the hypothalamus, hippocampus, amygdala and the thalamus to name a few, which exists to support a variety of functions including reviewing and responding to emotional events, as well as being instrumental in behaviour responses and memory processing (Catani et al. 2013).

Lesions of the anterior thalamic nuclei results in decreased expression of the neural plasticity marker *zif268* in the subiculum as well as reductions to pCREB (Dumont et al. 2012), indicating the role of the thalamus as part of the extended hippocampal system, crucially involved in memory processing. The amygdala (AMY) contributes heavily to fear-motivated learning, with manipulations to the region significantly affecting behavioural outcomes in the presence of fear conditioning (Fanselow & LeDoux 1999). Changes to firing rates of neurons have also been observed in the AMY, however the limbic system circuitry as a whole heavily influences this learning also (Quirk et al. 1997). As for instance, the basolateral amygdala (BLA) receives input from the neocortex, thalamus and hippocampus, projecting to the CeA to generate and coordinate with other limbic brain areas, inducing fear-related behaviour (Swanson & Petrovich 1998; Bolton et al. 2018).

1.4. The Hippocampus

The hippocampus (HC) is a structure of the brain that forms part of the limbic system and plays a key role in spatial navigation and episodic memory (O'Keefe & Speakman 1987). Both human and animal studies have found that stress impairs hippocampal-dependent memory tasks, altering the synaptic plasticity and firing properties of neurons involved in consolidation processes (Benoit et al. 2015).

The ventral HC and ventral subiculum largely control the response to HPA axis activity, as CORT pellets implanted into these areas present with a flattened circadian CORT rhythm, but also because stimulation of the vHC inhibits HPA axis activity (Slusher 1966; Casady & Taylor 1976). The HC primarily exerts an inhibitory effect on the PVN, with gross HC lesions elevating basal CORT levels (Fendler et al. 1961; Knigge 1961). However, lesions to specific areas have differing effects on HPA axis activity. Lesioning the dorsal HC, the

main projection to the hypothalamus, disrupts the circadian CORT rhythm and elevates resting CORT levels (Fischette et al. 1980), whereas lesions to the hippocampus proper (i.e. CA1-3) prolong the CORT response to stress, indicating the HC is important in controlling the rhythm and inhibition of the HPA axis in response to stress and circadian timing.

1.4.1 Input

The afferent and efferent pathways of the HC are vast, signifying its importance in the regulation of many circuits and regions of the brain. The primary afferent pathway of the HC is the perforant pathway, which originates in the entorhinal cortex (EC) and synapses predominantly in the granular cells of the dentate gyrus (DG), a region of the hippocampus formation (Witter 2007). These fibres predominantly project from the lateral EC to the outer layers of the DG, whereas fibres projecting from the medial area of the EC project to deeper regions of the DG.

The lateral and medial EC (MEC) process spatial information. The lateral EC (LEC) processes local spatial frameworks, whereas the medial EC processes global spatial frameworks (Knierim et al. 2014; Neunuebel et al. 2013). Lesioning of the LEC impairs local spatial framework tasks. Impaired memory was also observed during an object recognition task when involving multiple local stimuli but was unimpaired when recognising a single familiar object (Kuruvilla & Ainge 2017).

Further afferent projections of the HC include the cingulate gyrus, the contralateral HC, the medial septal nuclei and the fornix (Fuhrmann et al. 2015; Hamani et al. 2011). The precommissural branch of the fornix connects to the septal nuclei and ventral striatum to link the reward pathway (Schultz & Engelhardt 2014), the preoptic nuclei to regulate body temperature (McKinley et al. 2015), the orbitofrontal cortex which processes decision making (Rushworth et al. 2011), and the anterior cingulate cortex which connects the limbic system to the prefrontal cortex, combining the emotional response to cognitive processing (Bush et al. 2000). The postcommissural branch of the fornix projects to the anterior nuclei of the thalamus, a key component of the hippocampal system for episodic memory as well to the mammillary bodies of the hypothalamus, which act as a relay for indirect hippocampal inputs to the thalamic anterior nuclei and are often referred to as a

constituent of an extension of the hippocampus (Aggleton & Brown 1999). The afferent pathways of the HC provide insight into the vast actions of this structure, and its importance in multiple systems and circuits of the brain, in particular the limbic system.

1.4.2 Cell types and neuroanatomy

The HC is often described as the hippocampus proper, and hippocampus formation. The hippocampus proper is composed of the Cornu Ammonis (CA) regions (CA1-3) only, whereas the hippocampus formation consists of the CA regions, the dentate gyrus (DG) and subiculum (SUB) (Grønli et al. 2006; Roelink 2000). Principal neurons of the trisynaptic circuit of the HC formation (DG – CA3 – CA1) fire spatially modulated spikes in a particular area of the environment to form a neural representation of its surroundings, supporting its involvement in spatial navigation and episodic memories (Buzsáki 2010; Leutgeb et al. 2005).

The CA regions of the HC are structurally defined by their strata. The stratum oriens is composed of the cell bodies of inhibitory basket cells and the horizontal trilaminar cells – oriens, pyramidal and radiatum (Thal et al. 2000). The dendrites of pyramidal cells are located in the oriens, and receive information from pyramidal cells, septal fibres and commissural fibres of the contralateral HC (Lacaille et al. 1987). The stratum pyramidale is composed of the cell bodies of the pyramidal neurons, which are the principal excitatory neurons of the HC (Miles et al. 1996). Within the CA3 region, this stratum contains the synapses from mossy fibres which project through the stratum lucidum and is only found in the CA3 region where mossy fibres from the DG pass through this layer and synapse in the stratum pyramidale (Frotscher 1985). The stratum lacunosum contains Schaeffer collateral fibres as well as perforant path fibres from the EC. The stratum moleculare is the most superficial stratum in the HC, and where the perforant path fibres form synapses onto the distal, apical dendrites of pyramidal neurons (Andersen et al. 1966). Theta rhythm varies throughout the strata, and therefore the sulcus, which is a cell free area, is often used as a fixed-point reference for electroencephalography (EEG) recordings.

1.4.2.1 CA1 region

The CA1 region of the hippocampus has been extensively studied for its role in memory processing. It receives external information from the EC, arriving at the most distal dendritic regions of principal neurons. Internal information, predominantly from the CA3 region arrives at proximal perisomatic dendrites (Steward 1976; Megías et al. 2001; Suh et al. 2011; Witter et al. 2000). The CA1, CA3 and EC circuit drives the CA1 region to associate contextual and spatial information, therefore generating and maintaining context-dependent spatial maps (Takahashi & Magee 2009; Wood et al. 2000; Markus et al. 1995; Frank et al. 2000; Leutgeb et al. 2005).

In CA1 neurons, the glucocorticoid receptor is nuclear in the presence of glucocorticoids, and cytoplasmic in the absence of glucocorticoids (Conway-Campbell et al. 2010), presenting a rapid and transient effect of GCs on the GR at the level of these neurons. The expression of the molecular clock activators, CLOCK and BMAL1 in the CA1 region exhibit a significant circadian oscillation across the day and in the presence of a chronic unpredictable stress (CUS) paradigm, providing evidence for the role and importance of the molecular clock in depressive-like behaviour (Jiang & Salton 2013) in the hippocampus proper, and possibly, specifically in the CA1 region. *Per1* expression within CA1 has been shown, with expression susceptible to differing conditions such as restricted feeding, which increasing the expression in the CA1 region (Feillet et al. 2008). The CA1 region, along with CA3 and DG have the highest level of *Per1*, *Per2*, *Clock* and *Bmal1* (Shieh 2003; Segall & Amir 2010; Yamamoto et al. 2001), with these genes being rhythmic (Jilg et al. 2009). Further, the expression profiles of clock genes, *Per1*, *Per2* and *Bmal1* are altered in the CA1 region following chronic mild stress (Christiansen et al. 2016).

1.4.2.2 CA2 region

The CA2 region of the hippocampus is the least studied area of the hippocampus, with little known about its functional properties and behavioural role. The region contains pyramidal neurons and although projections to the EC are sparse from CA2, clear and robust projections occur at CA1 and CA3 regions, with the densest projections observed in the stratum oriens (Hitti & Siegelbaum 2014). Hypothalamic input to CA2, specifically from the PVN offers mixed results, with projections observed (Cui et al. 2013) and not (Hitti &

Siegelbaum 2014) in this area, potentially indicating an inability from a methodological point of view to identify this projection. CA2 projections to the CA1 region are clear and robust, with CA1 stratum oriens and radiatum regions evoking robust monosynaptic postsynaptic potentials (mPSPs) in principal neurons of the region. However, a functional inactivation of the CA2 region does not alter activity or anxiety-like behaviour. Nor does it affect spatial memory as assessed using the Morris water maze (Morris 2008).

Although the CA2 region has been shown to not affect spatial memory, it may play an important role in non-spatial tasks. Synaptic input was identified from the LEC, which delivers non-spatial memory (Hargreaves et al. 2005), as well as sub-cortical input from the median raphe nucleus which produces serotonin to act as an inhibitory relay onto the HPA axis (Hensler 2006) and the hypothalamic supramammillary nucleus (SuM) (Pan & McNaughton 2004). The SuM is instrumental in regulating the frequency in theta activity in the hippocampus, and therefore could influence hippocampal contributions to cognition and emotion (Pan & McNaughton 2002).

Per1$^{(-/-)}$ mice exhibit deficits to hippocampal specific memory formation. The phosphorylation of CREB was severely diminished in the CA2 region of these animals, in particular at a time when CREB phosphorylation is elevated in wild types to promote the transcription of genes required for long-term memory formation (Rawashdeh et al. 2014b).

1.4.2.3 CA3 region

The CA3 region of the HC is located in the lateral portion of the hippocampus proper. Neurons in this region project to neurons of the CA1 region via the Schaeffer collateral pathway (Gruart et al. 2006).

The region is composed primarily of pyramidal neurons, as well as inhibitory interneurons that synapse on pyramidal cells (Ishizuka et al. 1990). The most common inhibitory neuron of the CA3 region is the basket cell, which synapse on the cell bodies of CA3 pyramidal neurons, mediating somatic inhibition. Interneurons also synapse on the dendrites of the pyramidal neurons to inhibit dendritic activation (Buzsáki 2002). The pyramidal neurons receive excitatory input from the dentate granule neurons via the mossy fibre pathway and also through the perforant pathway input from the EC (Marchal & Mulle 2004; Lee &

Kesner 2004). Pyramidal neurons of the CA3 region project out of the ipsilateral HC via the alveus and fimbria of the fornix, which in turn project to the septal nuclei and contralateral HC (Li et al. 1994).

The CA3 region is largely involved in memory processing but is also susceptible to seizures and neurodegeneration (Scharfman et al. 2000). The internal connectivity of the CA3 region is denser than any other hippocampal region, with pyramidal neurons extensively making contacts with neighbouring excitatory and inhibitory neurons (Lei & McBain 2004). It receives input from the EC either directly through the perforant path or indirectly from the DG via mossy fibres (Amaral & Dent 1981), with the mossy fibre pathway translating densely coded cortical signals into specific hippocampal code essential to the formation of memory.

Per1, *Per2* and *Clock* are expressed in the CA3 region, and exhibit clear circadian rhythm in timing with the SCN (O'Callaghan et al. 2012). In *Per1*$^{(-/-)}$ mice, CREB activity is altered in the CA3 region, along with impaired spatial memory (Phan et al. 2011).

1.4.2.4 Dentate gyrus

The dentate gyrus (DG), similarly to the CA regions, is composed of a series of well-defined strata – the molecular layer, the principal cell layer and the polymorphic layer. The DG contains dentate granule cells, of which the dendrites are located predominantly in the molecular layer of the three-layer structure (Kuhn et al. 1996). Fibres originating from the EC project down the perforant path to this layer.

The principal cell layer is composed of densely packed granule cells. The cell body of the dentate pyramidal basket cell is often located within the border of the granule cell layer with the polymorphic layer. The polymorphic layer is composed mainly of mossy cells and interneurons. The axons of dentate granule cells pass through this layer to target the CA3 region of the HC proper (Amaral & Lavenex 2007). The stratum granulosum contains the cell bodies of the dentate granule cells (Schlessinger et al. 1975). The stratum moleculare can be divided into the inner third and outer two thirds. Commissural fibres from the contralateral DG run through the inner third and form synapses (Gottlieb & Cowan 1973). Medial septum input terminates here, on proximal dendrites of the granule cells (Frey et al.

2003). The outer two thirds are located superficial to the HC sulcus and across from the stratum moleculare in the CA fields. Perforant path fibres project through here, making excitatory synapses onto the distal apical dendrites of granule cells (Witter 2007).

The DG expresses the components of the molecular clock, with SCN and DG *Per1* expression in phase, however when corticosterone rhythm is blocked, the rhythm of *Per1* in the DG is suppressed (Gilhooley et al. 2011). The DG relies on an intact circadian CORT rhythm to exhibit effective stimulating anti-depressant drug effects, as blocking CORT rhythms here, prevented the stimulating action of fluoxetine (Pinnock et al. 2009).

1.4.2.5 Subiculum

The subiculum (SUB), which is encapsulated in the hippocampus formation terminology, is located caudal to the hippocampal formation, between the CA1 and subcortical regions including the EC and perirhinal cortex (PrhC). The plasticity of synaptic transmission and the functionality of the hippocampal-subicular axis is not as well understood as the pathways within the hippocampus proper.

The ventral subiculum (vSUB) projects to the PVN inhibiting the activity of the HPA and hypothalamic-spinal-adrenal (HSA) axes, with lesion studies confirming this (Herman & Spencer 1998; Herman et al. 1995)**.** There are multiple reciprocal connections between the SUB and other brain regions, including the hypothalamic nuclei. The ventral premammillary nucleus, the medial septal nuclei, as well as the anteroventral and anteromedial nuclei of the thalamus all project to the SUB (Köhler 1990; Risold & Swanson 1997). The projections from the vSUB target the hypothalamus via the postcommissural fornix, the medial corticohypothalamic tract and the AMY, where these projections innervate the MPOA, the VMH and DMH, as well as the ventral premammillary and medial mammillary nuclei (Canteras & Swanson 1992).

Inhibition of the HPA axis via the SUB is transynaptically mediated through GABAergic neurons that project to the PVN via neurons in the bed nucleus of the stria terminalis, the MPOA and the dorsomedial hypothalamus (Herman et al. 2003). Neurons of the median raphe nucleus project to the vSUB projecting area, indicating the role of SUB projections

to the PVN, which principally act to inhibit the HPA axis, limiting the response to stress (Herman et al. 1995).

Long range projections from the SCN to the SUB have been reported, and GABAergic input along this projection is rhythmic (Kalsbeek et al. 2008). However, little data has examined the role of the clock mechanism within this region. SCN lesions to animals after training showed hippocampal-dependent memory deficits (Phan et al. 2011), providing evidence of the importance of the master clock and its connectivity with the SUB and wider hippocampal structure. *Bmal1* is expressed in the SUB (Kondratova et al. 2010). The circadian input from the SCN to the HC via the SUB may regulate the excitability of the HC.

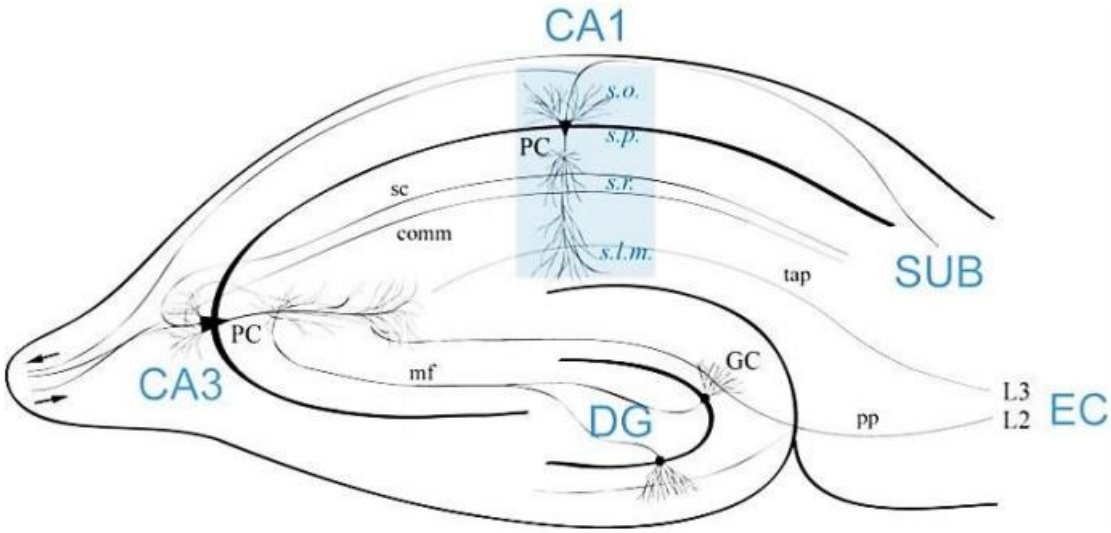

Figure 1.6 The hippocampal interconnectivity between sub regions. Projections from the entorhinal cortex and subiculum synapse predominantly on granule cells in the dentate gyrus (DG) project to the CA3 region, which project further to the CA1 region. Projections from the CA1 region to the entorhinal cortex closes the hippocampal loop. EC – entorhinal cortex, SUB – subiculum, DG – Dentate gyrus, CA3 – Cornu Ammonis 3, CA1 – Cornu Ammonis 1, PP – perforant path, sc – Schaeffer collateral, Blue box – s.o. stratum oriens, s.p. stratum pyramidale, s.r. stratum radiatum, s.l.m. stratum moleculare. (Björefeldt 2015).

1.4.3 Glucocorticoid response

The HC is an area extensively studied, providing a bridge between stress and brain plasticity, and its interconnected brain regions, such as the AMY, prefrontal cortex (PFC), PVN and SCN and as the HC provides negative feedback to the HPA axis, the role of glucocorticoids in hippocampal processes have been extensively studied. The HC acts as the hub in the memory and navigation network, with research assessing what effect differing levels of GCs, and at different points of the activity of the HPA axis, have on memory processing.

In 1985, the glucocorticoid (GR) and mineralocorticoid (MR) receptors were demonstrated in the HC (Reul & Kloet 1985), and following shortly after, the distribution and expression of these receptors were shown to vary depending upon their location. The dorsal subiculum and CA1 regions express both receptors, but with a 7-fold increase in MR expression compared to the GR. The dentate gyrus (DG) and CA3 region express both receptors equally and at a similar level to that of MR in the CA1 region (Reul & de Kloet 1986). The finding of GRs and MRs in the HC led to studies assessing glucocorticoid action on the brain, not only to regulate hypothalamic function, but also to influence neurological, cognitive and emotional functions throughout the brain. GCs facilitate memory processing during highly aversive memory testing paradigms, such as fear conditioning and passive avoidance tasks (Conrad et al. 1999; Conrad et al. 2004) but impair memory during less aversive memory tasks, such as during Y-maze and non-emotional declarative memory (Conrad et al. 1996). Immediate post-training injections of GC agonists in adrenalectomised (ADX) rats impair Y-maze performance , however GC antagonists given similarly also impair performance (Oitzl & de Kloet 1992), proposing that not only are glucocorticoids required for memory consolidation processes, but at a particular dose.

In addition to the hippocampus expressing the GR and MR, it is also driven by the master regulator of the molecular clock to regulate neurogenesis by controlling cellular timing to ~24h (Bouchard-Cannon et al. 2013). *Per1* expression for instance, a major component of the molecular clock, is rhythmically expressed in the HC (Jilg et al. 2009) and can be driven by chemical or electrical seizure-inducing stimulations (Eun et al. 2011) but importantly, also with GC treatment (Conway-Campbell et al. 2010), where robust upregulation in the expression of *Per1* mRNA and protein in the hippocampal formation is evident.

The 24hr cellular clock controls different aspects of hippocampal memory, however it's the consolidation period that seems heavily dependent on hippocampal neurons (Wood et al. 2000). HC memory consolidation requires the phosphorylation of cAMP Response Element Binding (CREB) protein to promote the transcription of genes for long term memory formation (Williams et al. 2008; Morris & Gold 2012). PER1 regulates the phosphorylation of CREB in the HC in a time of day dependent manner, where PER1 and pP90RSK co-translocate into the nucleus as in for example *Per1*$^{(-/-)}$ mice, pP90RSK remains perinuclear and unable to phosphorylate nuclear CREB, indicating that the presence of PER1 in a time of day dependent manner drives the phosphorylation of CREB, offering a functional link between circadian rhythms, GC exposure and learning efficiency (Rawashdeh et al. 2016).

1.4.4 Involvement in memory and sleep

The hippocampus determines memory acquisition, consolidation and retrieval with hippocampal specific cellular and molecular dynamics driven by: the time of day, activation through the HPA axis and stress, and reliance on the output of the SCN (Ruby et al. 2008; Phan et al. 2011).

During sleep, memories are vulnerable to manipulation, as a period of sleep is beneficial during the consolidation of memory stage (Stickgold et al. 2000; Graves et al. 2003). The critical signalling period, between 0.5h and 3h, occurs within the first few hours of post-learning. Sleep loss or alterations to the sleep period during this time overlap with critical molecular signalling that promotes the gene transcription of proteins that consolidate labile memories into long-term memories, such as the activation of CREB (Ahmed & Frey 2005). Disruption to CREB activation during this early phase following behavioural testing can impair the consolidation of memories (Graves et al. 2003; Palchykova et al. 2006).

Multiple systems contribute to the control of sleep, however as the molecular clock is instrumental in driving the circadian activity of tissues to day and night oscillations, it has been a target of research. PER1, along with PER2 have been shown to regulate the response of metabolism-associated transcripts that contribute to sleep disruption (Husse et al. 2012).

During sleep, both the nadir and major portion of GC secretion occur. In the earliest stages of sleep, GC levels are low, whereas as the night progresses, the first large pulse of GC occurs, in preparation for awakening. During the early hours of the sleep period, the majority of slow wave sleep (SWS) occurs, whereas in the second half of sleep, SWS is rare but rapid eye movement (REM) sleep predominates (Weitzman 1976), indicating an important interaction between the different sleep states and architecture with the activity of the HPA axis.

It is well established that sleep quality deteriorates with aging, as decreased SWS and slow wave activity (SWA) are observed in the aged population (Garfinkel et al. 1995; Landolt et al. 1996). However, the relationship with CORT secretion needs to be assessed further as HPA axis activity affects sleep. An infusion of CRH during the sleep period decreases SWS, but increases the REM period (Ehlers et al. 1986; Marrosu et al. 1990). As CRH impairs sleep, but CORT promotes SWS, this is most likely due to its inhibitory effect on the HPA axis.

1.5. Endogenous and Synthetic glucocorticoids

1.5.1 Endogenous glucocorticoids

Endogenous glucocorticoids are secreted from the adrenal cortex as an end product of the activation of the HPA axis. The axis consists of the paraventricular nucleus (PVN) of the hypothalamus, the anterior pituitary and the adrenal gland. The PVN is activated in the presence of circadian cues from the SCN, but also in the presence of a stressor. Activation leads to the secretion of CRH and AVP which in turn activates the secretion of ACTH from the anterior pituitary. ACTH drives the secretion of CORT from the adrenal gland.

In the absence of a stressor, this system is driven by circadian cues, with 24hr profiling of endogenous glucocorticoids in blood exhibiting a clear daily rhythm. An ultradian rhythm is also described, explained by the feedback of CORT onto the anterior pituitary and PVN, preventing the release of ACTH and CRH, respectively. Peak CORT secretion occurs just prior to wakening, in preparation for the onset of activity, with the levels decreasing throughout the day, in preparation for rest during the inactive period.

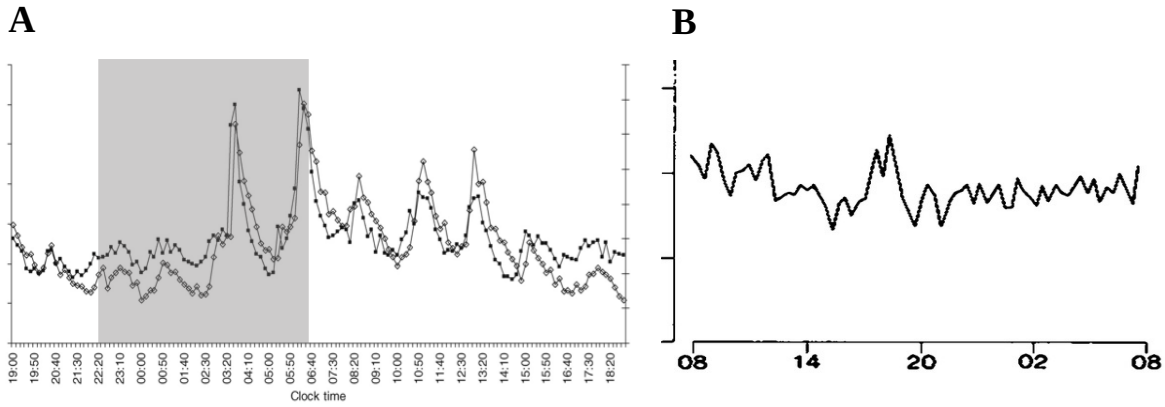

Figure 1.7 The HPA axis in Cushing's disease. A measure of cortisol over a 24h period in a healthy individual (**A**) and from a patient diagnosed with Cushing's disease (**B**). (Henley et al. 2009; Van Cauter & Refetoff 1985)

Cushing's disease can be characterised by excess levels of cortisol secretion, caused by a cortisol secreting adenoma in the cortex of the adrenal gland (~30%) or as a small benign tumour in the pituitary (70%). In these examples, the adrenal adenoma secretes cortisol at a high level irrespective of time of day, and negative feedback onto the pituitary from this high cortisol level, causes ACTH levels to remain low. However, a tumour of the pituitary produces excess levels of ACTH, in turn causing the adrenal gland to secrete prolonged, high levels of cortisol. Cushing's symptoms are varied, but can include, excessive or sudden weight gain, a decrease in muscle mass and bone density, as well as cognitive dysfunction, sleep impairment and depression (Nieman et al. 2008).

Although Cushing's can be characterised as an adrenal or pituitary tumour that allows for the continuous secretion of cortisol, the most common cause of Cushing's syndrome is glucocorticoid treatment. Steroids prescribed for a prolonged period of time, such as for asthma, arthritis or colitis, can induce similar effects to what is observed in patients with Cushing's disease. The incidence of Cushing's is 1 in 200,000, however the frequency is believed to be higher as the symptoms are so wide ranging, the diagnosis may not be considered (Newell-Price et al. 2006).

1.5.2 Synthetic glucocorticoids

Since the discovery of cortisone and cortisol in 1935 and the subsequent successful use of cortisone as a treatment of rheumatoid arthritis, glucocorticoids have been recognised to be beneficial in the treatment of many disorders (Barrow et al. 1951).

Synthetic glucocorticoids are a commonly prescribed class of drugs that are used to treat a variety of conditions. They are administered as replacement therapy in patients with primary and secondary adrenal insufficiency, as well as for adrenal suppression therapy in congenital adrenal hyperplasia and glucocorticoid resistance. They are also used for a range of non-endocrine disorders, such as treating skin conditions like dermatitis and rheumatological diseases like systemic lupus erythematosus due to their immunosuppressive and anti-inflammatory properties. In the UK, nearly 2% of the adult population use oral GCs at any given time (Overman et al. 2013; van Staa et al. 2000). Dosing, route of delivery and timeline of treatment range significantly and depend on the severity, and responsiveness of the condition being treated.

Methylprednisolone is Prednisolone with a methyl group attached at position 6 rendering it water soluble and can therefore be given intravenously and at very high doses over a short period of time. It was first given approval for medical use in 1955. It is primarily prescribed as an immunosuppressant, with clinical use ranging from alleviating skin inflammation, to organ transplantation and spinal cord injury inflammatory suppression (Tambe et al. 2010; Hurlbert 2000). In rat, the plasma corticosterone half-life is 15min (Sainio et al. 1988). In humans, plasma cortisol half-life is 66min (Weitzman et al. 1971) whereas the plasma methylprednisolone half-life ranged from 2.2 - 4.14h (Uhl et al. 2002; Sprague 1966; Al-Habet & Rogers 1989).

Table 1.3 Steroid dosage and disease state.

Dose	**mg per day**	**Condition**
Low	<10	Rheumatoid arthritis (Conn 2001)
Medium	10-20	Ulcerative colitis, Crohn's (Sandborn et al. 2012)
High	>20	Giant cell arteritis (Hayreh & Zimmerman 2003)

1.5.2.1 Side effects of synthetic glucocorticoid use

As with most prescribed treatments, glucocorticoids do not come without side effects. Side effects of glucocorticoid treatment vary greatly, depending on the method of application, dose and period of treatment required. Low dose steroids, commonly found in asthma inhalers have few side effects, with the most common being hoarseness of the throat (Lévy et al. 2003). Whereas mid to high dose steroid use can result in more serious side effects, however these are more often prescribed in acute serious illness, rather than as long-term care (Bone et al. 1987; Short et al. 2000; Zorzon et al. 2005). However, following high dose glucocorticoid treatment, a patient study found evidence of mania and depression, as well as changes to cognitive function, assessed using verbal and declarative working memory tasks (Brown & Chandler 2001).

1.6. Corticosteroid receptor signalling and action

The steroid hormone receptors are an evolutionary conserved subset of the nuclear receptor superfamily. Nuclear receptors are a group of proteins with sequence and structure similarity, with all possessing three major functional domains: the C-terminal ligand binding domain, a DNA binding domain and the N-terminal domain. Nuclear receptors are diverse in their functional output, controlling homeostasis, metabolism and development. These receptors are ligand activated transcription factors, and following activation by hormone binding, the receptors bind to regulatory DNA regions of target genes to initiate transcriptional activation or repression.

1.6.1 Steroid receptor structure

Steroid receptors have three important, functional regions: The N-terminal domain (NTD), which contains the activation function domain 1 (AF1), and acts in a ligand-independent manner. A central DNA binding domain (DBD) and a C-terminal ligand-binding domain (LBD), containing the ligand-dependent activation function 2 (AF2) site, which is tightly regulated by hormone binding. The LBD is connected to the NTD by a hinge region, enabling the receptors to act as ligand-activated transcription factors, binding to specific DNA sequences and recruiting other factors via the AF sites to evoke a high level of

transcriptional regulation (Carson-Jurica et al. 1990; Kumar & Thompson 1999; Kumar & Thompson 2005; Khan et al. 2011).

The type 1 and type 2 corticosteroid receptors (GR and MR) were both cloned by 1987 (Giguere et al. 1986; Arriza et al. 1987) and were found to be very similar in structure and function, which has led to research into MR versus GR specificity, in particular in tissues such as the hippocampus, where they are co-expressed.

The LBD consists of 12 helices that fold into a globular structure, each consisting of three sets of helices forming the sides and top of the globule, creating a central hydrophobic pocket where the ligand can bind. For the glucocorticoid receptor (GR), this structure is held in an open configuration by the association of chaperone proteins such as heat shock proteins (HSPs).

The DBD contains two zinc finger motifs which are responsible for recognition and binding to target regions of DNA known as glucocorticoid response elements (GREs). With GR, the first zinc finger comprises a P-box with a glycine, serine and valine that interact with specificity to the GRE. The second zinc finger is required for receptor dimerization, which for GR is vital for transactivation of target genes. *In vitro* studies have showed that GR binds as an inverted dimer to two 6bp palindromic sequences, separated by a 3bp spacer. These two zinc fingers can therefore work together to promote GR binding with the first zinc finger binding to the first half of the palindromic sequence, and the second zinc finger enabling the binding of another GR to the other half of the palindromic sequence. Binding of a homodimer to the GRE of specific genes can promote transactivation.

The NTD is highly variable depending on the receptor but contains the ligand-independent activation function 1 site. AF1 in this region has been shown to communicate with coactivators, chromatin modulators as well as basal transcription factors including RNA polymerase II and TATA binding protein to initiate transcription. In the GR, the AF1 site remains relatively unfolded in the basal state, whilst it forms a significantly complex helical structure in response to binding to cofactors, including TBP and p160 coactivators (Khan et al. 2011).

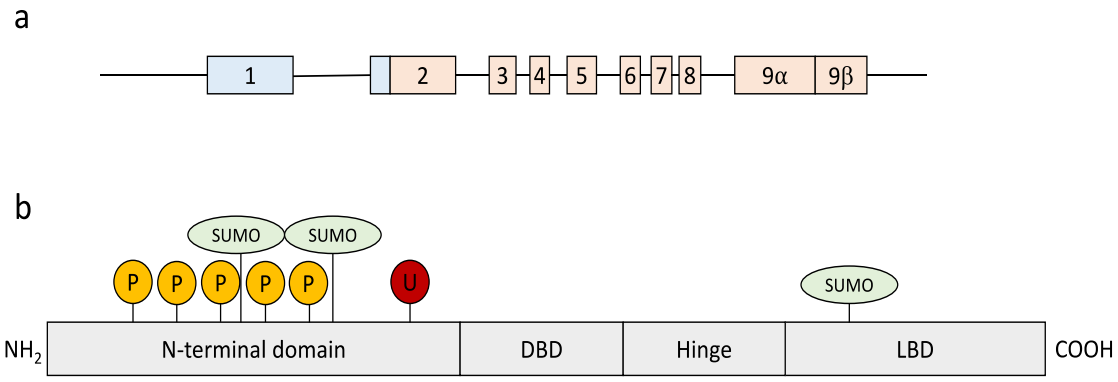

Figure 1.8 Structure of the glucocorticoid receptor. (**a**) Gene encoding the glucocorticoid receptor. The receptor is encoded by 9 exons, with the encoding region indicated by peach coloured boxes. Alternative splicing of exon 9 produces the a and b isoforms. (**b**) The structure of the receptor. The NTD contains the major transactivation function domain AF-1. The DBD consists of two a-helices, coordinating two zinc atoms and is important for dimerization, nuclear translocation and binding to glucocorticoid response elements. The LBD and DBD are joined by a hinge region. The LBD undergoes a conformational change when it binds ligand, enabling the interaction with other coregulator proteins. Heat-shock proteins bind in this region and it also contains the activation function domain AF-2. The receptor is subject to post-translational modification, impacting on its function. Abbreviations: P, sites of phosphorylation on serine and threonine residues; U, site of ubiquitination; SUMO, sites of SUMOylation (post-translational modification mediated by small, ubiquitin-related modifier proteins). Adapted from Rekers et al. 2016.

1.6.2 Steroid receptor binding

Endogenous mammalian GC actions are mediated via two corticosteroid receptors. The high affinity mineralocorticoid receptor (MR), originally termed the Type 1 corticosteroid receptor but now termed NR3C2 and the low affinity glucocorticoid receptor (GR), originally termed the Type 2 corticosteroid receptor but now termed NR3C1.

1.6.2.1 Binding affinities for CORT, MPL and DEX

Glucocorticoids are secreted from the adrenal gland in a circadian pattern which is driven by ultradian pulses of increasing amplitude in anticipation of the active period. The endogenous Corticosterone, or cortisol in human, binds to the MR in a 10-fold greater affinity than that of the GR (Reul & Kloet 1985). During low levels of glucocorticoid secretion from the adrenal i.e. during the inactive phase, the MR remains occupied, but the GR is not. It is only during higher levels of circulating glucocorticoid that the GR becomes occupied, i.e. during the active phase, or during a stress response (Mifsud & Reul 2016). The ultradian rhythm of 1hr pulses of CORT release are also important to note. During the active phase, CORT will bind to the GR for ~20 minutes, before dissociating from the GR following GR:DNA binding (Conway-Campbell et al. 2012). This dissociation occurs as circulating CORT decreases in these individual pulses. Previously, the MR was believed to remain at near maximal ligand occupancy during the circadian peak and nadir (Reul & Kloet 1985; Reul & de Kloet 1986), however more recent evidence suggests that the MR, similarly to GR, is bound in a circadian pattern, at least on the *Fkbp5, Per1 and Sgk1* gene, and that in the presence of an acute stressor, the binding of MR on *Fkbp5* is further increased (Mifsud & Reul 2016).

Methylprednisolone binds to the GR and MR with similar affinity to that of endogenous glucocorticoids. However, the binding period is significantly different, with methylprednisolone binding to the GR for ~6h. Dexamethasone, another glucocorticoid steroid significantly more potent than methylprednisolone binds to the GR for ~12h (E Earl et al. 2018).

1.6.3 Expression of GR and MR

GR is widely expressed throughout most cells and tissue types in the body. In the brain, GR has been found to be highly abundant in the hippocampus (HC) and medial prefrontal cortex (mPFC), as well as being expressed within the AMY, areas that are associated with memory and learning processes (Reul & de Kloet 1986). The pyramidal cells of the CA1 and CA2 regions of the HC have been shown to express GR highly, as well as the granular cells of the DG (Van Eekelen et al. 1988). High levels of GR have also been shown in the

cerebellar cortex, olfactory cortex, thalamus, hypothalamus, dorsal nucleus raphe and locus coeruleus (Ahima & Harlan 1990; Reul & Kloet 1985).

MR is generally reported to exhibit a more restricted expression profile throughout the body, with notably high levels of expression in the kidney and adipose tissue (Edwards et al. 1988). In the brain MR expression has been reported in the PFC, the MeA and CeA, lateral septum, thalamic nuclei and hypothalamic nuclei (Diorio et al. 1993; Mitra et al. 2009; Han et al. 2005). However, the highest expression of MR has been reported in the CA1, CA2, CA3 and the DG of the hippocampus (Reul & de Kloet 1986). However, a recent study in the *Parus major* has shown that MR is prevalent across many areas of the brain including the locus coeruleus and the oculomotor nerve (Senft et al. 2016), therefore it may still remain to be seen how widespread MR expression is in humans and experimental rodents.

In previous studies, the GR and MR were undetectable within the SCN, leading researchers to believe that glucocorticoid steroids do not bind and regulate within this highly significant brain area. However, these receptors are expressed in high abundance in the HC to detect circulating GCs and modulate the negative feedback inhibition of the HPA axis through stress and circadian variations of GCs (Buchanan et al. 2004). Blocking or deleting the GR in the HC diminished the inhibitory influence on the HPA axis, increased CORT levels and caused GC resistance to negative feedback inhibition of the axis (Boyle et al. 2005).

1.7. Research statement

Circadian rhythms and the genes that comprise the molecular clock are important for driving the daily changes to the environment that one is presented with. The molecular clock has been studied extensively, with affected change observed in psychiatric and mood-related disorders, an increased risk in cardiovascular and diabetes diseases, as well as affective state changes to sleep and memory loss. However, the underlying mechanisms driving these changes remains unknown.

Glucocorticoids, which are produced endogenously and driven by circadian cues target almost every area of the body, influencing a variety of physiological processes such as glucose metabolism, immune and inflammatory responses, and mental functions, such as

promoting memory processing. They maintain homeostatic mechanisms and are the major factor secreted in response to stress. However, glucocorticoids are the most important and most frequently prescribed class of anti-inflammatory drugs to this day, with almost 2% of the UK population being prescribed oral glucocorticoids at any given time, with little evidence to show what effects taking glucocorticoids has on the brain, when taken throughout the day. Unlike endogenous glucocorticoids which are rapidly metabolised *in vivo* to produce short lived pulses and associated GR activation, synthetic glucocorticoids, and in particular, Methylprednisolone, has a prolonged half-life (biological – 18-36h) in the circulation that activates the GR and MR for much longer than its endogenous counterpart. Methylprednisolone was synthetised from the endogenous glucocorticoid, Cortisol, and therefore binds to both the GR and MR with similar affinity.

Patients who are prescribed synthetic glucocorticoids often complain of poor sleep, and evidence-based studies indicate an effect of memory impairment in patients prescribed glucocorticoids, however the mechanism causing this remains unknown.

Glucocorticoids have been shown to promote the transcription of Period 1, a major component of the molecular clock, in the liver and hippocampus, with alterations to this gene causing memory deficits and sleep disturbances in the latter.

1.8. Hypothesis and aims

Therefore, using Methylprednisolone to blunt the endogenous secretion of glucocorticoid whilst maintaining high circulating levels of synthetic glucocorticoid, I hypothesise that prolonged activation of the glucocorticoid receptor in peripheral tissues to the master clock in the SCN, such as the hippocampus, would lead to dysregulation of the molecular clock, uncoupling the timing of the peripheral clock from the central clock, affecting sleep and memory processing.

Chapter 3: Compare the expression of core clock genes in the SCN in response to MPL treatment to confirm a lack of effect of this synthetic glucocorticoid on the master clock

Chapter 4: Assess the expression of core clock genes and glucocorticoid regulated genes in the hippocampus using RNAseq in response to treatment with MPL

Chapter 5: Measure locomotor activity and core body temperature in animals following MPL treatment

Chapter 6: Measure brain activity, in particular during sleep, following a hippocampal specific memory task in the presence of MPL treatment

Chapter 2

Materials and Methods

2.1. Animals and treatments

Adult male Lister hooded rats (250-350g, 9-11 weeks) (Envigo, UK) were used in all experimental procedures. Animals were maintained in standard housing conditions under a 12:12 light/dark cycle. Food and water were available *ad libitum.* All procedures were carried out in accordance with the UK Animals (Scientific Procedures) Act 1986 under PPL 30/3114 and PIL I04092F5F.

2.1.1 Surgery under general anaesthesia

Animals used in the described experiments were subjected to a combination of procedures detailed below. Individual chapter methods sections provide exact details of the combination of surgeries and treatments applied for each experiment. Rats were anaesthetised using a combination of gaseous isoflurane (Merial, UK) and medical grade air. During all surgical procedures and recovery, body temperature was maintained using heat pads. Aseptic technique, sterilized drapes and autoclaved surgical tools were used throughout.

2.1.2 Telemetry probe implantation

Anaesthetised rats were placed on their front. A section of the mid-back was shaved and disinfected with Hibitane. A midline incision was made along the midline rostro-caudally to expose subcutaneous tissue and muscle sitting over the rib cage. Following identification of landmarks along the spine, an incision was made through the muscle wall and into the peritoneal cavity near to the liver. Blunt scissors stretched the incision site to allow for the implantation of the telemeter (PTD 4000 E-mitter, Starr Life Sciences Corp). The sterilised telemeter was inserted into the abdominal space and sutured to the muscle wall closing in the process. The midline skin incision was closed using individual suture knots. The wound was cleaned and treated with wound powder to aid healing.

2.1.3 Antagonist implantation

Following telemetry probe implantation, the rats received subcutaneous implantation of a slow-release pellet (Innovative Research of America, US) between the shoulder blades. At

the start of surgery, a section of the nape of the neck was shaved and disinfected with Hibitane. An incision along the midline of the back was made followed by blunt dissection to make a pocket for pellet placement. The slow-release pellet was placed under the skin far enough away from the incision site to cause adverse effects. When implanting the GR (Mifepristone (RU-486), cat no. X-999) and MR (Spironolactone, cat no. M-161) antagonists together, they were placed on opposing sides of the midline to prevent cross reaction. The wound was sutured using conventional techniques and wound powder was applied to aid healing.

2.1.4 Local field potential drive implantation

Rats were implanted with multi-site electrode arrays (EIB-36, Neurolynx, US) targeting the Prelimbic (PrL) area of the prefrontal cortex and the dorsal CA1 area of the hippocampus. A minimum of 1 week was allowed for recovery, during which the animals were handled daily and habituated to the behavioural arena and recording environment 5 days prior to experiment start.

2.1.5 Post-operative care

Immediate post-operative pain relief was administered with 1mg subcutaneous Carprofen (Rimadyl, Pfizer, UK). Fluids were replaced by subcutaneous injection of 2.5ml of glucose saline (0.9% NaCl, 5% Glucose) (Braun, Germany). Following surgical recovery defined by reacquisition of the righting reflex, animals were transferred to clean housing ready for experimental procedures.

2.1.6 Administration of drug

Methylprednisolone (MPL) (Solu-Medrone, Pfizer, UK) solution was provided in drinking water *ad libitum.* Treatment lasted five days. MPL was made up in accordance with the supplier directions, then diluted with tap water to give a final concentration of 1mg/ml. To preserve stability of MPL, bottles were protected from light and drinking solution was replaced every two days. MPL was provided in drinking water to limit possible stress effects of administration via other routes such as oral gavage, and subcutaneous and intraperitoneal injections. As the biological half-life of MPL is 18-36h, multiple injections

would be required to retain elevated circulating glucocorticoid levels. Providing treatment ad libitum in drinking water was able to bypass such parameters. Rats were individually housed and drinking water was monitored daily to confirm drug administration. Body weight was also measured daily as a known measure of steroid therapy (Azcue et al. 1997).

2.1.7 Death and Dissection

For all experimental settings animals were anaesthetised using a combination of gaseous isoflurane and medical grade air and then decapitated. Brains were either rapidly dissected on ice for hippocampal isolation or whole brains frozen on dry ice for dissection on a cryostat. Hippocampal tissue was rapidly dissected and frozen in liquid Nitrogen. Blood was collected from the trunk into tubes containing Ethylenediaminetetraacetic acid (EDTA) and plasma was obtained following centrifugation at 4000rpm for 10 minutes at 4°C and stored at -20°C until corticosterone was measured by radioimmunoassay.

2.2. RNA extraction

2.2.1 Sample preparation

Whole brains were rapidly removed from the skull following decapitation. Hippocampal tissue was dissected immediately on ice and flash frozen in liquid nitrogen in preparation for RNA extraction. SCN tissue was sliced using a cryostat on whole brains that were frozen rapidly on dry ice.

2.2.2 RNA quality assessment

All extracted RNA samples were first assessed for RNA quality and quantity using a Nanodrop (ThermoScientific, US). Samples sent for RNA sequencing were further assessed for RNA integrity on the 2200 Tapestation system (Agilent, US).

2.2.3 RNA extraction protocol

2.2.3.1 Suprachiasmatic nucleus

Frozen whole brains were given time to increase in temperature to be able to slice accurately within the cryostat. Object and chamber temperature were both set at -10°C for slices 200µm thick to prevent tissue cracking. SCN coordinates were identified from The Rat Brain in Stereotaxic Coordinates (Paxinos & Watson 2007). Brains were sliced rostro-caudally and the start of the SCN was identified at Bregma -0.92mm. Serial slices 200µm thick were taken and ceased at bregma -1.72, within the retrochiasmatic area. A single 1mm punch (Sample corer, 18035-01, Fine Science Tools, Germany) was taken from each of the four slices in the location of the SCN and stored in a 1.5mL eppendorf tube, kept on dry ice until transferred the RNA extraction protocol. 400µL of TRIzol (ThermoFisher Scientific, US) was added to each tube and vortexed at high speed for 2x10 seconds, with a rest period in between. Direct-zol total RNA extraction kit (Zymo Research, US) was used, following the manufacturer's protocol, including the DNase digestion step. Samples were stored at -80°C.

2.2.3.2 Hippocampus

Frozen whole hippocampal tissue was placed into individual tubes stored in dry ice. 1mL of TRIzol (ThermoFisher Scientific, US) was added to each tube and each sample was immediately homogenised using a mechanical homogeniser (Polytron PT-2100, Kinematica, Switzerland). Following complete homogenisation of sample, 300µL of chloroform (Sigma-Aldrich, UK) was added to each sample and mixed by inversion. Samples were spun for 15 minutes at 4°C, >10,000rpm for phase separation. The aqueous phase was removed by pipette, avoiding the organic phase below and placed into a fresh 1.5mL tube. Total RNA was extracted using the miRNeasy total RNA extraction kit protocol (Qiagen, US) following the manufacturer's guide and included a DNase digestion step. Samples were stored at -80°C.

2.2.4 cDNA synthesis

RNA samples were measured for purity and quantity on a Nanodrop 2000C (ThermoFisher Scientific, US) and a total of 1μg of RNA was used to synthesise cDNA using iScript cDNA synthesis kit (BioRad, US), as per the manufacturer's protocol.

2.3. RNA sequencing

2.3.1 Sample preparation

RNA sequencing of hippocampal tissue was carried out using TruSeq Stranded Total RNA kit and protocols (Illumina, US). A 1ug aliquot of total RNA from each hippocampus was prepared for RNA sequencing. 48 samples total. First, bioanalyzer traces were carried out on all samples for RNA quantity and quality check. RIN scores above 8.0 were deemed high enough quality to take through to RNA sequencing. Below is a workflow of the library preparation (Figure 2.1).

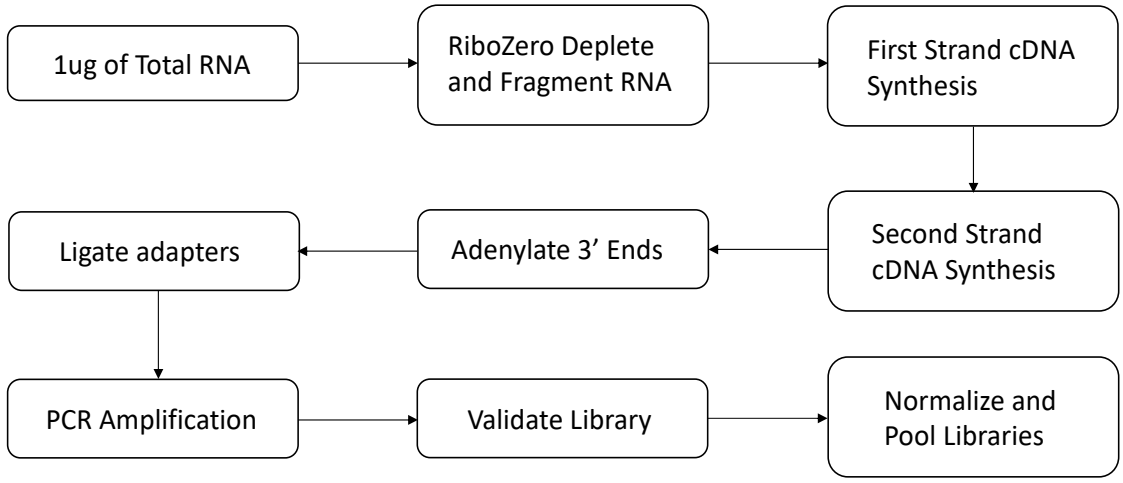

Figure 2.1 Workflow of TruSeq sample preparation protocol. Adapted from Illumina TruSeq Stranded Total RNA Sample Preparation Guide.

2.3.2 RNA sequencing protocol

Following library preparation, the samples were run on a HiSeq 2500 machine (Illumina, US). 8 samples were run in each lane, in a paired end sequencing run, generating

approximately 300 million reads across the 8 samples. This equated to ~37.5million reads per sample.

2.4. Quantitative Polymerase Chain Reaction

Quantitative Polymerase Chain Reaction was used to assess mRNA transcript levels across time points and treatments using ThermoFisher Scientific reagents.

2.4.1 Sample preparation and primer design

Primers for RNA analysis were designed NCBI BLAST Primer design tool (https://blast.ncbi.nlm.nih.gov/Blast.cgi) or taken from the literature for all Sybr Green assays. Primer length was designed to be between 60-150bp in length. Nuclease free water was added to each lyophilised primer to give a stock concentration of 100μM. 20μL of stock primer was added to 980μL of nuclease free water, creating a working primer concentration of 2μM. A standard curve for each primer was produced to assess primer efficiency and to validate the absence of primer dimers. Serial dilutions of cDNA for RNA analysis were prepared to provide a range of cycle threshold (Ct) values that were anticipated would cover the range of values expected to be produced by samples. Taqman primers were designed by Life Technologies (ThermoFisher Scientific, US).

Table 2.1 mRNA primer sequences used for Sybr Green qPCR

Gene	Forward Primer	Reverse Primer
Per 1	CCTCGATGTAACGGCTTGTGT	GTCCGAGTGGCCAGGATCT
Per 2	CGAAGCGCCTCATTCCAGAG	TGCTCATGTCCACGTCTTCC
Cry 1	AGAGGACGCACAGAGTGTTG	CCTCCCGCATGCTTTCGTAT
Cry 2	CTGCGTCTACATCCTCGACC	GCAGTAGGAACCTCCATCGG
Bmal1	TGCCACTGACTACCAAGAAAGT	GGGCCTCCCTTGCATTTTTG
Clock	CACAAGGCATGTCACAGTTTCA	TCTATCATGCGTGTCCGCTG
Npas2	CCGCCTCTCCTTACTGCTTA	AGAGGCTCTCTTTGCTCTATCC
Rev-erbα	CCCTGGCATGACCAAGAGTC	TGAAGAAGCCCTTACAGCCT
Rorα	GGGATCAAACCCGAACCCAT	GCAAGGTGTTCTAGTTCCGC
Actβ	CGCGAGTACAACCTTCTTGC	CGTCATCCATGGCGAACTGG

Table 2.2 mRNA primer accession codes for Taqman qPCR

Gene	Accession code
Period 1	Rn01325256_m1
Period 2	Rn01427704_m1
Bmal1	Rn00577590_m1
Actβ	Rn00667869_m1

Table 2.3 Reaction quantities for Sybr Green qPCR

Reaction component	**Volume per well (µL)**
Fast Sybr®Green Master mix	5
Forward Primer	1.5
Reverse Primer	1.5
Nuclease-free water	1
cDNA sample	1
Total Reaction volume	10

Table 2.4 Reaction quantities for Taqman qPCR

Reaction component	**Volume per well (µL)**
Taqman Mastermix (2x)	5
Taqman Assay (20x)	0.5
Nuclease-free water	3.5
cDNA sample	1
Total Reaction volume	10

2.4.2 qPCR reaction

qPCR determined the approximate levels of mRNA transcripts in RNA samples. Experiments were performed using 96-well plates (Applied Biosystems, Life Technologies, UK) with a 10µL final reaction per well (Tables 2.3 and 2.4). Each PCR reaction contained 1µL of cDNA. Samples were pipetted in duplicate and a no template control (NTC) was added to each plate to assess for contamination. MicroAmp Optical Adhesive film (Applied Biosystems, Life Technologies, UK) was used to seal plates. Plates

were spun to ensure samples were at the bottom of each well prior to amplification. A StepOnePlus PCR machine (Applied Biosystems, Life Technologies, UK) was used. The Taqman and Sybr®Green qPCR runs consisted of an initial 95°C holding stage for 20 seconds, followed by 40 cycles of 95°C (1 second) and 60°C (20 second). However, the Sybr®Green run also contained a melt curve step, consisting of 40 cycles of 95°C (15 seconds) and 60°C (1 minute), with a final denaturing step of 95°C (15 seconds).

2.5. Radioimmunoassay for Corticosterone

Using an automated gamma counter (PerkinElmer, US), a CORT radioimmunoassay was carried out to assess CORT levels in blood samples collected from trunk blood.

An 11-point standard curve of known CORT concentrations was prepared in B-buffer (25mM tri-sodium citrate, 50mM sodium dihydrogen orthophosphate, 1mg/mL bovine serum albumin: pH3). Plasma obtained either from the automated blood sampler or trunk blood was diluted in triplicate at a ratio of either 1:10 or 1:50 in B-buffer, respectively. A specific CORT antibody (kindly provided by G. Makara, Institute of Experimental Medicine, Budapest, Hungary) was diluted at a ratio of 1:50 in B-buffer and 50µl added to 100uL standards, unknown samples, and Quality Control (QC20 and QC100) tubes. Tracer (Izotop, Institute of Isotopes, Hungary) was diluted in B-buffer to give total counts of 3750cpm in 50µl and added to all tubes (50µl/tube). Tubes were incubated overnight at 4°C.

Charcoal suspension (5g charcoal added to 0.5g Dextran T70 dissolved in 1L B-buffer) was prepared and 500µl added to all tubes and briefly vortexed. Blocks were centrifuged at 4000rpm at 4°C and the resulting supernatant aspirated off. Unknown samples were determined from interpolation of the standard curve

2.6. Behavioural Testing

2.6.1 Telemetry recording

Animals were individually housed for telemetry recordings due to technical reasons. Cages were placed upon signal receivers (ER-4000 receiver, Starr Life Sciences Corp, US) which were connected to a computer that recorded data collection using the VitalView software package (Starr Life Sciences Corp, US), from 24 hours post-surgery, into 10-minute epochs. Four of eight animals were implanted with telemeters. All received either vehicle or MPL in drinking water, or MPL with either GR (X-999, Innovative Research of America, US) or MR (M-161, Innovative Research of America, US) antagonism, or a combination of both. MPL treatment started 1 day following surgery. Locomotor activity and body temperature recording continued for 5 days.

2.6.2 Novel Object Location task

The novel object location task, a hippocampal specific memory task, was used in conjunction with the electrophysiology experiments.

2.6.2.1 Apparatus

Exploration occurred in an open-top arena (50 x 90 x 100cm) made of wood. The walls inside the arena were black in colour and floor covered in sawdust. An overhead camera and video recorder were used to monitor behaviour for analysis at a later date. The objects presented as stimuli were constructed from Duplo blocks and varied in shape, size and colour, which were too heavy for the animals to displace.

2.6.2.2. Pre-training

After acclimatising to the facility and being handled for a week prior to experimental start, the animals were habituated to the arena without stimuli for 10 minutes daily for 5 days before the start of behavioural testing.

2.6.2.3 Novel Object Location task

The task comprised of an acquisition and test phase separated by a 6h delay. During the acquisition phase, each rat was placed into the arena at the same position facing the wall. The arena contained identical objects in the far side corners of the arena, 10cm away from the walls to allow full access around the object. The rats were allowed to investigate the objects for 4 minutes and then returned to the sleep box until the test phase. In between each animal, the objects were cleaned with ethanol and the sawdust reset. The test phase lasted 3 minutes and consisted of one of the objects being moved to the opposite corner with the other object remaining in its original position. The position of the object was counter balanced between rats. Throughout the task, the rat was tethered for electrophysiology recordings.

2.6.3 Electrophysiology recordings

Electrical signal was acquired using a Digital Lynx 4 SX system (Neuralynx, USA) and recording using the PC software Cheetah (Neuralynx, USA). All behavioural and sleep recordings were carried out during the active period of the rat. The rats were placed in a sound-attenuating chamber for a 2h recording, followed by a 4min object location sample phase experiment in a behavioural arena. The rats were placed back into the sound-attenuating chamber for a further 6h recording. Following the 6h delay period, the rats were replaced into the behavioural arena with one of the objects moved to a novel location. In order to measure the rats movement, a video recording was captured above the sound-attenuating chamber and above the behavioural arena. These movement data were used alongside the electrophysiology data to manually score arousal state in 10sec epochs. Epochs was scored as wake if movement was high. Non-rapid eye movement (NREM) was scored if there was low movement and ripples and slow-waves on the local field potential (LFP) drive. After the final experiment, animals were deeply anaesthetised with sodium pentobarbital (60mg/kg). A positive current of 30μM was passed through each channel in order to create a lesion at the tip of the electrode before the rat was perfused transcardially with 0.9% saline (Braun, Germany) followed by 4% paraformaldehyde (Sigma-Aldrich, UK). Brains were dissected and stored for 48h in paraformaldehyde before being transferred to 30% sucrose. 50μm coronal sections were cut using a freezing microtome

and Nissl-stained with thionin. Lesions were identified as a darkened ring of damaged tissue and checked for correct location using the rat brain atlas (Paxinos & Watson 2007). n = 5 per group.

2.7. Statistical Analyses

GraphPad Prism version 7 (GraphPad software Inc., US) was used to analyse data by One-way or Two-way ANOVA with suitable post-hoc test. T-tests were also carried out in Prism. For each result, the statistical test used is stated. The mean and standard error of the mean (SEM) were also calculated.

2.7.1 Whole genome RNA sequencing

High-throughput RNA sequencing raw data were uploaded to Galaxy, an open access portal for next-generation sequencing analysis (www.galaxyproject.org). For each condition, a N of 4 was used in each group, and three lanes of data were collected for each sample. A workflow was run to generate a BAM file (Sequence aligned data file) (Figure 2.2). The BAM files from each of the three lanes were merged. The merged BAM files were then analysed for gene expression differences using CuffDiff analysis. The CuffDiff parameters included geometric library organisation, pooled dispersion estimation and the false discovery rate was set at 0.05. Minimum alignment count – 10, multi-read correct, bias correction and CuffLinks effective length correction. Differential gene expression was calculated from fragments per kilobase per million mapped reads (FKPM) values. Differential expression was assessed between all time points and across both treatment groups using CuffDiff, a statistical package widely used which encompasses a test statistical model of $T = E[\log(y)]/\mathrm{Var}[\log(y)]$, where y is the ratio of the normalized counts between two conditions, and this ratio approximately follows a normal distribution, which is why a t-test is used to calculate the P-value. Multiple hypothesis correction was carried out using the Benjamini-Hochberg test, which lowers the false discovery rate using the formula (i/m)Q, where i = individual P value, m = total number of tests and Q is the false discovery rate. Data deemed statistically significant by the programme were FDR < 0.05. supraHex analysis was used to aid visualisation of expression patterns in the data (Fang & Gough 2014).

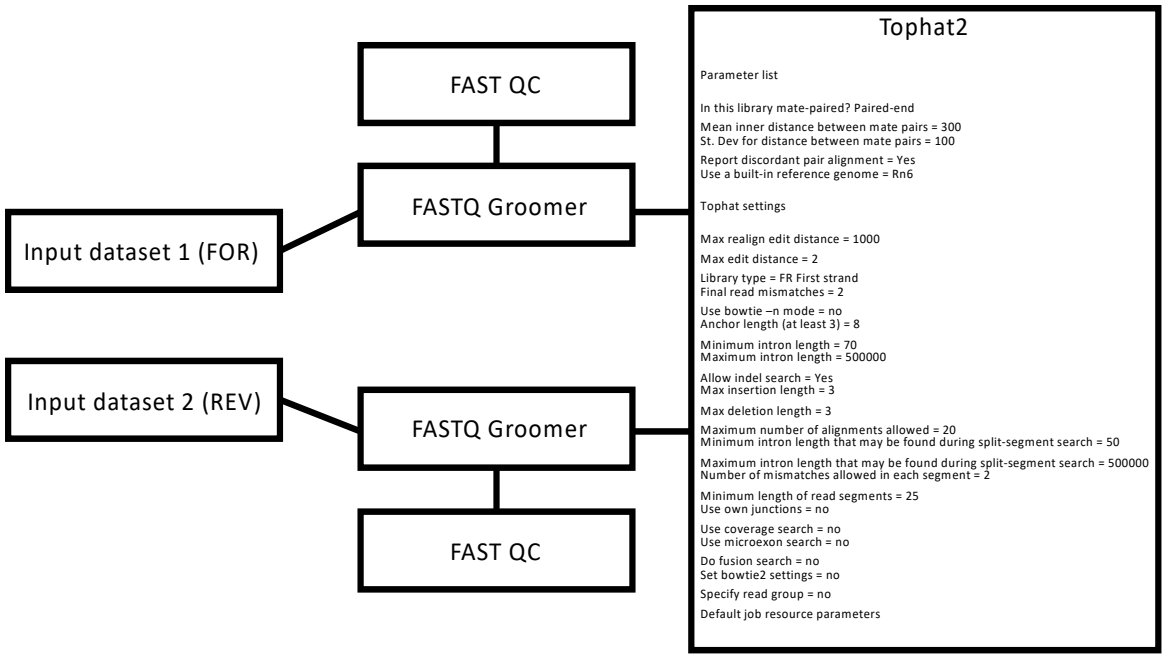

Figure 2.2 Schematic of the differential gene expression pipeline (www.Galaxyproject.org).

2.7.2 quantitative PCR

StepOne Software (Life Technologies, UK) was used to analyse all samples. Baselines and thresholds were defined and set automatically. The corresponding data file was exported to Microsoft Excel for further analysis.

All Sybr Green data were analysed using the standard curve method. All Taqman data were analysed using the ΔΔCt method. β actin was used as an endogenous control throughout. Fold change was determined relative to ZT2 samples. Analysis methods described below:

Standard curve analysis:

1. The numbers generated from the standard curve for each duplicate for the gene of interest (GOI) and endogenous control (ECon) was obtained
2. An average of the ZT2 GOI and ECon values were obtained (ΔCt calibrator)
3. The value from each GOI and ECon was divided with result from step 2
4. The output from step 3 was divided (GOI/ECon) for each sample
5. An average of the duplicate sample was taken, giving fold change data

ΔΔCt analysis:

1. The Ct values generated for the gene of interest (GOI) and endogenous control (ECon) was obtained
2. An average of the ZT2 GOI and ECon values were obtained
3. The Ct of each sample of the ECon was subtracted from the GOI (ΔCt)
4. $\Delta\Delta Ct = 2^{-(\Delta Ct - \Delta Ct\ calibrator)}$ produced relative expression across samples

Normalised data were further analysed using GraphPad Prism (Version 7.0; GraphPad Software, Inc., USA). All graphs are expressed as mean ± SEM unless otherwise stated. Specific analysis methods used are described with each result. Calculated values of $P<0.05$ were considered statistically significant.

2.7.3 Locomotor activity and core body temperature

Locomotor activity and core body temperature data were collected in 10-minute epochs using VitalView software (Starr Life Sciences Corp, US). MATLAB (v2016b, MathWorks, US) was used to analyse and plot the data using an in-house script consisting of Wavelet transform spectral analysis and Lomb-Scargle Periodogram. Rhythms are commonly assessed in biology, with varying analysis packages and techniques to understand rhythmic periods in a dataset. Often, actograms are used to analyse locomotor activity however these datasets are generally large, consisting of 2+ weeks of data (Leise et al. 2013). However, due to the experimental design, LA and cBT were recorded for only 5 days, which is an insufficient period length to run with actogram programs. Therefore, wavelet transform was utilised to assess periodicity. It has been used for many years in the field of physical sciences but is relatively new to the field of circadian biology. It is a technique that processes rhythmic signals, or wavelets, in a dataset. This is a unique property to this signal processing technique, as these signals can be symmetric or non-symmetric, high or low frequency, and be identified in regular or irregular datasets (Hoang Dang 2014). It allows for discrete identification of rhythms, or independent frequencies within a dataset, and in conjunction with using the Lomb-Scargle periodogram, which detects rhythmic signals

based upon a least squares fit of sinusoidal data (Hocke 1998) from sample data with zero mean, allows for period length to be measured.

The wavelet transform analysis subsequently identified wavelets, or rhythmic signals within the data as a measure of time. The Lomb-Scargle periodogram fits the detrended data under the pretense that it is sinusoidal, using the least squares fit method. The script was made available by Dr. Amitesh Pratap.

2.7.4 Electrophysiology

All sleep electrophysiology data were analysed using MATLAB (v2016b, MathWorks, US). In order to measure the animals movement, a video recording was captured above the sound-attenuating chamber. These movement data were used alongside the electrophysiology data to manually score arousal state in 10 second epochs. Epochs were scored as wake if movement was high. Non-rapid eye movement sleep (NREM) was scored if there was low movement and ripples and slow-waves were recorded on the LFP (Delta wave; 0.5-2Hz). Ripples were characterized by sharp bursts of neural activity within slow waves. Rapid eye movement sleep (REM) was scored as low levels of movement and theta waves on the LFP (Theta wave; 6-10Hz). All analysis was carried out using in-house scripts written by members of Prof. Matt Jones' lab.

Chapter 3

Methylprednisolone alters clock gene expression in the SCN

3.1 Introduction

The molecular clock is a robust mechanism that drives the daily rhythm of cells and tissues in preparation for daily environmental changes. This clock is present in all mammalian cells tested, however the central clock, located in the SCN, drives peripheral clocks, such as those found in the rest of the brain, skeletal muscle, liver and heart, to remain in rhythm (Gillette & Tischkau 1999). Light input to the SCN via the retinohypothalamic tract is the master entraining signal of daily rhythms (Foster & Hankins 2007; LeGates et al. 2014), however, skeletal muscle and liver can be further regulated by food intake and activity periods (Hodge et al. 2015).

The importance of circadian rhythms is vast, determining sleeping and feeding patterns, whilst also controlling brain activity, hormone production and cell regeneration (Xie et al. 2015; Welsh et al. 1985; Qian et al. 2012). Sleep-wake disorders, which affects a large proportion of the UK, are believed to be caused by alterations in the SCN clock timing, its entraining systems, or due to a misalignment of the internal clock rhythm with the external environment. Recently, a dissociation between central and peripheral clocks has been linked to depression and mental illness in patients (Partonen et al. 2007; Soria et al. 2010; Jagannath et al. 2013). It has furthermore been suggested that an altered clock, which is observed in patients with Alzheimer's may be an underlying cause of the disease as the sleep/wake cycle regulates the production of amyloid-beta peptide and an alteration to this cycle may therefore increase the levels of this peptide in the brain (Bellanti et al. 2017).

Glucocorticoids are the most commonly prescribed class of drugs in the UK today, with 2% of the population prescribed oral glucocorticoids at any given time (Overman et al. 2013), with a third reporting continued use of longer than five years. Prolonged use of glucocorticoid steroids can lead to several detrimental side effects. A significant number of long-term users complain of alterations to their daily activity, sleep period, and impairment to memory (Keenan et al. 1996; Coluccia et al. 2008). Side effects observed during glucocorticoid therapy are vast, predominantly targeting endocrine systems and metabolic systems but they also affect the central nervous system with patients often complaining of changes to mood, with a proportion of these reporting bouts of depression, and in severe cases, mania (Naber et al. 1996). Therefore, it is important to understand the molecular

mechanisms that underlie these severe side effects, a fundamentally important question in glucocorticoid research.

The effect of glucocorticoids on the central clock within the SCN has previously been assessed, using the potent GR specific agonist, Dexamethasone (Balsalobre et al. 2000). No change to the rhythm and timing of the molecular clock or any of its components was observed in the SCN, however a phase shift in mRNA expression of the components of the molecular clock in the liver, kidney and heart were noted. As glucocorticoids act through binding to their cognate receptors, these results were somewhat expected, as previously, binding assays targeting the GR and MR could not detect their expression in the SCN (Reul & Kloet 1985). In contrast, GR and MR were found to be expressed highly in the HC and liver, regions that have since been extensively studied.

The GR and MR reside in the cell cytoplasm and upon binding to ligand, translocate into the nucleus, where they bind to specific sequences on DNA called glucocorticoid response elements (GREs) to facilitate the recruitment of transcription factors to promote the transcription of glucocorticoid regulated genes. In peripheral tissues to the SCN, such as the hippocampus and liver, glucocorticoids binding through its receptors, promote the expression of the major clock gene *Per1*, through the glucocorticoid binding site upstream of the *Per1* transcriptional start site (Reddy et al. 2012). Therefore, in this first chapter, the rhythmic expression of *Per1*, *Per2* and one of its transcriptional activators *Bmal1*, were assessed in the SCN following treatment with the glucocorticoid and mineralocorticoid agonist Methylprednisolone. Based upon previous findings, no difference was expected between the rhythms of the central clock with steroid treatment, even though *Per1* is a glucocorticoid sensitive and regulated gene (Conway-Campbell et al. 2010; Balsalobre et al. 2000), because of a lack of GR in this brain area. Instead the daily rhythm and clock machinery was expected to remain in time and rhythm with the controls, driven by the major regulator of the clock, the light/dark cycle.

Although the potent glucocorticoid agonist Dexamethasone does not affect clock gene expression in the SCN, the well-known glucocorticoid MPL has not been assessed. In this chapter, I assessed the effect of MPL on clock gene expression in the SCN, to identify if this commonly prescribed glucocorticoid could affect clock function.

3.2 Methods

3.2.1 Animal housing and Home Office

96 adult male Lister Hooded rats (250-300g; 9-11 weeks) were obtained from Harlan Laboratories, now Envigo (Bicester, UK) and maintained under standard housing conditions with a 12:12 light/dark cycle. Food and water were available *ad libitum*. Rats were given an initial period to acclimatise to the facility. All procedures were carried out in accordance with the UK Home Office guidelines and the UK Animals (Scientific Procedures) Act under PPL 30/3114 and PIL I04092F5F.

3.2.2 Experimental design

Rats were housed in pairs for experimental purposes and were habituated to the experimenter for five days prior to the start of experimental procedures and during to eliminate effects of stress. Methylprednisolone (1mg/ml in drinking water (Demski-Allen 2014) (20mg/per day)) treatment lasted five days. Following five days treatment, the animals (n=8 per time and treatment) were killed at zeitgeber (ZT) times 2, 6, 10, 14, 18 and 22. Whole brains were frozen on dry ice and stored at -80°C for subsequent RNA expression studies. Trunk blood was collected to assess the levels of circulating endogenous glucocorticoid in the blood at the time of kill. Group size was determined by literature review.

3.2.3 RNA extraction and qPCR

Suprachiasmatic nucleus coordinates were assessed (Paxinos & Watson 2007) and coronal sections (4 x 200um) were cut on a cryostat. The SCN was removed using a 1mm micropunch. Total RNA was extracted using Direct-zol Miniprep reagents (Zymo Research, USA). RNA quality and concentration was assessed using a Nanodrop (ThermoFisher Scientific, USA). cDNA was synthesised using the iScript cDNA synthesis kit (Biorad, USA). All gene expression assays were carried out using inventoried Taqman assays (ThermoFisher Scientific, USA) using a 7500 thermal cycler (ABI systems, USA) to assess expression. *Period1* (Rn01325256_m1), *Period2* (Rn1427704_m1) and *Bmal1*

(Rn00577590_m1). Brains were dissected and all molecular biology techniques were blinded to the experimenter.

3.2.4 Radioimmunoassay (RIA)

Trunk blood was collected at all time points and treatment immediately following decapitation. Corticosterone levels were measured following an in-house corticosterone assay using a gamma counter (Perkin Elmer, USA) (for full details, please see methods section 2.5).

3.3 Results

3.3.1 Assessment of corticosterone levels in blood in control and MPL treated rats

The hypothalamic-pituitary-adrenal (HPA) axis regulates corticosterone secretion from the adrenal gland in a circadian profile, driven by activation of the PVN from the SCN. This circadian profile is highly conserved across species with the highest levels of CORT secreted prior to the onset of the active period. The secretion and presence of CORT is vital for many processes, including driving gluconeogenesis in the liver, preparing glucose uptake in skeletal muscle for the active period, whilst also driving the consolidation of memories and promoting sleep processes, including REM and NREM sleep (Yabaluri & Bashyam 2010; Van Cauter et al. 2000; Tatomir et al. 2014). Glucocorticoids are known to regulate gene expression, in particular in the liver, where synchronisation of 60% of the circadian transcriptome occurs (Reddy et al. 2007). The HPA axis however, can be interrupted in the presence of a stressor, where a transient spike of CORT is released from the adrenal gland in response to a stress response, to initiate glucocorticoid target systems into action. Although the hypothesis was that glucocorticoids would not affect gene expression in the SCN, it was still important, for completeness, to assess circulating levels of corticosterone in the blood at each time point and treatment to ensure that the molecular clock was not affected by stimuli outside of a circadian paradigm, for instance, through stress. Using known reference points, from our lab and others, levels deemed ‘stress’ and not part of the ‘normal’ CORT levels could be assessed measuring CORT levels in the blood. It was also important to confirm that the MPL treated animals were HPA axis suppressed, as expected following GC treatment due to negative feedback of the axis.

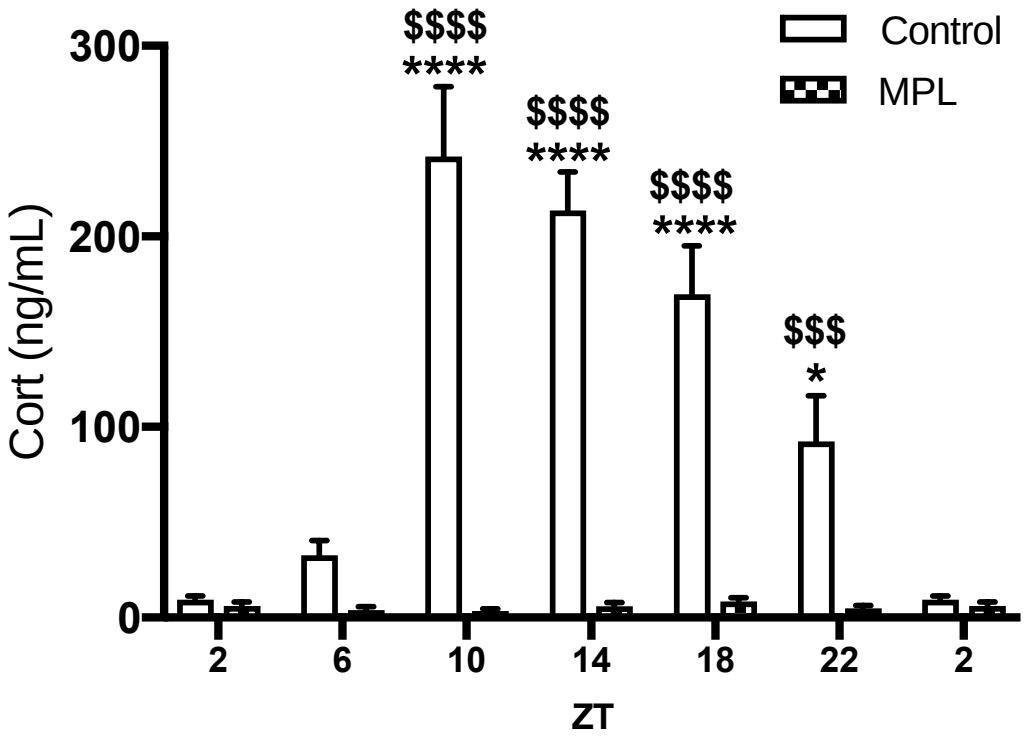

Figure 3.1 RIA of the circadian corticosterone profile in control animals and reduced corticosterone levels with MPL treatment. In control animals, circulating CORT is circadian, as expected from previously published data. Circulating CORT levels in MPL treated animals are significantly blunted, with no circadian profile observed and no significant difference observed across time points. All data represented as mean ± SEM. N = 8 per group. Analysis with Two-way ANOVA with Sidak's post-hoc test. * represent significant effect of time, $ represent significant effect of treatment. All statistical significance indicated at $P < 0.05$ (*), $P < 0.01$ (**), $P < 0.001$ (***) and $P < 0.0001$ (****). ZT2 is repeated for visualisation purposes.

The secretion of corticosterone in rodent from the adrenal gland is in response to a cascade of hormone production originating from the release of CRH from the PVN. The PVN is activated primarily from direct contact with the SCN and therefore is driven predominantly by circadian cues. However, the PVN is also activated in the presence of a stressor. Before assessing the expression of clock genes within the SCN, it was important to assess the circulating levels of GCs in the blood to confirm that the data were a result of circadian drive, and not one of a stressor. While the SCN is reported to be unaffected by acute stress, we nevertheless wanted to ensure all rats used in the experiment exhibited the expected

CORT circadian profile. It was also important to ensure that all MPL treated rats were suppressed at this dose, as previously reported (Spiga et al. 2011).

In the control animals there was a clear and significant circadian release of GCs into the circulating blood ($F_{6,49} = 4.48$, $p<0.0001$). The levels of CORT were expectantly low during the early periods of inactivity (ZT2 – 9.4ng/mL) (ZT6 – 32.5ng/mL) before a clear and robust increase in CORT levels was observed (ZT10 – 241.9ng/mL, P=0.0001), 2 hours prior to the onset of activity/dark phase, in preparation for the active period. The levels of CORT decreased throughout the active period (ZT14 – 213.5ng/mL, P=0.0001), (ZT18 – 169.6ng/mL, P=0.0001) (ZT22 – 92.3ng/mL, P=0.0344) in preparation for low levels of CORT during the early phase of inactivity/sleep phase. Following MPL treatment, the secretion of CORT was no longer in a circadian rhythm, with a significant effect of time ($F_{6,95} = 20.83$, $P < 0.0001$) and treatment ($F_{1,95} = 163.2$, $P < 0.0001$) observed between groups, (ZT10 – $P < 0.0001$), (ZT14 – $P < 0.0001$), (ZT18 – $P < 0.0001$), (ZT22– P=0.001). It should be noted that both of these profiles were expected based on previous findings and based upon the known activity and feedback circuitry of the HPA axis.

3.3.2 The expression of *Per1* in the SCN is altered with MPL treatment

Following confirmation of the expected CORT profile in the control group and suppressed CORT in the MPL group, I assessed the effects of time of day and MPL treatment on SCN *Per1* mRNA expression with reasonable confidence that I had minimised the possibility of a potentially confounding stress response.

The rhythmic expression of *Per1* mRNA has been extensively studied, both in the SCN and in many peripheral tissues. As a major repressor of the molecular clock, PER1's importance in maintaining rhythms has been widely researched with a range of techniques including luciferase reporter assays, in situ hybridisation histochemistry and qPCR all showing a robust circadian profile. The highest levels of expression are evident prior to the active period. Following this high level of expression, the *Per1* mRNA is translated to PER protein to repress its own activation, as described previously. Therefore, as the day progresses further into the active period, the level of *Per1* decreases until low levels are recorded prior to the sleep period (Peirson et al. 2006; Schwartz et al. 2011).

Balsalobre et al. 2000 looked at the expression of core clock genes in the SCN, liver, kidney and heart following glucocorticoid treatment, using the potent GR agonist DEX. No effects on expression of the SCN clock components were observed following DEX treatment, but a shift in phase was observed in the tissues peripheral to the SCN. At the time, the presence of the glucocorticoid response element upstream of the *Per1* transcriptional start site was unknown, however it was recently shown that glucocorticoids can regulate the expression of *Per1* through this site. The GR is known to be abundantly expressed in the peripheral tissues that were sensitive to glucocorticoid-induced phase shift but has not been detected in the SCN. Therefore, SCN *Per1* mRNA was expected to be unaffected by MPL treatment, and to retain its circadian rhythmicity irrespective of GC treatment.

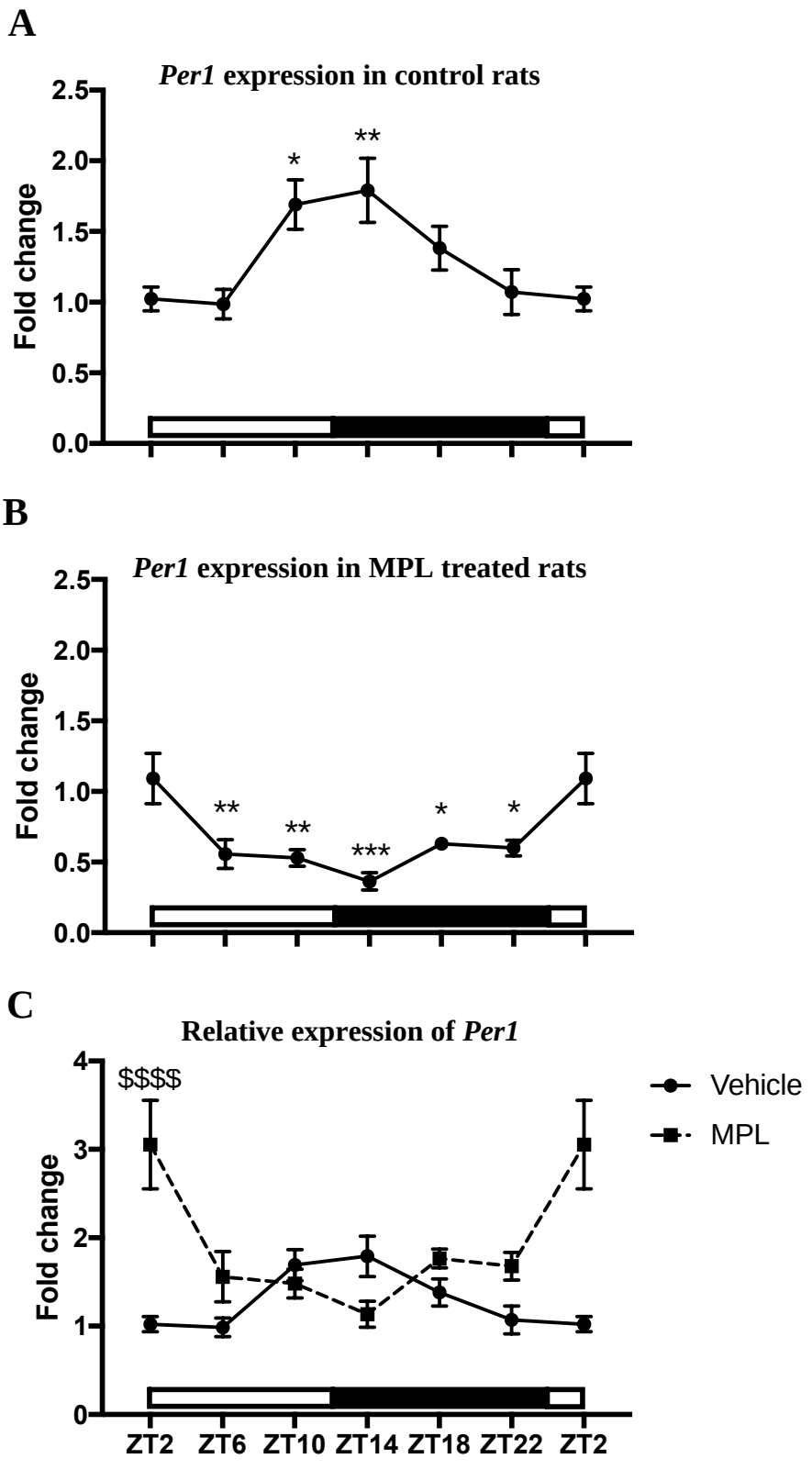

Figure 3.2 Treatment with MPL alters the circadian expression of *Per1* mRNA in the SCN. In control rats (**A**), a clear and robust circadian rhythm of *Per*1 expression is observed, with peak expression prior to the onset of the dark, or active phase. Following MPL treatment (**B**), the circadian expression of *Per1* mRNA expression is inverted,

compared to controls. When assessing the relative levels between groups (**C**), a significant increase in expression of *Per1* mRNA in the MPL group was evident at ZT2, compared to controls, but no significant difference was observed at any other time point. All data represented as mean ± SEM. N = 8 per group. One-way ANOVA with Dunnett's post-hoc test was used, with all comparisons to ZT2 in graphs (**A**) and (**B**). Two-way ANOVA with Sidak's post-hoc test was used in (**C**). All statistical significance indicated at $P < 0.05$ (*), $P < 0.01$ (**), $P < 0.001$ (***) and $P < 0.0001$ (****). ZT2 is repeated for visualisation purposes.

The mRNA expression of *Per1* has been well characterised in the SCN. In the control group (**A**), an obvious and robust circadian variation in expression was reported (One-way ANOVA $F_{6,49} = 6.286$, $p<0.0001$). Low levels of *Per1* mRNA were measured during the inactive period before a significant increase in expression was shown prior to the animals entering the active phase (ZT10 – P=0.0176). The level of *Per1* mRNA remained significantly elevated four hours later (ZT14 – P=0.0028) before returning to baseline levels during the most active period (ZT18 – P=0.2529), (ZT22 – P=0.9996).

Following treatment with MPL (**B**), the expression profile of *Per1* remained significant across time (One-way ANOVA $F_{6,48} = 8.006$, $p<0.0001$). The level of *Per1* mRNA was most abundant at ZT2, with a repression in expression observed at all other time points throughout the day (ZT6 – P=0.0073), (ZT10 – P=0.0062), (ZT14 – P=0.0006), (ZT18 – P=0.0256), (ZT22 – P=0.0154).

However, when assessing the relative levels of *Per1* mRNA expression between treatment and across time by Two Way ANOVA (**C**), a significant effect was observed across time ($F_{6,97} = 6.537$, $p<0.0001$), treatment ($F1,97 = 155.8$, $p<0.0001$) and an interaction between both ($F_{6,97} = 9.537$, $p<0.0001$). A surprising and significant increase in *Per1* mRNA expression was observed in the MPL treated group at ZT2, when compared to its control counterpart ($P<0.0001$). However, following this rapid increase, which occurred shortly after the onset of lights, no other time point was significantly different from controls (ZT6 – P=0.5136), (ZT10 – P=0.9985), (ZT14 – P=0.4771), (ZT18 – P=0.8872), (ZT22 – P=0.4401), suggesting an elevated level of *Per1* mRNA expression in the MPL group throughout.

3.3.3 The expression of *Per2* mRNA in the SCN is altered with MPL treatment

Clock gene expression in the SCN has been extensively studied. However, in previous studies, the only way that the SCN clock components have been altered is either by changes to the light/dark cycle or by using a targeted gene approach. Examples of this include *Bmal1*$^{(-/-)}$, *Per*$^{(-/-)}$ and *Cry*$^{(-/-)}$ mice (Bae et al. 2001; Horst et al. 1999; Kondratov et al. 2006).

I have shown that the synthetic glucocorticoid MPL can change the expression of *Per1*, a major component of the primary transcriptional loop of the molecular clock. However importantly, *Bmal1*$^{(-/-)}$ mice become arrhythmic, whereas *Per1*$^{(-/-)}$ mice present with a shorter free-running period. *Bmal*1 is also a major component of the clock, being a transcriptional activator, however no other gene has been shown to compensate for its loss, leading to the arrhythmic phenotype. *Per1*$^{(-/-)}$ mice however, were shown to be compensated by *Per*2, retaining rhythm, albeit slightly shorter in period length. Therefore, following the result that MPL treatment significantly affected the expression of *Per1* in the SCN, it was important to assess the expression of *Per2* in these animals, as a compensatory effect of the altered expression of *Per1* may occur, and therefore retain rhythmicity of physiological systems to ~24h.

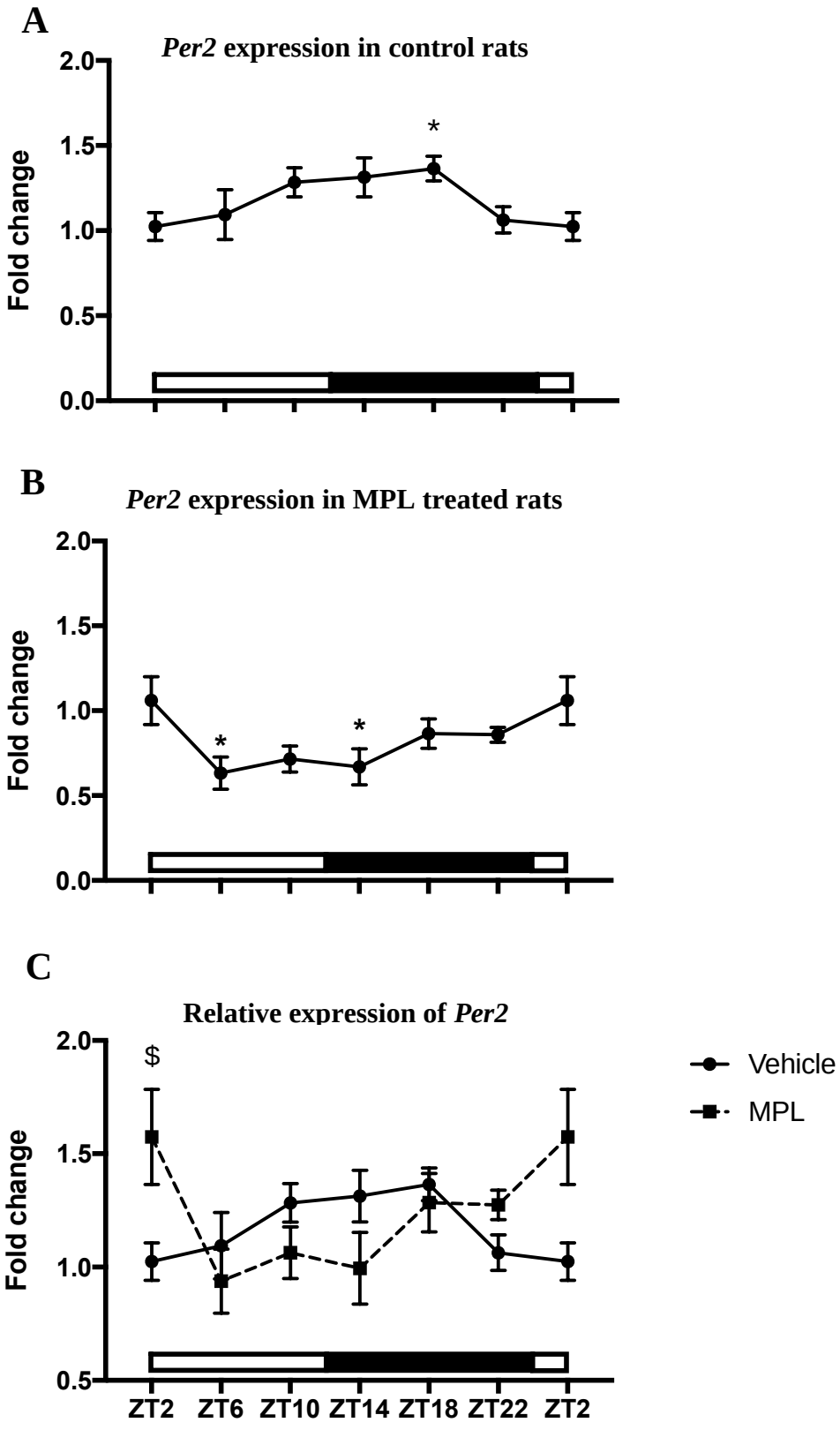
A
Per2 expression in control rats
Fold change
2.0
1.5
1.0
0.5
0.0
*
B
Per2 expression in MPL treated rats
Fold change
2.0
1.5
1.0
0.5
0.0
*
*
C
Relative expression of Per2
Fold change
2.0
1.5
1.0
0.5
$
ZT2
ZT6
ZT10
ZT14
ZT18
ZT22
ZT2
Vehicle
MPL

Figure 3.3 *Per2* does not compensate for *Per1* in the SCN following MPL treatment. The expression of *Per2* in control animals (**A**) exhibited clear circadian rhythm, with a delay in peak expression observed between *Per1* and *Per2*, where peak expression occurred at ZT18, rather than ZT10 in *Per1*. Following MPL treatment, a significant effect of treatment was observed (**B**). The expression of *Per2* was altered, with peak expression occurring at ZT2, and a repression of expression evident between ZT6 and ZT14. The relative expression of *Per2* between treatments was assessed (**C**) and showed a strikingly similar result to that seen in the *Per1* data. A significant increase was observed at ZT2 in the MPL group only. All data represented as mean ± SEM. N = 8 per group. One-way ANOVA with Dunnett's post-hoc test was used, with all comparisons to ZT2 in graphs (**A**) and (**B**). Two-way ANOVA with Sidak's post-hoc test was used in (**C**). All statistical significance indicated at $P < 0.05$ (*). ZT2 is repeated for visualisation purposes.

Per2, which has previously been shown to compensate for *Per1* expression in *Per1*$^{(-/-)}$ mice keeping animals in rhythm was also shown to be significantly affected by glucocorticoid treatment. In the control group (**A**), circadian variation was evident by (One Way ANOVA $F_{6,47} = 4.276$, $p = 0.0016$), although significance was only found at ZT18 ($P = 0.0311$), but a trend to significance was also found at ZT14 ($P = 0.0863$).

Following MPL treatment (**B**), the expression of *Per2* across the day was significantly altered by One Way ANOVA ($F_{6,49} = 2.872$, $p = 0.0177$), with peak expression occurring at ZT2, and a repression of expression evident at ZT6 ($P = 0.0262$) and ZT14 (0.0498).

However, when assessing the relative expression between treatments (**C**), a significant effect of treatment over time was observed by Two Way ANOVA ($F_{6,98} = 3.961$, $p = 0.0014$), where a robust increase in expression was observed at ZT2 in the MPL group ($P = 0.0224$), indicating that the expression of *Per2* remains elevated through the active period and into the most inactive period, before returning to low expression levels observed in the late inactive period.

3.3.4 The expression of *Bmal1* mRNA in the SCN is altered with MPL treatment

Bmal1 is one of the major components of the molecular clock that drives the transcription of *Per1*, dimerising with CLOCK and binding to E-box elements upstream of the *Per1* TSS. *Bmal1* has been a major target of gene manipulation to affect the clock, with *Bmal1*$^{(-/-)}$ mice exhibiting a loss of circadian rhythmicity in activity periods. A GRE has not been described for this gene, and it is not reported to be directly regulated by glucocorticoids. Its expression is controlled predominantly through the secondary loop of the molecular clock and the expression of REV-ERBs and RORs, with BMAL1 in turn regulating the expression of RORs and REV-ERBs.

As *Bmal1* has currently not been shown to contain a GRE or be driven by glucocorticoid exposure, the levels of *Bmal1* mRNA in control and MPL treated animals may be expected to remain the same. However, an alteration in *Per1* expression may in turn affect the timing and rhythm of *Bmal1* expression.

A

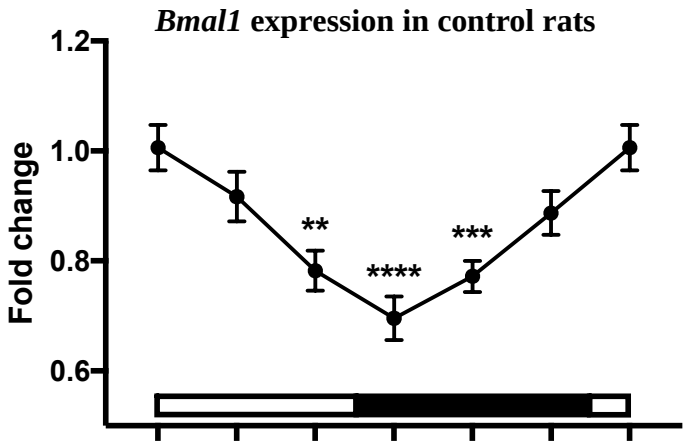
Bmal1 expression in control rats
Fold change
1.2
1.0
0.8
0.6
**
****
***

B

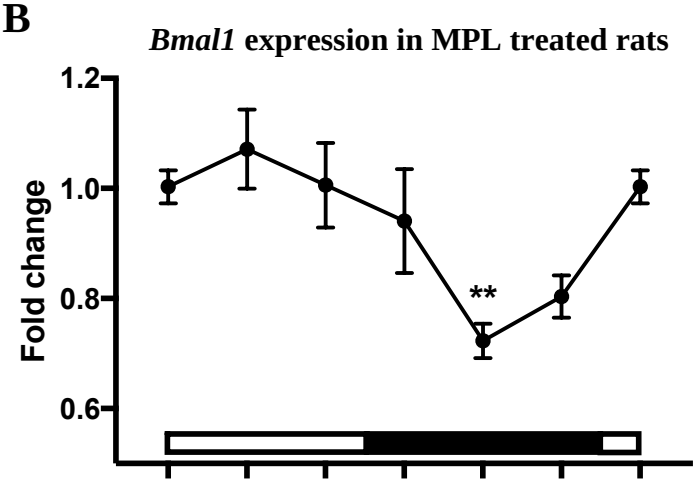
Bmal1 expression in MPL treated rats
Fold change
1.2
1.0
0.8
0.6
**

C

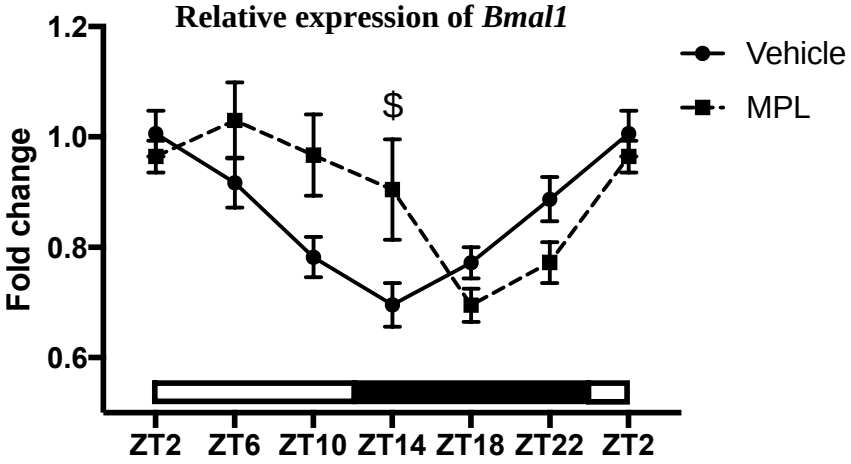
Relative expression of *Bmal1*
Fold change
1.2
1.0
0.8
0.6
$
Vehicle
MPL
ZT2
ZT6
ZT10
ZT14
ZT18
ZT22
ZT2

Figure 3.4 Treatment with MPL shifts the expression pattern of *Bmal1* mRNA in the SCN. In control rats (**A**), a clear and robust circadian expression of *Bmal1* mRNA expression was observed, with peak expression evident at ZT2, and a decrease in expression leading up to the most active period of the rat. Following MPL treatment (**B**), *Bmal1* expression was phase shifted with steady expression observed through to the most active period before a decrease is observed. Assessment of the relative levels between control and MPL treatment confirmed the effect of an elevated level of expression in the MPL group at ZT14 (**C**). All data represented as mean ± SEM. N = 8 per group. One-way ANOVA with Dunnett's post-hoc test was used, with all comparisons to ZT2 in graphs (**A**) and (**B**). Two-way ANOVA with Sidak's post-hoc test was used in (**C**). All statistical significance indicated at $P < 0.05$ (*), $P < 0.01$ (**), $P < 0.001$ (***) and $P < 0.0001$ (****). ZT2 is repeated for visualisation purposes.

The transcriptional activator of the molecular clock BMAL1 exhibits robust *Bmal1* circadian expression pattern as expected in the control group (**A**), being in clear antiphase with the *Per1* expression pattern of the control group (Figure 3.2a). The most abundant levels of *Bmal1* expression occur during the lowest levels of *Per1*, and vice versa. There is a significant effect of time of day in the expression of *Bmal1* (One Way ANOVA $F_{6,49} = 9.44$, $p<0.0001$), with the highest levels occurring at ZT2, during the most inactive period, before a decrease in expression is observed with significance noted just prior to, and during the most active period (ZT10 – P=0.0011), (ZT14 – P=0.0001), (ZT18 – P=0.0006).

Following treatment with MPL (**B**), the expression profile altered, however significant variation was detected across time (One Way ANOVA $F_{6,49} = 4.58$, $p = 0.0009$). The mRNA level in this group remained consistently high during the inactive period and largely into the active period, with no significant difference observed. However, a decrease in expression was observed at ZT18 (P=0.0078).

When assessing the relative levels of *Bmal1* mRNA expression between control and MPL treated groups by Two Way ANOVA (**C**), significant effects of time ($F6,98 = 8.608$, $p<0.0001$) and treatment ($F1,98 = 3.71$, $p = 0.0023$) were detected. Sidak's post tests indicated that the significant difference between control and MPL treated rats was found at ZT14 (P=0.0213). At ZT14, the control animals had a significant decrease in expression

relative to ZT2, whereas the MPL group was not significantly different from its highest level of expression observed at ZT2.

3.3.5. *Glucocorticoid receptor* mRNA is expressed in the SCN and exhibits an altered pattern with MPL treatment

Although previous data described no effect of glucocorticoid treatment on the clock machinery in the SCN due to the absence of GRs in this region, it was important to assess whether the *glucocorticoid receptor* mRNA was present following the striking effect that was observed in *Per1* expression following MPL treatment, as this could account for the effect observed with *Per1* mRNA.

The expression of *Gr* mRNA has not been described in the SCN, however it has been published in other brain regions, notably in the hippocampus, a brain region known to abundantly express the receptor. Different regions of the hippocampus were assessed over a day, with the expression of *Gr* mRNA published in all sub regions of the hippocampus proper (CA1-3) and the cortex, describing a clear daily rhythm (Herman et al. 1993). Therefore, based on those data, if the receptor mRNA was to be present in the SCN, a similar expression profile would be expected.

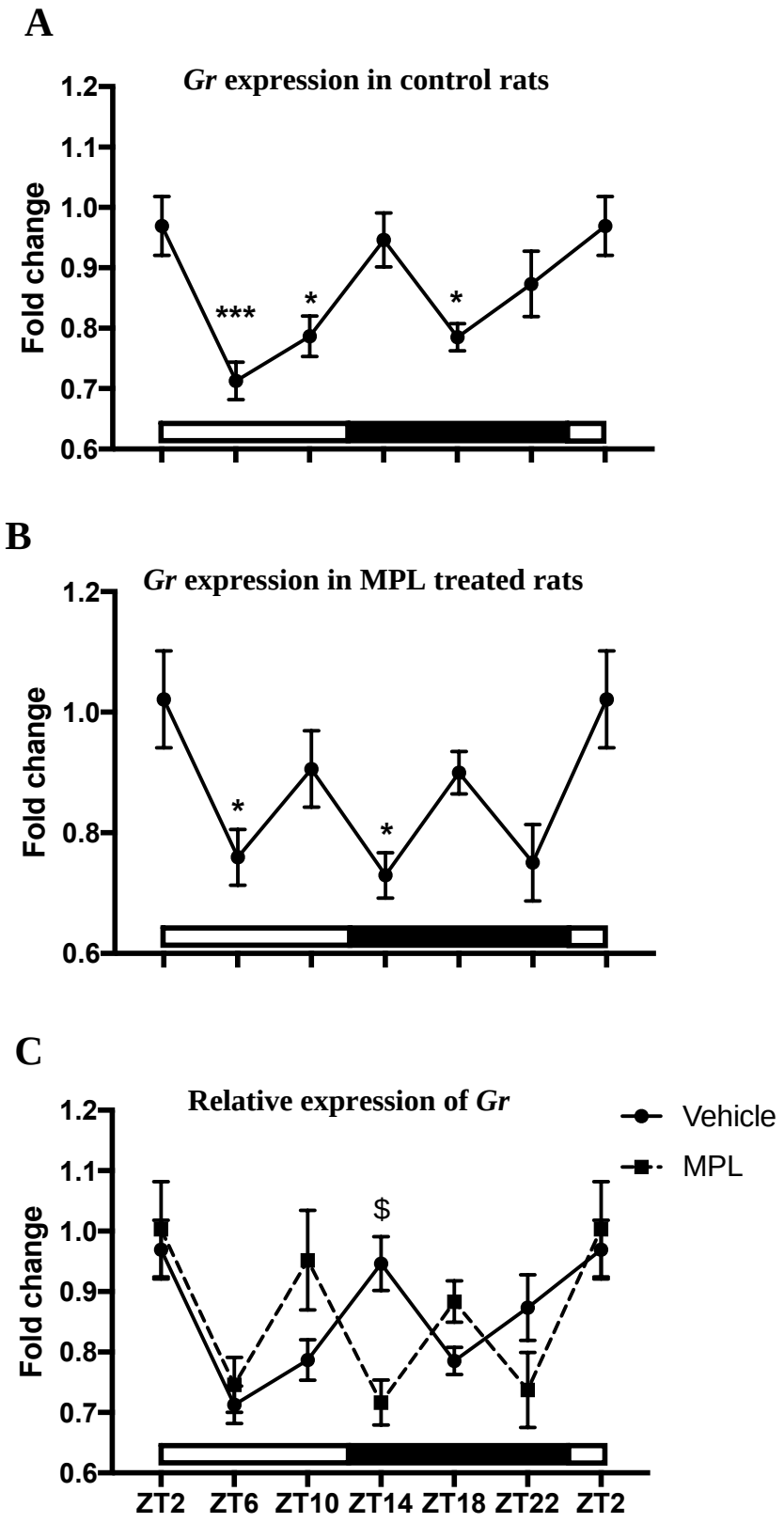

Figure 3.5 *Gr* mRNA is expressed in the SCN. In control rats (**A**), a clear and robust expression profile of *Gr* was observed, with peak levels of expression occurring at ZT2 and ZT14, with a significant decrease in expression observed at ZT6, ZT10 and ZT18. Following MPL treatment (**B**), *Gr* mRNA exhibited a similar pattern to the control group

at ZT6, however the biphasic expression was not present in this group, as at ZT14, *Gr* mRNA was still repressed. Relative expression (**C**) confirmed an expected significant difference at ZT14, where the expression of *Gr* in the control group returned to levels similar to ZT2, whereas the MPL group did not. All data represented as mean ± SEM. N = 8 per group. One-way ANOVA with Dunnett's post-hoc test was used, with all comparisons to ZT2 in graphs (**A**) and (**B**). Two-way ANOVA with Sidak's post-hoc test was used in (**C**). All statistical significance indicated at $P < 0.05$ (*), $P < 0.01$ (**) and $P < 0.001$ (***). ZT2 is repeated for visualisation purposes.

The expression of *Gr* has previously been shown to be rhythmic, made of a biphasic profile across the daily cycle. The control group exhibited a significant effect of time on *Gr* levels ($F_{6,42} = 5.348$, $p = 0.0004$) in the SCN (**A**), with the highest levels of expression at ZT2 and ZT14. A significant decrease of expression was observed at ZT6 (P=0.0007) and ZT10 (P=0.0222) before returning to non-significant baseline levels at ZT14 (P=0.8411). The second decrease in expression was observed at ZT18 (P=0.0207), before returning to non-significant baseline levels at ZT22 (P=0.4260).

With MPL treatment (**B**), the expression profile of *Gr* was altered in its expression profile, although still significant across time ($F_{6,46} = 3.348$, $p = 0.0080$). The biphasic activity of the mRNA which was shown in the control is no longer represented. A significant decrease in expression was observed at ZT6 (P=0.0224), similarly to that of the control group. However, whereas in the control group it remained low before returning to non-significant levels at ZT14, with MPL treatment, the mRNA levels returned to non-significant levels at ZT10 (P=0.6343), before a significant repression of expression reoccurred at ZT14 (P=0.0122), significantly altered compared to the control. The levels of GR mRNA returned to non-significant levels at ZT18 (P=0.5852) and ZT22 (P=0.1643).

This alteration in *Gr* mRNA expression was confirmed by Two way ANOVA (**C**), with a significant effect of time ($F_{6,86} = 5.93$, $p<0.0001$) and an interaction between time and treatment ($F_{6,86} = 2.845$, $p = 0.0142$) observed. Sidaks post hoc tests revealed a significant difference between control and MPL at ZT14 (P=0.0466), where *Gr* mRNA was at its highest level of the day in the control group, but lowest in the MPL group.

3.3.6. The expression of the housekeeping gene *Actb* in the SCN in control and MPL treated animals

Following the data presented above, it was important to show the expression of *Actb* across all tested samples in the SCN, to ensure that the expression changes observed were of changes to the gene of interest rather than an effect of *Actb* circadian variability.

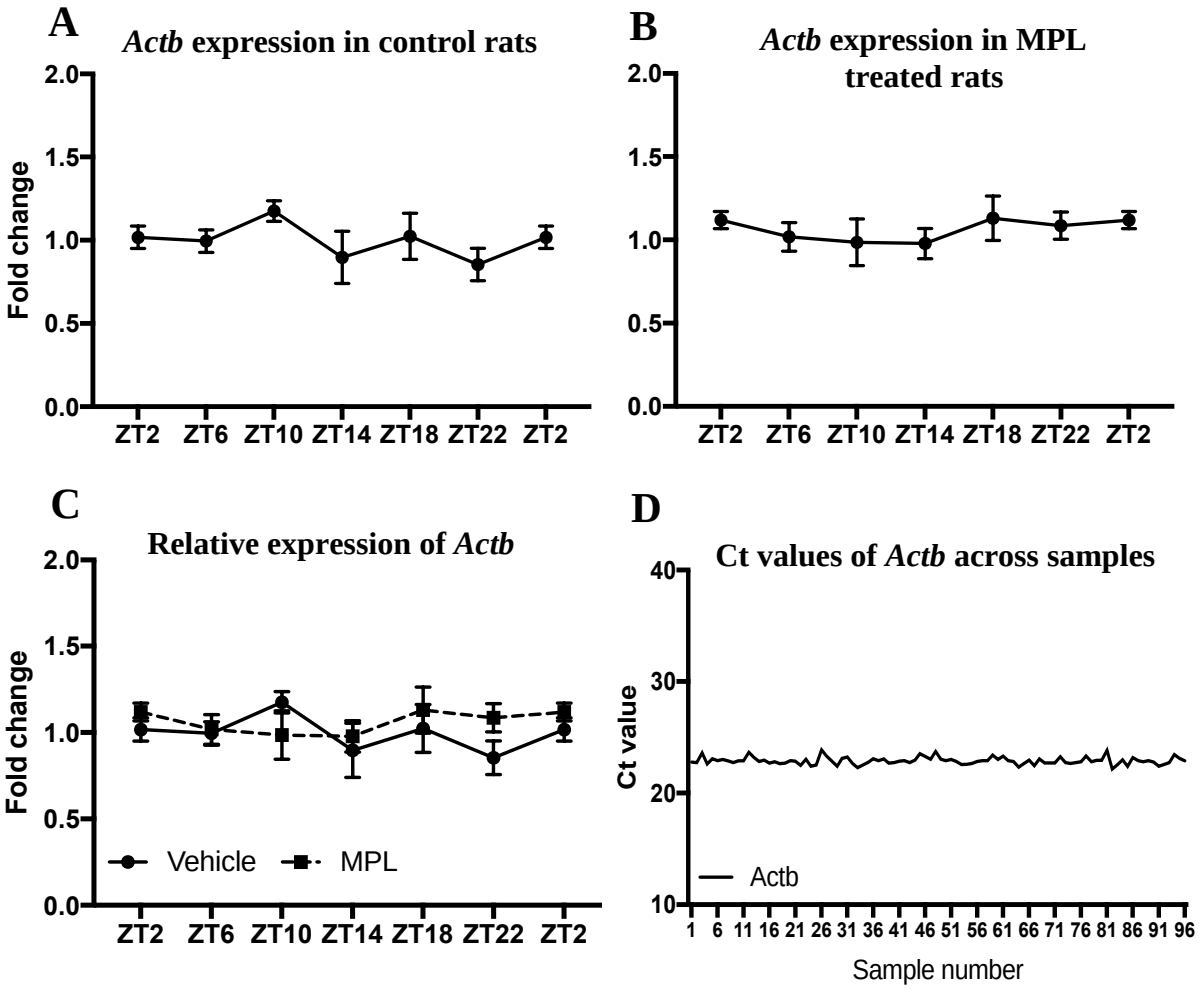

Figure 3.6. *Actb* mRNA levels remained consistent across samples independent of time of day or exposure to MPL treatment. No circadian expression was observed in control rats across one day (**A**) or rats treated with MPL (**B**). The relative expression of *Actb* between treatments was not affected (**C**) and the stability of Actb was consistent across all samples tested (**D**). All data represented as mean ± SEM. N = 8 per group. One-way ANOVA with Dunnett's post-hoc test was used, with all comparisons to ZT2 in graphs (**A**)

and (**B**). Two-way ANOVA with Sidak's post-hoc test was used in (**C**). ZT2 is repeated for visualisation purposes.

It was important to assess the expression of *Actb* across time and treatment to ensure that the expression of the genes of interest were not influenced by changing levels of the endogenous control. In control rats (**A**), the expression of *Actb* did not change across time points and therefore no significant difference across the day was observed ($F_{6,49} = 1.411$, $p = 0.4034$). This was also evident in the MPL treated group (**B**) ($F_{6,49} = 1.062$, $p = 0.8219$).

Although no effect was observed in *Actb* expression across the day in both control and MPL treatment, it was further important to assess the relative expression of *Actb* to ensure that MPL did not alter the overall expression levels between groups. The relative levels between treatments were found to be non-significant (**C)**, with two-way ANOVA indicating no effect of time ($P = 0.6476$), treatment ($P = 0.2172$) or an interaction between both ($P = 0.5339$).

These data therefore provide confirmation that the effects observed in clock gene expression in this chapter are either an effect of time and treatment, and therefore are not influenced by changing expression in the endogenous control.

3.4 Discussion

In this chapter, the mRNA expression profiles of core clock genes *Per1, Per2* and *Bmal1* were assessed within the SCN following treatment with the synthetic glucocorticoid, MPL. Previously, no effect on the core clock components within the SCN was reported when using the potent glucocorticoid agonist DEX, with the core clock machinery retaining a robust daily rhythm in timing with the light/dark cycle (Balsalobre et al. 2000). Therefore, this study was designed to provide a robust control for circadian regulated genes synchronised to a standard 12:12 light/dark cycle.

Glucocorticoids are secreted from the adrenal gland in a circadian manner, driven by SCN activation of the HPA axis. Internal HPA axis feedback maintains CORT at optimum levels, targeting the anterior pituitary and PVN to suppress the secretion of ACTH and CRH, respectively. The circadian levels of CORT were measurable in these data (Figure

3.1). In the control group, a clear circadian rhythm of CORT secretion was evident, with the highest levels observed prior to waking and during the active period. With MPL treatment, the HPA axis was significantly suppressed. This was expected based on previously published data (Spiga et al. 2011).

The expression profile of *Per1* in the control group exhibited clear rhythmicity in timing with the circadian period. *Per1* expression has been extensively studied, both its profile within the SCN, as well as in peripheral tissues including the heart, liver and skeletal muscle (Peirson et al. 2006; Marcheva et al. 2010). In these data, *Per1* accumulated during the inactive phase (Figure 3.2A), with absolute levels decreasing through the active period as they are translated to PER proteins, where they act to inhibit the transcription of *Per1*.

Similarly to *Per1*, the circadian profile of *Bmal1* expression has been published in the SCN and peripheral tissues (Peirson et al. 2006; Barca-Mayo et al. 2017). BMAL1, along with CLOCK, act as transcriptional activators, driving the expression of *Per* and *Cry*. In the control group, *Per1* expression peaked during the nadir of *Bmal1* expression, whilst peak levels of *Bmal1* were evident during the nadir of *Per1* expression (Figure 3.4A). Therefore, *Bmal1* expression is in antiphase to *Per1*, and an alteration to either of these could push the other to a new rhythm (Oishi et al. 1998a).

In this chapter, I have shown for the first time that MPL can alter these core clock components of the primary loop. It is well known that glucocorticoids can induce the *Per1* transcript via a receptor dependent mechanism, where GR and/or MR binds to GREs located upstream of the transcriptional start site of *Per1*, driving transcriptional output. However, this has only been described in areas that abundantly express these receptors, for example the GR rich liver, and the GR/MR rich hippocampus (Reddy et al. 2007; Conway-Campbell et al. 2010). The SCN was deemed devoid of GR and MR following the inability to detect either (Reul & Kloet 1985; Reul & de Kloet 1986), and therefore the *Per1* gene was not expected to be modulated by glucocorticoid exposure here.

However, under normal light/dark cycles, the expression of *Per1* in the SCN following MPL treatment was significantly altered. MPL acts via the GR and MR, and so this may indicate that the receptors are present in the SCN to drive *Per1* expression to desynchronise the molecular clock (Figure 3.2C). The MPL group presented with prolonged *Per1*

expression throughout the inactive period. The elevated expression at the onset of the inactive period, and expression level similar to peak levels in the control group, could indicate an underlying mechanistic cause for disturbances to the sleep/wake cycle, as seen in patients with Cushing's disease, where elevated glucocorticoid levels are evident (Van den Berg et al. 1995). *Per2* expression was also assessed following this result. In *Per1*$^{(-/-)}$ mice, a compensatory effect was observed, with activity rhythm shortened 0.5h due to *Per2* retaining clock rhythm, whereas in *Per1/Per2*$^{(-/-)}$ mice, they become arrhythmic (Bae et al. 2001; Zheng et al. 2001). In these data, the circadian expression of *Per2* was also significantly affected with MPL treatment, indicating that a compensatory effect did not occur here. *Bmal1* expression in the presence of MPL treatment resulted in a phase delay (Figure 3.4B), further supporting the notion that MPL affects the synchrony between these core components of the clock.

Fundamentally, to affect the molecular clock in this way, MPL treatment would need to target the expression of *Per1* through the GR and/or MR, leading to the revised hypothesis that the GR and MR are present in this brain area. In previous studies, affecting the clock components within the SCN has required either gene manipulation or alterations to the light/dark cycle, as no previous study targeting the clock machinery was altered with drug treatment *in vivo* (Balsalobre et al. 2000). DEX is a potent GR agonist and failed to alter expression of the core clock genes, whereas MPL binds both GR and MR, therefore suggesting a requirement for the co-activation of the GR and MR to alter the expression of the core clock machinery. The identification of *Gr* in the SCN further supported that the effects observed following MPL treatment in the SCN were due to the presence and activation of GRs. *Gr* mRNA was robustly expressed here, the first time this has been shown.

The altered expression of *Per1* and *Bmal1*, and the presence of *Gr* expression in the SCN was not expected. However, these findings are the first to provide evidence that glucocorticoids can target the clock machinery of the SCN. These data suggest that treatment with synthetic glucocorticoids can adversely affect the central clock, leading to a dissociation between the light/dark cycle and the internal clock rhythm. Classically, a dissociation between central and peripheral pacemakers have been suggested as a root cause for illness, in particular, in patients with depression and/or sleep disturbances (Sequeira et al. 2012; Bunney et al. 2015). Patients receiving glucocorticoid therapy often

complain of alterations to the sleep/wake period following steroid treatment (Vázquez-Palacios et al. 2001; Antonijevic & Steiger 2003). A dissociation between the master and peripheral clocks has been suggested for this, as glucocorticoid treatment failed to show an effect on the master clock. However, the robust effect presented here reveals that MPL can target and alter the expression of the clock mechanism.

Following on from these data, it was important to assess the clock machinery peripheral to the SCN, but within the brain. Glucocorticoid therapy has been shown to affect memory and the sleep/wake cycle (Keenan et al. 1996; Coluccia et al. 2008). The hippocampus is instrumental in regulating both of these processes and is a regulator of negative feedback of HPA axis activity (Walker & Stickgold 2004). Patients with Cushing's disease, who present with an elevated level of glucocorticoids, complain of memory impairment, disturbances to sleep and in post mortem, often present with hippocampal atrophy (Starkman et al. 1992). Therefore, in the following chapter I have assessed the effect of MPL treatment on the clock machinery in the hippocampus.

Chapter 4

Methylprednisolone alters gene expression in the HC

4.1 Introduction

The hippocampus is a brain structure which is a major part of the limbic system that plays a key role in spatial navigation and sleep processing (Girardeau et al. 2009; Jones & Wilson 2005; O'Keefe & Speakman 1987). Lesions to the hippocampus significantly impair memory consolidation (Zola-Morgan et al. 1986; Morris et al. 1982). CORT can also impair or enhance the consolidation of memories, depending upon the level of glucocorticoids present (Sandi et al. 1997; Schaaf et al. 2000; Hui et al. 2004; Roozendaal et al. 1998; McLay et al. 1998). However, high levels and low levels of glucocorticoid exposure can impair the memory processing of certain tasks, indicating an optimum level of glucocorticoid exposure to enhance memory formation (Diamond et al. 1992; Rey et al. 1994; Pavlides et al. 1996; de Kloet et al. 1999; Joëls et al. 2011).

The HC is indirectly driven by the master clock in the SCN to regulate neurogenesis by controlling the timing of a large proportion of molecular processes to ~24hr (Schibler & Sassone-Corsi 2002; Phan et al. 2011; Eckel-Mahan et al. 2008). Gene expression of the components of the molecular clock within the hippocampus has been published, with all major elements of the molecular clock expressed in the sub regions of the HC, displaying clear circadian timing, albeit with a slight delay in peak expression compared to the SCN (Bouchard-Cannon et al. 2013; Conway-Campbell et al. 2010; L. M.-C. Wang et al. 2009; Summa et al. 2015). The CA1 region of the HC has been extensively studied, mainly for its role in memory processing. *Per1* mRNA expression in the CA1 region has been shown, and is susceptible to external stimuli, such as a restricted feeding paradigm, which increased baseline expression (Conway-Campbell et al. 2010; Yamamoto et al. 2001). The CA1, CA3 and DG highly express the molecular clock components *Per1*, *Per2*, *Clock* and *Bmal1* and are circadian rhythmic (Feillet et al. 2008), however following a mild stress paradigm, in which glucocorticoids are subsequently released and target the HC, the expression of *Per1*, *Per2* and *Bmal1* are altered in the CA1 region (Christiansen et al. 2016), reinforcing that GCs target and alter the expression of these glucocorticoid sensitive clock genes.

The SCN drives the sleep/wake cycle. Its projection to the medial septal nuclei directly acts on the HC to regulate theta-burst firing in neurons driving theta oscillations in the HC, controlling REM and NREM sleep periods, as well as ensuring the timing of the molecular

clock within the HC (Kang et al. 2015). Lesions to the SCN alter the sleep period, due to a lack of circadian timing (Ibuka & Kawamura 1975), driving the HC but also because the projection from the SCN to the medial septal nuclei is abolished (Eastman et al. 1984), therefore affecting neuron firing and REM and NREM sleep architecture.

Although memory consolidation processes in the HC are significantly affected by the amount, and quality of sleep attained, the cellular and molecular processes driving sleep-enhancing memories are still not fully understood, or even what parameters of sleep, or what molecular processes within the HC are targeted for optimal memory consolidation (Rasch & Born 2013; Abel et al. 2013; Wilhelm et al. 2011; Gais et al. 2002; Siegel 2001; Born 2010; Bliss & Collingridge 1993). However, it is clear that the molecular clock, or at least components of the molecular clock are instrumental in driving memory consolidation and sleep processes, as using a targeted gene approach, *Per1*$^{(-/-)}$ mice exhibited altered sleep/wake rhythms, and deficits to memory (Rawashdeh et al. 2016; Husse et al. 2012).

The glucocorticoid and mineralocorticoid receptors are abundantly expressed in the hippocampus, with distinct differences in the levels of expression exhibited across the different sub regions. The dorsal subiculum and CA1 region express the MR 7-fold greater than the GR whereas the dentate gyrus, CA3 and ventral hippocampus express the receptors equally (Reul & Kloet 1985). The presence of the receptors allows for the HC to modulate the negative inhibition of the HPA axis during the circadian variation and stress induction of GCs (Herman et al. 1989).

Glucocorticoid steroids are a commonly prescribed class of drugs, used to combat illnesses from asthma to lupus, indicating their broad spectrum of use and therefore accounting for the large number of users and long prescription periods (Overman et al. 2013). MPL, a synthetic glucocorticoid steroid variant of Prednisolone was synthetised from endogenous CORT. Being a derivative of CORT, it binds to the GR and MR with similar efficacy (Ye et al. 2014; Andrews et al. 2012). Once activated by ligand, both GR and MR can bind to glucocorticoid response elements on the DNA, promoting the transcription of glucocorticoid regulated genes (Herman & Spencer 1998; George et al. 2017; Paskitti et al. 2000). However, the dynamics of endogenous and synthetic glucocorticoids differ greatly. Endogenous GCs transiently activate the GR to facilitate the transcription of GC target genes for short periods of time, and only when sufficient levels of GCs are present. For

example, during the inactive period when circulating glucocorticoids are low, GC regulated gene transcription is stalled, but when circulating glucocorticoids are high, gene transcription readily occurs. As endogenous GCs transiently bind the GR to facilitate transcription, one would expect the same from synthetic GCs prescribed to patients. However, the timing of glucocorticoid binding differs significantly, with endogenous binding occurring for ~20 minutes, whereas the synthetic glucocorticoid binds for ~3h (Earl et al. 2018).

Almost half of the protein coding transcriptome is circadian rhythmic, and in the liver, glucocorticoids have been shown to affect almost 60% of these (Reddy et al. 2007), indicating the GCs ability to act on a large proportion of circadian regulated genes. In the HC, glucocorticoids target an array of genes, upregulating glucocorticoid regulated targets such as *Serum Glucocorticoid Kinase 1* (*Sgk1*) and *Glucocorticoid Induced Leucine Zipper* (*Gilz*) to induce and regulate neuron excitability, inflammation, apoptosis and a range of other processes (Anacker et al. 2013; Lang et al. 2010; Kajiyama et al. 2010). A reduced expression of *Sgk1* and *Gilz* during high *interleukin 6* (*Il6*) levels reduced hippocampal volume (Frodl et al. 2012). However, as well as these glucocorticoid targets, the clock gene *Per1* contains a GRE upstream of the transcriptional start site which facilitates the transcription of *Per1*. As the glucocorticoid receptor is abundantly expressed in the HC, the expression of *Per1* can be driven independently of SCN control, through glucocorticoid action independent of the classically known light/dark cycle (Conway-Campbell et al. 2010).

Glucocorticoid therapy often leads to alterations to sleep patterns and an effect of memory processing (Keenan et al. 1996). Therefore, following the results of chapter 3, where I showed a significant change to major components of the primary loop of the molecular clock, it was important to assess the effects of the glucocorticoid steroid MPL, on a peripheral target of the SCN, and as the HC has been extensively studied for its role in glucocorticoid regulation, sleep processing and the consolidation of memory, it was an obvious target brain region to assess, to see if this synthetic GC affects the molecular clock within this area as well as other glucocorticoid regulated targets. In this chapter, I have used RNAseq, a deep sequencing technology to profile the whole transcriptome in a sample. RNAseq not only provides data on the whole transcriptome, it is also a far more precise

measurement of levels of transcripts and their isoforms than any other method (Z. Wang et al. 2009).

4.2 Methods

4.2.1 Animal housing and Home Office

48 adult male Lister Hooded rats (250-300g; 9-11 weeks) were obtained from Harlan Laboratories, now Envigo (Bicester, UK) and maintained under standard housing conditions with a 12:12 light/dark cycle. Food and water were available *ad libitum*. Rats were given an initial period to acclimatise to the facility. All procedures were carried out in accordance with the UK Home Office guidelines and the UK Animals (Scientific Procedures) Act under PPL 30/3114 and PIL I04092F5F.

4.2.2 Experimental design

Rats were housed in fours for experimental purposes and were habituated to the experimenter for five days prior to the start of experimental procedures and during to eliminate effects of stress. Methylprednisolone (1mg/ml in drinking water (Demski-Allen 2014) (20mg/per day)) lasted five days. Following five days treatment, the animals (n=4 per time and treatment) were killed at zeitgeber (ZT) times 2, 6, 10, 14, 18 and 22. Whole hippocampus was immediately dissected and snap frozen in liquid nitrogen before storage at -80°C for subsequent RNA expression studies. Trunk blood was collected to assess the levels of circulating endogenous glucocorticoid in the blood at the time of kill. Group size was determined by literature review.

4.2.3 RNA extraction and qPCR

Whole hippocampi were dissected as per an in-house technique. Total RNA was extracted from individual whole hippocampi using miRNeasy mini reagents (Qiagen, USA). RNA quality and concentration was assessed for each sample on a Tapestation RNA screentape (Agilent Technologies, USA). RNA Integrity Number (RIN) of < 8, to a maximum of 10 was recorded for all samples. cDNA was synthesised using the iScript cDNA synthesis kit

(Biorad, USA). All gene expression assays were carried out using in-house designed primers (NCBI BLAST and Sigma, USA) using a 7500 thermal cycler (ABI systems, USA) to assay expression.

4.2.4 RNAseq

High throughput RNA sequencing was carried out across all time points and over both treatments using TruSeq Stranded Total RNA sequencing (Illumina, USA). 16 samples were run per lane (total read 560 million), average reads per sample 33 million. Following quality control checks, the samples were analysed using the open access high throughput sequencing portal, UseGalaxy.org. Significantly different genes were further analysed using supraHex.

4.2.5 Radioimmunoassay (RIA)

Trunk blood was collected at all time points and treatment immediately following decapitation. Corticosterone levels were measured following an in-house corticosterone assay using a gamma counter (Perkin Elmer, USA) (for full details, please see methods section).

4.3 Results

4.3.1 Assessment of corticosterone levels in blood in control and MPL treated

The PVN of the hypothalamus releases CRH in the presence of a circadian cue from the SCN or in response to stress which activates the release of ACTH from the pituitary gland. The release of ACTH in turn acts on the adrenal gland to secret CORT. As the PVN is activated in the presence of a circadian cue or the presence of a stressor, the secretion profile of CORT in circulating blood is circadian in rhythm in a non-stressed animal. The secretion of CORT in this way is vital for many processes, in particular in the hippocampus, where it is instrumental in the mechanisms involved in memory processing and sleep. Glucocorticoids have been shown to regulate gene expression, both in a circadian manner but also following a stress response. Glucocorticoids targeting of the hippocampus should affect gene transcription. However, it was still important to assess the circulating levels of

CORT in the animals used for the RNAseq studies, to confirm that in the control group, expectant levels of circulating CORT were measured (based on data from our lab and others), and that the MPL treated animals were HPA axis suppressed, as expected following GC treatment due to the negative feedback systems of the axis.

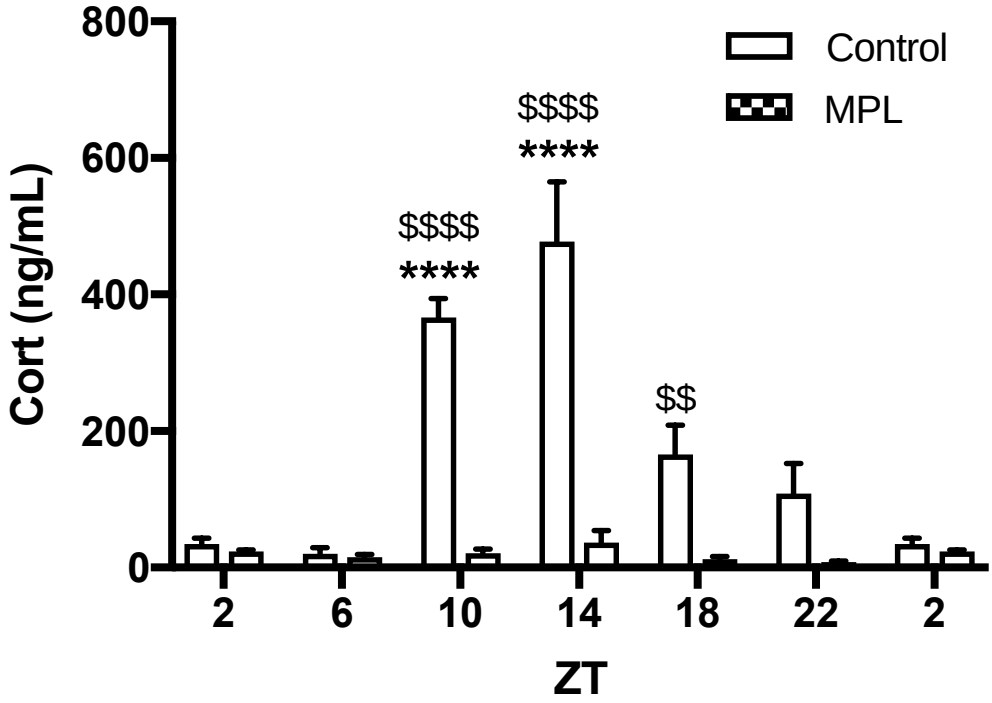

Figure 4.1 RIA of the circadian secretion of corticosterone in control animals and the loss of circadian CORT secretion with MPL treatment. In control animals, the secretion of CORT increases in preparation for the active period, with clear circadian rhythm evident. Circulating CORT levels in the MPL treated group are significantly blunted, with no circadian profile evident. All data represented as mean ± SEM. N = 4 per group. Analysis with Two-way ANOVA with Sidak's post-hoc test. * represent significant effect of time, $ represent significant effect of treatment. All statistical significance indicated at $P < 0.05$ (*), $P < 0.01$ (**), $P < 0.001$ (***) and $P < 0.0001$ (****). ZT2 repeated for visualisation purposes.

The secretion of CORT in control animals exhibit a clear circadian profile with no elevated levels observed in individual animals. The secretion of CORT is significantly blunted in the MPL treated group, with no evidence of a circadian rhythm evident. All data represented as mean ± SEM. N = 4 per group. Two-way ANOVA with Sidak's post-hoc

test was used in (**d**). All statistical significance indicated at $P < 0.05$ (*), $P < 0.01$ (**), $P < 0.001$ (***) and $P < 0.0001$ (****).

Corticosterone is secreted from the adrenal gland following the activation of the HPA axis. The PVN is activated in the presence of circadian cues from the SCN, as well as in the presence of a stressor. Prior to assessing the whole transcriptome for gene expression changes in the presence of synthetic glucocorticoid treatment, it was important to assess the circulating levels of endogenous glucocorticoids in the blood, to confirm that gene expression changes did not occur due to a stressor. In control rats, there was a clear and significant circadian rhythm of CORT in the blood. The levels of CORT were low during the inactive period (ZT2 – 34.00ng/mL) (ZT6 – 20.00ng/mL), as expected, before reaching its circadian peak just prior to, and during the onset of activity (ZT10 – 366.40ng/mL – P=0.0001) (ZT14 – 477.56ng/mL – P=0.0001) and then returning to low levels in preparation for the inactive period (ZT18 – 165.65ng/mL) (ZT22 – 108.06ng/mL). Following treatment with MPL, the secretion of CORT is no longer circadian with no significant difference observed across time points (ZT2 – 23.50ng/mL) (ZT6 – 15.04ng/mL – P = 0.8281) (ZT10 – 21.16ng/mL – P = 0.9996) (ZT14 – 36.21ng/mL – P = 0.5753) (ZT18 – 12.38ng/mL – P = 0.6255) (ZT22 – 7.948ng/mL – P = 0.3123). Two-way ANOVA identified a significant effect of treatment at (ZT10 – P<0.0001) (ZT14 – P<0.0001) (ZT18 – P = 0.0069).

4.3.2 Profiling of mRNA in hippocampus using RNA sequencing

Following assessment of circulating CORT in the blood of control and MPL treated animals, with a circadian profile evident in the controls and a suppression of CORT in the MPL treated group, I assessed gene expression in the hippocampus, focusing on circadian regulated genes and genes that were controlled by glucocorticoid exposure, in the absence of a stress.

The hippocampus is a major structure of the limbic system that plays a vital role in spatial navigation and sleep processing. Stress paradigms can impair hippocampal dependent memory tasks, as well as a lack of the stress hormone, altering the optimal synaptic plasticity and firing properties of neurons of the CA1 region of the hippocampus (Benoit et al. 2015).

The GR and MR are abundantly expressed in the HC; however, their expression varies depending on the sub region of the HC itself. Circulating glucocorticoids target the HC promoting gene expression of glucocorticoid regulated genes, including *Per1*. The HC also modulates the response to stress and circadian variations in GCs forming negative feedback inhibition of the HPA axis, preventing further secretion of GCs. Blocking the GR in the HC reduces the HC's inhibitory influence on the HPA axis, and therefore increases CORT levels (Boyle et al. 2005).

Here, whole transcriptomic gene expression has been characterised from the whole HC, rather than individual sub regions. Using whole transcriptomic sequencing enabled me to assess the effects of the glucocorticoid steroid, as well as the changes in gene expression of control animals, across the whole genome for significant changes rather than a subset of genes of interest. Here I have presented the significantly regulated gene targets as characterised by RNAseq analysis, DAVID pathway analysis and further looked at the expression of the core clock components in the HC. qPCR analysis of these targets was used to confirm the analysis carried out during RNAseq.

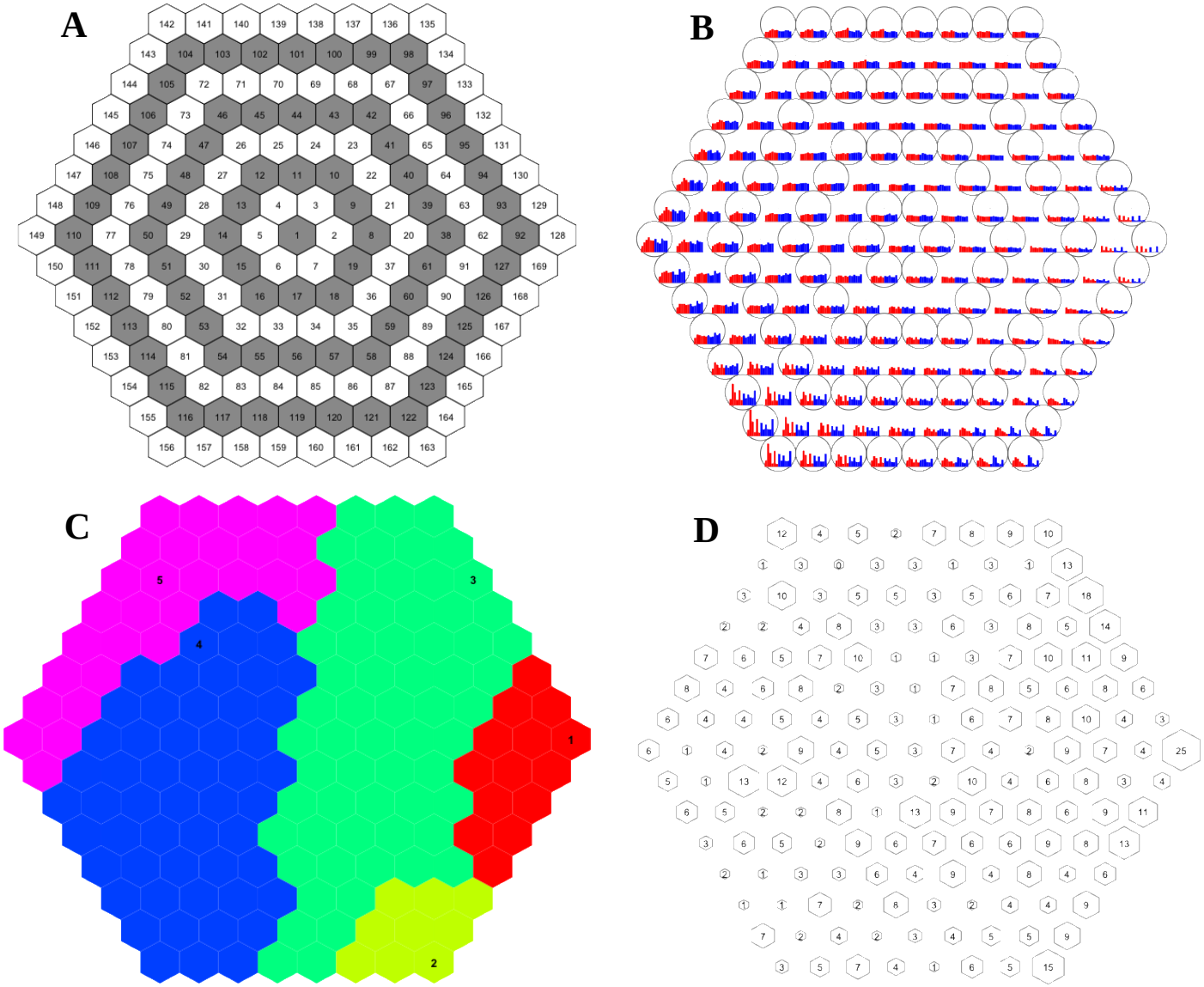
A
B
C
D

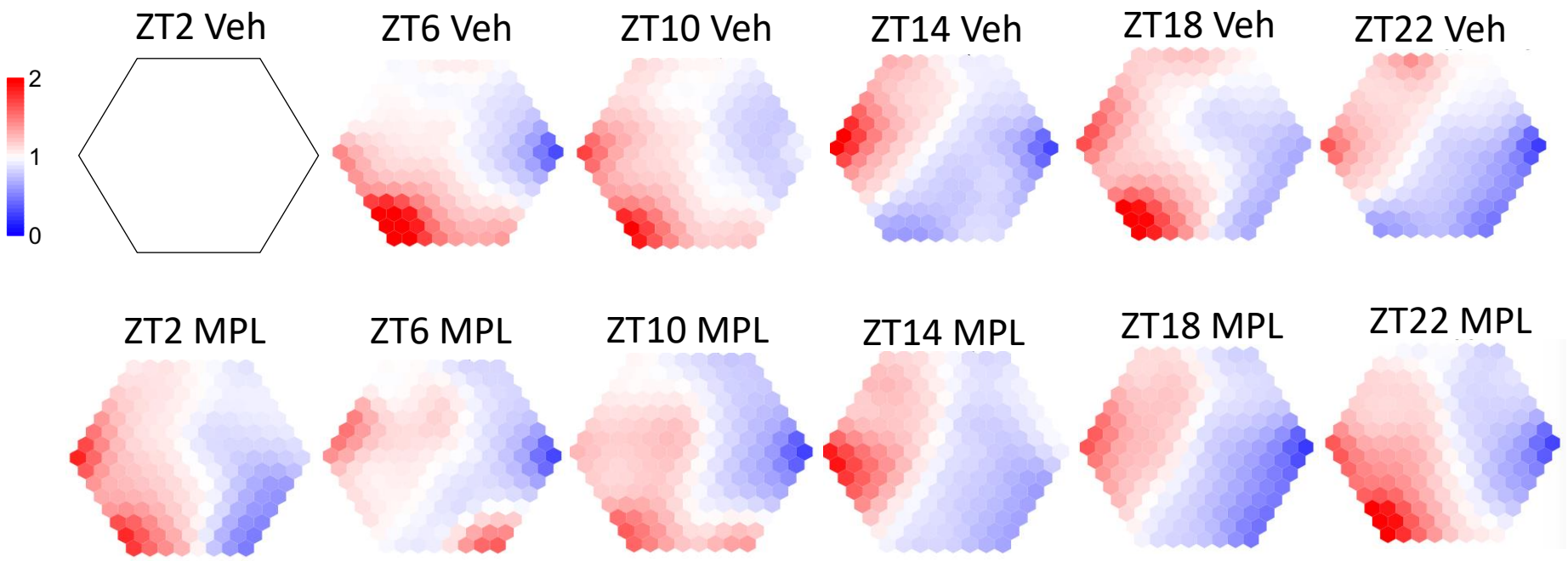

Figure 4.2 supraHEX analysis of high throughput RNA sequencing data comparing control and MPL treated rats. supraHEX is a suprahexagonal map that utilises hierarchical clustering to place significantly regulated genes into smaller hexagons based on basal expression (**A**). Expression profiles based on basal expression (**B**). Genes are further clustered into larger groups of similar expressing values (**C**). The number of genes clustered into each hexagon (**D**). A suprahexagonal hierarchical clustering heatmap mapping gene expression changes through time (**E**), where RED = high expression and BLUE = low expression. RNAseq data from control and MPL treated animals over 6 time points throughout the day were analysed using Galaxy (methods) with differential expression. CuffDiff revealed 946 genes that were significantly differentially expressed. Significance in CuffDiff is calculated using Benjamini-Hochberg correction for multiple testing of P-values less than the false discovery rate set by the program at $P < 0.05$.

4.3.2.1 supraHex analysis of high throughput RNA sequencing data

948 significantly regulated genes were found using the Galaxy Next-Generation sequencing portal and were analysed further using supraHex, a bioinformatics program that places gene expression data using a hierarchical clustering paradigm, of which 517 genes were identified to be significantly regulated in the control group and 663 genes were identified to be significant regulated in the MPL treated group. supraHex arranges genome-wide data into groups of similar gene expression profiles, and position them into either the same, or nearby small hexagons that make up the supraHex. This analysis program allows for the hierarchical clustering of a large dataset to place gene patterns into specific hexagons based upon their basal expression, with the heatmap indicating the change in expression over time and across treatments. Control ZT2, ZT6, ZT10, ZT14, ZT18 and ZT22, as well as MPL treated animals at equivalent time points were assessed. Significantly regulated genes are positioned based upon basal expression of control ZT2, and at each time point following, the heatmap distinguishes their relative expression, either induction (shown in red) or repression (shown in blue). Gene expression changes can be visualised in (**E**), where changes in expression of genes in each node is shown by a change in colour of that particular hexagon. Darkest red contains the highest expressing genes, with darkest blue representing the lowest expressing genes. The colour gradient represents the intermediate expression levels, with the colour key representing log2 data.

Each sub-hexagon is numbered according to the layout shown (**A**) with the number of genes assigned to each sub-hexagon denoted (**D**). The gene expression profiles that correspond to each sub-hexagon are shown in (**B**), with a simple colour key to denote control or MPL treatment and time. The sub-hexagons are further clustered into 5 meta-clusters, representing larger groups of similar expression (**C**). 111 genes were located in cluster 1, 62 genes in cluster 2, 394 in cluster 3, 246 in cluster 4 and 132 in cluster 5. A selection of genes from each cluster are shown in table 4.1. The meta-cluster that represents circadian rhythmic genes are located in meta-cluster 5 such as *Per1* in sub-hexagon 105 and *Per2* in sub-hexagon 106 along with glucocorticoid regulated gene targets *Sgk1* and *Gilz*, located in sub-hexagon 147. A selection of genes and the meta-cluster in which they fall can be observed in table 4.1.

Table 4.1. Selection of genes identified in each metacluster and the expression profile associated with each metacluster.

Metacluster	Gene	Expression profile
1	*Ddit4, NeuroD4, Tph1, Fos, Ptgds, Kif19, Hspb1, Eno2, Cdkn1a, Pear1, Grk1*	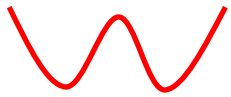
2	*Igf2, Igfbp2, Pla2g5, Mmp2, Glycam1, Slc2a12, Dsg2, Mfrp, Tmem27, Lect1*	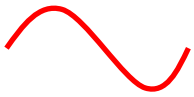
3	*Egr1, Grin2a, Rgs9, Il1r1, Fkbp4, Kif26b, Wnt4, Camk2a, Fnbp1, Notch1, Fkbp8, Sox2*	
4	*Dbp, Gh1, Klf13, Camk2d, Olfm2, Grm2, Klf9, Per3, Nr4a2, Mt2A, Vapb, Lhx2, Mt1m*	
5	*Nfkbiz, Gpd1, Sgk1, Tsc22d3, Dusp5, Cryab, Klf15, Per1, Per2, Fkbp5, Nt5e*	

4.3.2.2 Assessment of changes in gene expression using supraHex

Basal expression of genes in each hexagon is shown in the ZT2 control group, where expression is forced to 1, with all other hexagons expressed as an induction or repression of that number. As each gene is maintained in the same sub-hexagon in the defined supra-hexagonal map, differences in expression between control and MPL treated, as well as differences in time can be observed as differences in the colour of corresponding sub-hexagons in a direct comparison to either ZT2 control, or its equivalent time, between treatments.

A robust example to show the change in expression can be observed in sub-hexagon 105, where PER1 is placed, in the top left corner of the supraHex. In control animals over time, a steady increase in expression is evident, with the highest levels occurring at ZT10-18, before returning close to baseline at ZT22. In the MPL group however, where it is placed in the same sub-hexagonal position, the expression of *Per1* at ZT2 is significantly different from control, with an increase evident, before lowering to similar levels at ZT6, as what is seen at ZT2 in control. The elevated level of expression of *Per*1 in MPL appears to be

highest at ZT14-22, eluding to a possible phase shift in expression of *Per1* in the presence of MPL.

4.3.2.3 Navigating the supraHex model

The dataset is 'trained' in a highly specific manner and is therefore unique to this particular dataset. The central sub-hexagon (1) represents genes with a median level of expression. To the right of the central sub-hexagon are genes that decrease in overall expression, where sub-hexagon 128 contains low abundant but significant regulated genes such as *NeuroD4* and *Tph1*, and the left of the central sub-hexagon (149) that contains genes that are the most abundant and significantly regulated in overall expression, such as *Calcium/Calmodulin Dependent Protein Kinase II Delta* (*Camk2δ*) and *Solute Carrier family 19 member 3* (*SLC19A3*).

The supraHex map shows overall that a large number of genes are under circadian control and in the presence of the glucocorticoid steroid MPL, the expression profile of those genes become dysregulated. For instance, the expression of *Per1*, *Per2* and *Cry1* are all significantly altered in the presence of MPL. Glucocorticoid target genes such as *Sgk1* and *Gilz* are also significantly dysregulated in the presence of this long acting glucocorticoid steroid.

4.3.2.4 Pathway analysis of RNAseq data using DAVID

RNA sequencing allows for the identification of the transcriptome and to accurately measure the levels of transcripts and their isoforms far more precisely than any other technique. It therefore also provides the experimenter with a large dataset to analyse. DAVID (Database for Annotation, Visualisation and Integrated Discovery) (Huang, Brad T. Sherman, et al. 2009; Huang, Brad T Sherman, et al. 2009) is an open access program that clusters related groups of genes and identifies pathways affected, gene-disease association and uses KEGG, which is a collection of biological pathways, diseases and drugs databases to understand what effect individual gene transcripts may have.

Further analysis of the supraHEX dataset in DAVID identified multiple pathways involved as displayed in table 4.2 and figures 4.3 - 4.7.

Table 4.2. DAVID analysis identifying pathways targeted

Sublist	Category	Term	RT	Genes	Count	%	P-Value	Benjamini
	KEGG_PATHWAY	ECM-receptor interaction	RT		23	2.6	8.3E-11	2.1E-8
	KEGG_PATHWAY	Focal adhesion	RT		34	3.9	7.6E-10	9.4E-8
	KEGG_PATHWAY	PI3K-Akt signaling pathway	RT		41	4.6	6.0E-8	5.0E-6
	KEGG_PATHWAY	Circadian entrainment	RT		19	2.2	5.0E-7	3.1E-5
	KEGG_PATHWAY	Cholinergic synapse	RT		20	2.3	1.0E-6	5.1E-5
	KEGG_PATHWAY	Glutamatergic synapse	RT		19	2.2	6.5E-6	2.7E-4
	KEGG_PATHWAY	Calcium signaling pathway	RT		24	2.7	1.9E-5	6.7E-4
	KEGG_PATHWAY	Protein digestion and absorption	RT		15	1.7	6.6E-5	2.0E-3
	KEGG_PATHWAY	Proteoglycans in cancer	RT		24	2.7	7.1E-5	2.0E-3
	KEGG_PATHWAY	Gastric acid secretion	RT		13	1.5	1.4E-4	3.5E-3
	KEGG_PATHWAY	cAMP signaling pathway	RT		22	2.5	3.4E-4	7.7E-3
	KEGG_PATHWAY	Bile secretion	RT		12	1.4	4.5E-4	9.4E-3
	KEGG_PATHWAY	Pathways in cancer	RT		35	4.0	5.4E-4	1.0E-2
	KEGG_PATHWAY	Retrograde endocannabinoid signaling	RT		14	1.6	1.1E-3	1.9E-2
	KEGG_PATHWAY	GnRH signaling pathway	RT		13	1.5	1.2E-3	2.0E-2
	KEGG_PATHWAY	Cocaine addiction	RT		9	1.0	1.2E-3	1.9E-2
	KEGG_PATHWAY	Estrogen signaling pathway	RT		13	1.5	1.8E-3	2.6E-2
	KEGG_PATHWAY	Amoebiasis	RT		14	1.6	2.3E-3	3.2E-2
	KEGG_PATHWAY	Nicotine addiction	RT		8	0.9	2.4E-3	3.1E-2
	KEGG_PATHWAY	Amphetamine addiction	RT		10	1.1	2.9E-3	3.6E-2
	KEGG_PATHWAY	Oxytocin signaling pathway	RT		17	1.9	3.6E-3	4.2E-2
	KEGG_PATHWAY	Serotonergic synapse	RT		14	1.6	5.6E-3	6.2E-2
	KEGG_PATHWAY	Neuroactive ligand-receptor interaction	RT		25	2.8	5.7E-3	6.0E-2
	KEGG_PATHWAY	Aldosterone synthesis and secretion	RT		11	1.2	6.0E-3	6.1E-2
	KEGG_PATHWAY	Axon guidance	RT		14	1.6	7.3E-3	7.1E-2
	KEGG_PATHWAY	GABAergic synapse	RT		11	1.2	7.7E-3	7.1E-2
	KEGG_PATHWAY	Dopaminergic synapse	RT		14	1.6	7.8E-3	7.0E-2
	KEGG_PATHWAY	Salivary secretion	RT		10	1.1	9.3E-3	8.0E-2
	KEGG_PATHWAY	Circadian rhythm	RT		6	0.7	1.2E-2	1.0E-1
	KEGG_PATHWAY	Vascular smooth muscle contraction	RT		13	1.5	1.2E-2	9.9E-2
	KEGG_PATHWAY	Hypertrophic cardiomyopathy (HCM)	RT		10	1.1	1.3E-2	9.8E-2
	KEGG_PATHWAY	Rap1 signaling pathway	RT		19	2.2	1.4E-2	1.0E-1
	KEGG_PATHWAY	Pancreatic secretion	RT		11	1.2	1.5E-2	1.1E-1
	KEGG_PATHWAY	Dilated cardiomyopathy	RT		10	1.1	1.7E-2	1.2E-1
	KEGG_PATHWAY	Arrhythmogenic right ventricular cardiomyopathy (ARVC)	RT		9	1.0	1.8E-2	1.2E-1
	KEGG_PATHWAY	Gap junction	RT		10	1.1	2.3E-2	1.5E-1
	KEGG_PATHWAY	Ras signaling pathway	RT		19	2.2	2.5E-2	1.6E-1
	KEGG_PATHWAY	Phototransduction	RT		5	0.6	2.8E-2	1.7E-1
	KEGG_PATHWAY	Morphine addiction	RT		10	1.1	2.9E-2	1.7E-1
	KEGG_PATHWAY	MicroRNAs in cancer	RT		13	1.5	3.8E-2	2.1E-1
	KEGG_PATHWAY	Alcoholism	RT		15	1.7	3.9E-2	2.1E-1
	KEGG_PATHWAY	Osteoclast differentiation	RT		12	1.4	4.1E-2	2.2E-1
	KEGG_PATHWAY	Thyroid hormone signaling pathway	RT		11	1.2	4.5E-2	2.3E-1
	KEGG_PATHWAY	TGF-beta signaling pathway	RT		9	1.0	5.0E-2	2.5E-1
	KEGG_PATHWAY	Platelet activation	RT		12	1.4	5.4E-2	2.7E-1
	KEGG_PATHWAY	HTLV-I infection	RT		21	2.4	5.9E-2	2.8E-1
	KEGG_PATHWAY	MAPK signaling pathway	RT		19	2.2	6.4E-2	3.0E-1
	KEGG_PATHWAY	ErbB signaling pathway	RT		9	1.0	6.5E-2	3.0E-1
	KEGG_PATHWAY	Chemokine signaling pathway	RT		14	1.6	7.6E-2	3.3E-1
	KEGG_PATHWAY	Vitamin digestion and absorption	RT		4	0.5	8.3E-2	3.5E-1
	KEGG_PATHWAY	Long-term potentiation	RT		7	0.8	8.6E-2	3.5E-1
	KEGG_PATHWAY	Inflammatory mediator regulation of TRP channels	RT		10	1.1	9.4E-2	3.8E-1

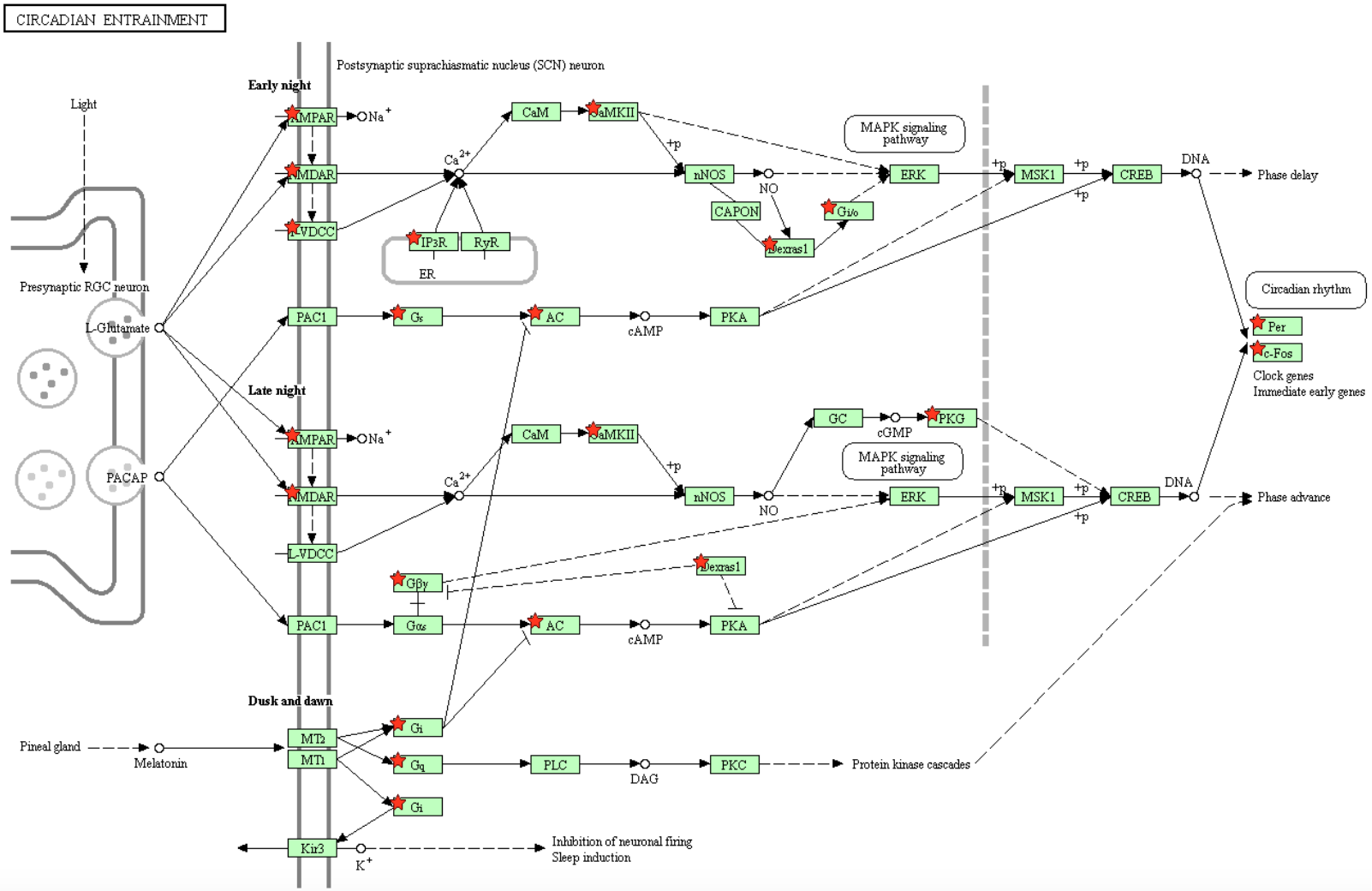

Figure 4.3 Circadian entrainment pathway

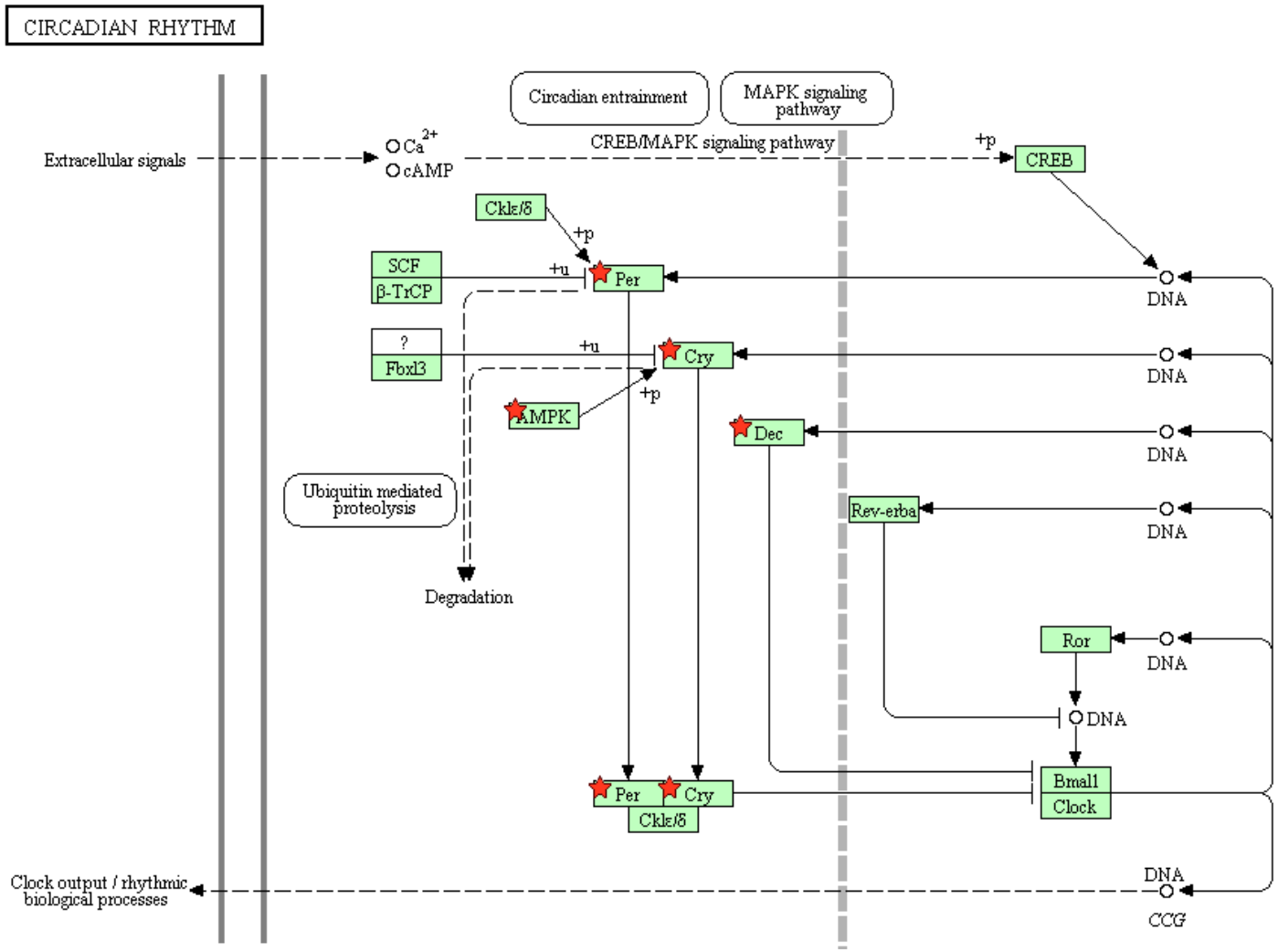

Figure 4.4 Circadian rhythm pathway

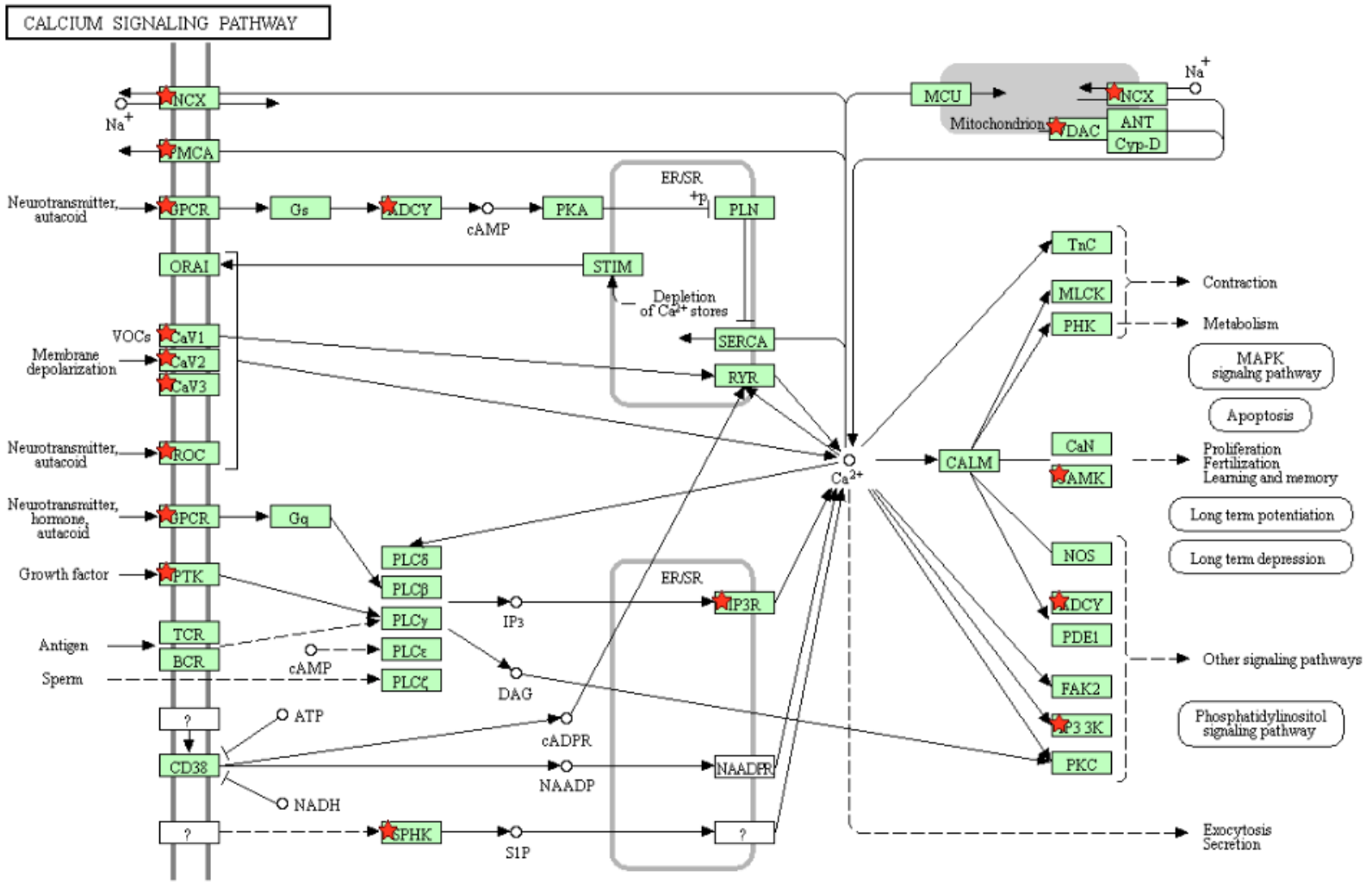

Figure 4.5 Calcium Signalling pathway

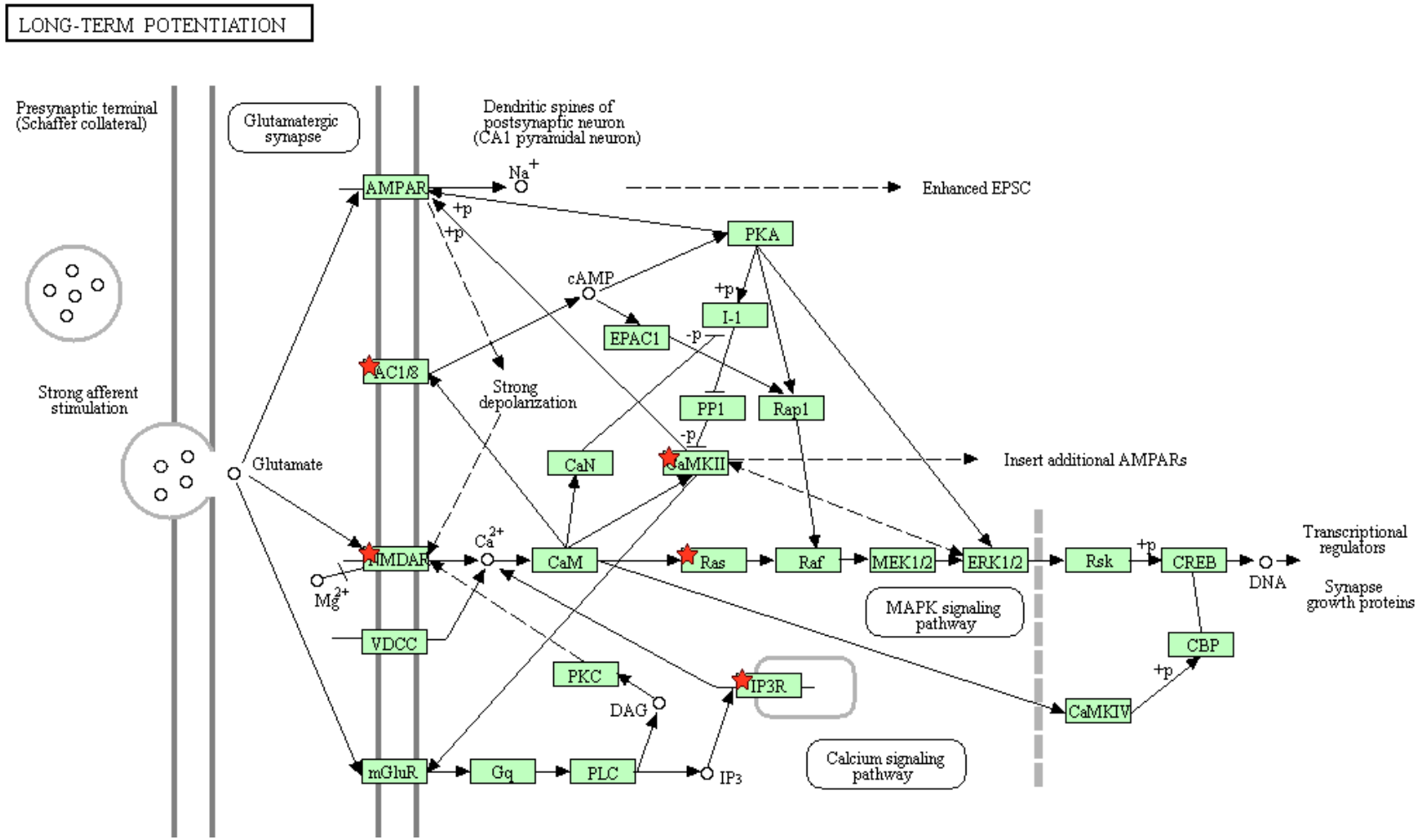

Figure 4.6 Long-term potentiation pathway

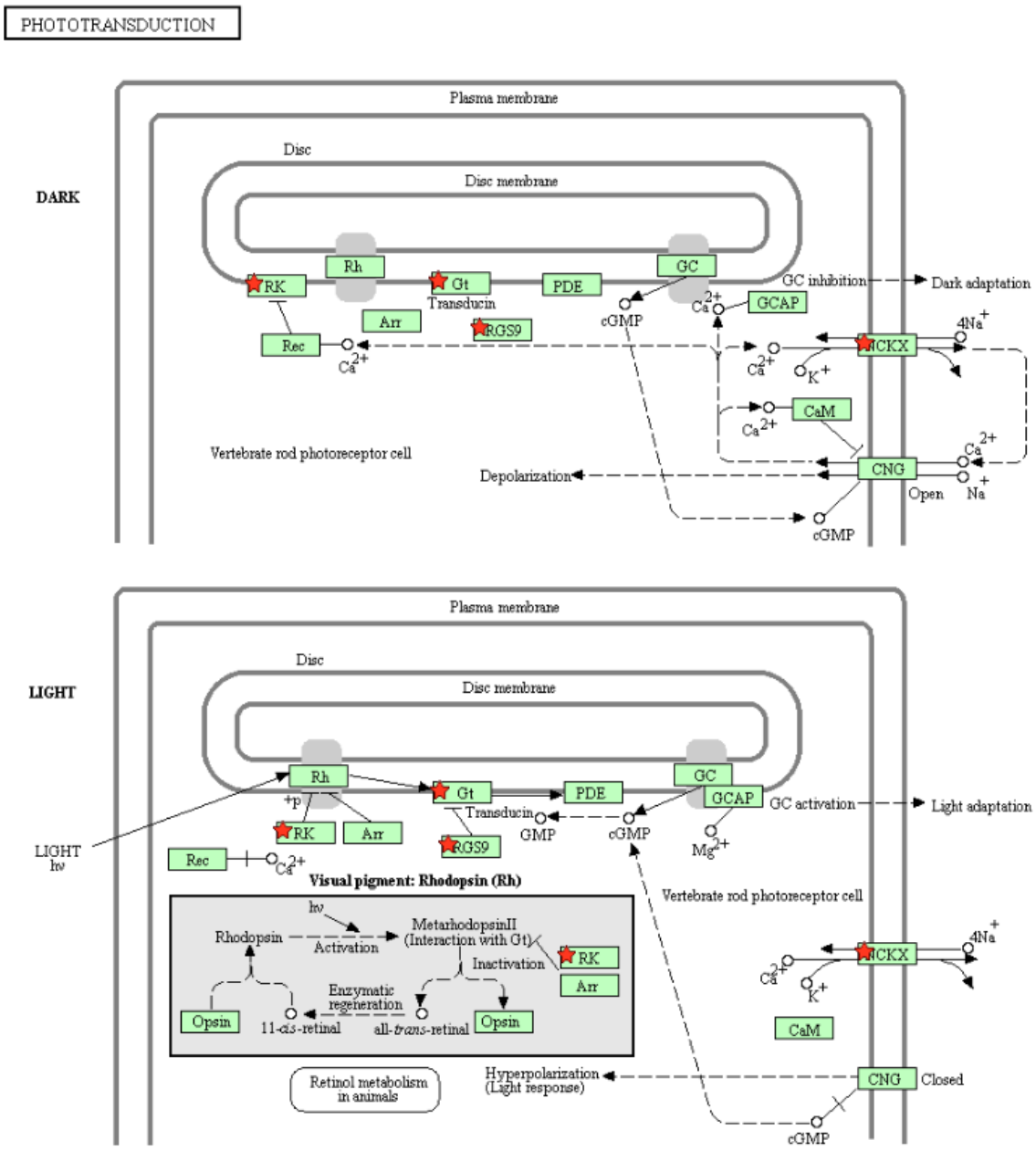

Figure 4.7 Phototransduction pathway

A number of pathways were identified using DAVID as shown in table 4.2 and expanded further with a selection of pathways in figures 4.3-7. DAVID provides a useful overview of pathways targeted from this experimental design, however further analysis would need to be carried out to identify if these individual pathways are affected. Importantly, DAVID did provide pathway identification for circadian entrainment (Figure 4.3) and rhythms (Figure 4.4) as well as calcium signalling (Figure 4.5) and long-term potentiation (Figure 4.6), both of which are important for learning and memory processes. Following supraHex

and DAVID pathway analysis, it was important to confirm the gene expression profiles as confirmation of data analysis.

4.3.3 Clock gene expression analysis from supraHex using qPCR

The supraHex model of high throughput RNA sequencing data analysis carried out using Galaxy yielded hypothesised results and expectant results based on the literature and gene expression studies previously carried out, albeit in different tissues. However, it was still important to validate the results collected using an independent method assessing the gene expression using the same samples ran to analyse from RNAseq. Following the RNAseq analysis, it was clear that the clock mechanism was a major target, with it showing robust changes throughout the day in control, but also because glucocorticoids target the major transcriptional repressor of the clock system, *Per1*. Therefore, based upon this and the data shown in the SCN shown in chapter 3, I have assessed using qPCR, the levels of mRNA in control and MPL treated animals over the circadian period.

4.3.3.1 *Per1* mRNA expression

Following analysis of the RNAseq data using CuffDiff and visualization with supraHex, assessment of the expression of *Per1* mRNA in the HC over one circadian cycle in control and following treatment with MPL was carried out. The expression of *Per1* in the HC has previously been shown, with a circadian rhythm evident, and notably delayed in peak expression compared to the master clock, located in the SCN, where peak expression occurs during the light phase, and in the hippocampus, peak expression occurs at the onset of activity, in the dark period. Also, following the expression changes observed of *Per1* in the SCN following MPL treatment in chapter 3, it was important to see if it affected the expression of *Per1* in this major brain region, which is also a target of SCN daily rhythms.

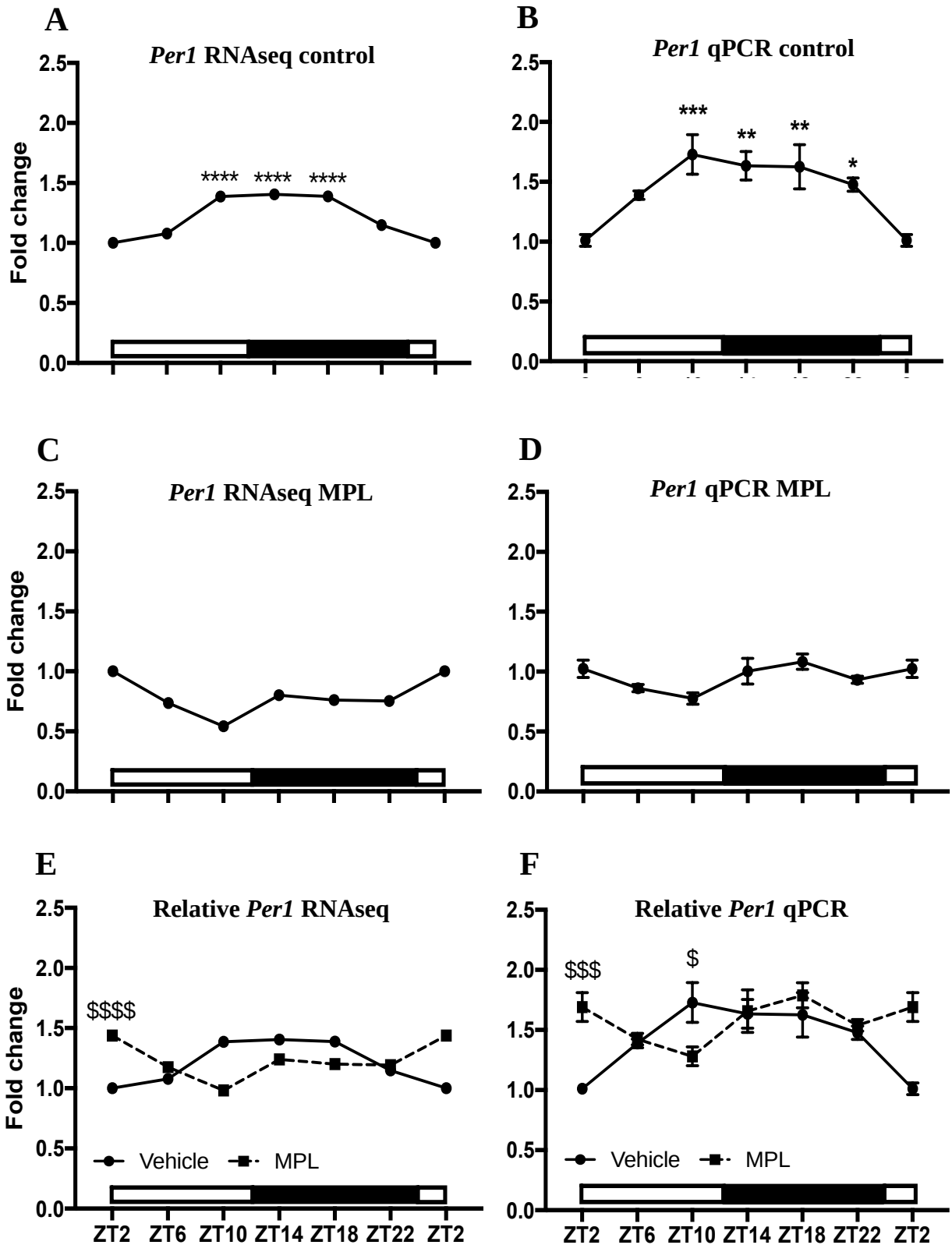

Figure 4.8 *Per1* mRNA expression is altered in the HC with MPL treatment. Analysis from RNAseq and qPCR show *Per1* mRNA expression is altered following MPL treatment. From RNAseq, in control animals (**A**), mRNA expression is circadian with the highest

levels occurring during the most active period of the animal between ZT10-18. qPCR of this target validated the RNAseq data (**B**). Following MPL treatment, the circadian profile of *Per1* expression was lost, with a flattening evident in both the RNAseq dataset (**C**) and qPCR (**D**). Assessment of the relative levels of *Per*1 expression between controls and MPL treated presented a significant elevation in expression at ZT2 in the MPL treated group only in the RNAseq dataset (**E**), whereas there was an additional significant difference at ZT10 in the qPCR dataset (**F**). RNAseq data represented as mean. N = 4 per group. One-way ANOVA with Benjamini-Hochberg post-hoc test was used, with all comparisons to ZT2 in graphs (**A**) and (**C**). Two-way ANOVA with Benjamini-Hochberg post-hoc was used in graph (**E**). qPCR data represented as mean ± SEM. N = 4 per group. One-way ANOVA with Dunnett's post-hoc test was used, with all comparisons to ZT2 in graphs (**B**) and (**D**). Two-way ANOVA with Sidak's post-hoc test was used in (**F**). All statistical significance indicated at $P < 0.05$ (*), $P < 0.01$ (**), $P < 0.001$ (***) and $P < 0.0001$ (****). ZT2 repeated for visualisation purposes.

The expression of *Per1* in the hippocampus is robust in these data. In the RNAseq analysis, *Per1* mRNA expression in controls (**A**) was robustly circadian, with P value and Q value significance reported at ZT10 ($P < 0.00005$, $Q = 0.0158$), ZT14 ($P < 0.00005$, $Q = 0.0066$) and ZT18 ($P < 0.00005$, $Q = 0.0133$). A trend to P value significance was calculated at ZT22 ($P = 0.0511$), however the false discovery rate indicated that no effect of time was observed here ($Q = 0.623$). qPCR validation of *Per1* (**B**) also confirmed the expected significant circadian rhythm of expression, with the expression profiles nearly identical between RNAseq and qPCR analysis ($F_{6,21} = 7.151$, $p = 0.0003$). A significant increase in gene expression was observed at ZT10 ($P = 0.0008$), ZT14 ($P = 0.0034$), ZT18 ($P = 0.0038$) and ZT22 ($P = 0.0329$). Following MPL treatment, analysis from RNAseq (**C**) and qPCR (**D**) produced a consistent result, with no significant change in expression observed across any time point, and a flattening of the circadian profile observed. When the relative expression was assessed using these techniques, a significant effect of *Per1* expression was evident in the RNAseq analysis (**E**) at ZT2 ($P < 0.00005$, $Q = 0.0130$). P value significance was also observed at ZT10 ($P = 0.0215$), ZT14 ($P = 0.0062$) and ZT18 ($P = 0.01535$), however the FDR calculated these differences to be non-significant ZT10 ($Q = 0.6626$), ZT14 ($Q = 0.3208$) and ZT18 ($Q = 0.2607$). Analysis of relative expression from qPCR data (**F**) also exhibited a significant effect of time ($F_{6,42} = 3.283$, $p = 0.0097$), treatment ($F_{1,42} = 8.512$, $p = 0.0056$) and interaction between time and treatment ($F_{6,42} = 6.668$, p

<0.0001). Post hoc analysis showed the robust and significant increase in expression of *Per1* at ZT2 (P = 0.0005), but also at ZT10 (P = 0.0408).

4.3.3.2 *Per2* mRNA expression

Per2 expression in the HC has been assessed, with the expression shown to increase as the day progresses into the active period (Moriya et al. 2014). In *Per1*$^{(-/-)}$ mice, *Per2* will compensate for *Per1* and act to regulate the clock mechanism. Therefore, the rhythm of *Per2* would be expected to be similar to that of *Per1* in the HC. Conflicting evidence of a GRE driving *Per2* expression have been published, however this is still unknown (Cheon et al. 2013). Like *Per1* in the HC, the expression of *Per2* is delayed in peak expression to the master clock in the SCN. Following the effect of *Per1* alteration in the HC, and due to the literature eluding to a compensatory mechanism of *Per2*, it was important to see if *Per2* mRNA expression remained circadian and in timing with controls, following treatment with MPL.

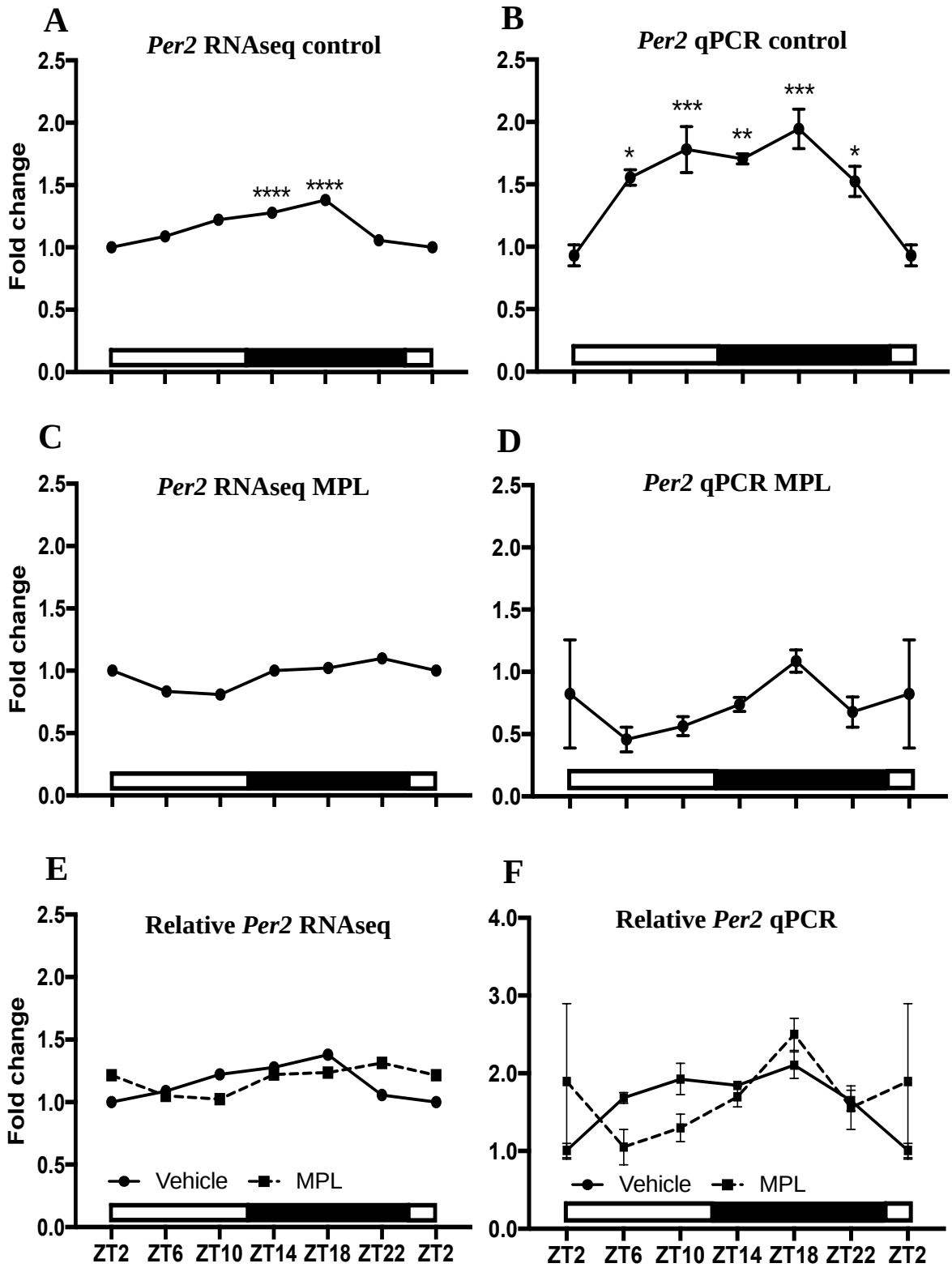

Figure 4.9 *Per2* mRNA exhibits a similar profile to *Per1* in the HC with MPL treatment. Similarly, to the expression of *Per1*, *Per2* mRNA was characterised from RNAseq data and qPCR data. From RNAseq, in control animals (**A**), *Per2* mRNA was significantly circadian in rhythm with the highest levels of expression evident during the

most active period, like *Per1* at ZT14 and ZT18. qPCR confirmed this result (**B**). Following MPL treatment, the circadian profile of *Per2* expression was blunted, with no significant difference observed in both RNAseq (**C**) and qPCR (**D**) techniques. Relative levels of mRNA expression were assessed between control and MPL treated rats, with neither RNAseq (**C**) nor qPCR (**F**) exhibiting significant differences between expression at individual time points. RNAseq data represented as mean. N = 4 per group. One-way ANOVA with Benjamini-Hochberg post-hoc test was used, with all comparisons to ZT2 in graphs (**A**) and (**C**). Two-way ANOVA with Benjamini-Hochberg post-hoc was used in graph (**E**). qPCR data represented as mean ± SEM. N = 4 per group. One-way ANOVA with Dunnett's post-hoc test was used, with all comparisons to ZT2 in graphs (**B**) and (**D**). Two-way ANOVA with Sidak's post-hoc test was used in (**F**). All statistical significance indicated at $P < 0.05$ (*), $P < 0.01$ (**), $P < 0.001$ (***) and $P < 0.0001$ (****). ZT2 repeated for visualisation purposes.

Similarly, to *Per1* mRNA expression in the HC, the expression of *Per2* is robust and circadian in pattern. RNAseq analysis of *Per2* expression in controls (**A**) exhibited a clear circadian rhythm, with peak significant expression evident between ZT14 ($P < 0.00005$, $Q = 0.0066$) and ZT18 ($P < 0.00005$, $Q = 0.01334$). P value significance was also quantified at ZT10 ($P = 0.00335$), however the FDR deemed this non-significant ($Q = 0.303161$). Validation of the RNAseq data using qPCR also showed the expected circadian profile (**B**), with qPCR analysis accentuating this rhythm, showing a clear significant effect of time on *Per2* expression ($F_{6,19} = 9.816$, $p < 0.0001$). A significant increase in expression was observed at ZT6 ($P = 0.0118$), ZT10 ($P = 0.0007$), ZT14 ($P = 0.0018$), ZT18 ($P = 0.0001$) and ZT22 (0.0173). The expression of *Per2* following MPL treatment was similar to that shown of *Per1* expression following MPL treatment. RNAseq data analysis (**C**), showed the circadian profile was blunted, with no significant difference observed across time points. This was also matched following qPCR analysis (**D**), however the spread of data at ZT2 in qPCR may have accounted for the lack of difference seen here. Differences in expression between treatments were assessed. RNAseq analysis (**E**) showed no significant difference between treatments, ZT2 was deemed P value significant ($P = 0.00465$), the FDR deemed this difference non-significant ($Q = 0.339815$). qPCR analysis (**F**) also did not yield a significant difference between time, treatment or interaction.

4.3.3.3 *Cry1* mRNA expression

The expression profiles of *Per1* and *Per2* being significantly altered following MPL treatment in the HC, led to the assessment of *Cry1* in the HC. As CRY proteins dimerise with PER proteins to prevent their own transcription, it was important to assess the expression of *Cry1* to see if the glucocorticoid effect through *Per1* would cause secondary effects on other, vital clock components.

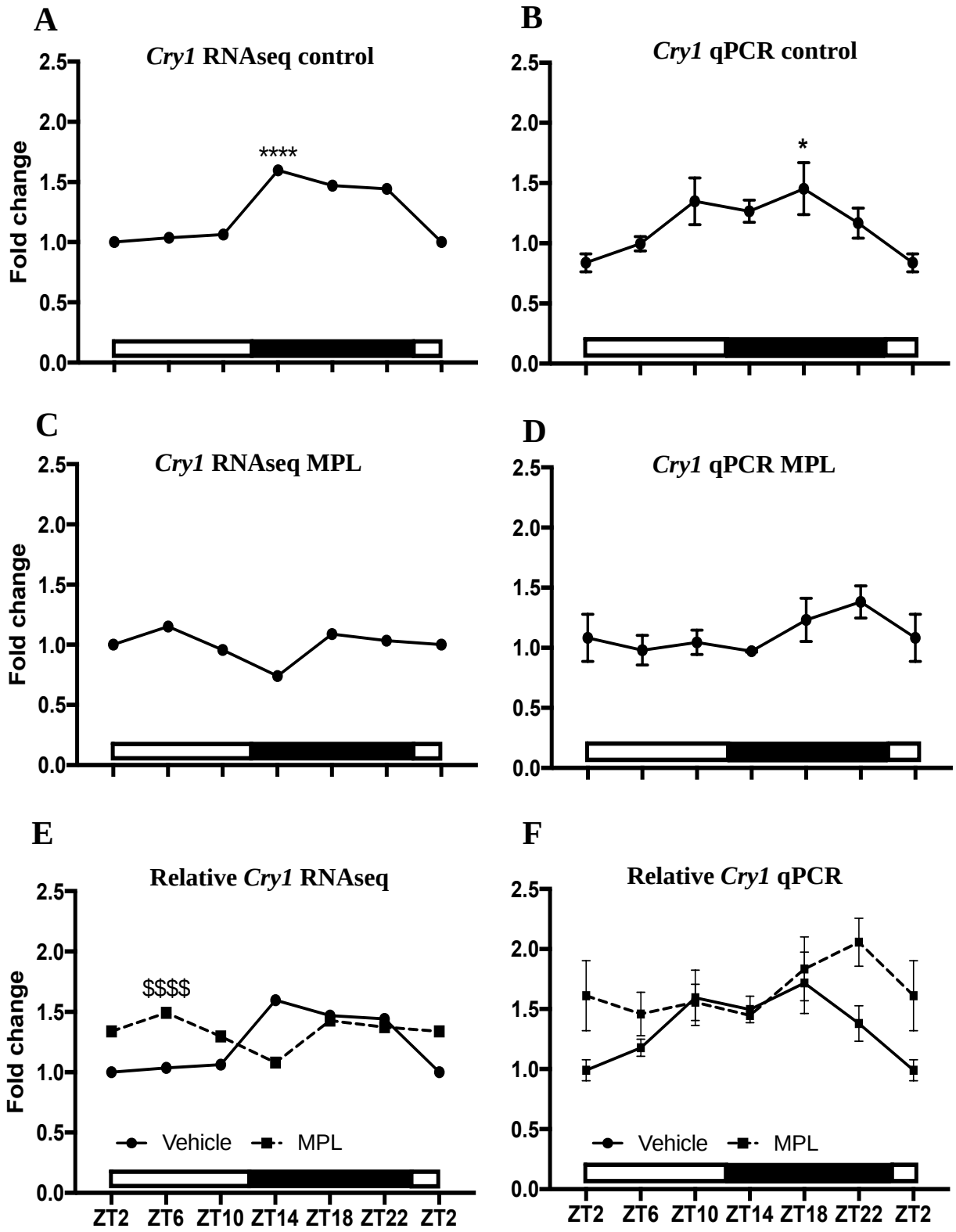
A
Cry1 RNAseq control
Fold change
2.5
2.0
1.5
1.0
0.5
0.0
****
B
Cry1 qPCR control
*
C
Cry1 RNAseq MPL
D
Cry1 qPCR MPL
E
Relative Cry1 RNAseq
$$$$
Vehicle
MPL
ZT2
ZT6
ZT10
ZT14
ZT18
ZT22
ZT2
F
Relative Cry1 qPCR

Figure 4.10 *Cry1* mRNA expression is blunted in the HC with MPL treatment. The expression of *Cry1* was firstly assessed using RNAseq and further using qPCR. From RNAseq, the expression of *Cry1* mRNA in the control group (**A**) was circadian, with significant increase in expression observed at ZT14. A significant increase in expression was also observed following qPCR (**B**), however it was noted at ZT18. With MPL treatment, the expression of *Cry1* was significantly altered, with no circadian expression evident, from RNAseq (**C**) and qPCR (**D**) analyses. Relative levels of mRNA showed a significant increase in expression from the RNAseq dataset (**E**) at ZT6, however this was not confirmed with qPCR (**F**). RNAseq data represented as mean. N = 4 per group. One-way ANOVA with Benjamini-Hochberg post-hoc test was used, with all comparisons to ZT2 in graphs (**A**) and (**C**). Two-way ANOVA with Benjamini-Hochberg post-hoc was used in graph (**E**). qPCR data represented as mean ± SEM. N = 4 per group. One-way ANOVA with Dunnett's post-hoc test was used, with all comparisons to ZT2 in graphs (**B**) and (**D**). Two-way ANOVA with Sidak's post-hoc test was used in (**F**). All statistical significance indicated at $P < 0.05$ (*), $P < 0.01$ (**), $P < 0.001$ (***) and $P < 0.0001$ (****). ZT2 repeated for visualisation purposes.

PER and CLOCK proteins dimerise and bind at the E-box element of their genes to prevent transcription from occurring. Following the significant effect that was observed in both *Per1* and *Per2* mRNA expression following treatment, *Cry1* expression was assessed. RNAseq data in controls (**A**) exhibited the clear circadian rhythm of expression that was expected, with significant increase in expression evident at ZT14 ($P < 0.00005$, $Q = 0.00665$). No other time point passed significance thresholds in controls, even though at ZT18 and ZT22, P value significance passed the minimum threshold ($P = 0.00285$) and ($P = 0.0019$), however the FDR deemed these changes non-significant ($Q = 0.234888$) and ($Q = 0.111477$), respectively. Again, this was validated with qPCR (**B**), with a significant effect of time observed in *Cry1* mRNA expression ($F_{6,19} – 2.822$, $p = 0.0389$). A significant increase was observed at ZT18 ($P = 0.0376$). *Cry1* mRNA assessed following MPL treatment significantly affected the circadian profile of expression in both RNAseq (**C**) and qPCR (**D**) analyses, with the profile flattening and resembling a similar profile to that of *Per1* (Fig. 4.3 C/D**)** and *Per2* (Fig. 4.4 C/D**)**. Relative expression between control and MPL treated animals showed a significant effect of treatment of ZT6 ($P = 0.0001$, $Q = 0.0191257$), where *Cry1* mRNA was elevated in the MPL treatment group, as shown from

the RNAseq (**E**). qPCR analysis (**F**) however did not show a significant difference between treatments at any time point, with only a trend of significance observed at ZT22 (P = 0.1190).

4.3.3.4 *Cry2* mRNA expression

Cry2 expression was assessed in the HC using RNAseq and qPCR data. The expression profile of *Cry2* is delayed compared to the expression of *Cry1*, however this was shown in liver, and although it is peripheral to the master clock, the delay may not be evident in the hippocampus (Filiano et al. 2013).

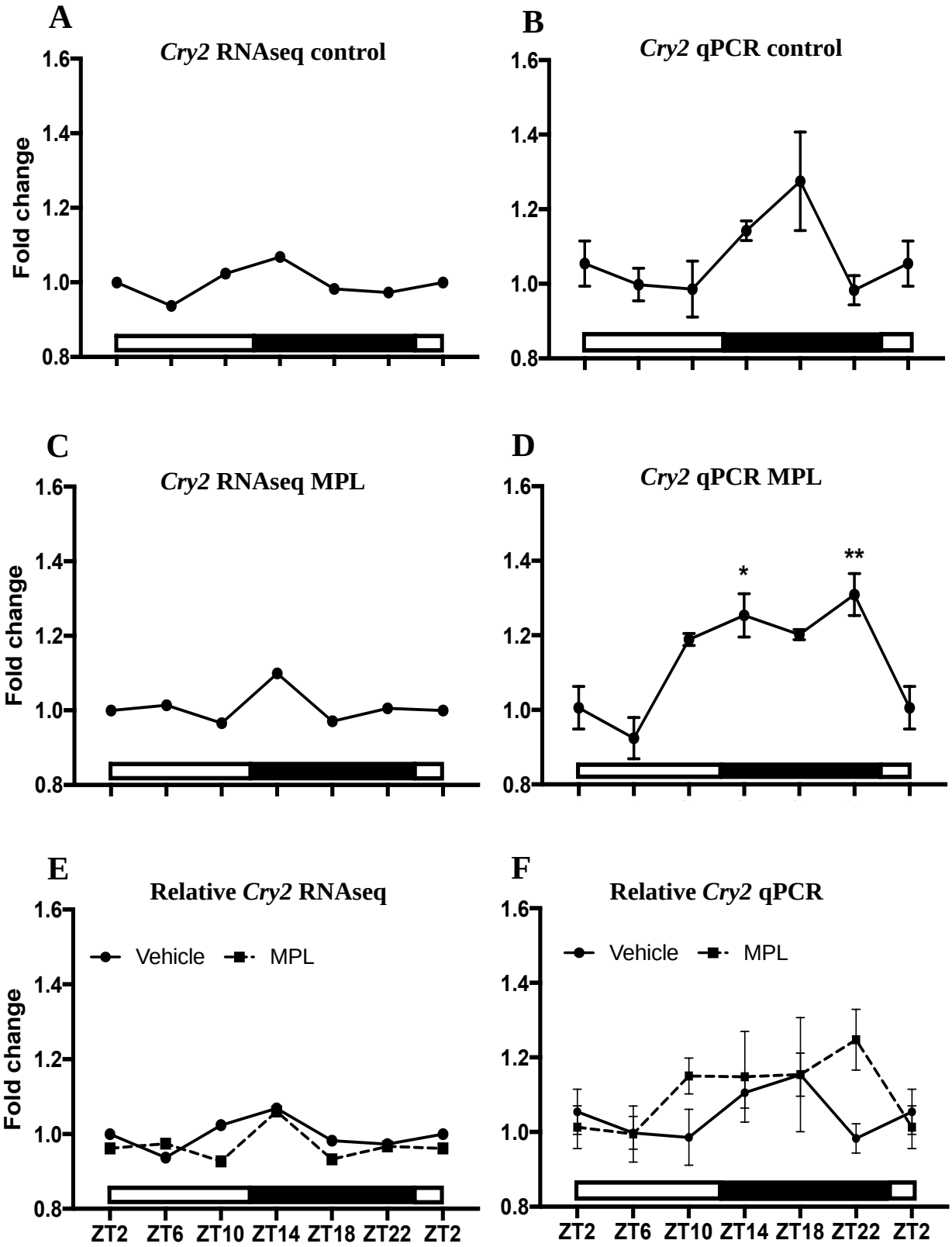
A
Cry2 RNAseq control
B
Cry2 qPCR control
C
Cry2 RNAseq MPL
D
Cry2 qPCR MPL
E
Relative Cry2 RNAseq
F
Relative Cry2 qPCR
Fold change
1.6
1.4
1.2
1.0
0.8
Vehicle
MPL
*
**
ZT2
ZT6
ZT10
ZT14
ZT18
ZT22
ZT2

Figure 4.11 *Cry2* mRNA expression in the HC with MPL treatment displays circadian rhythm. The expression of *Cry2* in the hippocampus did not exhibit a significant circadian profile from RNAseq (**A**) and qPCR (**B**) in control animals. Following MPL treatment, a similar response was shown to controls, with a non-significant change in expression observed across all time points, in the RNAseq data analysis (**C**). However, qPCR (**D**) exhibited a robust a circadian rhythmicity of expression with a significant increase observed at ZT14 and ZT22. Relative levels between treatment groups showed no significant difference at any time point in RNAseq (**E**) or qPCR (**F**). RNAseq data represented as mean. N = 4 per group. One-way ANOVA with Benjamini-Hochberg post-hoc test was used, with all comparisons to ZT2 in graphs (**A**) and (**C**). Two-way ANOVA with Benjamini-Hochberg post-hoc was used in graph (**F**). qPCR data represented as mean ± SEM. N = 4 per group. One-way ANOVA with Dunnett's post-hoc test was used, with all comparisons to ZT2 in graphs (**B**) and (**D**). Two-way ANOVA with Sidak's post-hoc test was used in (**F**). All statistical significance indicated at $P < 0.05$ (*), $P < 0.01$ (**). ZT2 repeated for visualisation purposes.

Analysis of *Cry2* mRNA in the HC yielded some surprising results. Although no significant effect of time was observed in the RNAseq data (**A**), nor following qPCR analysis (**B**), a trend of significance was observed using qPCR ($F_{6,19} – 2.281$, $p = 0.0793$), however the spread of data at each time point meant that no time point was significant (ZT18 – $P = 0.1424$). With MPL treatment, the expression profile from RNAseq (**C**) was similar to its control equivalent, with no significance reported across time points. However, qPCR analysis (**D**) of *Cry2* mRNA following MPL treatment showed a clear, significant circadian profile of expression ($F_{6,16} – 8.018$, $p = 0.0004$), with a significant effect observed at ZT14 ($P = 0.0142$) and ZT22 ($P = 0.0029$), and a trend of significance at ZT18 ($P = 0.0603$). Assessment of relative expression however, showed no significant difference between treatments using both RNAseq (**E**) and qPCR (**F**) paradigms. A trend of significance was observed at ZT22 ($P = 0.1180$).

4.3.3.5 *Bmal1* mRNA expression

Following RNAseq and qPCR assessment of the transcriptional repressors of the molecular clock, it was important to assess the transcriptional activators of the molecular clock, to evaluate if the alteration observed to the primary clock components would affect the transcriptional output of these important components. *Bmal1*, the transcriptional activator of *Per* and *Cry* was assessed in the HC across the circadian period and with MPL treatment.

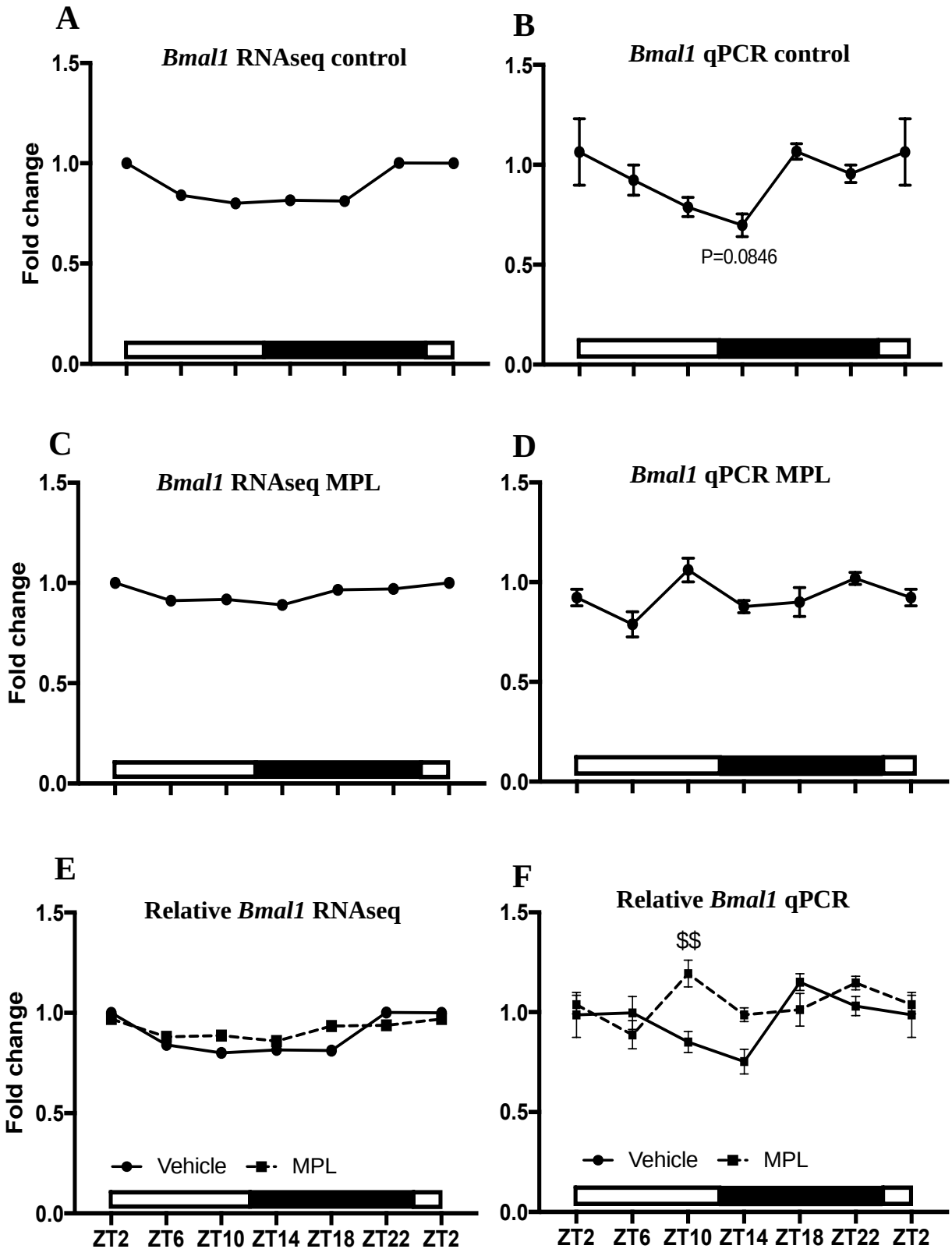

Figure 4.12 *Bmal1* mRNA expression is elevated with MPL treatment. *Bmal1* mRNA expression was assessed using RNAseq and qPCR. A non-significant decrease in expression was observed in the control group from RNAseq (**A**) and qPCR (**B**). MPL

treatment flattened the mRNA expression of *Bmal1* in both RNAseq (**C**) and qPCR (**D**) data. No significant difference was observed when looking at the relative levels of expression in the RNAseq analysis (**E**), however a significant difference was observed following qPCR (**F**) at ZT10, where mRNA decreased in the control group but remained elevated in the MPL group. RNAseq data represented as mean. N = 4 per group. One-way ANOVA with Benjamini-Hochberg post-hoc test was used, with all comparisons to ZT2 in graphs (**A**) and (**C**). Two-way ANOVA with Benjamini-Hochberg post-hoc was used in graph (**F**). qPCR data represented as mean ± SEM. N = 4 per group. One-way ANOVA with Dunnett's post-hoc test was used, with all comparisons to ZT2 in graphs (**D**) and (**D**). Two-way ANOVA with Sidak's post-hoc test was used in (**F**). All statistical significance indicated at $P < 0.05$ (*) and $P < 0.01$ (**). ZT2 repeated for visualisation purposes.

RNAseq analysis showed differential expression of *Bmal1* in control animals to be non-significant (**A**), however P value significance was evident at ZT6 (P = 0.02035, Q = 0.723869), ZT10 (P = 0.00225, Q = 0.231868), ZT14 (P = 0.00355, Q = 0.166757) and ZT18 (P = 0.00705, Q = 0.40783), yet the FDR for each time point deemed those results non-significant. qPCR analysis of control (**B**) indicated a trend of significance ($F_{6,20}$ – 1.996, p = 0.1141), with a trend of significance observed at ZT14 (P = 0.0846).

Although a circadian profile was not significantly shown in controls, with MPL treatment the profile was flattened further, with no significant difference observed at any time point from RNAseq (**C**) and qPCR (**D**) analyses. Relative expression assessment of *Bmal1* expression showed no significant difference between treatments at any time based on FDR values (**E**), however qPCR analysis (**F**) showed a significant effect of time ($F_{6,34}$ – 2.537, p = 0.0388), treatment ($F_{1,34}$ – 4.427, p = 0.0429) and an interaction between both ($F_{6,34}$ – 3.246, p = 0.0125), with ZT10 exhibiting clear significance between treatments (P = 0.0088).

4.3.3.6 *Clock* mRNA expression

The transcriptional activator CLOCK was assessed in the HC following MPL treatment. *Clock* mRNA has previously been shown in tissues to be constitutively expressed (Ripperger & Merrow 2011), and although that could be expected here, it was still important to assess the expression profile, in control and following MPL treatment.

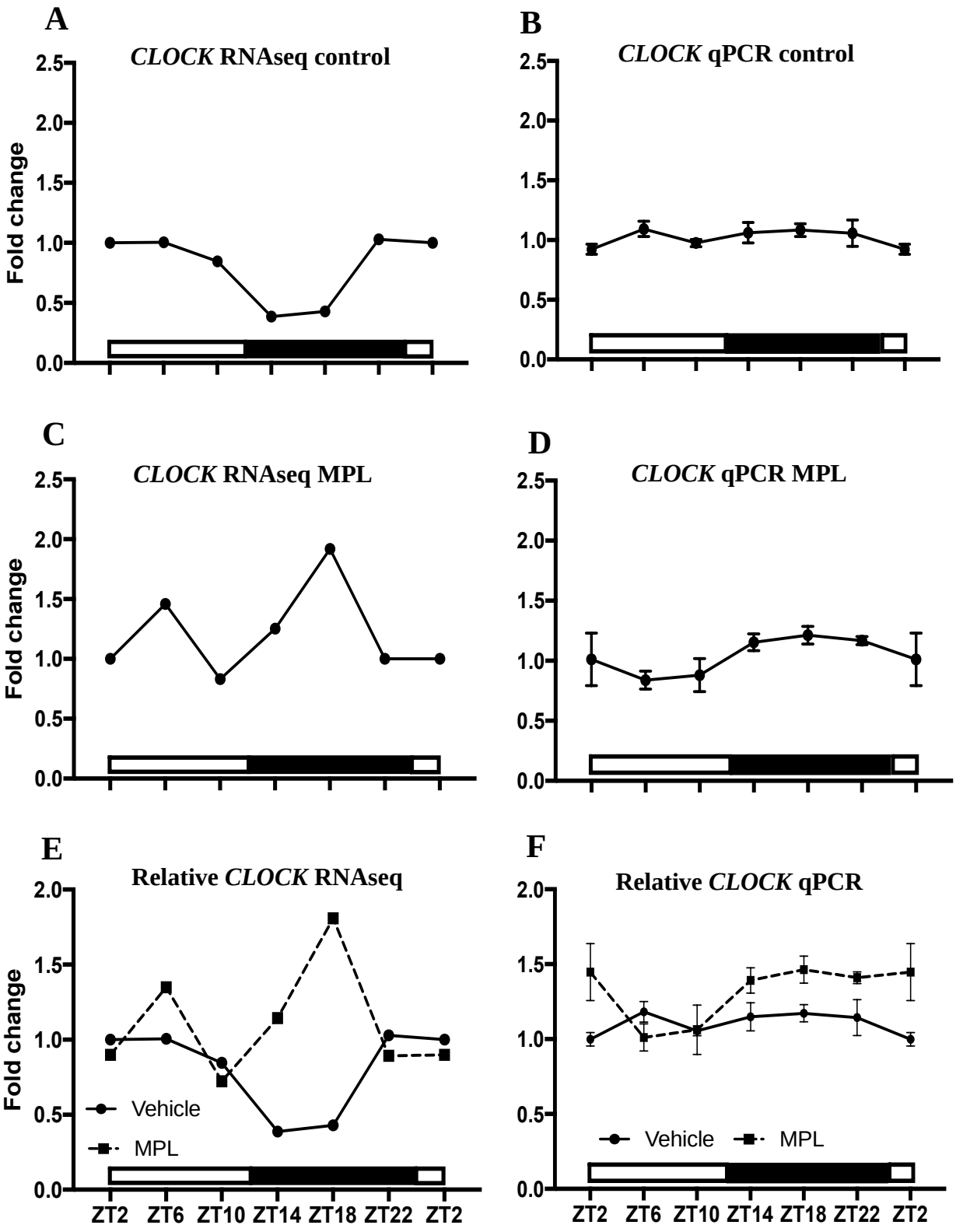
A
CLOCK RNAseq control
B
CLOCK qPCR control
C
CLOCK RNAseq MPL
D
CLOCK qPCR MPL
E
Relative CLOCK RNAseq
F
Relative CLOCK qPCR
Fold change
2.5
2.0
1.5
1.0
0.5
0.0
Vehicle
MPL
ZT2 ZT6 ZT10 ZT14 ZT18 ZT22 ZT2

Figure 4.13 *Clock* mRNA expression remained constitutively expressed in the HC irrespective of MPL treatment. In control animals, *Clock* mRNA remained constitutively expressed throughout, with no significant difference observed following RNAseq (**A**) and qPCR (**B**) analyses. MPL treatment did not affect the expression of *Clock* with both RNAseq (**C**) and qPCR (**D**) showing non-significant changes throughout. The relative levels of expression remained unchanged and non-significant from RNAseq (**E**) and qPCR (**F**). RNAseq data represented as mean. N = 4 per group. One-way ANOVA with Benjamini-Hochberg post-hoc test was used, with all comparisons to ZT2 in graphs (**A**) and (**C**). Two-way ANOVA with Benjamini-Hochberg post-hoc was used in graph (**F**). qPCR data represented as mean ± SEM. N = 4 per group. One-way ANOVA with Dunnett's post-hoc test was used, with all comparisons to ZT2 in graphs (**B**) and (**D**). Two-way ANOVA with Sidak's post-hoc test was used in (**F**). All statistical significance indicated at $P < 0.05$ (*). ZT2 repeated for visualisation purposes.

Based upon published data, the mRNA expression of *Clock* was expected to remain at a steady state level, as it has been shown to be constitutively expressed. RNAseq (**A**) and qPCR (**B**) analysis confirmed this, as no significant effect of time was evident, and although there appeared to be a repression in expression in the RNAseq analysis, neither P value, nor Q value were deemed significant (ZT14, P = 0.32865, Q = 0.915714) (ZT18, P = 0.37515, Q = 0.995783). Like the control group, no effect of MPL was observed on *Clock* mRNA expression following RNAseq (**C**) and qPCR (**D**) analyses, with the large variation in the RNAseq time points not passing FDR parameters. The relative levels of expression between control and MPL were assessed. No effect was observed in the individual control and MPL analyses, and no effect was observed in the RNAseq analysis (**E**), however an effect of treatment was found when assessing between groups and across time ($F_{1,38} – 15.88$, p = 0.0003) as well as a significant interaction ($F_{6,38} – 2.442$, p = 0.0427), using qPCR (**F**) however no significant effect was observed between time points, with a trend of an effect observed at ZT2 (P = 0.0547).

4.3.3.7 *Npas2* mRNA expression

The expression of *Npas2*, which replaces CLOCK to bind to BMAL1 and promote the transcription of *Per* and *Cry* genes was assessed. The expression of *Npas2* would also be

expected to express constitutively through the day, however profiling of this target in the HC is not as well-known as other clock gene components.

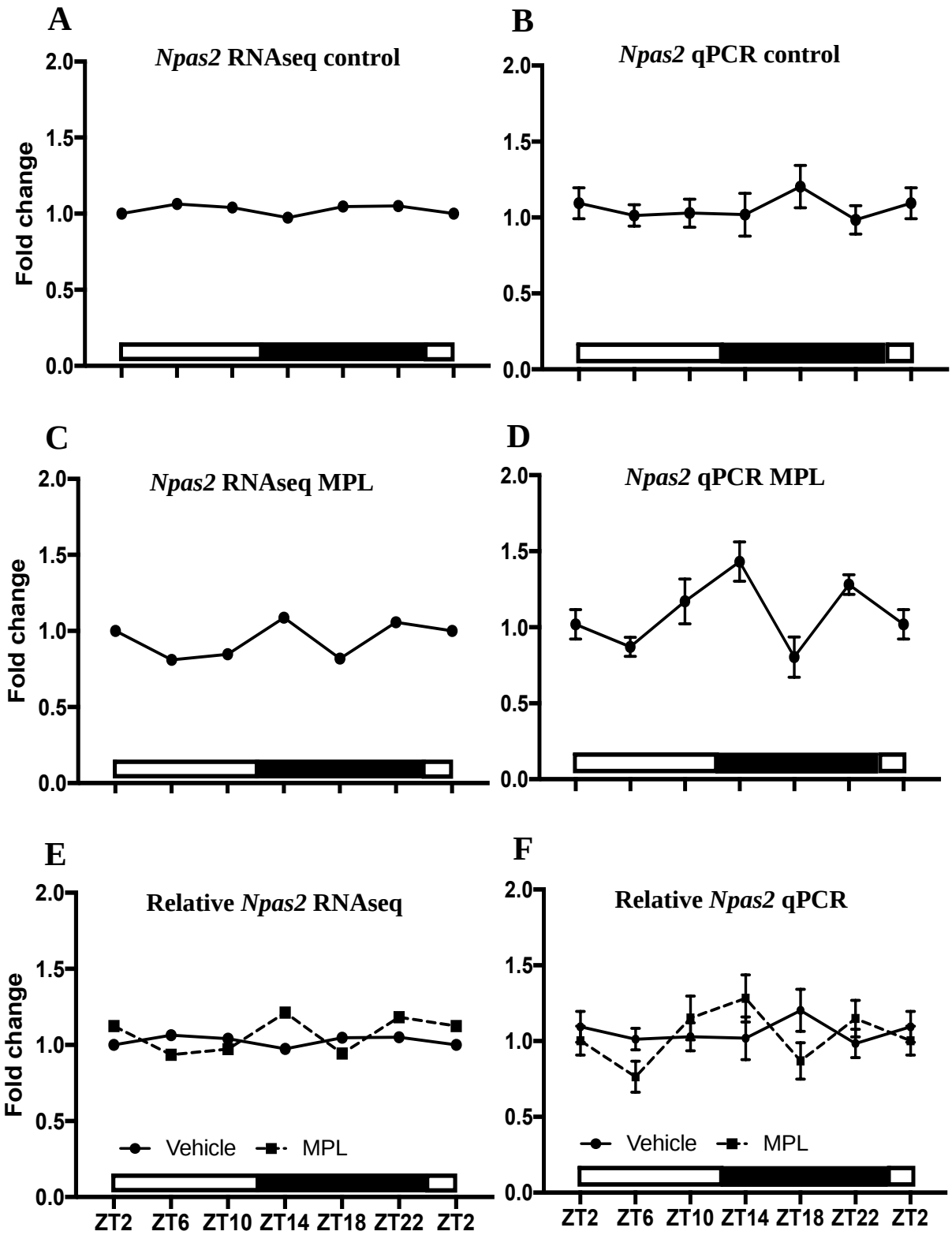

Figure 4.14 No effect was observed on *Npas2* mRNA expression in the HC with MPL treatment. RNAseq (**A**) and qPCR (**B**) analysis of *Npas2* in control animals showed no significant difference at any time point, with the levels of mRNA remaining constant throughout the day. Following MPL treatment, no effect of glucocorticoids was observed from RNAseq (**C**) or qPCR (**D**), with the levels of mRNA remaining the same as the controls. This was shown further when looking at the relative levels of expression, with neither RNAseq (**E**) or qPCR (**F**) exhibiting a significant change. RNAseq data represented as mean. N = 4 per group. One-way ANOVA with Benjamini-Hochberg post-hoc test was used, with all comparisons to ZT2 in graphs (**A**) and (**C**). Two-way ANOVA with Benjamini-Hochberg post-hoc was used in graph (**E**). qPCR data represented as mean ± SEM. N = 4 per group. One-way ANOVA with Dunnett's post-hoc test was used, with all comparisons to ZT2 in graphs (**B**) and (**D**). Two-way ANOVA with Sidak's post-hoc test was used in (**F**). All statistical significance indicated at $P < 0.05$ (*). ZT2 repeated for visualisation purposes.

Like *Clock* gene expression, the expression of *Npas2* in control animals following RNAseq (**A**) and qPCR (**B**) analyses were non-significant and remained constitutively active throughout the day. Treatment with MPL did not affect the expression profile from RNAseq data (**C**), however qPCR showed a significant effect of time (**D**) ($F_{6,17} – 3.494$, $p = 0.0195$), however only a trend of significance was observed at ZT14 ($P = 0.0826$). Relative levels of *Npas2* mRNA expression were also assessed. RNAseq analysis (**E**) showed no difference between treatments across time points. qPCR analysis (**F**) showed no significant effect of time, treatment or an interaction of both.

4.3.3.8 *Rev-erbα* mRNA expression

REV-ERBα, a major component of the molecular clock, in the accessory loop drives the transcription of *Bmal1*, which in turn promotes the transcription of *Per1*, which is be targeted by glucocorticoids. *Rev-erbα* is also known to contain a glucocorticoid response element, and it was therefore important to assess the regulation of this gene in control and MPL treated animals.

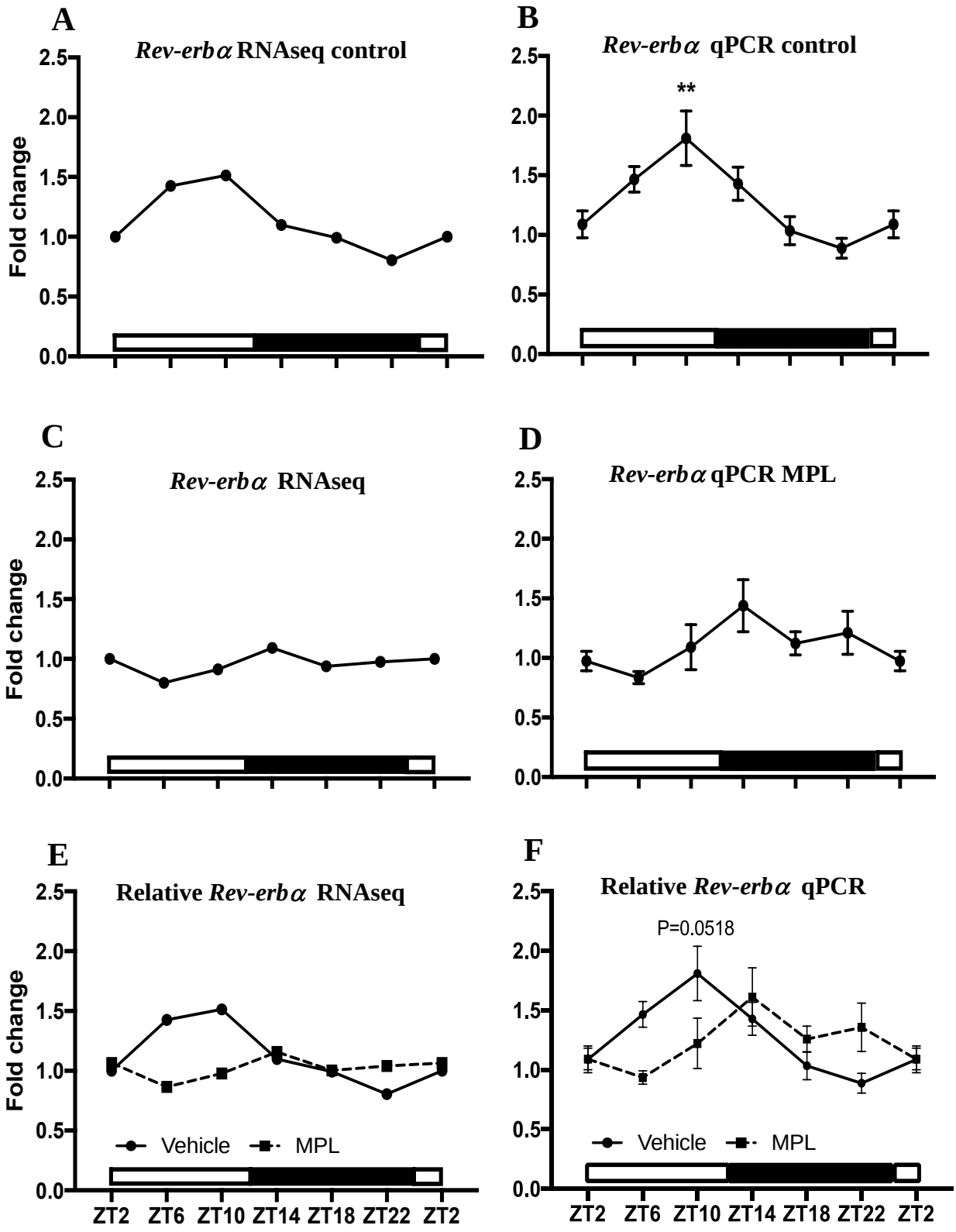
A
Rev-erbα RNAseq control
Fold change
2.5
2.0
1.5
1.0
0.5
0.0
B
Rev-erbα qPCR control
**
C
Rev-erbα RNAseq
D
Rev-erbα qPCR MPL
E
Relative Rev-erbα RNAseq
Vehicle
MPL
ZT2 ZT6 ZT10 ZT14 ZT18 ZT22 ZT2
F
Relative Rev-erbα qPCR
P=0.0518

Figure 4.15 *Rev-erbα* mRNA expression following treatment with MPL is blunted. Although the pattern of expression detected between RNAseq and qPCR in controls was highly similar**,** RNAseq analysis did not detect any significant circadian variation in control animals (**A**). However, a robust significant circadian profile was observed using qPCR (**B**), with a significant increase in expression observed at ZT10. The circadian rhythmicity observed in controls, was lost following MPL treatment using both RNAseq (**C**) and qPCR (**D**) techniques. However, when assessing the relative expression, no significant difference was observed in the RNAseq data set (**E**), however a trend of a significance was observed following qPCR (**F**), at ZT10. RNAseq data represented as mean. N = 4 per group. One-way ANOVA with Benjamini-Hochberg post-hoc test was used, with all comparisons to ZT2 in graphs (**A**) and (**C**). Two-way ANOVA with Benjamini-Hochberg post-hoc was used in graph (**E**). qPCR data represented as mean ± SEM. N = 4 per group. One-way ANOVA with Dunnett's post-hoc test was used, with all comparisons to ZT2 in graphs (**B**) and (**D**). Two-way ANOVA with Sidak's post-hoc test was used in (**F**). All statistical significance indicated at $P < 0.05$ (*) and $P < 0.01$ (**). ZT2 repeated for visualisation purposes.

The expression of *Rev-erbα* has been shown in multiple tissues of the body, and consistently is shown to express highly during the inactive/light period before levels lower during the active/dark period. RNAseq analysis (**A**) did not yield a significant effect of time in *Rev-erbα* expression, however qPCR analysis of the same samples (**B**) showed a significant effect of time ($F_{6,21} – 5.608$, $p = 0.0013$), with a significant effect observed at ZT10 ($P = 0.0059$), consistent with published data indicating an increase in expression during the inactive/light period. MPL treatment blunted the circadian pattern of expression in both RNAseq (**C**) and qPCR (**D**) analyses, with no significant difference observed across time. Relative expression was assessed between treatments, with an effect of time ($F_{6,42} – 3.4$, $p = 0.0080$) and an interaction ($F_{6,42} – 3.507$, $p = 0.0067$) observed (**F**), however no significant difference was observed between treatment at individual time points (ZT6, $P = 0.1014$) (ZT10, $P = 0.0518$).

4.3.3.9 *Rorα* mRNA expression

Assessment of the transcriptional repressor of *Bmal1* was important to assess following the changes observed to expression in *Rev-erbα* following MPL treatment.

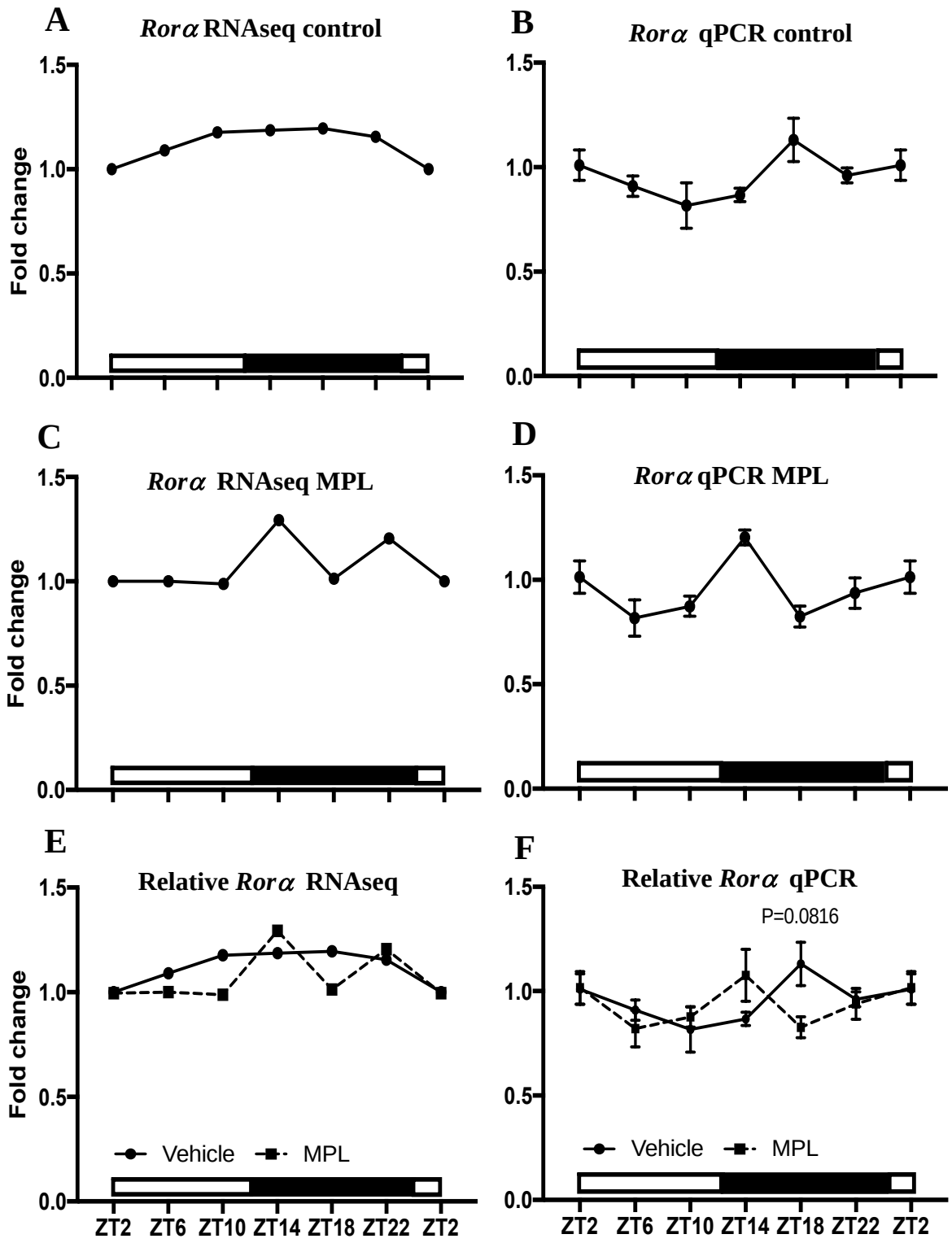

Figure 4.16 *Rorα* mRNA expression was not affected following MPL treatment. In control animals, the mRNA levels of *RORα* remained constant throughout, with no change observed at any time point in the RNAseq (**A**) and qPCR (**B**) analyses. MPL treatment did not affect mRNA expression as shown by RNAseq (**C**) and qPCR (**D**). The relative levels of mRNA expression were assessed, with no significant difference observed from RNAseq (**E**), however a trend to significance was observed from qPCR analysis (**F**) at ZT18. RNAseq data represented as mean. N = 4 per group. One-way ANOVA with Benjamini-Hochberg post-hoc test was used, with all comparisons to ZT2 in graphs (**A**) and (**C**). Two-way ANOVA with Benjamini-Hochberg post-hoc was used in graph (**F**). qPCR data represented as mean ± SEM. N = 4 per group. One-way ANOVA with Dunnett's post-hoc test was used, with all comparisons to ZT2 in graphs (**B**) and (**D**). Two-way ANOVA with Sidak's post-hoc test was used in (**c**). All statistical significance indicated at $P < 0.05$ (*). ZT2 repeated for visualisation purposes.

Rorα mRNA expression in RNAseq (**A**) and qPCR (**B**) was not affected by time, with no significant changes observed across the circadian period. Although no significance was calculated from the RNAseq set (**C**), a significant effect of time was evident following qPCR analysis (**D**) ($F_{6,18} – 3.428$, $p = 0.0193$). Assessment of control and MPL treatment exhibited significance in the RNAseq data (**E**), however the FDR deemed these non-significant (ZT10, $P = 0.0119$, $Q = 0.459648$) (ZT18, $P = 0.03645$, $Q = 0.486015$). qPCR analysis (**F**) did not yield a significant effect, with only a trend observed ($F_{6,33} – 1.888$, $p = 0.1124$) and a trend to significance at ZT18 ($P = 0.0816$).

4.4 Discussion

The hippocampus is a brain region that has been extensively studied for its role in memory processing and sleep regulation. Since the role of the hippocampus in spatial navigation and episodic memory was established, a huge amount of research followed, looking into the molecular mechanisms that account for these processes. However, to this day, although significant advancements have been made, there is still a huge void in the knowledge of what mechanisms control these processes.

Basic research looking at mechanisms that control memory and sleep in the HC have focused largely on the long-term potentiation (LTP) and long-term depression (LTD)

phenomena, where neuronal synapses are strengthened or weakened for an extended period of time following a stimulus, respectively (Bliss & Lomo 1973; Collingridge et al. 1983; Bannerman et al. 1995; Stevens 1998; Muller et al. 2002). This synaptic activity can affect memory consolidation and is altered in neurological disorders, with long-term potentiation-like plasticity disrupted in Alzheimer's disease (Di Lorenzo et al. 2016). However, this process accounts for a small cog in a large system, as memory and sleep are affected by a magnitude of other molecular and physiological processes, including HPA axis activity and the release of hormones, and the interconnectivity between sleep and memory itself, as sleep is required to consolidate long-term memories (Aisa et al. 2007; Stickgold 2005; Marshall et al. 2006; Born 2010).

The molecular clock, has proved in recent years to be fundamental to regulating our daily rhythms, including controlling the sleep/wake cycle, metabolic processes and being instrumental in controlling, to an extent, memory processing (Jin et al. 1999; Kondratova et al. 2010). Glucocorticoids, endogenous and synthetic, have been shown to affect these processes (Keenan et al. 1996; Rebuffé-Scrive et al. 1992). However, although glucocorticoids are known to entrain peripheral clocks, little has been shown of the link between the molecular clock and glucocorticoid activity in the brain, in particular in the HC, an area fundamental for memory and sleep processing and what becomes significantly affected in patients with elevated glucocorticoid levels, either through endogenous or exogenous means.

In this chapter, I show that the mRNA expression of the major components of the molecular clock within the HC become dysregulated following synthetic glucocorticoid treatment using high throughput RNA sequencing, DAVID pathway analysis, supraHEX gene expression clustering and validation using qPCR. A primary target of glucocorticoids to the molecular clock is *Per1*. The GRE upstream of the *Per1* gene specifically regulates the expression of *Per1* in the HC (Conway-Campbell et al. 2010), as well as the expression of other circadian regulated genes, although this was shown in A549 cells and with DEX treatment (Reddy et al. 2012). Clock gene expression is also affected with Prednisolone treatment, with the glucocorticoid treatment repressing the circadian oscillations in HepG2 cells, but also in the liver and skeletal muscle of mice (Koyanagi et al. 2006).

.

The expression of the core components of the molecular clock, circadian regulated genes and glucocorticoid regulated genes were assessed using RNAseq over one circadian cycle. Consistent with the RNAseq analysis, the expression profiles and quantity using qPCR analysis were strikingly similar, indicating the robustness of the techniques, and enabling me to assess further the expression of multiple components of the molecular clock, firstly looking at the expression in RNAseq, and later confirming with qPCR analysis.

The *Per1* gene has been extensively studied, with peripheral expression of this gene remaining circadian, although peak expression is delayed when compared to the master clock in the SCN (Jilg et al. 2009). Targeting the *Per1* gene using a knockout model, results in a shorter free-running period, however *Per2* compensates and retains the circadian rhythm in the clock (Bae et al. 2001). In my data, in the control group, clear circadian rhythm with peak mRNA expression occurring prior to the onset of activity was evident, indicating no delay in expression compared to that of the SCN, possibly eluding to peripheral clocks within the brain remaining in rhythm and timing with the master clock, and that other peripheral clocks, such as the liver and skeletal muscle may be delayed due to other clock controlling factors, such as feeding and exercise affecting the liver and skeletal clock transcriptome (Gatfield & Schibler 2008; Zhou et al. 2014). Assessment of *Per1*, *Per2*, *Rev-erbα* and *Bmal*1 following subcutaneous administration of Prednisolone for 7 days in liver and skeletal muscle showed striking results to the expression profiles of these genes (Koyanagi et al. 2006). The expression of *Per1* in the liver and skeletal muscle in controls exhibited clear circadian rhythm, with peak expression occurring at ZT14, reinforcing the delay between peripheral and central clocks. However, in that study the expression of *Per1* mRNA lost its circadian oscillation, with elevated levels during the light/inactive phase, and non-significant changes during the active period when compared to controls (Koyanagi et al. 2006). In these data shown here, the expression of *Per1* in the HC following MPL treatment exhibited remarkably similar results with the expression of *Per1* significantly elevated at ZT2 compared to controls. DAVID analysis may elude to a mechanistic role of the phototransduction pathway which is targeted in the presence of glucocorticoid treatment at ZT2, however this would need to be assessed further.

As *Per1*$^{(-/-)}$ mice are protected by the incumbent compensatory mechanism of *Per2*, it was important to assess *Per2* expression in the HC following MPL treatment, as it could keep the peripheral clock components in rhythm, independent of *Per1* expression. The expression of *Per2*, following RNAseq and qPCR analysis showed robust circadian oscillations, as expected, with peak expression occurring 4 hours later than that of *Per1* expression. However, as in the *Per1*$^{(-/-)}$ mouse where *Per2* takes over, following MPL treatment I show that the expression of *Per2* is also significantly altered, and exhibited a similar pattern to that of *Per1* following MPL treatment. The expression of *Per1* can be explained by the presence of the GRE that is known to drive transcription, however evidence of a GRE, either upstream of the TSS or through long ranging interactions is limited for *Per2* data (Segall et al. 2006; Cheon et al. 2013). But, these data suggest that glucocorticoids are able to alter the expression of the *Per2* gene, at least within the HC.

The molecular clock genes *Cry1* and *Cry2* were assessed. The *Cryptochrome* genes drive multiple processes, and interestingly were recently shown to mediate the rhythmic expression of the glucocorticoid receptor in HEK293T cells, and mouse liver (Lamia et al. 2011). In this dataset, rhythmic expression of *Cry1* in control was observed, with peak expression occurring during the active/dark phase, consistent with other published data (Peirson et al. 2006; Soták et al. 2016). However following MPL treatment, the expression was significantly altered with an elevated level of expression occurring in the early light/inactive phase, again linking to a phase shift in clock gene expression in the HC following MPL administration, most likely driven by the dysregulation of the transcriptional repressor *Per1*. The expression of *Cry2* in controls, showed similar expression to *Cry1*, with no significant differences observed across the day. However surprisingly, following MPL treatment, although the RNAseq data did not show a significant difference over time in *Cry2* transcript expression, the qPCR exhibited a robust circadian profile, with a significant increase in transcript observed during the most active period of the rat, providing evidence for glucocorticoid regulation or a compensatory mechanism of *Cry*2 in the HC.

Following the significant effects observed in the transcriptional repressors of the molecular clock, led to the assessment of the transcriptional activators BMAL1, CLOCK and NPAS2. Classically in circadian biology research, BMAL1, the major transcriptional activator of the molecular clock, has been a dominant target to affect and assess for altered downstream

processes. *Bmal1*$^{(-/-)}$ mice become circadian arrhythmic (Rakai et al. 2014), indicating its importance in regulating circadian oscillations and driving circadian rhythms in biology. BMAL1 and CLOCK dimerise and promote the transcription of *Per1* through binding at E-box elements upstream of the *Per1* TSS. The expression of *Per1* in the HC following glucocorticoid treatment was significantly altered, and with MPL treatment a significant effect was observed in *Bmal1* transcript expression, as *Bmal1* expression should be in antiphase to the expression of *Per1* (Oishi et al. 1998a), as shown in controls. Following MPL treatment this was not evident, indicating an effect on the molecular clock. Yet, although with RNAseq the expression of *Bmal1* was not significant across time points, this could be explained, in part, to the stringency of the false discovery rate in the RNAseq analysis, where the Benjamini-Hochberg post hoc test was used to calculate the false discovery rates (Benjamini & Hochberg 1995). However, if only looking at the P value, the expression of *Bmal1* was significantly repressed at ZT6-18, as expected based upon previously published data, and the robustness of the SCN *Bmal1* data that I showed in chapter 3. Again however, following qPCR no significant difference was observed but this could be an example of where the effect size was too small, and that a larger group was needed for each time point and treatment to show clear significance. This was evident also with *Rev-erbα* expression, where P-value significance was observed, however the variation across samples lead to the data being non-significant, although significance was observed following qPCR analysis.

REV-ERBα was the first nuclear receptor (NR) to provide a mechanistic link for direct NR regulation of the clock, as *Rev-erbα*$^{(-/-)}$ mice showed constitutively elevated *Bmal1* transcript levels (Preitner et al. 2002). Mechanistically, REV-ERBα binds to the C-terminal portion of heat shock protein 90 (HSP90), with GR binding to the N-terminal portion and influences the stability and nuclear localisation of the GR, therefore affecting gene expression of target GR responsive genes (Okabe et al. 2016). Because of this, the delay observed in the *Rev-erbα* expression could again account for the phase shift observed in the components of the primary loop, as GR stability is necessary and required for the GR to bind to PER1 and promote *Per1* gene transcription.

Following MPL treatment, *Per1*, *Per2*, *Cry1*, *Cry2*, *Bmal1*, components of the primary loop of the molecular clock exhibited varying changes to expression when compared to controls.

Of the accessory loop, no clock components became dysregulated, with only *Rev-erbα* offering a trend to a phase shift in peak expression caused by treatment.

The well-established glucocorticoid target *Per1* (Conway-Campbell et al. 2010) was significantly affected by synthetic glucocorticoid treatment, with the levels of mRNA expression remaining elevated through the inactive and active periods. Such the intricacy of the molecular clock circuitry, the overexpression during the inactive period could act to drive the other clock components out of rhythm, as observed in the primary loop components *Per2*, *Bmal1*, *Cry1*, but also in the accessory loop, where a delay in expression was observed in *Rev-erbα.* That being said, the primary loop of the clock appeared to be the major target of glucocorticoid action, specifically through *Per1* expression driving the primary loop to fall out of synchronisation, driving the dysregulation of other clock targets.

These data indicate that the synthetic glucocorticoid MPL significantly alters the expression of major components of the molecular clock, most likely through binding of the glucocorticoid receptor to the *Per1* GRE, driving the transcription of this gene and overriding the dominant light/dark cycling. As the hippocampus is a major component involved in memory consolidation and sleep processing, an alteration of the clock, as shown here with glucocorticoid treatment, could provide evidence for the mechanism that drives glucocorticoid-determined sleep and memory related processing in patients (Keenan et al. 1996; Pivonello et al. 2015; Antonijevic & Steiger 2003; Sonino & Fava 2001), and could offer a potential mechanism for dysregulating the timing of the molecular processes in the hippocampus, which would affect the optimum timing and activity of the hippocampus to increase memory consolidation and enter the appropriate sleep stages to enhance and store memories during the sleep period.

The following two chapters will explore physiological outcomes arising from the transcriptional changes I have reported in Chapters 3 and 4.

Chapter 5

Locomotor activity and core body temperature recordings following MPL treatment and in the presence of GR and MR antagonists

5.1 Introduction

The molecular clock within the SCN and peripheral clocks within tissue are instrumental in retaining physiological, chemical and metabolic processes to a periodicity of ~24h, in timing with the daily cycle of light and dark. Locomotor activity (LA) and core body temperature (cBT) are just two examples which are under the control of daily rhythms through central and peripheral clock processes.

The master clock in the SCN drives 24h rhythmicity through the activation of photosensitive retinal ganglion cells in the eye, which transmit signal down the retinohypothalamic tract directly to the SCN, initiating the components of the molecular clock in hypothalamic nuclei to entrain to the light/dark cycle. Lesions to the SCN ablate the circadian oscillations observed in LA and cBT (Eastman et al. 1984; Refinetti et al. 1994; Waite et al. 2012). Similarly, animals placed in constant light exhibit a loss of circadian rhythmicity in LA and cBT (Ohta et al. 2005; Waite et al. 2012). Gene knockouts of core components of the clock significantly affect the activity period, with *Bmal1*$^{(-/-)}$ and *Per2*$^{(ldc)}$ mice exhibiting arrhythmic activity periods (Mieda & Sakurai 2011; Bae et al. 2001).

The SCN projects to the ventral lateral preoptic nucleus (VLPO) and dorsomedial hypothalamus (DMH) to control core body temperature (Zhao et al. 2017). The subparaventricular zone (sPVZ) also relays signals to the SCN to further regulate cBT and LA, as well as sleep regulation (Lu et al. 2001; Saper et al. 2005). LA and cBT can be further regulated by peripheral clock systems in liver and skeletal muscle (Cornu et al. 2014; Stokkan et al. 2001), as restricted feeding or running wheel access can produce significantly different patterns of activity when compared to *ad libitum* food or no cage enrichment, irrespective of the light cycle (Damiola et al. 2000; Reebs & Mrosovsky 1989).

Patients prescribed glucocorticoid treatment often complain of changes to their activity periods, with increased sleep noted in the day and a lack of sleep in the night (Antonijevic & Steiger 2003). MPL binds to the glucocorticoid and mineralocorticoid receptors and is commonly prescribed in the clinic (Overman et al. 2013). In chapters 3 and 4, I showed that glucocorticoid sensitive genes can be dysregulated in the presence of this long acting steroid, in particular in genes fundamental to the molecular clock that drive daily rhythms.

The action of glucocorticoids can be blocked in the presence of GR and MR antagonists, Mifepristone and Spironolactone, respectively. Mifepristone (RU-486), is a GR antagonist that specifically antagonises cortisol (or similar) action competitively at the receptor level (Zhang et al. 2007; Chu et al. 2001) with its binding affinity 3x the potent GR agonist DEX, and 10x that of CORT (Gagne et al. 1985). Spironolactone is medically used as a diuretic to block the effects of Aldosterone, primarily in the kidney. It binds to the MR in tissues inhibiting the action of aldosterone and cortisol (Rupprecht et al. 1993).

Previously, it has been reported that treatment with MPL significantly altered the periodicity of LA and cBT (Figure 5.1). However, no further analysis characterised the period length in control or MPL treated animals. Rhythms are commonly assessed in biology, with varying analysis packages and techniques to understand rhythmic periods in a dataset. Classically, actograms of locomotor activity are presented in research articles (Leise et al. 2013), which visually show animals entraining to light/dark cycles, their activity during constant darkness as well as during constant light (Chen et al. 2008). Wavelet transform has been used for many years in the field of physical sciences but is relatively new to the field of circadian biology. It is a technique that processes rhythmic signals, or wavelets, in a dataset. This is a unique property to this signal processing technique, as these signals can be symmetric or non-symmetric, high or low frequency, and be identified in regular or irregular datasets (Hoang Dang 2014). It allows for discrete identification of rhythms, or independent frequencies within a dataset, and in conjunction with using the Lomb-Scargle periodogram, which detects rhythmic signals based upon a least squares fit of sinusoidal data (Hocke 1998) from sample data with zero mean, allows for period length to be measured.

In this chapter, I have analysed the periodicity exhibited in control and MPL treated animals. Additionally, following the results shown in chapter 3, where treatment with MPL dysregulated the pivotal clock gene *Per1* in the SCN, I have assessed if blocking the activity of the glucocorticoid receptor and the mineralocorticoid receptor, therefore preventing MPL from binding to the receptors and prevent GC regulated transcription of the *Per1* gene, would retain the clock at the dominant light/dark cycle.

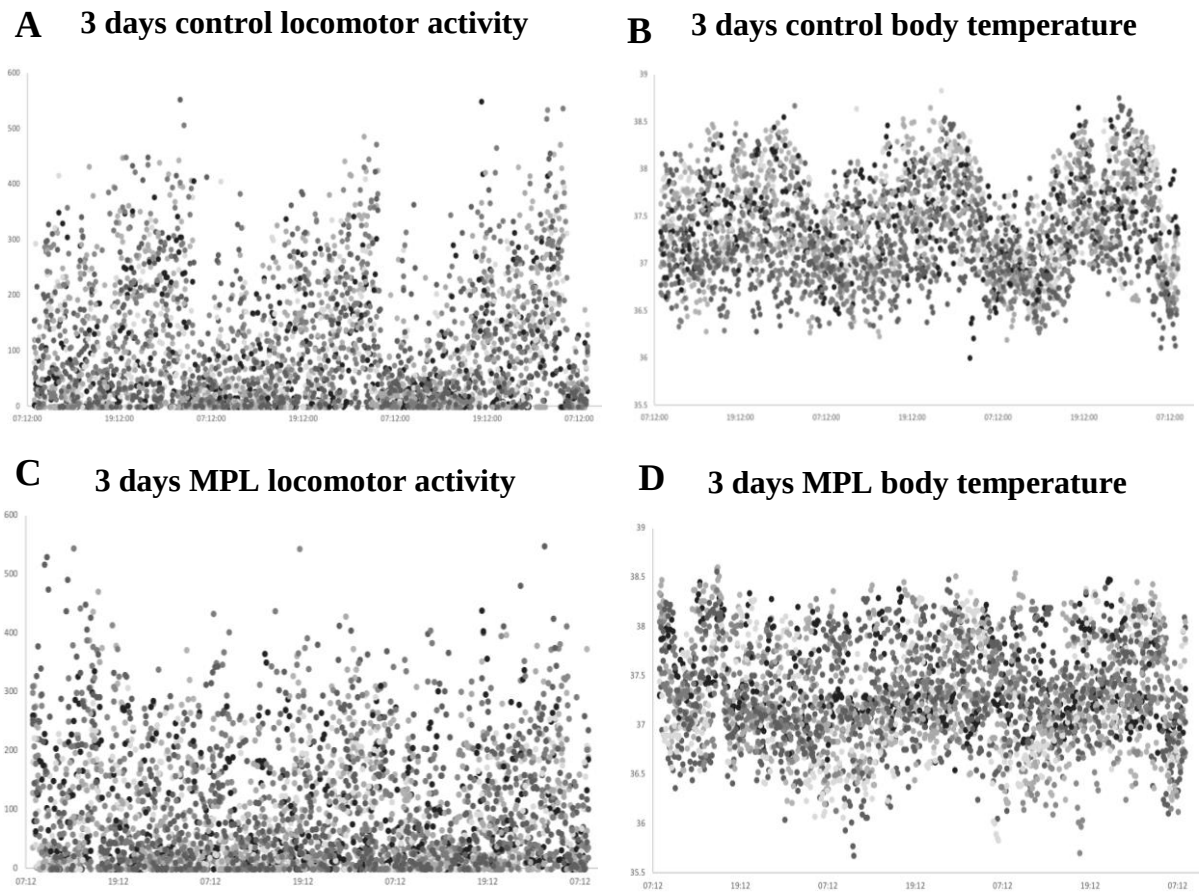

Figure 5.1 Locomotor activity and core body temperature are dysregulated following MPL treatment. Locomotor activity (**A**) and core body temperature (**B**) in controls showed circadian oscillations across three days of recordings. During MPL treatment, locomotor activity (**C**) and core body temperature (**D**) showed a lack of rhythm (Demski-Allen 2014).

5.2 Methods

5.2.1 Animal housing and Home Office

32 adult male Lister Hooded rats (250-300g; 9-11 weeks) were obtained from Harlan Laboratories, now Envigo (Bicester, UK) and maintained under standard housing conditions with a 12:12 light/dark cycle. Food and water were available *ad libitum*. Rats were given an initial period to acclimatise to the facility. All procedures were carried out

in accordance with the UK Home Office guidelines and the UK Animals (Scientific Procedures) Act under PPL 30/3114 and PIL I04092F5F. Group size was determined by literature review and previous experience in Prof. Stafford Lightman's laboratory.

5.2.2 Experimental design

During the experimental period, rats were individually housed for technical purposes. Methylprednisolone (1mg/ml in drinking water (Demski-Allen 2014) (20mg/per day)) lasted five days. Telemetry recordings of locomotor activity and body temperature were measured throughout the course of MPL treatment and in the presence of a subcutaneous pellet containing either Mifepristone, Spironolactone or placebo. In the repeated data, all MPL treated animals received either a combination of GR and MR antagonism, GR or MR separately, or the placebo pellet. N = 4-8 per group.

5.2.3 Surgery

Surgery was performed under balanced anaesthesia (veterinary isoflurane; Merial Animal Health Ltd., UK). Post-surgery, rats received subcutaneous injections (SC) of 0.2mg/mL Rimadyl (Carprofen 5% w/v, Benzyl alcohol 1% w/v; Pfizer., UK) diluted in sterile 10 IU/mL heparinised saline and 2.5mL s/c glucose saline (Sodium chloride 0.45% w/v and Glucose 2.5% w/v solution for infusion BP; Baxter Healthcare Ltd., UK) to aid recovery.

5.2.3.1 Locomotor activity and body temperature recordings

Intraperitoneal implantation of a PDT-4000 E-Mitter radiotelemetry probe (Respironics, US) was performed with subcutaneous implantation of a slow release pellet containing either Mifepristone, Spironolactone or Placebo (5mg/day (Nasca et al. 2015)) (Innovative Research of America, USA). Following surgical recovery, animals were housed in individual cages for telemetry recording in soundproof rooms. Radiotelemetry data collection began 2 days following surgery. Sample collection frequency of 10 minutes was set and viewed using Respironics VitalView software (Mini Mitter Co. USA). Activity counts are generated when the E-Mitter changes position relative to the charging signal received from any of 3 concentric charge/receive grids inside the ER-4000 Receiver. Position change can be in any plane or from place to cause activity counts to be recorded. One cannot determine how far a given movement is in terms of precise distances based on

number of counts. There is not a specific distance that must be moved in order to generate a count. These data are simply a relative measure of gross motor activity level over time.

5.2.4 Analysis using Wavelet Transform and Lomb-Scargle periodogram

Locomotor activity and core body temperature were analysed using computer program MATLAB v2016b (MathWorks, USA). In house scripts for wavelet spectrum analysis and Lomb-Scargle periodogram were provided by Dr. Amitesh Pratap. Full script available in chapter 2 (Methods). Analysis of wavelet periodicity was assessed using GraphPad Prism 7.0.

5.3 Results

5.3.1 Locomotor activity and core body temperature with wavelet spectral analysis

Previously, it was shown that MPL significantly altered the periodicity of LA and cBT (Figure 5.1). Here, using the same raw data, I have reanalysed this dataset using wavelet spectral analysis with the Lomb-Scargle periodogram to assess underlying frequencies in the LA and cBT datasets of control and MPL treated animals. Following the results of chapter 3, where SCN clock genes were dysregulated with MPL treatment, I hypothesised that there should be a relationship between dysregulating the master clock in the SCN, and dysregulation of peripheral clocks driving these two physiological processes. For instance, similar to what has been shown in LA and cBT following constant light and constant dark experimental parameters.

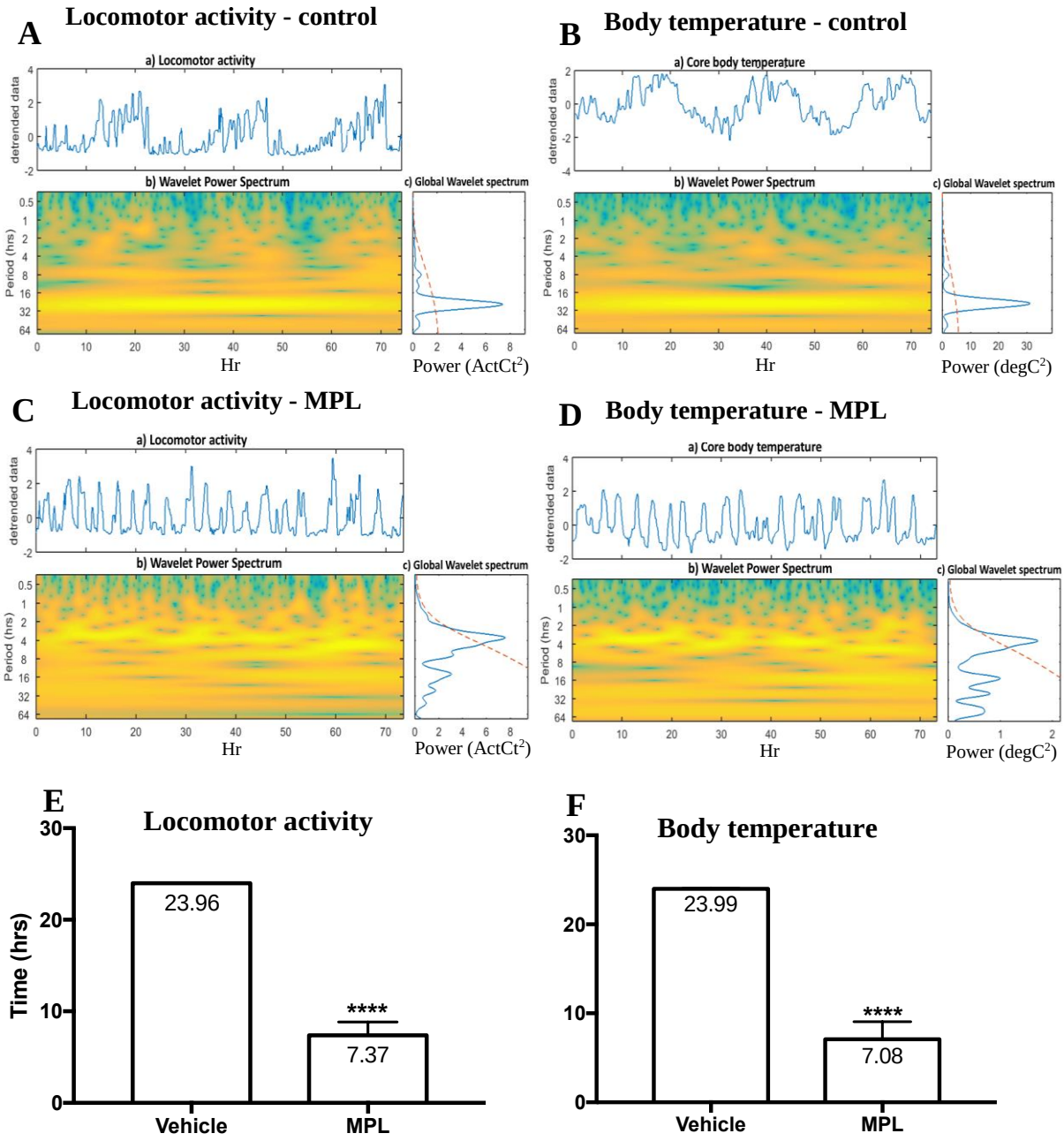

Figure 5.2 Wavelet analysis of locomotor activity and core body temperature. LA (**A**) and cBT (**B**) in control animals exhibited a clear circadian rhythm using this analysis technique. Following MPL treatment, LA (**C**) and cBT (**D**) were significantly affected, with a loss of circadian oscillation but a dominant ultradian rhythm evident. The frequency periods of LA (**E**) and cBT (**F**) are shown, comparing controls with MPL treated animals. N = 8 per group. Detrended data and representative plot. Black bars indicate period of dark. Wavelet spectral analysis with Lomb-Scargle periodogram (**a** - raw, detrended data; **b** – wavelet spectral analysis; **c** – Lomb-Scargle periodogram). Red dotted line indicates P<0.05. Bar graphs – mean ± SEM. Analysed with unpaired t-test, $P < 0.05$, $P < 0.01$, $P < 0.001$ and $P < 0.0001$.

Locomotor activity and core body temperature are known to be under circadian control. Here, three days of locomotor activity and core body temperature are presented. In the control group, a clear and robust circadian oscillation was observed in locomotor activity (**A/E** 23.96 ± 0.06**)** and core body temperature (**B/F** 23.99 ± 0.04) output. Visually, an ultradian rhythm was evident in these control animals, however the dominance of the circadian rhythm rendered the underlying ultradian rhythm non-significant. Following MPL treatment, the circadian rhythm of locomotor activity (**C/E** 7.372 ± 1.432) and core body temperature (**D/F** 7.083 ± 1.989) was ablated, with the ultradian rhythm becoming the dominant rhythm in these animals. Analysis of the Lomb-Scargle periodicity output showed a significant effect of MPL treatment on LA (**E** – $t(8) = 12.82$, $p < 0.0001$) and cBT (**F** – $t(8) = 12.67$, $p < 0.0001$).

5.3.2 Locomotor activity and core body temperature during MPL treatment with GR and MR antagonists

Previous work in our group identified a striking effect of MPL treatment on the circadian rhythm of LA and cBT, which I have gone on to quantify using wavelet analysis. The predominant rhythm of LA (Figure 5.2E) and cBT (Figure 5.2F) were calculated at 24h in controls, consistent with published entraining rhythms data (Stenvers et al. 2016). In contrast, MPL treated rats exhibited a significantly different frequency period of 7h. In chapter 3, I showed significant MPL dependent alteration of the circadian expression profiles of core clock genes *Per1*, *Per2* and *Bmal1* in the SCN. As *Per1* is a well-established glucocorticoid target gene and is known to be induced via glucocorticoid receptor dependent regulation at a conserved binding site in the *Per1* proximal promoter, I hypothesised that blocking the activity of either the glucocorticoid receptor or mineralocorticoid receptor would block the MPL effects on LC and cBT. With MPL dysregulation blocked, I hypothesised that LC and cBT should cycle at a dominant 24h period controlled by the light/dark cycle.

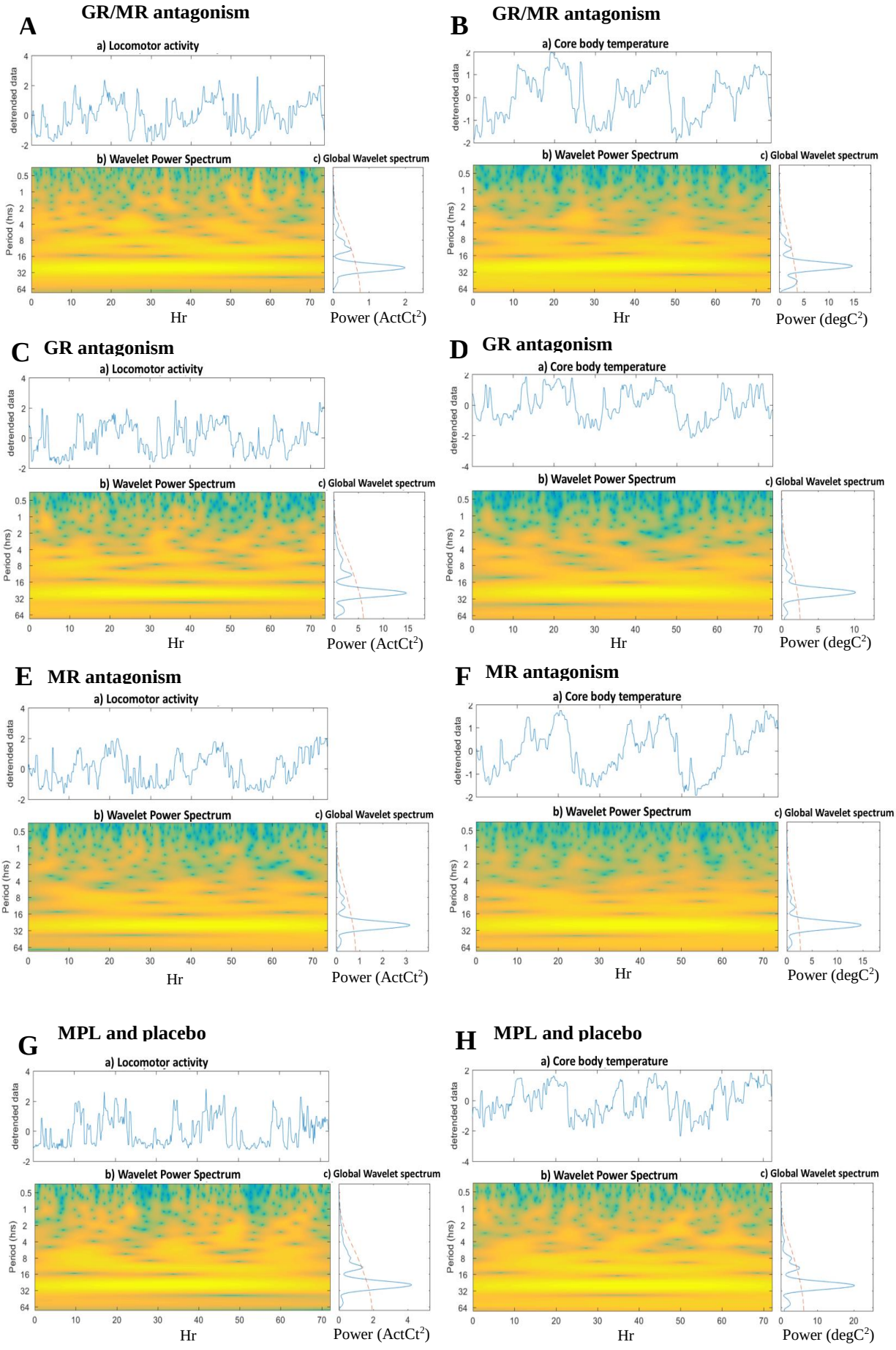
A
GR/MR antagonism
a) Locomotor activity
b) Wavelet Power Spectrum
c) Global Wavelet spectrum
detrended data
Period (hrs)
Hr
Power (ActCt²)
B
GR/MR antagonism
a) Core body temperature
b) Wavelet Power Spectrum
c) Global Wavelet spectrum
detrended data
Period (hrs)
Hr
Power (degC²)
C
GR antagonism
a) Locomotor activity
b) Wavelet Power Spectrum
c) Global Wavelet spectrum
detrended data
Period (hrs)
Hr
Power (ActCt²)
D
GR antagonism
a) Core body temperature
b) Wavelet Power Spectrum
c) Global Wavelet spectrum
detrended data
Period (hrs)
Hr
Power (degC²)
E
MR antagonism
a) Locomotor activity
b) Wavelet Power Spectrum
c) Global Wavelet spectrum
detrended data
Period (hrs)
Hr
Power (ActCt²)
F
MR antagonism
a) Core body temperature
b) Wavelet Power Spectrum
c) Global Wavelet spectrum
detrended data
Period (hrs)
Hr
Power (degC²)
G
MPL and placebo
a) Locomotor activity
b) Wavelet Power Spectrum
c) Global Wavelet spectrum
detrended data
Period (hrs)
Hr
Power (ActCt²)
H
MPL and placebo
a) Core body temperature
b) Wavelet Power Spectrum
c) Global Wavelet spectrum
detrended data
Period (hrs)
Hr
Power (degC²)

Figure 5.3 The effects of the GR and MR antagonists Mifepristone and Spironolactone on locomotor activity and body temperature during MPL treatment. Circadian oscillations in locomotor activity (**A**) and core body temperature (**B**) were observed in MPL treated rats following combined GR and MR antagonism. MPL treated rats cotreated with the GR antagonist Mifepristone also exhibited circadian oscillations of locomotor activity (**C**) and core body temperature (**D**). MPL treated rats cotreated with Spironolactone, which targets the MR, also exhibited circadian oscillations of locomotor activity (**E**) and core body temperature (**F**). However, when assessing the locomotor activity (**G**) and body temperature (**H)** of MPL treated rats cotreated with a vehicle pellet, circadian oscillations were observed. N = 4 per group. Detrended data and representative plot. Wavelet spectral analysis with Lomb-Scargle periodogram (**a** - raw, detrended data; **b** – wavelet spectral analysis; **c** – Lomb-Scargle periodogram). Red dotted line indicating $P<0.05$.

Treatment with MPL was previously found to significantly alter the rhythm of locomotor activity and core body temperature in rats (Figure 1.1) (Demski-Allen 2014). Treatment with the GR and MR antagonists Mifepristone and Spironolactone appeared to reverse the effect of MPL treatment on locomotor activity and core body temperature, with the frequency significantly lengthening from 7h to ~24h. The combination of the GR and MR antagonists drove locomotor activity (**A** 25.66 ± 0.3735) and core body temperature (**B** 24.83 ± 0.3522) to a dominant free running period. Assessment of the effect of the GR specific antagonist, Mifepristone during MPL treatment, also resulted in a similar effect to GR/MR treatment, with a return of the free running period length of locomotor activity (**C** 25.00 ± 0.1477) and core body temperature (**D** 23.95 ± 0.4684) apparent. This surprising effect was also observed in the presence of the MR specific antagonist, Spironolactone, where the periodicity of locomotor activity (**E** 25.00 ± 0.1447) and core body temperature (**F** 25.26 ± 0.1938) was circadian rhythmic. However, implantation of a vehicle pellet into MPL treated rats resulted in a similar periodicity in locomotor activity (**G** – 24.87 ± 0.211) and core body temperature (**H** - 24.96 ± 0.2074).

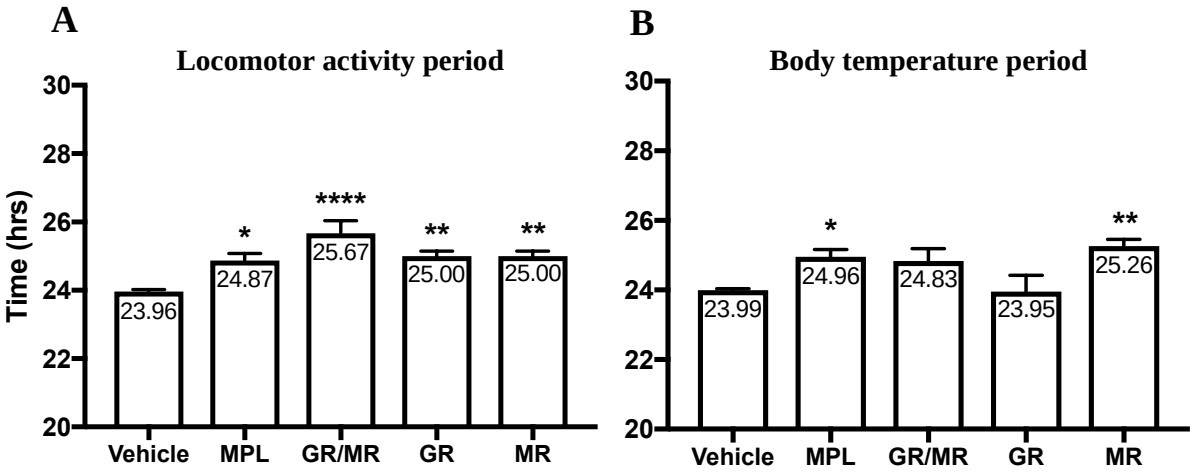

Figure 5.4 Analysis of locomotor activity and core body temperature period length following GR and MR antagonism. Locomotor activity (**A**) in the presence of GR, MR or both showed an increase in period length compared to the control group. This effect was also observed in core body temperature (**B**) for GR and MR combined, and MR only. But with GR antagonism, core body temperature exhibited circadian oscillations similar to control. Animals given the placebo pellet presented with similar periodicity to that of the antagonists. N = 4 per group. Bar graphs – mean ± SEM from Lomb-Scargle periodogram (Figure 5.3). One-way ANOVA with Dunnett's multiple comparison post-hoc test, $P < 0.05$, $P < 0.01$, $P < 0.001$ and $P < 0.0001$.

Using the Lomb-Scargle periodogram with wavelet spectral analysis allowed for the assessment of periodicity in these animals following MPL treatment with either GR, MR or both GR/MR antagonists to block the effect that was previously observed with MPL treatment alone. Locomotor activity in the control group robustly entrained to the light/dark cycle (**A** – 23.96 ± 0.05), as did core body temperature (**B** – 23.99 ± 0.04). MPL treatment with placebo pellet resulted in an increase in period length in both locomotor activity (**A** – $P = 0.0108$), and core body temperature (**B** – $P = 0.0250$). Co-treatment with the GR and MR antagonists exhibited an increase in periodicity similar to what is observed in free running in locomotor activity and was significantly different from the control group (**A** – 25.67 ± 0.37, $P < 0.0001$). However, no difference was observed in body temperature (**B** – 24.83 ± 0.35, $P = 0.0549$). The effects of GR and MR antagonism were further assessed alone. Locomotor activity with GR antagonism resulted in a similar effect to that observed with GR and MR antagonism, exhibiting a significant increase in periodicity for LA (25 ±

0.15, P = 0.0037), however cBT retained rhythm similar to the control group (23.95 ± 0.04). Locomotor activity with MPL treatment and MR antagonism was significantly different from control (25 ± 0.15, P = 0.0037). cBT was also significantly elongated in rhythm compared to the control group (25.26 ± 0.19, P = 0.0030). The findings here clearly show that MPL, in the presence of a placebo pellet, did not induce the predominant ultradian periodicity analysed in Figure 5.2 (7.372 ± 1.432 (LA) and 7.083 ± 1.989 (cBT)). Therefore, this led to the reassessment of LA and cBT with MPL treatment only.

5.3.3 Reproducibility of the effect of MPL treatment on locomotor activity and core body temperature

The initial findings showing that the GR and MR antagonists Mifepristone and Spironolactone, respectively, could prevent the circadian dysregulation observed in MPL treated animals was exciting. Combined with the results that I showed in chapter 3, where *Per1* expression was altered and *Gr* was expressed in the SCN, this supported the notion that glucocorticoids may target this area and significantly affect its output. However, MPL treated rats implanted with placebo pellet exhibited a vastly different rhythm to that of the original MPL treated rats. The MPL treated group was now more similar to the control group, with only a small albeit significant difference in rhythm compared to control. Therefore, based upon these findings, it was important to repeat the initial experiment of MPL treatment only, to assess the frequency period in LA and cBT.

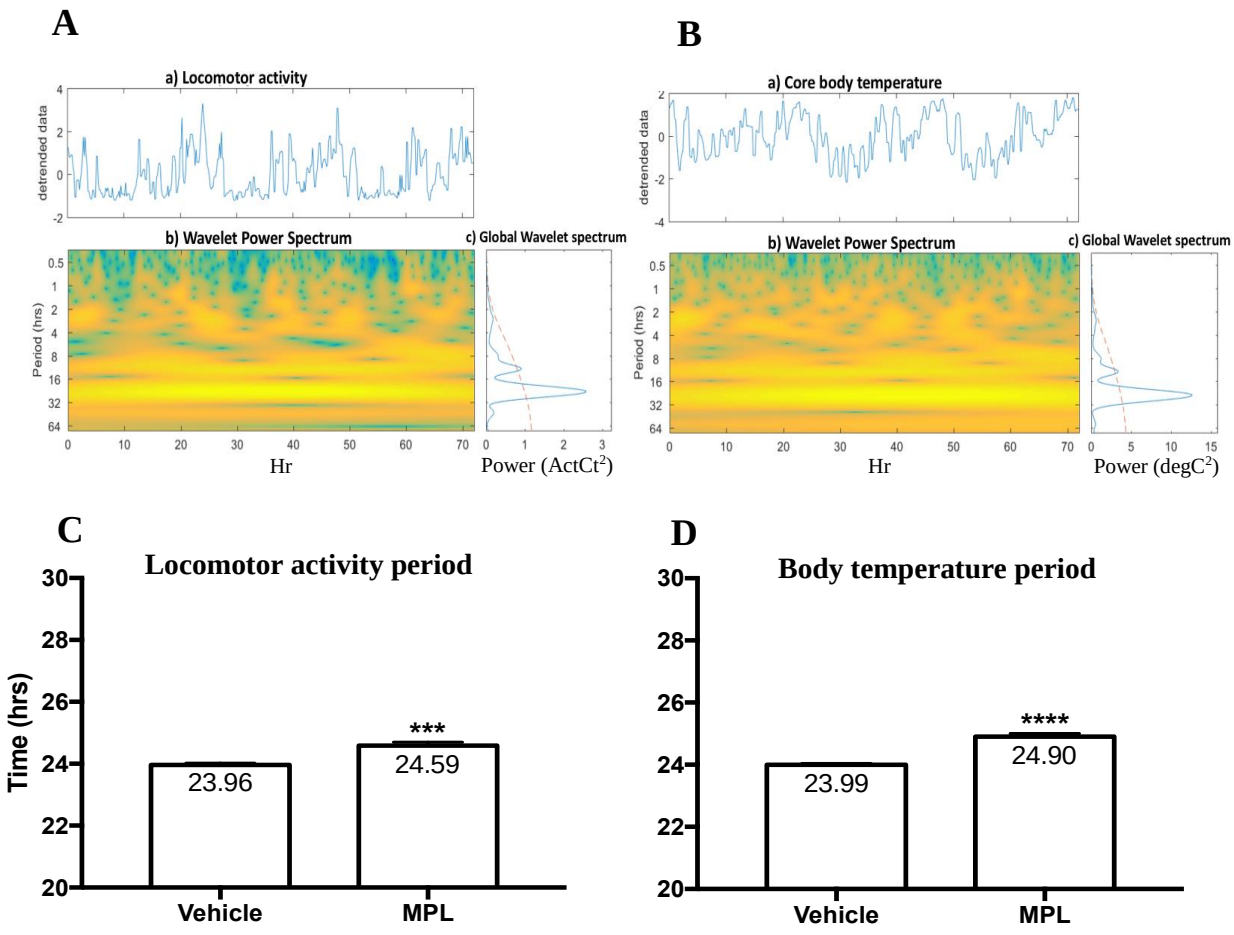

Figure 5.5 A repeated experiment looking at the locomotor activity and core body temperature in rats treated with MPL showed a different periodicity to that shown previously. Following MPL treatment, the rhythmicity of locomotor activity (**A**) and core body temperature (**B**) exhibited a different profile than what was previously shown, with rhythmicity no longer dominant to a ~7h frequency but instead, more similar to that shown in the control group. The periodicity of LA (**C**) and cBT (**D**) are shown between control and MPL treated animals. A significant increase in period length was observed in the MPL treated group for LA (**C**) and cBT (**D**). N = 8 per group. Detrended data and representative plot. Wavelet spectral analysis with Lomb-Scargle periodogram (**a** - raw, detrended data; **b** – wavelet spectral analysis; **c** – Lomb-Scargle periodogram). Red dotted line indicating P<0.05. Bar graphs; Mean ± SEM. Unpaired t-tests. P < 0.05, P < 0.01, P < 0.001 and P < 0.0001.

Based on previous data, the expectant rhythm was anticipated to lack circadian rhythmicity with a dominant ultradian rhythm present. However, locomotor activity (**A/C** - 24.59 ± 0.1114), although not 24h, exhibited a periodicity much more similar to that of controls, albeit with a period lengthening, similar to the period observed in free running. Core body

temperature, similarly to locomotor activity was also more similar to controls than the previous experiment, but again with a lengthening of the period, similar to what is seen in free running (**B/D** - 24.9 ± 0.1056). The periodicity was assessed between groups in LA (**C**) and cBT (**D**), with a significant increase in period length observed in both LA (**C**) and cBT (**D**) in the MPL treated group (**C** – t(8) – 4.992, p = 0.0005) (**D** – t(8) – 8.98, p < 0.0001).

5.4 Discussion

Locomotor activity (LA) and core body temperature (cBT) are tightly regulated to remain in rhythm with the light/dark cycle, maintaining a 24h periodicity (Stenvers et al. 2016). In a 12:12 light cycle, rats entrain to this rhythm, with both robustly synchronized by the external stimuli (Panda et al. 2002). In constant dark, rats revert to a free running rhythm with a lengthened period of 24.5h observed (Chen et al. 2008), resulting in a daily shift in phase continuing over time. In constant light, which acts as both a circadian disruptor and a chronic stressor, rats become arrhythmic (Waite et al. 2012). Analysis of these data using wavelet spectral analysis showed a similar periodicity to what was evident in the original MPL treated LA and cBT (Figure 5.7) providing evidence that MPL treatment could robustly and rapidly dysregulate the clock mechanism at the level of the SCN, an effect that took 4 weeks of constant light to evoke.

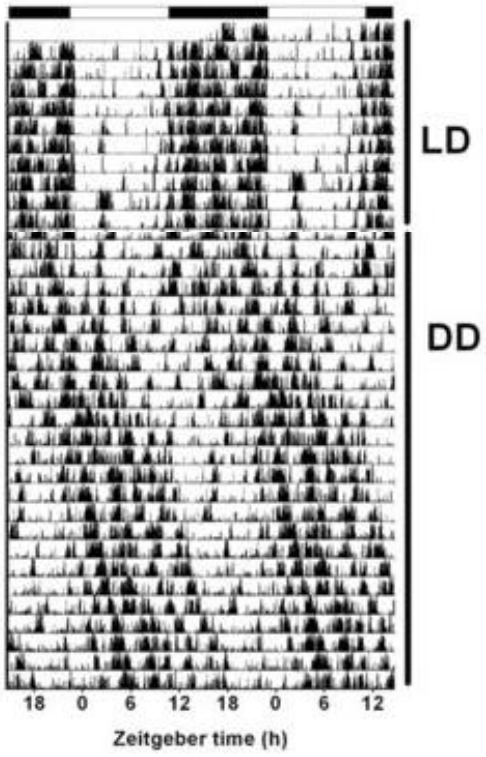

Figure 5.6 Actogram data of 12:12 light/dark schedule, free running during constant darkness and arrhythmic activity during constant light. These data show rats entrained to the 12:12 light/dark cycle, with LA rhythm entrained to 24h. However, during constant dark, mice free run, whereas during constant light they present with arrhythmic activity periods *(Adapted from* Stenvers et al. 2016)**.**

Patients who are prescribed glucocorticoid steroids often report altered activity periods, including sleep disruption. However, this has been difficult to evaluate, as differences in dosage and disease per patient makes it hard to analyse for a significant effect. Previously, it was shown that the glucocorticoid steroid MPL significantly affects the periodicity of LA and cBT in rats (Figure 1.1), however no further analysis was carried out, with only an observational effect noted. However, the rapid effect observed in those data, were similar to the effect observed in rats following 6 weeks of constant light, indicating that MPL rapidly targets the master clock, whereas constant light exposure requires 4 weeks to induce a similar effect.

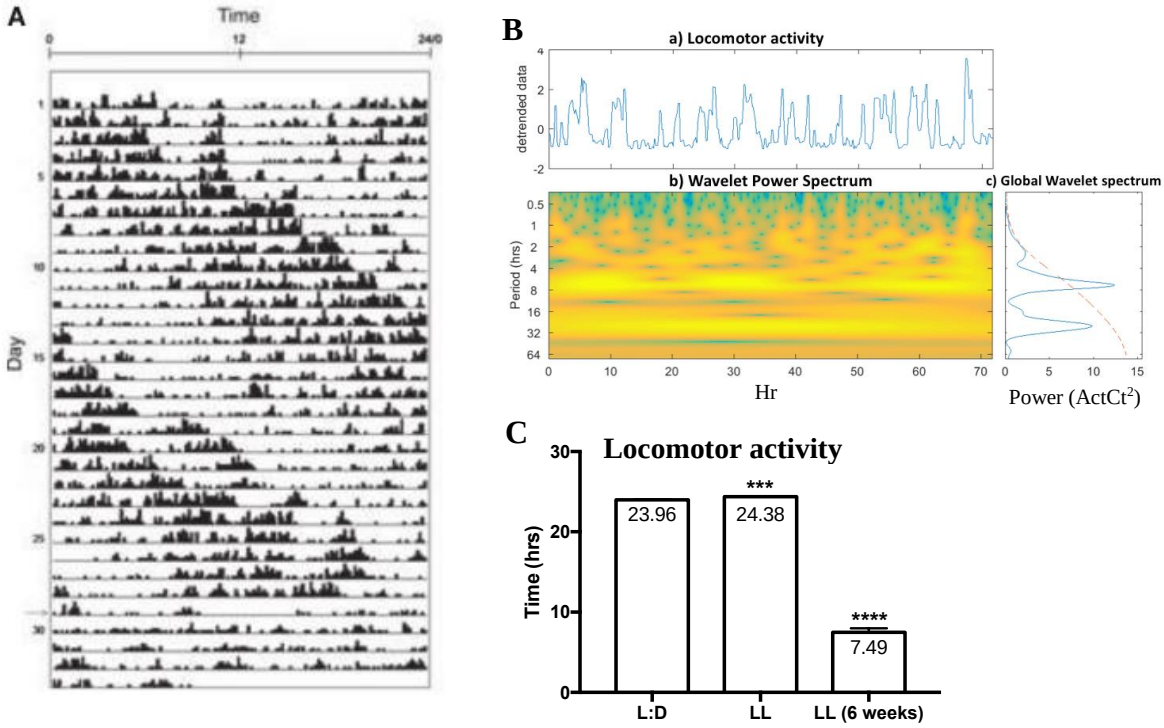

Figure 5.7 Constant light evokes free running in rats followed by arrhythmic activity after four weeks in actogram data and wavelet spectral analysis. During the first four weeks of constant light exposure, rats exhibit a free running LA behavior that is similar to rats kept in constant dark (**A**). However, after five weeks of constant light the rats become arrhythmic (shown with arrow) (Waite et al. 2012). Using wavelet spectral analysis and the Lomb-Scargle periodogram (**B**), the arrhythmic activity is evident over the three-day period analysed. Output of the wavelet analysis and Lomb-Scargle periodogram (**C**) showed that in constant light, the rats entered a free running periodicity (24.38 ± 0.06843) compared to the light/dark entrained group (23.96 ± 0.05545). Following four weeks of constant light,

the rats became arrhythmic, with the periodicity of activity sharply falling (7.486 ± 0.493). N = 8 per group. Detrended data and representative plot. Wavelet spectral analysis with Lomb-Scargle periodogram (**a** - raw, detrended data; **b** – wavelet spectral analysis; **c** – Lomb-Scargle periodogram). Red dotted line indicating P<0.05. Bar graphs; Mean ± SEM. Unpaired t-tests. $P < 0.05$, $P < 0.01$, $P < 0.001$ and $P < 0.0001$.

Here, I used wavelet spectral analysis with a Lomb-Scargle periodogram to assess the periodicity of these data. Continuous wavelet spectral analysis, used previously to assess body temperature (Leise 2013) and PER2:LUC oscillations (Price et al. 2008) finds a correlation between a time series across specific points in a dataset with a scaled version of the wavelet function to define the frequency that best describes the dataset analysed. Further, using the Lomb-Scargle periodogram, which although is well-known for its algorithm to detect and characterize periodic signals from unevenly sampled data (Ruf 1999), can be utilized here, in particular in conjunction with the wavelet analysis to assess dominant and/or hidden frequencies within these data (Mallat 2009). It estimates the Fourier power, which decomposes a function of time, as a function of period oscillation, and therefore reads the oscillation as a period of time (Abramovich et al. 2000). Using this analysis technique allowed for the assessment of periodicity across a short period of time. Actogram data of LA in particular, is usually assessed following a significant period of recording, i.e. regularly 2+ weeks (Ben-Hamo et al. 2016; Sabbar et al. 2017; Chabot et al. 2012; Riccio & Goldman 2000). However, I was unable to do this due to experimental constraints, and therefore an adaptation to the analysis program was required. Using two analysis programs built into one, provided the most suitable option for this.

Clear daily rhythm in LA and cBT in the control group was observed using the wavelet analysis, as expected, with a light/dark entrainment evident, and further with the Lomb-Scargle periodogram which identified the same periodicity. Assessment of the MPL periodicity presented an exciting result, with an ultradian rhythm dominant in both LA and cBT. The ultradian rhythm showed here is not the first time LA and cBT have been shown to exhibit a dominant ultradian rhythm. Lesioning the SCN results in arrhythmic locomotor activity and core body temperature rhythms as well as rats kept in constant light for 6 weeks (Waite et al. 2012). However, in the MPL experiments, the SCN remained intact, and the light cycle remained on a 12:12 light/dark cycle, indicating that the effect observed was through the action of the glucocorticoid steroid, MPL.

Following on from this, and the results of chapter 3 where I showed that MPL dysregulated clock genes *Per1*, *Per2* and *Bmal1* in the SCN, assessment of LA and cBT in the presence of GR and MR antagonists was carried out. A rhythm close to 24h was observed in all antagonist datasets, however this was also observed in the placebo dataset, and therefore significantly differed from the original MPL treated dataset from 2013 (Demski-Allen 2014). It was therefore important to return to the original experiment and repeat to confirm that I could match the initial result. The outcome was that I couldn't replicate those findings, however the periodicity of LA and cBT remained significantly different from control. Interestingly, the effect that I observed was one of an elongation to the period length. The extended period was consistent with that detected in free running animals (Verwey et al. 2013).

The latest rhythmic periodicity shown in the MPL treated group (Figure 5.5) would indicate that the GR and MR antagonist study was unable to inhibit the effect of the glucocorticoid MPL on LA and cBT, as the periodicity in the GR, MR and GR/MR combined antagonist study also produced a longer periodicity than the 24h profile (Figure 5.4). The dose given to antagonize GR and MR was not assessed in house but was taken from an experiment shown to block the effects of stress during a behavioural task (Nasca et al. 2015). Therefore, I cannot conclude with certainty that the GR and MR were effectively inhibited in my experiment. The potential role of GR and MR in the MPL-dependent rhythm changes would need to be assessed further, after optimization and characterisation of antagonist doses.

Furthermore, it is also important to address the differences between my experimental findings and the previous data. In an ideal world, we would want to be able to understand and find the cause of the rhythm disturbance that was observed previously. Reproducibility is vital in scientific research and therefore understanding what could account for the differences observed between the two sets of experiments are paramount. There were a number of factors that might account for the differences observed between MPL groups. Firstly, although the animals (male Lister hooded rat, Harlan, UK) were purchased from the same supplier, the initial experiments were carried out in mid 2013, whereas the most recent experiments were carried out in early 2018. During this five-year period, the genetic lineage may have changed and could have resulted in increased or decreased susceptibility

to GC treatment (Charmandari et al. 2008). Others have previously shown differential effects of using the same animal but with different genetic backgrounds (Ceolin et al. 2011; Wood et al. 2017). Secondly, my experiments were conducted on rats with surgically implanted IP telemeters. Whereas the previous experiment was conducted on rats with a combination of surgically implanted IP telemeters and jugular vein cannulation for continuous blood sampling with a spring and swivel tethering system (Windle et al. 1997). It may be possible that the combination of the extra surgical procedures and tethering induced a different physiological outcome during MPL treatment.

Despite the caveats detailed in this chapter, the results from my own series of experiments are both robust and reproducible. Taken together my data are internally consistent, with an alteration of the central clock at both the molecular and physiological level. MPL treatment induced an elongation in LA and cBT period length along with disrupted expression profiles of core clock genes in the SCN. The prolonged elevation of *Per1* mRNA expression – i.e. high expression from ZT10 through to ZT2 on the following day - could account for the prolonged period observed in LA and cBT in the MPL treated group.

Using wavelet analysis on actogram data from a previous constant light experiment (Figure 5.7), I detected a four-week duration of free running rhythm that is similar to rats kept in constant dark. After the fourth week of constant light, the rats displayed arrhythmic behaviour that was similar to SCN lesioned rats. The data that I have presented here indicated that treatment with MPL also induced a free running periodicity in animals without manipulating light/dark cues. This may imply a disconnect between the light/dark entraining rhythm of the SCN, with MPL being able to significantly override the dominant light/dark entraining signal to induce free running behaviour in these animals. In the following chapter, I explore how this alteration in circadian activity may also affect sleep and hippocampal circuitry during memory consolidation.

Chapter 6

The effects of MPL on hippocampal activity and sleep following the NOL task

6.1 Introduction

Treatment with MPL impacts cognitive function, with hippocampal specific memory significantly affected (Figure 6.1). Glucocorticoids are known to target the hippocampus through the abundantly expressed GR and MR (Reul & Kloet 1985; Conway-Campbell et al. 2010). Hippocampal specific memory consolidation, routinely assessed using the novel object location (NOL) task in rodents, has previously been reported to be impaired by glucocorticoid administration during the sleep period (Lupien & Lepage 2001; Kelemen et al. 2014), and memory impairments have been detected in patients during chronic prednisolone treatment (Keenan et al. 1996). Furthermore, the most commonly reported cognitive side effects associated with high dose intravenous MPL are memory loss and sleep disturbances (Kupersmith et al. 1994). However, these effects appear to be reversible, as memory processing and the sleep cycle recover after 60 days following treatment (Oliveri et al. 1998).

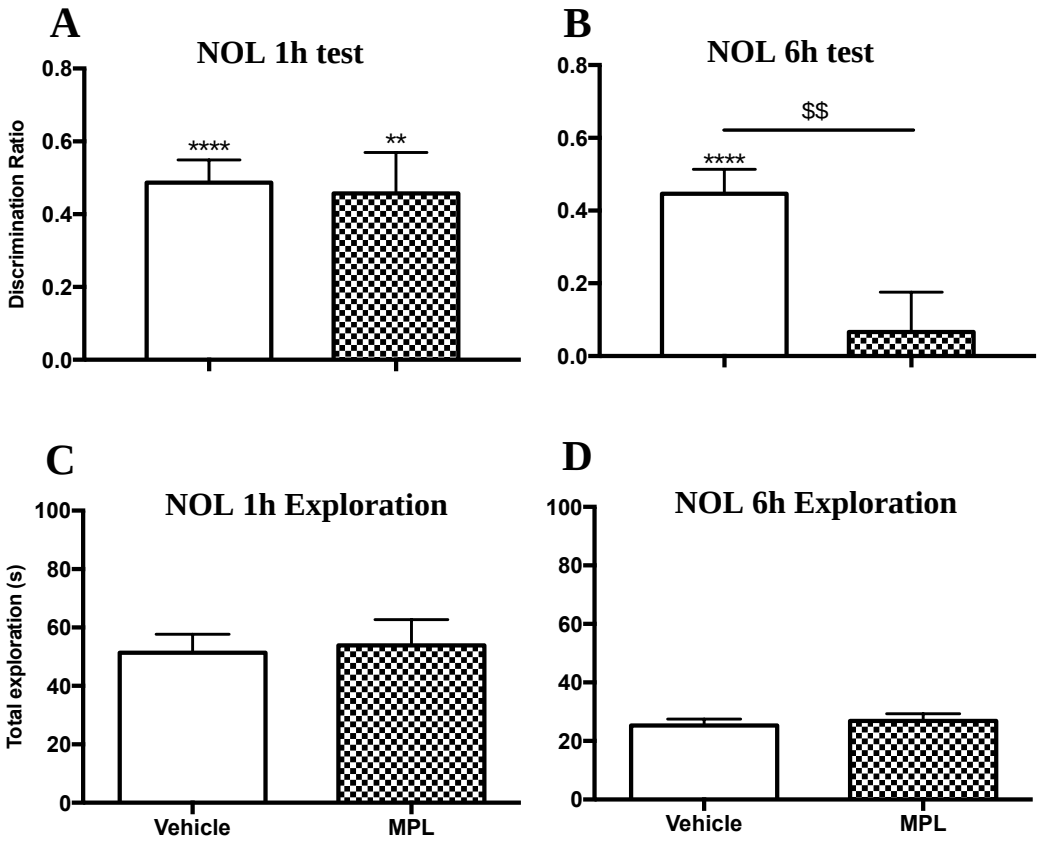

Figure 6.1 MPL treatment significantly affected memory performance in the novel object location task. Following a 1h delay between sample and test phases (**A**), both control and MPL treated rats were able to discriminate between novel and familiar object

locations. However, following a 6h delay (**B**), only the control group could discriminate between novel and familiar object locations. In contrast, the MPL group spent equal time at each object. Total exploration time was assessed at both time points, 1h (**C**) and 6h (**D**), showing no significant difference between treatments. Discrimination ratio equation ($\tau N - \tau F)/\Sigma\tau$, where τ = time, Σ = sum, N = novel and F = familiar. Figure adapted from Demski-Allen 2014.

In 'normal' healthy animals, there is a large variation in endogenous glucocorticoid levels between the circadian active and inactive phases. The highest circulating CORT levels occur prior to wakening, with levels falling throughout the night in nocturnal animals in anticipation of the sleep period (Weitzman et al. 1983; Henley et al. 2009), stabilising the sleep/wake cycle to the photoperiod (Sage et al. 2004). Exogenous glucocorticoid treatment has been shown to profoundly affect the sleep/wake cycle, dependent upon the time of administration (Born et al. 1991; Xie et al. 2015). Interestingly, there is a striking concentration dependent differential effect of glucocorticoids on sleep. Low dose hydrocortisone increases SWS, while high dose hydrocortisone decreases SWS (Vázquez-Palacios et al. 2001; Bradbury et al. 1998). Consistent with this, HPA axis alterations to corticotropin-releasing hormone can affect REM and SWS sleep (Holsboer et al. 1988). There are also reciprocal interactions between these systems, as alterations in sleep can significantly impact the secretion of CORT (Mirescu et al. 2006).

Sleep can be separated into rapid eye movement sleep (REM) and non-rapid eye movement sleep (NREM). NREM sleep, which comprises slow wave sleep (SWS) predominantly occurs during the first half of the sleep period, during which glucocorticoid levels are low (Born et al. 1988; Bierwolf et al. 2003; Plihal & Born 1999b; Henley et al. 2009) (Figure 6.2). Long-term memories are consolidated during SWS (Marshall et al. 2006; Rasch et al. 2007). Slow wave activity is evident in neuronal firing in the hippocampus, during which time the reactivation of recently encoded neuronal memory representations occur and are transformed for integration into long term memories (Wilson & McNaughton 1994; Skaggs & McNaughton 1996; Rasch & Born 2013). Therefore, timing of exposure to elevated glucocorticoid levels during the sleep period may have functionally significant effects on memory consolidation.

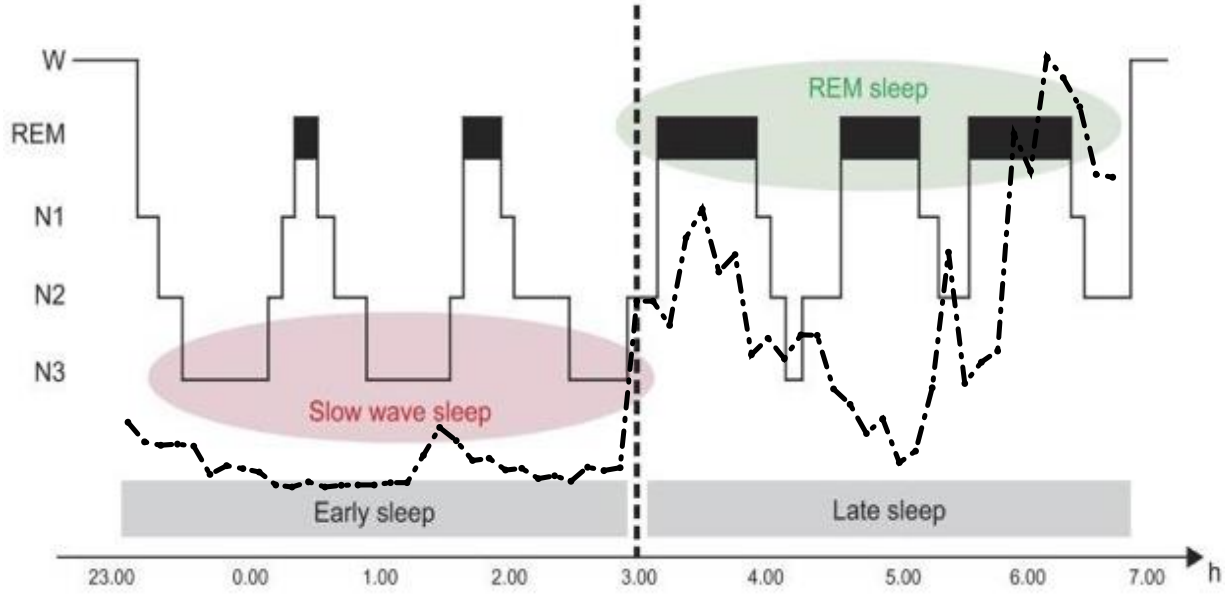

Figure 6.2 Cortisol secretion from continuous blood sampling during the different stages of sleep. During the early period of sleep, cortisol levels are low and SWS dominates, with small bouts of REM sleep evident. However, as the sleep period progresses, cortisol begins to rise in preparation for wakening where REM sleep dominates, with less SWS. W - wake, REM – Rapid Eye Movement, N1 – Non-REM1, N2 – Non-REM2, N3 – Non-REM3. N1-3 are collectively referred to as NREM sleep, N3 – Slow wave sleep. Circulating cortisol profile – black dotted line. (Adapted from Henley et al. 2009; Rasch & Born 2013)

In the previous chapters I showed a dysregulation to major components of the primary loop of the molecular clock in the SCN, a concomitant change in circadian activity period, and an alteration to the hippocampal circadian clock transcriptional machinery following MPL treatment. Therefore, I hypothesised that an MPL-induced sleep impairment may be responsible for impaired memory during the hippocampal specific NOL task. However, the NOL memory task was performed during the rats active phase, and impaired memory was detected at the 6h timepoint, which was also within the rats active phase. Therefore, the consolidation mechanism affected by MPL treatment must occur prior to the sleep phase (inactive period). However, rats sleep for short periods within the active phase, where during these bouts of sleep, characteristic sleep architecture is evident, with both REM and NREM sleep detected (Figure. 6.3).

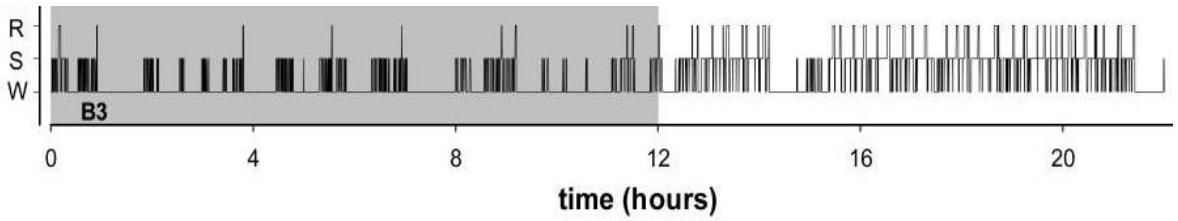

Figure 6.3 A representative hypnogram displaying periods of sleep across the active and inactive phase in the rat. During the active period (shaded), rats exhibit short periods of NREM (SWS) sleep with short bursts of REM sleep, interspersed with long periods of wake. During the inactive period (non-shaded), rats exhibit long periods of NREM (SWS) sleep and bursts of REM sleep, with only short periods of wake. Shaded region – active period. W – wake, S – slow-wave sleep, R – REM. (Adapted from Simasko & Mukherjee 2009).

Therefore, we hypothesised that we would see altered sleep architecture in the MPL treated rats during these bouts of sleep in the 6h memory consolidation period of the NOL task.

6.2 Methods

6.2.1 Animal housing and Home Office

5 adult male Lister Hooded rats (250-300g; 9-11 weeks) were obtained from Harlan Laboratories, now Envigo (Bicester, UK) and maintained under standard housing conditions with a 12:12 light/dark cycle. Food and water were available *ad libitum*. Rats were given an initial period of at least one week to acclimatise to the facility. All procedures were carried out in accordance with the UK Home Office guidelines and the UK Animals (Scientific Procedures) Act under PIL I04092F5F. Sample size was generated based upon known effect size in Prof. Matt Jones' laboratory.

6.2.2 Experimental design

During the experimental period, rats were individually housed for technical purposes. Rats were handled by the experimenter for 5 days prior to the start of experiments to eliminate effects of stress on memory processing during sleep. Rats were placed into a sleep box for 2hr prior to the NOL sample phase. Following the 4-minute NOL sample phase, the rats

were placed into the sleep box for 6 hours. The NOL test phase was then carried out (3-minute). Methylprednisolone (1mg/ml in drinking water (Demski-Allen 2014) (20mg/per day)) lasted five days. Sleep experiments were carried out on day 5 of treatment. N = 5 per group.

6.2.3 Surgery

Surgery was performed under balanced anaesthesia (veterinary isoflurane; Merial Animal Health Ltd., UK). Post-surgery, rats received subcutaneous injections (SC) of 0.2mg/mL Rimadyl (Carprofen 5% w/v, Benzyl alcohol 1% w/v; Pfizer., UK) diluted in sterile 10 IU/mL heparinised saline and 2.5mL s/c glucose saline (Sodium chloride 0.45% w/v and Glucose 2.5% w/v solution for infusion BP; Baxter Healthcare Ltd., UK) to aid recovery.

6.2.3.2 *In vivo* electrophysiology recordings of sleep

Rats were implanted with multi-site electrode arrays targeting the Prelimbic (PrL) area of the prefrontal cortex and the dorsal CA1 area of the hippocampus. The animals were handled daily and habituated to the behavioural arena and recording environment 5 days prior to experiment start. Electrical signal was acquired using a Digital Lynx 4 SX system (Neuralynx, USA) and recording using the PC software Cheetah (Neuralynx, USA). All behavioural and sleep recordings were carried out during the rats' active phase. The rats were placed in a sound-attenuating chamber for a 2hr recording, followed by a 4min object location sample phase experiment in a behavioural arena. The rats were placed back into the sound-attenuating chamber for a further 6hr recording. Following the 6hr delay period, the rats were replaced into the behavioural arena with one of the objects moved to a novel location. In order to measure the rats movement, a video recording was captured above the sound-attenuating chamber and above the behavioural arena. These movement data were used alongside the electrophysiology data to manually score arousal state in 10sec epochs. Epochs was scored as wake if movement was high. REM sleep was scored during periods of low movement combined with the presence of short wave activity (Theta frequency – 6-10Hz) on the local field potential (LFP) drive. Non-rapid eye movement (NREM) was scored if there was low movement and ripples and slow-waves (Delta frequency – 0.5-2Hz) on the LFP drive.

6.2.4 Novel object location task

The task comprised of an acquisition phase and a test phase separated by a 6h delay. In the acquisition phase, each rat was placed into the arena (wall facing) opposite to where duplicate objects were placed. The rats were allowed to investigate the objects for a total of 4 minutes before being placed into the sleep box. Six hours later, the rats were placed back into the arena but with one object now moved into the opposite corner (Figure 6.4). Exploration behaviour was recorded via a camera placed directly above the arena. Behavioural analysis was carried out post-experiment unblinded, by the experimenter.

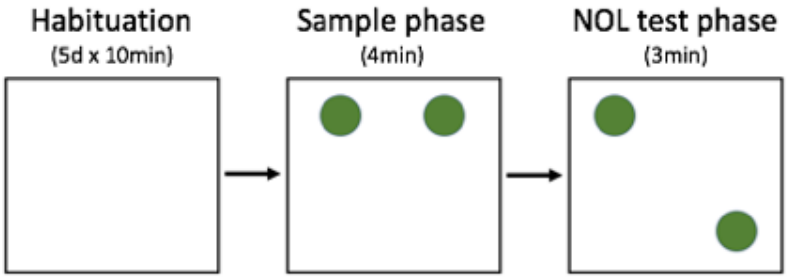

Figure 6.4. Representation of the Novel Object Location task.

6.3 Results

6.3.1 Recordings during the memory consolidation period reveal a significant effect of MPL treatment

Hippocampal specific memory was impaired by MPL treatment when the rats were tested with a 6h delay, but not following a 1h delay. Here, I have recorded brain activity for 6h following the sample phase of the NOL task to assess if MPL treatment altered hippocampal activity and may therefore account for the deficits in memory consolidation observed.

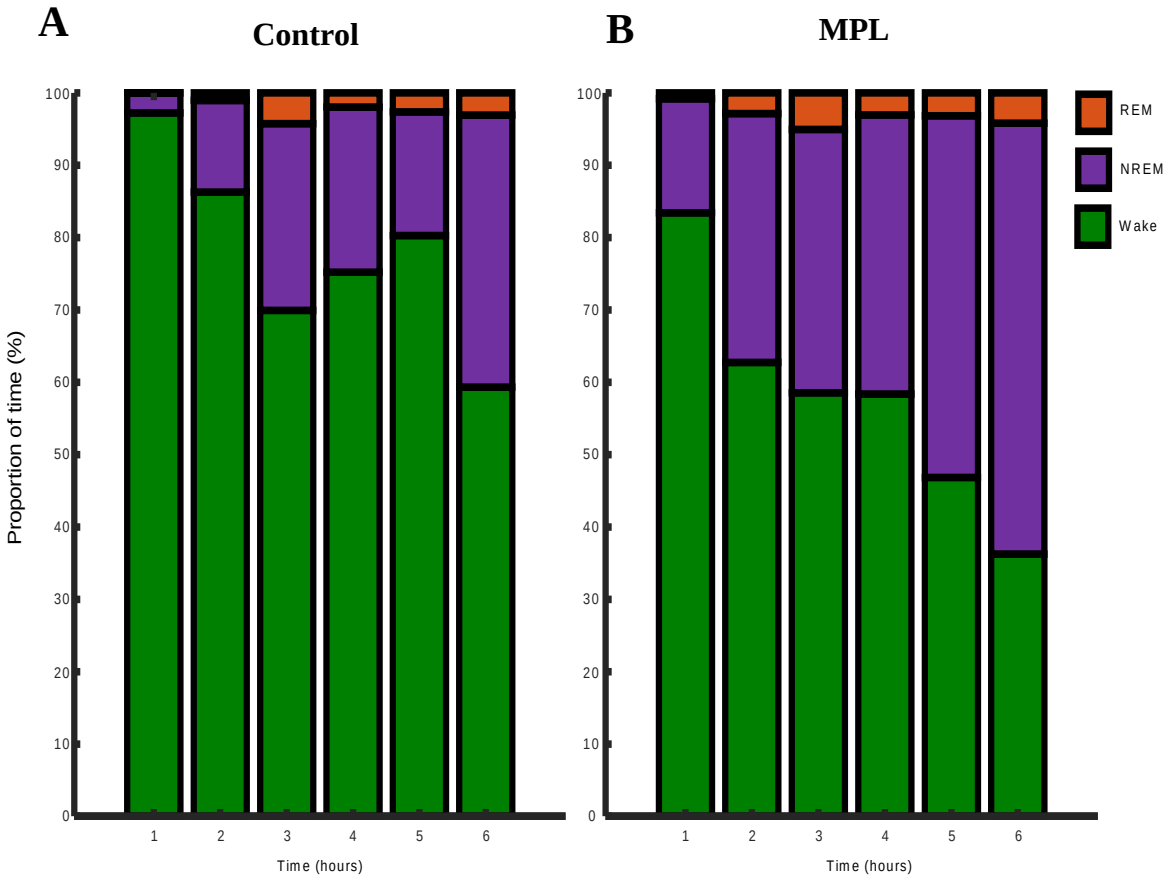

Figure 6.5 *In vivo* electrophysiology recordings of hippocampal activity for 6h following the NOL sample phase. Hippocampal activity in the control group (**A**) showed dominant periods of wake activity, as expected, with small bouts of REM and NREM sleep across each of the 1h epochs. In the MPL treated group (**B**), the rats were also active across all hours following the NOL sample phase, however a significant increase in NREM sleep was observed. Data represented as mean as a percentage of time. N = 5 per group.

In vivo electrophysiology recordings of hippocampal activity showed the expected level of wake activity, REM and NREM periods of sleep in the control group (**A**). No REM sleep was evident in the first hour following the NOL sample phase, with REM sleep occurring across the following five hours. NREM sleep occurred across all hours assessed, stabilised in hours 3, 4 and 5 then reached maximal levels during the final hour prior to the NOL test phase. In the MPL treated group (**B**), REM sleep was observed during all time periods. A significant portion of each hour was spent in NREM sleep, and similarly to the control group, maximal levels of NREM sleep were observed in the final hour.

6.3.2 REM sleep following the NOL sample phase

Figure 6.3 showed differences in hippocampal activity between treatment groups and therefore differences between the REM sleep period were analysed for significant differences.

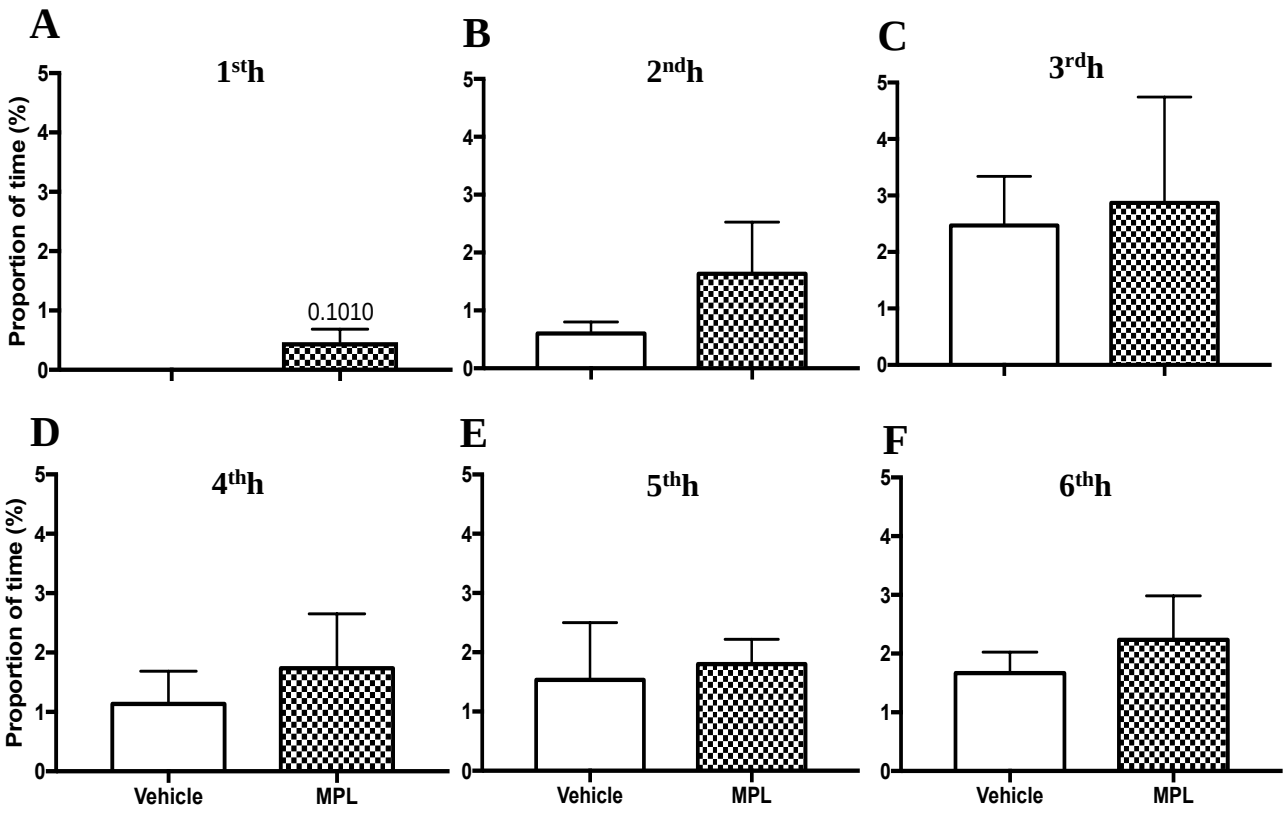

Figure 6.6 REM sleep was unchanged following MPL treatment. In the first hour (**A**) following NOL sample phase, the control group did not go into REM sleep but the MPL treated group did. In the second (**B**), third (**C**), fourth (**D**), fifth (**E**) and sixth (**F**) hour following the NOL sample phase, both treatment groups exhibited REM sleep, but no difference was observed between groups. N = 5. Data represented as mean ± SEM. Paired t-test. Significance set at $P < 0.05$.

Assessment of REM sleep between control and MPL was carried out. During the first hour following the NOL sample phase, the control group did not go into REM sleep at any point, however the MPL group did (**A**). However, as a percentage of total time per hour (control

– 0%, MPL – 0.46%, or 28secs of the hour), no significant difference was observed here. No significant difference was observed across any other hour, with REM sleep during the total assessment period not increasing over 2.47% of total time in control, and 2.87% in the MPL group, observed at 3h.

6.3.3 NREM sleep following the NOL sample phase

Although no significant difference was observed in REM sleep over the assessed period, an obvious increase in NREM sleep was evident. Therefore, individual assessment of each hour following the NOL sample phase was assessed for significant difference between groups.

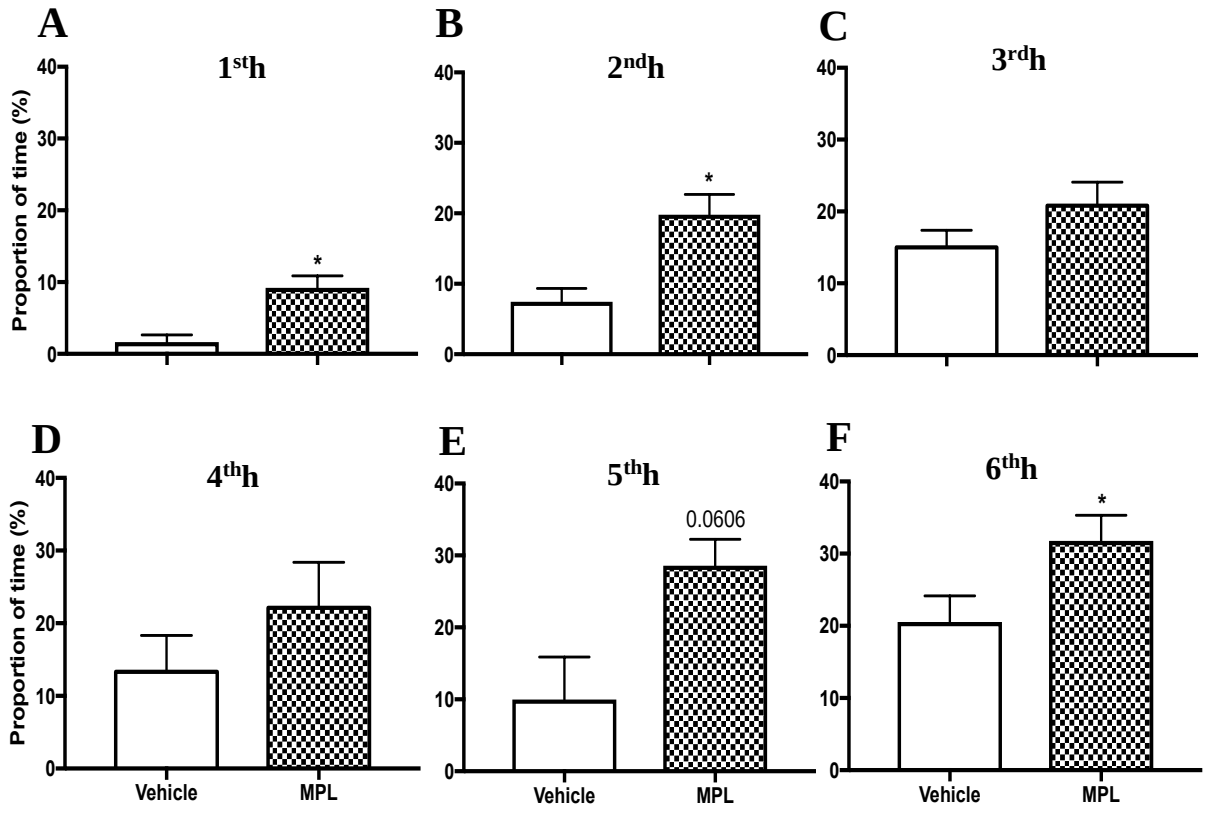

Figure 6.7 NREM sleep was affected following the NOL sample phase with MPL treatment. NREM sleep was evident within 1h (**A**), 2h (**B**), 3h (**C**), 4h (**D**), 5h (**E**) and 6h (**F**) following the NOL sample phase in both treatment groups. However, a significant increase in NREM sleep was observed in the MPL group at 1h, 2h and 6h, with a trend of significance observed at 5h. N = 5. Data represented as mean ± SEM. Paired t-test. Significance set at $P < 0.05$.

The total percentage of time spent in NREM sleep was significantly greater than that observed in the REM sleep period. In the first hour following the NOL sample phase (**A**), a significant increase in NREM sleep was observed in the MPL treated group (**A** ($t(5) = 4.266$, $p = 0.013$)). This significant increase persisted into the second hour (**B** ($t(5) = 2.788$, $p = 0.0494$)). No significant difference in NREM sleep was observed between groups for the following three hours, with only a trend of significance observed in the fifth hour (**E** ($t(5) = 2.592$, $p = 0.0606$). However, 6h following the NOL sample phase, a significant increase in NREM sleep was observed in the MPL group (**F** $t(5) = 2.954$, $p = 0.0418$).

6.3.4 Novel object location task following MPL treatment

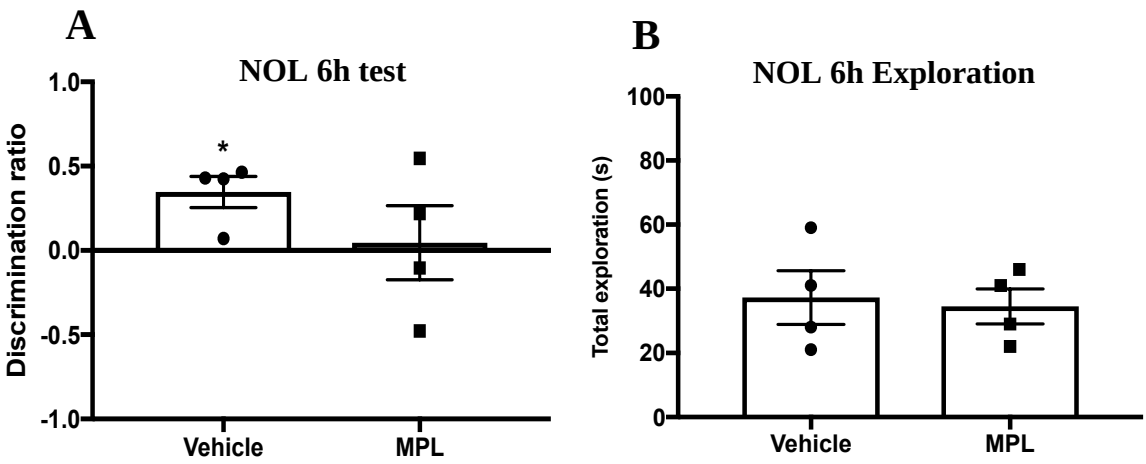

Figure 6.8 No difference was observed in memory performance between treatments in the novel object location task. Following a 6h delay in the NOL task (**A**), the control group were able to discriminate between novel and familiar objects, however the MPL group could not. However, no significant difference was observed between treatment. No significant difference was observed in exploration time between treatments (**B**). N = 4. * is comparison to hypothetical 0 using a t-test. Further analysed using Two-way ANOVA. Discrimination ratio equation $(\tau N - \tau F)/\Sigma\tau$, where τ = time, Σ = sum, N = novel and F = familiar.

Following on from previous published work, it was important to assess the NOL test phase following assessment of the sleep period to confirm the effect of memory impairment in

these animals. Using a hypothetical 0 to assess if both the control and MPL treated groups could discriminate between novel and familiar objects, the control group could (P = 0.0329), whereas the MPL group could not (P = 0.8478). Using a two-way ANOVA to assess for an interaction between treatments, no significant difference was observed (P = 0.2297).

6.4 Discussion

MPL has previously been shown to significantly impair memory processing during a hippocampal dependent memory task (Figure 6.1). In that experiment, short term memory remained intact, but memory was significantly impaired when tested 6h and 24h after the sample phase (Demski-Allen 2014). In those experiments, the sample phase of the behavioural test was carried out in the early active phase, when circulating glucocorticoids in the control rats were high. Therefore, the following 6h would still be within the active period, when circulating glucocorticoids remained elevated. In this chapter, I have looked at hippocampal activity during the 6h memory consolidation period of the NOL task, to assess for differences that could account for the memory impairment in the MPL treated rats.

A significant increase in NREM sleep was identified in the MPL treated group during the time period in which a deficit to hippocampal dependent memory was observed. Disrupted NREM sleep is known to impair hippocampal dependent memory (Mander et al. 2013), so an increase in NREM sleep was unexpected. However, as my recordings were carried out during the active phase, studies reporting associations between disrupted NREM sleep and impaired memory were conducted during the inactive phase, it is therefore difficult to draw further comparisons between the two sets of studies.

Assessment of the novel object location task yielded no effect of memory impairment between treatments. Although this result is not consistent with previously published data, it could be due to a number of factors. That being said, a significant difference was observed between a hypothetical 0 and control and MPL. However, the variability in the treatment group rendered further testing non-significant. To note, the sample size in this particular study was potentially underpowered, as in this cohort, 5 animals were used compared to 12 in the published study. Therefore, making conclusions based on these specific data may be

difficult and to identify a significant effect in behavioural analysis may have required a larger sample size.

However, although the behavioural data may be underpowered, it is still important to further analyse the NREM sleep data which may reveal important functional differences between the control and MPL treated rats. NREM sleep is composed of slow wave activity and sharp-wave ripples, which haven't yet been analysed in my dataset. In particular, ripple density during the first episodes of SWS after learning has been reported to be the more important for memory consolidation (Eschenko et al. 2008). As well as ripple density, magnitude and duration have been shown to increase during learning. Therefore, while the bouts of NREM sleep may be increased, the quality of sleep may be altered/decreased by MPL treatment.

While there is good evidence for interactions between sleep state, memory consolidation and the HPA axis, most of these studies are performed during the inactive phase. LFP and EEG recording are usually performed during the inactive phase in the rat, and memory testing is performed following a true period of sleep (Plihal & Born 1999a; Plihal & Born 1997; Wagner & Born 2008). However, here I show that discrete episodes of NREM sleep, with brain wave activity such as sharp-wave ripples and slow waves normally associated with memory consolidation processes, also occur during the rats' active phase. The findings in this chapter highlight the importance of these types of brain waves during memory consolidation processes at this time of day. Future characterisation of ripple density, magnitude and duration within the episodes of NREM sleep during memory consolidation, as well as assessing differences in sleep bouts between treatment groups, will hopefully elucidate mechanisms that may become dysregulated with MPL treatment.

Chapter 7

General Discussion

7.1 Summary of findings

In this thesis, I have for the first time demonstrated that treatment with the synthetic glucocorticoid Methylprednisolone targets the gene expression of the core clock component, *Period1* in the suprachiasmatic nucleus, dysregulating other clock components and altering the rhythmic output of the master circadian oscillator. I have demonstrated that MPL targets the peripheral clock oscillator in the hippocampus, significantly dysregulating core clock genes throughout the day. Further to dysregulating the molecular clock both centrally and peripherally, I have presented altered physiological output, in the form of locomotor activity and core body temperature. Previously published data showed that methylprednisolone significantly affected memory following a novel object location task. Here, I have showed that altering the molecular clock with MPL resulted in altered hippocampal activity following the novel object location task which may account for the memory deficits observed.

7.2 The role of glucocorticoids in circadian physiology

Circadian rhythms are intrinsic ~24h cycles that persist in the absence of external cues (Rosenwasser et al. 2005). The SCN acts as the master clock in the brain, entraining peripheral clocks in the body to remain in rhythm (Chen et al. 2008) with light input via photosensitive retinal ganglion cells retaining this rhythm to the photoperiod (Hattar et al. 2002), as rats in constant dark free run to a period of ~24.5h (Nakamura et al. 2005). Neuroendocrine circadian function is under the control of the SCN, as circadian variation in glucocorticoid secretion is abolished in SCNx studies (Moore & Eichler 1972; Silver et al. 1996; Waite et al. 2012).

In the brain, glucocorticoids target multiple areas where the GR and MR are expressed (Reul & Kloet 1985). The GR and MR were estimated to be located throughout most brain areas based on findings from in vitro [^{3}H]CORT binding assays, identifying such areas as the hippocampus, amygdala, lateral septum, locus coeruleus, and dorsal raphe. The hippocampus, which is particularly rich in GR and MR expression, has been extensively studied due to its importance for stress, and memory and learning. However, the receptors were not detected in the SCN in these studies (Reul & Kloet 1985; Reul & de Kloet 1986). Further experimentation assessing glucocorticoid action on the SCN failed to exhibit an

effect on the clock components using the potent GR specific agonist, DEX, whereas peripheral clocks were altered (Balsalobre et al. 2000).

CORT, DEX and MPL differ considerably in their activities. CORT rapidly binds to the GR in short pulses of 20 minutes every hour, whereas it binds to the MR far longer (Conway-Campbell et al. 2010; Mifsud & Reul 2016). DEX is a potent GR specific agonist whose activity is considerably different to that of CORT and MPL. A single injection of DEX into ADX animals results in GR binding for 6h in the HC. MPL on the other hand, binds to both the GR and MR in similar affinities to that of endogenous CORT. Again, in ADX animals, a single injection of MPL results in GR binding for 3h in the HC (Emma Earl et al. 2018). Although DEX binds to the GR far longer than MPL in the brain, it doesn't bind the MR, whereas MPL binds both receptors.

The prolonged half-life of MPL *in vivo* effectively maintains extremely low levels of circulating endogenous glucocorticoids whilst the synthetic glucocorticoid levels remained high. Importantly though, in untreated animals, corticosterone binds to the glucocorticoid receptor in a circadian manner (Kitchener et al. 2004) whereas MR is bound at both the circadian peak and nadir (Reul & Kloet 1985; Mifsud & Reul 2016). GR monomers and dimers mediate transcriptional processes in vivo (Lim et al. 2015) and GR:MR interactions have been observed at the DNA, suggesting a transcriptional role (Pooley 2015).

With MPL treatment, the GR was bound to the synthetic glucocorticoid far longer and in absence of a circadian pattern, keeping the receptor active and facilitating increased gene expression of *Per1* (Figure 7.1) (Earl et al. 2018). However, although this was expected, it has only been shown in tissues that express the GR, and as the SCN was a brain area where the GR or MR had not previously been identified, the expression of glucocorticoid regulated genes shouldn't have been affected here.

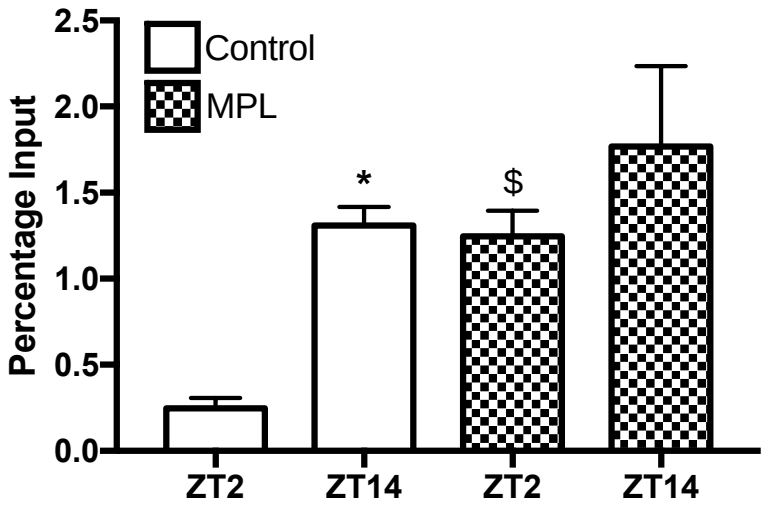

Figure 7.1 Hippocampal GR binding at the *Per1* gene distal GRE. Glucocorticoid receptor binding in control animals exhibit clear circadian rhythmic binding, with the binding at the *Per1* glucocorticoid response element significantly upregulated during peak CORT secretion. In the MPL treated group, endogenous glucocorticoids were suppressed, however GR binding persists in this group with the rhythmic binding lost. Data represented as mean ± SEM. N = 7 per group. Two-way ANOVA with Tukey's post-hoc test was used. All statistical significance indicated at $P < 0.05$ (*/$). * represents effect of time, $ represents effect of treatment. ZT2 repeated for visualisation purposes (Birnie 2018).

As DEX did not alter the core clock genes in the SCN, the data presented showing dysregulation in the SCN, potentially indicates a requirement of the activation of both the GR and MR to mediate the effects observed. Figure 7.2 potentially supports this hypothesis. Although I did not include these data in my results because it is only preliminary data, using RNAscope® (ACDBio, US), which detects RNA using a novel *in situ* hybridisation technique, I identified the presence of *Gr*, *Mr*, and *Per1* in nuclei of the SCN.

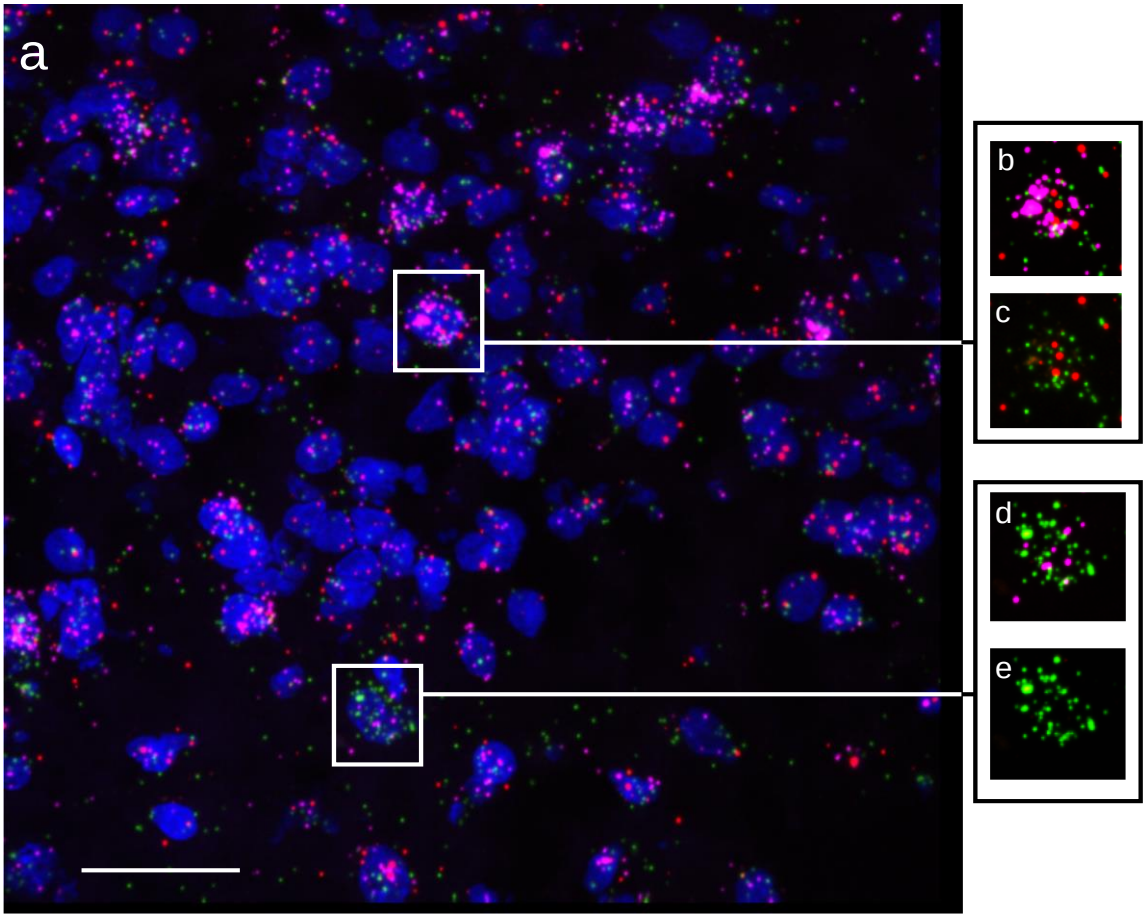

Figure 7.2 The colocalization of *Gr*, *Mr* and *Per1* mRNA in individual neurons within the SCN using RNAscope®. A wide field view of the neurons in the SCN shows abundant expression of *Per1*, *Gr* and *Mr* in the perinuclear area of individual neurons (**a**). Enlarged images of an individual nucleus indicate the perinuclear expression of *Gr*, *Mr* and *Per1*. (**b**) For visualisation purposes, only channels for *Gr* and *Mr* are shown in this image (**c**). Interestingly, another neuron is shown to lack MR expression, with only *Gr* and *Per1* expression evident (**d**). For visualisation purposes, only channels for *Gr* and *Mr* are shown in this image (**e**). *Gr* – green, *Mr* – red, *Per1* – pink, Nuclear Stain DAPI – blue. Scale bar – 10μm.

Further to the identification of *Gr*, *Mr* and *Per1* in SCN neurons, the effect observed in gene expression was most likely due to the use of a synthetic glucocorticoid that differs in temporal activation to its endogenous counterpart. GR activation with CORT is transient, lasting ~20 minutes during the highest levels of GC secretion, facilitating GC sensitive gene transcription at specific times of day. As Earl et al. 2018 showed, MPL binds to the

GR for over 3h, which would ultimately prolong GR activation and binding to DNA response elements to facilitate transcription, for example *Per1*. This prolonged activation of the receptor and transcriptional output of *Per1* would result in a dysregulation to the molecular clock shown.

However, SCN clock timing is also regulated by other brain areas such as the raphe nucleus as serotonergic projections from here to the SCN affect light entrainment of the clock. Adrenalectomy abolishes the circadian transcription of the serotonin rate limiting enzyme, *Tryptophan hydroxylase-2* (*Tph2*) in the raphe nucleus, indicating an indirect mechanism for glucocorticoid feedback (Malek et al. 2007; Meyer-Bernstein & Morin 1999). However, as Balsalobre et al. 2000 failed to report a change in clock gene expression in the SCN with DEX *in vivo*, it indicates that the raphe nuclei did not drive an indirect rhythmic change here, at least via a GR only mediated effect, again supporting the role for the activation of both GR and MR to bring about this effect.

However, I do not believe these results are limited to this synthetic GC, as Cushing's disease, in which patients exhibit elevated circulating GCs levels with an undefined circadian rhythm, complain of altered sleep periods and memory deficits (Keenan et al. 1996), leading to the hypothesis that elevated levels of endogenous GCs, may evoke a similar response in the SCN.

SCN expression of *Per1*, *Per2* and *Bmal1* exhibited the rhythmic expression profile in agreement with previously published data (Peirson et al. 2006). *Per1* and *Per2* expression increased prior to the onset of the active phase (Figure 3.2A and 3.4A), with *Bmal1* transcript expression in antiphase. The expression of the *Per1* gene following MPL treatment was robust and showed that glucocorticoids are able to target this brain region. In *Per1*$^{(-/-)}$ mice, a compensatory mechanism has been observed, with *Per2* regulating the clock (Bae et al. 2001) and so was tested to assess if this mechanism was evident. Interestingly, *Per2* expression was similar to *Per1*, indicating that either *Per1* was able to significantly dysregulate *Per2*, or that *Per2* in the SCN is also a glucocorticoid target, as it has been shown *in vivo* in the BNST and CeA (Amir et al. 2004; Lamont et al. 2005). The significant induction of *Per1* and *Per2* at ZT2 in the MPL group also raises the question of whether this effect would be observed in constant dark experimentation, as this effect could be due to a hypersensitivity to light following chronic treatment with glucocorticoid

therapy, although there is currently no clinical evidence for this. However the glucocorticoid and mineralocorticoid receptors are expressed in the retina (Zhao et al. 2010; Gallina et al. 2014), and therefore could potentially exert direct retinal to SCN input effects, and is certainly an area that is of importance to explore.

Peripheral to the SCN in the HC, ligand-activated GR can directly induce increased transcription of *Per1* irrespective of the time of day (Conway-Campbell et al. 2010) and in the liver and skeletal muscle, activated GR has been shown to phase shift clock genes (Balsalobre et al. 2000). The prolonged activation of the GR on the *Per1* gene (Figure 7.1) results in increased output of *Per1* transcription, which in turn could drive the dysregulation of peripheral clocks, in particular altering other core components of the primary loop such as *Cry1, Cry2, Bmal1* and *Clock*, to desynchronise internal clocks from external stimuli. Although I haven't shown this in the SCN, this is a mechanism that could be expected based upon these data.

Interestingly, the expression of *Per1* in the HC in the MPL group was similar to *Per1* expression in the SCN, with a significant increase in transcript observed at ZT2, in both the RNA sequencing and qPCR data. However, as the SCN drives peripheral clocks to remain in rhythm, one could say this was unsurprising, however as the SCN was not expected to be altered with GC treatment, this provides further evidence that glucocorticoids can target the SCN.

That being said, further assessment of *Per*1 and *Bmal1* expression in the HC following MPL treatment provided evidence of a 4h phase shift (Figure 7.3) in a manner similar to that observed in other peripheral tissues following GC treatment (Balsalobre et al. 2000).

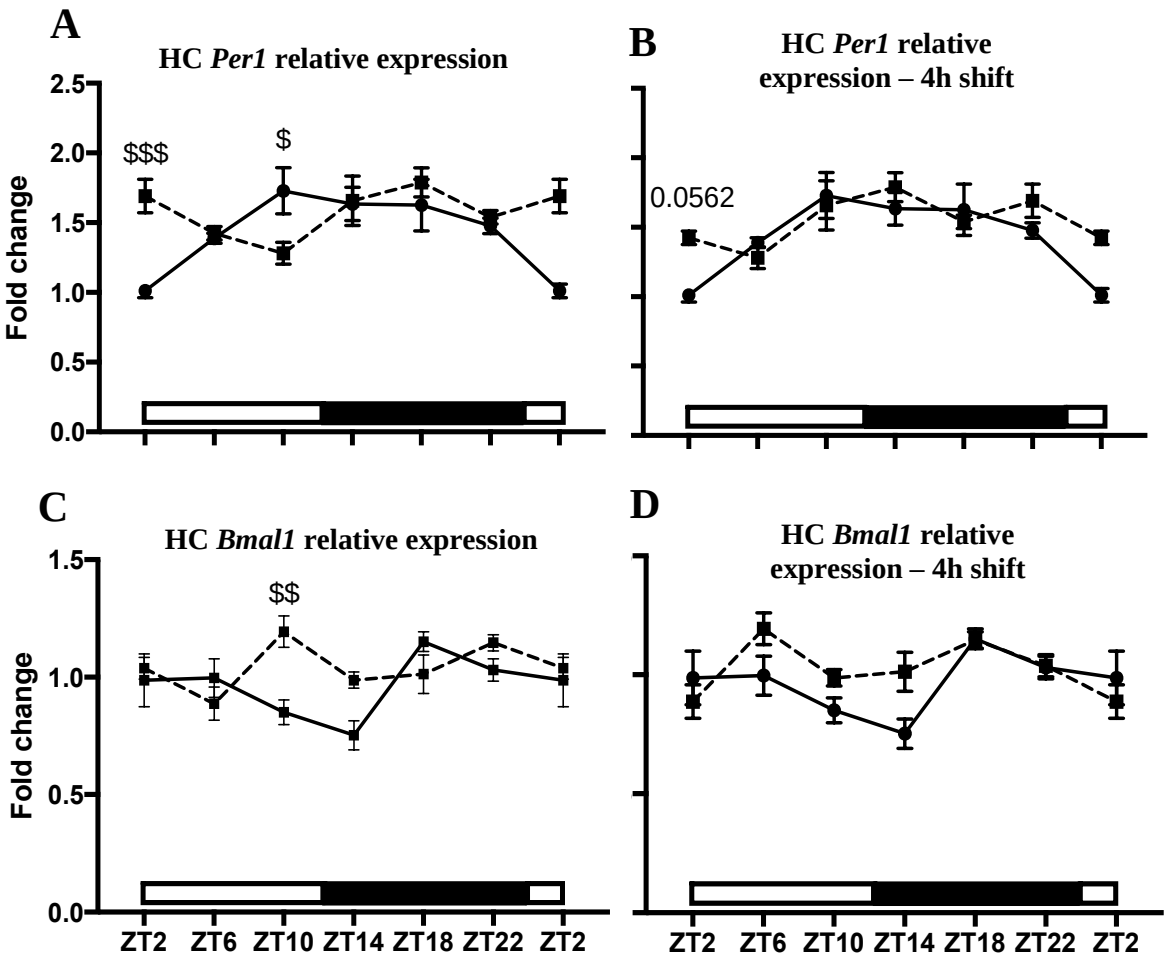

Figure 7.3 Phase shifting the expression of *Per1* and *Bmal1* in the MPL group by 4h results in no effect of treatment in the HC. A significant effect of MPL treatment on Per1 expression was observed in the HC, with a significant increase in transcript expression observed at ZT2, followed by a repression of expression at ZT10 (**A**). However, replotting the data after shifting the phase of expression of the MPL group 4h back, resulted in no significant difference between groups (**B**). Bmal1 expression was affected by MPL treated (**C**), however, replotting the data after shifting the phase by 4h in the MPL group, resulted in no significant difference between treatments. MPL – dotted line. qPCR data represented as mean ± SEM. N = 4 per group. Two-way ANOVA with Sidak's post-hoc test was used. All statistical significance indicated at $P < 0.05$ (*). ZT2 repeated for visualisation purposes.

This phase delay in clock gene expression here, may have resulted in the extended phase of locomotor activity and core body temperature identified in these animals. In the 12:12 light/dark cycle, they should retain rhythm to the photoperiod, similarly to controls (Riccio & Goldman 2000). However, the alteration to the master clock and peripheral clocks may account for the extended period length in these animals. The light/dark cycle may still act as a zeitgeiber in these animals, to retain a circadian rhythm. Therefore, assessing these animals in constant dark with MPL treatment would provide further understanding of the effect MPL has on the master clock to affect physiological output.

Similarly, hippocampal activity was assessed following a novel object location task. Although the behavioural data did not yield a significant effect of treatment as shown previously, this could be due to the sample size used. However, the neural activity data indicated an increase in slow wave activity in the MPL treated group, further supporting the notion that MPL can target central and peripheral clocks to alter the sleep phase in relation to the light/dark cycle, which may account for this increase in hippocampal slow wave activity during the active period. The underlying mechanism that accounted for the memory disturbances in those animals remains unknown and although differences were observed in the neural activity of these animals, no difference was observed in the ability to consolidate memories at this stage, and therefore indicates that these two events may occur independently of one another. However, hippocampal plasticity is vital for consolidating new memories, and importantly, exhibits a striking time-of-day difference, indicating that timing is key to forming new memories (Jilg et al. 2009).

I have showed in this thesis that MPL significantly dysregulates the core clock gene *Per1*. The rhythmic phosphorylation of CREB is critically regulated by *Per1* (Rawashdeh et al. 2016) and CREB is central to learning and memory (Kida & Serita 2014). Further evidence of a requirement of *Per1* in memory processing was evident with $Per1^{(-/-)}$ mice, who exhibit reduced LTP, a marker of long-term memory in electrophysiology experiments (Rawashdeh et al. 2014b), whilst also testing poorly in the hippocampal specific radial arm maze (Jilg et al. 2009).

Although these data provide a novel role in which glucocorticoids can target the SCN, there are a number of limitations that were noted. Firstly, the metabolic effects of glucocorticoid treatment render this experimental design to a maximum of five days treatment, which

limits the ability to assess long term effects on activity and temperature recordings. The method of delivery too, via ad libitum oral treatment, which although is medically relevant to the clinic, limits the known dose that each rat received during each experimental study. To combat this, future studies employing direct infusions to the brain areas of interest would certainly be a method to combat these limitations.

Glucocorticoids are one of the most commonly prescribed classes of drugs today, with 2% of the UK adult population prescribed oral glucocorticoid therapy at any given time (Overman et al. 2013). Reports of depression and psychiatric illness have been reported following synthetic glucocorticoid use (Muzyk & Holt 2010), as well as in patients with Cushing's disease and Cushing's syndrome, who present with elevated levels of glucocorticoid hormones throughout the day (Pereira et al. 2010; Pivonello et al. 2015). Sleep disturbances are commonly reported in the clinic and studies have revealed that memory is significantly impaired with long-term Prednisolone treatment (Keenan et al. 1996; Brown 2009; Judd et al. 2014). In this thesis, I believe I have identified a novel mechanism that will increase the understanding of glucocorticoid action on circadian biology, with particular relevance to glucocorticoid related sleep disturbances, memory impairment and mental health in patients treated chronically with long-acting synthetic glucocorticoids.

8. References

Abarca, C., Albrecht, U. & Spanagel, R., 2002. Cocaine sensitization and reward are under the influence of circadian genes and rhythm. *Proceedings of the National Academy of Sciences of the United States of America*, 99(13), pp.9026–30. Available at: http://www.ncbi.nlm.nih.gov/pubmed/12084940.

Abe, M. et al., 2002. Circadian rhythms in isolated brain regions. *The Journal of neuroscience : the official journal of the Society for Neuroscience*, 22(1), pp.350–6. Available at: http://www.ncbi.nlm.nih.gov/pubmed/11756518.

Abel, T. et al., 2013. Sleep, Plasticity and Memory from Molecules to Whole-Brain Networks. *Current Biology*, 23(17), pp.R774–R788. Available at: https://www.sciencedirect.com/science/article/pii/S0960982213008488.

Abraham, U. et al., 2005. Independent circadian oscillations of Period1 in specific brain areas in vivo and in vitro. *Soc Neuroscience*. Available at: http://www.jneurosci.org/content/25/38/8620.short.

Abrahamson, E.E. & Moore, R.Y., 2001. Suprachiasmatic nucleus in the mouse: retinal innervation, intrinsic organization and efferent projections. *Brain research*, 916(1–2), pp.172–91. Available at: http://www.ncbi.nlm.nih.gov/pubmed/11597605.

Abramovich, F., Bailey, T.C. & Sapatinas, T., 2000. Wavelet Analysis and its Statistical Applications. *Journal of the Royal Statistical Society: Series D (The Statistician)*, 49(1), pp.1–29. Available at: http://doi.wiley.com/10.1111/1467-9884.00216.

Adelmant, G. et al., 1996. A functional Rev-erb alpha responsive element located in the human Rev-erb alpha promoter mediates a repressing activity. *Proceedings of the National Academy of Sciences of the United States of America*, 93(8), pp.3553–8. Available at: http://www.ncbi.nlm.nih.gov/pubmed/8622974.

Aggleton, J.P. & Brown, M.W., 1999. Episodic memory, amnesia, and the hippocampal-anterior thalamic axis. *The Behavioral and brain sciences*, 22(3), pp.425-44; discussion 444-89. Available at: http://www.ncbi.nlm.nih.gov/pubmed/11301518.

Ahima, R.S. & Harlan, R.E., 1990. Charting of Type II glucocorticoid receptor-like immunoreactivity in the rat central nervous system. *Neuroscience*, 39(3), pp.579–604. Available at: https://www.sciencedirect.com/science/article/pii/030645229090244X.

Ahmad, M. & Cashmore, A.R., 1993. HY4 gene of A. thaliana encodes a protein with characteristics of a blue-light photoreceptor. *Nature*, 366(6451), pp.162–166. Available at: http://www.ncbi.nlm.nih.gov/pubmed/8232555.

Ahmed, T. & Frey, J.U., 2005. Plasticity-specific phosphorylation of CaMKII, MAP-kinases and CREB during late-LTP in rat hippocampal slices in vitro. *Neuropharmacology*, 49(4), pp.477–492. Available at: https://www.sciencedirect.com/science/article/pii/S0028390805001498.

Aisa, B. et al., 2007. Cognitive impairment associated to HPA axis hyperactivity after maternal separation in rats. *Psychoneuroendocrinology*, 32(3), pp.256–266. Available at: https://www.sciencedirect.com/science/article/pii/S030645300700008X.

Akashi, M. & Takumi, T., 2005. The orphan nuclear receptor RORα regulates circadian transcription of the mammalian core-clock Bmal1. *Nature Structural & Molecular Biology*, 12(5), pp.441–448. Available at: http://www.ncbi.nlm.nih.gov/pubmed/15821743.

Akhtar, R.A. et al., 2002. Circadian cycling of the mouse liver transcriptome, as revealed by cDNA microarray, is driven by the suprachiasmatic nucleus. *Current biology :*

CB, 12(7), pp.540–50. Available at: http://www.ncbi.nlm.nih.gov/pubmed/11937022.
Al-Habet, S.M. & Rogers, H.J., 1989. Methylprednisolone pharmacokinetics after intravenous and oral administration. *British journal of clinical pharmacology*, 27(3), pp.285–90. Available at: http://www.ncbi.nlm.nih.gov/pubmed/2655680.
Albers, H.E. & Ferris, C.F., 1984. Neuropeptide Y: role in light-dark cycle entrainment of hamster circadian rhythms. *Neuroscience letters*, 50(1–3), pp.163–8. Available at: http://www.ncbi.nlm.nih.gov/pubmed/6548555.
Amaral, D.G. & Dent, J.A., 1981. Development of the mossy fibers of the dentate gyrus: I. A light and electron microscopic study of the mossy fibers and their expansions. *The Journal of Comparative Neurology*, 195(1), pp.51–86. Available at: http://www.ncbi.nlm.nih.gov/pubmed/7204652.
Amaral, D.G. & Lavenex, P., 2007. The dentate gyrus: fundamental neuroanatomical organization (dentate gyrus for dummies). *Progress in Brain Research*, 163, pp.3–790. Available at: https://www.sciencedirect.com/science/article/pii/S0079612307630015.
Amato, M.P. et al., 2004. Neocortical volume decrease in relapsing-remitting MS patients with mild cognitive impairment. *Neurology*, 63(1), pp.89–93. Available at: http://www.ncbi.nlm.nih.gov/pubmed/15249616.
Amir, S. et al., 2004. A Circadian Rhythm in the Expression of PERIOD2 Protein Reveals a Novel SCN-Controlled Oscillator in the Oval Nucleus of the Bed Nucleus of the Stria Terminalis. *Journal of Neuroscience*, 24(4), pp.781–790. Available at: http://www.ncbi.nlm.nih.gov/pubmed/14749422.
Anacker, C. et al., 2013. Role for the kinase SGK1 in stress, depression, and glucocorticoid effects on hippocampal neurogenesis. *Proceedings of the National Academy of Sciences of the United States of America*, 110(21), pp.8708–13. Available at: http://www.ncbi.nlm.nih.gov/pubmed/23650397.
Anand, S.N. et al., 2013. Distinct and Separable Roles for Endogenous CRY1 and CRY2 within the Circadian Molecular Clockwork of the Suprachiasmatic Nucleus, as Revealed by the Fbxl3Afh Mutation. *Journal of Neuroscience*, 33(17), pp.7145–7153. Available at: http://www.ncbi.nlm.nih.gov/pubmed/23616524.
Andersen, P., Holmqvist, B. & Voorhoeve, P.E., 1966. Excitatory Synapses on Hippocampal Apical Dendrites Activated by Entorhinal Stimulation. *Acta Physiologica Scandinavica*, 66(4), pp.461–472. Available at: http://doi.wiley.com/10.1111/j.1748-1716.1966.tb03224.x.
André, E. et al., 1998. Disruption of retinoid-related orphan receptor β changes circadian behavior, causes retinal degeneration and leads to vacillans phenotype in mice. *The EMBO Journal*, 17(14), pp.3867–3877. Available at: http://www.ncbi.nlm.nih.gov/pubmed/9670004.
Andrews, M.H. et al., 2012. Acute glucocorticoid administration rapidly suppresses basal and stress-induced hypothalamo-pituitary-adrenal axis activity. *Endocrinology*, 153(1), pp.200–11. Available at: http://www.ncbi.nlm.nih.gov/pubmed/22087024.
Antle, M.C. & Silver, R., 2005. Orchestrating time: arrangements of the brain circadian clock. *Trends in Neurosciences*, 28(3), pp.145–151. Available at: http://www.ncbi.nlm.nih.gov/pubmed/15749168.
Antonijevic, I.A. & Steiger, A., 2003. Depression-like changes of the sleep-EEG during high dose corticosteroid treatment in patients with multiple sclerosis. , 28, pp.780–795.
Archer, S.N. et al., 2003. A length polymorphism in the circadian clock gene Per3 is linked to delayed sleep phase syndrome and extreme diurnal preference. *Sleep*,

26(4), pp.413–5. Available at: http://www.ncbi.nlm.nih.gov/pubmed/12841365.
Arens, D. et al., 2007. Seasonal changes in bone metabolism in sheep. *The Veterinary Journal*, 174(3), pp.585–591. Available at: https://www.sciencedirect.com/science/article/pii/S1090023306001985.
Arriza, J.L. et al., 1987. Cloning of Human Mineralocorticoid Receptor Complementary DNA: Structural and Functional Kinship with the Glucocorticoid Receptor Cloning of Human Mineralocorticoid Receptor Complementary DNA: Structural and Functional IKinship with the Glucocorticoid Receptor. *Source: Science, New Series*, 237222117(17), pp.268–275. Available at: http://www.jstor.org/stable/1699970.
Asher, G. et al., 2008. SIRT1 Regulates Circadian Clock Gene Expression through PER2 Deacetylation. *Cell*, 134(2), pp.317–328. Available at: http://www.ncbi.nlm.nih.gov/pubmed/18662546.
Azcue, M. et al., 1997. Energy expenditure and body composition in children with Crohn's disease: effect of enteral nutrition and treatment with prednisolone. *Gut*, 41(2), pp.203–8. Available at: http://www.ncbi.nlm.nih.gov/pubmed/9301499.
Bae, K. et al., 2001. Differential functions of mPer1, mPer2, and mPer3 in the SCN circadian clock. *Neuron*, 30(2), pp.525–36. Available at: http://www.ncbi.nlm.nih.gov/pubmed/11395012.
Baldock, N.M., Sibly, R.M. & Penning, P.D., 1988. Behaviour and seasonal variation in heart rate in domestic sheep, Ovis aries. *Animal Behaviour*, 36(1), pp.35–43. Available at: https://www.sciencedirect.com/science/article/pii/S0003347288802471.
Balsalobre, A. et al., 2000. Resetting of Circadian Time in Peripheral Tissues by Glucocorticoid Signaling. *Science* , 289(5488), pp.2344–2347.
Bannerman, D.M. et al., 1995. Distinct components of spatial learning revealed by prior training and NMDA receptor blockade. *Nature*, 378(6553), pp.182–186. Available at: http://www.ncbi.nlm.nih.gov/pubmed/7477320.
Barca-Mayo, O. et al., 2017. Astrocyte deletion of Bmal1 alters daily locomotor activity and cognitive functions via GABA signalling. *Nature Communications*, 8.
Barrow, J.G. et al., 1951. DECUBITUS ULCER IN RHEUMATIC FEVER TREATED WITH CORTISONE. *Journal of the American Medical Association*, 147(1), p.41. Available at: http://jama.jamanetwork.com/article.aspx?doi=10.1001/jama.1951.73670180002010a.
Baver, S.B. et al., 2008. Two types of melanopsin retinal ganglion cell differentially innervate the hypothalamic suprachiasmatic nucleus and the olivary pretectal nucleus. *European Journal of Neuroscience*, 27(7), pp.1763–1770. Available at: http://www.ncbi.nlm.nih.gov/pubmed/18371076.
van der Beek, E.M., 1996. Circadian control of reproduction in the female rat. *Progress in brain research*, 111, pp.295–320. Available at: http://www.ncbi.nlm.nih.gov/pubmed/8990922.
van der Beek, E.M. et al., 1997. Synaptic contacts between gonadotropin-releasing hormone-containing fibers and neurons in the suprachiasmatic nucleus and perichiasmatic area: an anatomical substrate for feedback regulation? *Brain research*, 755(1), pp.101–11. Available at: http://www.ncbi.nlm.nih.gov/pubmed/9163545.
Belden, W.J. & Dunlap, J.C., 2008. SIRT1 Is a Circadian Deacetylase for Core Clock Components. *Cell*, 134(2), p.212. Available at: http://www.ncbi.nlm.nih.gov/pubmed/18662537.
Bellanti, F. et al., 2017. Alterations of Clock Gene RNA Expression in Brain Regions of a

Triple Transgenic Model of Alzheimer's Disease. *Journal of Alzheimer's disease : JAD*, 59(2), pp.615–631. Available at: http://www.ncbi.nlm.nih.gov/pubmed/28671110.

Ben-Hamo, M. et al., 2016. Circadian Forced Desynchrony of the Master Clock Leads to Phenotypic Manifestation of Depression in Rats. *eneuro*, 3(6), p.ENEURO.0237-16.2016. Available at: http://eneuro.sfn.org/lookup/doi/10.1523/ENEURO.0237-16.2016.

Benedict, R.H.B. et al., 2006. Neocortical Atrophy, Third Ventricular Width, and Cognitive Dysfunction in Multiple Sclerosis. *Archives of Neurology*, 63(9), p.1301. Available at: http://archneur.jamanetwork.com/article.aspx?doi=10.1001/archneur.63.9.1301.

Benjamini, Y. & Hochberg, Y., 1995. Controlling the False Discovery Rate: A Practical and Powerful Approach to Multiple Testing. *Journal of the Royal Statistical Society. Series B (Methodological)*, 57, pp.289–300. Available at: https://www.jstor.org/stable/2346101.

Benoit, J.D., Rakic, P. & Frick, K.M., 2015. Prenatal stress induces spatial memory deficits and epigenetic changes in the hippocampus indicative of heterochromatin formation and reduced gene expression. *Behavioural Brain Research*, 281, pp.1–8. Available at: https://www.sciencedirect.com/science/article/pii/S0166432814007864.

Van den Berg, G. et al., 1995. Combined amplification of the pulsatile and basal modes of adrenocorticotropin and cortisol secretion in patients with Cushing's disease: Evidence for decreased responsiveness of the adrenal glands. *Journal of Clinical Endocrinology and Metabolism*, 80(12), pp.3750–3757.

Berk, M.L. & Finkelstein, J.A., 1981. An autoradiographic determination of the efferent projections of the suprachiasmatic nucleus of the hypothalamus. *Brain Research*, 226(1–2), pp.1–13. Available at: https://www.sciencedirect.com/science/article/pii/0006899381910799.

Bernardis, L.L., 1973. Disruption of diurnal feeding and weight gain cycles in weanling rats by ventromedial and dorsomedial hypothalamic lesions. *Physiology & behavior*, 10(5), pp.855–61. Available at: http://www.ncbi.nlm.nih.gov/pubmed/4715812.

Berson, D.M., Dunn, F.A. & Takao, M., 2002. Phototransduction by Retinal Ganglion Cells That Set the Circadian Clock. *Science*, 295(5557). Available at: http://science.sciencemag.org/content/295/5557/1070.

Berson, D.M., Dunn, F.A. & Takao, M., 2002. Phototransduction by Retinal Ganglion Cells That Set the Circadian Clock. *Science*, 295(5557), pp.1070–1073. Available at: http://www.ncbi.nlm.nih.gov/pubmed/11834835.

Bierwolf, C. et al., 2003. Slow Wave Sleep Drives Inhibition of Pituitary-AdrenalSecretion in Humans. *Journal of Neuroendocrinology*, 9(6), pp.479–484. Available at: http://doi.wiley.com/10.1046/j.1365-2826.1997.00605.x.

Billon, C., Sitaula, S. & Burris, T.P., 2017. Metabolic Characterization of a Novel RORα Knockout Mouse Model without Ataxia. *Frontiers in Endocrinology*, 8, p.141. Available at: http://www.ncbi.nlm.nih.gov/pubmed/28744254.

Birnie, M.T., 2018. Chronic synthetic glucocorticoid treatment induces circadian disturbances and memory impairments. *Acad. Med. Sci*.

Bisset, G.W., Errington, M.L. & Richards, C.D., 1973. The distribution of vasopressin and oxytocin in the hypothalamoneurohypophysial system of the guinea-pig. *Br. J. Pharmac*, 48, pp.263–272. Available at: https://bpspubs.onlinelibrary.wiley.com/doi/pdf/10.1111/j.1476-5381.1973.tb06912.x.

Björefeldt, A., 2015. Neuromodulation of hippocampal single cell-and network activity by human cerebrospinal fluid. *Thesis*. Available at: https://gupea.ub.gu.se/bitstream/2077/40445/1/gupea_2077_40445_1.pdf.

Blandina, P. et al., 2012. Histamine neurons in the tuberomamillary nucleus: a whole center or distinct subpopulations? *Frontiers in systems neuroscience*, 6, p.33. Available at: http://www.ncbi.nlm.nih.gov/pubmed/22586376.

Bliss, T. V & Lomo, T., 1973. Long-lasting potentiation of synaptic transmission in the dentate area of the anaesthetized rabbit following stimulation of the perforant path. *The Journal of physiology*, 232(2), pp.331–56. Available at: http://www.ncbi.nlm.nih.gov/pubmed/4727084.

Bliss, T.V.P. & Collingridge, G.L., 1993. A synaptic model of memory: long-term potentiation in the hippocampus. *Nature*, 361(6407), pp.31–39. Available at: http://www.nature.com/doifinder/10.1038/361031a0.

Bolton, J.L. et al., 2018. Anhedonia Following Early-Life Adversity Involves Aberrant Interaction of Reward and Anxiety Circuits and Is Reversed by Partial Silencing of Amygdala Corticotropin-Releasing Hormone Gene. *Biological Psychiatry*, 83(2), pp.137–147. Available at: http://www.ncbi.nlm.nih.gov/pubmed/29033027.

Bone, R.C. et al., 1987. A Controlled Clinical Trial of High-Dose Methylprednisolone in the Treatment of Severe Sepsis and Septic Shock. *New England Journal of Medicine*, 317(11), pp.653–658. Available at: http://www.nejm.org/doi/abs/10.1056/NEJM198709103171101.

Born, J. et al., 1991. Gluco- and antimineralocorticoid effects on human sleep: a role of central corticosteroid receptors. *American Journal of Physiology-Endocrinology and Metabolism*, 260(2), pp.E183–E188. Available at: http://www.ncbi.nlm.nih.gov/pubmed/1996621.

Born, J., 2010. Slow-wave sleep and the consolidation of long-term memory. *The World Journal of Biological Psychiatry*, 11(sup1), pp.16–21. Available at: http://www.tandfonline.com/doi/full/10.3109/15622971003637637.

Born, J., Muth, S. & Fehm, H.L., 1988. The significance of sleep onset and slow wave sleep for nocturnal release of growth hormone (GH) and cortisol. *Psychoneuroendocrinology*, 13(3), pp.233–43. Available at: http://www.ncbi.nlm.nih.gov/pubmed/3406323.

Bouchard-Cannon, P. et al., 2013. The Circadian Molecular Clock Regulates Adult Hippocampal Neurogenesis by Controlling the Timing of Cell-Cycle Entry and Exit. *Cell Reports*, 5(4), pp.961–973. Available at: http://www.ncbi.nlm.nih.gov/pubmed/24268780.

Boyle, M.P. et al., 2005. Acquired deficit of forebrain glucocorticoid receptor produces depression-like changes in adrenal axis regulation and behavior. *Proceedings of the National Academy of Sciences*, 102(2), pp.473–478. Available at: http://www.ncbi.nlm.nih.gov/pubmed/15623560.

Bradbury, M.J., Dement, W.C. & Edgar, D.M., 1998. Effects of adrenalectomy and subsequent corticosterone replacement on rat sleep state and EEG power spectra. *The American journal of physiology*, 275(2 Pt 2), pp.R555-65. Available at: http://www.ncbi.nlm.nih.gov/pubmed/9688693.

Brown, E.S., 2009. Effects of Glucocorticoids on Mood, Memory, and the Hippocampus. *Annals of the New York Academy of Sciences*, 1179(1), pp.41–55. Available at: http://doi.wiley.com/10.1111/j.1749-6632.2009.04981.x.

Brown, E.S. & Chandler, P.A., 2001. Mood and Cognitive Changes During Systemic Corticosteroid Therapy. *Primary care companion to the Journal of clinical psychiatry*, 3(1), pp.17–21. Available at:

http://www.ncbi.nlm.nih.gov/pubmed/15014624.
Buchanan, T.W. et al., 2004. Circadian regulation of cortisol after hippocampal damage in humans. *Biological Psychiatry*, 56(9), pp.651–656. Available at: https://www.sciencedirect.com/science/article/pii/S0006322304009011.
Bugge, A. et al., 2012. Rev-erbα and Rev-erbβ coordinately protect the circadian clock and normal metabolic function. *Genes & development*, 26(7), pp.657–67. Available at: http://www.ncbi.nlm.nih.gov/pubmed/22474260.
Buller, K.M., Xu, Y. & Day, T.A., 1998. Indomethacin attenuates oxytocin and hypothalamic-pituitary-adrenal axis responses to systemic interleukin-1 beta. *Journal of neuroendocrinology*, 10(7), pp.519–28. Available at: http://www.ncbi.nlm.nih.gov/pubmed/9700679.
Bunney, B.G. et al., 2015. Circadian dysregulation of clock genes: clues to rapid treatments in major depressive disorder. *Molecular psychiatry*, 20(1), pp.48–55. Available at: http://www.ncbi.nlm.nih.gov/pubmed/25349171.
Bush, G., Luu, P. & Posner, M.I., 2000. Cognitive and emotional influences in anterior cingulate cortex. *Trends in Cognitive Sciences*, 4(6), pp.215–222. Available at: https://www.sciencedirect.com/science/article/pii/S1364661300014832.
Buzsáki, G., 2010. Neural Syntax: Cell Assemblies, Synapsembles, and Readers. *Neuron*, 68(3), pp.362–385. Available at: http://www.ncbi.nlm.nih.gov/pubmed/21040841.
Buzsáki, G., 2002. Theta Oscillations in the Hippocampus. *Neuron*, 33(3), pp.325–340. Available at: https://www.sciencedirect.com/science/article/pii/S089662730200586X.
Canteras, N.S. & Swanson, L.W., 1992. Projections of the ventral subiculum to the amygdala, septum, and hypothalamus: A PHAL anterograde tract-tracing study in the rat. *The Journal of Comparative Neurology*, 324(2), pp.180–194. Available at: http://doi.wiley.com/10.1002/cne.903240204.
Card, J.P. & Moore, R.Y., 1988. Neuropeptide Y localization in the rat suprachiasmatic nucleus and periventricular hypothalamus. *Neuroscience letters*, 88(3), pp.241–6. Available at: http://www.ncbi.nlm.nih.gov/pubmed/3386869.
CARSON-JURICA, M.A., SCHRADER, W.T. & O'MALLEY, B.W., 1990. Steroid Receptor Family: Structure and Functions. *Endocrine Reviews*, 11(2), pp.201–220. Available at: http://press.endocrine.org/doi/abs/10.1210/edrv-11-2-201.
Casady, R.L. & Taylor, A.N., 1976. Effect of electrical stimulation of the hippocampus upon corticosteroid levels in the freely-behaving, non-stressed rat. *Neuroendocrinology*, 20(1), pp.68–78. Available at: http://www.ncbi.nlm.nih.gov/pubmed/934426.
Castel, M. & Morris, J.F., 2000. Morphological heterogeneity of the GABAergic network in the suprachiasmatic nucleus, the brain's circadian pacemaker. *Journal of anatomy*, 196 (Pt 1), pp.1–13. Available at: http://www.ncbi.nlm.nih.gov/pubmed/10697283.
Catani, M., Dell'Acqua, F. & Thiebaut de Schotten, M., 2013. A revised limbic system model for memory, emotion and behaviour. *Neuroscience & Biobehavioral Reviews*, 37(8), pp.1724–1737. Available at: https://www.sciencedirect.com/science/article/pii/S0149763413001711.
Van Cauter, E., Leproult, R. & Plat, L., 2000. Age-Related Changes in Slow Wave Sleep and REM Sleep and Relationship With Growth Hormone and Cortisol Levels in Healthy Men. *JAMA*, 284(7), p.861. Available at: http://jama.jamanetwork.com/article.aspx?doi=10.1001/jama.284.7.861.
Van Cauter, E. & Refetoff, S., 1985. Evidence for Two Subtypes of Cushing's Disease Based on the Analysis of Episodic Cortisol Secretion. *New England Journal of Medicine*, 312(21), pp.1343–1349. Available at:

http://www.nejm.org/doi/abs/10.1056/NEJM198505233122102.
Ceolin, L. et al., 2011. Study of Novel Selective mGlu2 Agonist in the Temporo-Ammonic Input to CA1 Neurons Reveals Reduced mGlu2 Receptor Expression in a Wistar Substrain with an Anxiety-Like Phenotype. *Journal of Neuroscience*, 31(18), pp.6721–6731. Available at: http://www.ncbi.nlm.nih.gov/pubmed/21543601.
Cermakian, N. et al., 2001. Altered behavioral rhythms and clock gene expression in mice with a targeted mutation in the Period1 gene. *The EMBO journal*, 20(15), pp.3967–74. Available at: http://www.ncbi.nlm.nih.gov/pubmed/11483500.
Chabot, C.C., Connolly, D.M. & Waring, B.B., 2012. The effects of lighting conditions and food restriction paradigms on locomotor activity of common spiny mice, Acomys cahirinus. *Journal of Circadian Rhythms*, 10(0), p.6. Available at: https://www.jcircadianrhythms.com/article/10.1186/1740-3391-10-6/.
Charmandari, E. et al., 2008. Generalized Glucocorticoid Resistance: Clinical Aspects, Molecular Mechanisms, and Implications of a Rare Genetic Disorder. *The Journal of Clinical Endocrinology & Metabolism*, 93(5), pp.1563–1572. Available at: https://academic.oup.com/jcem/article-lookup/doi/10.1210/jc.2008-0040.
Chen, C.-Y. et al., 2016. Effects of aging on circadian patterns of gene expression in the human prefrontal cortex. *Proceedings of the National Academy of Sciences*, 113(1), pp.206–211. Available at: http://www.ncbi.nlm.nih.gov/pubmed/26699485.
Chen, Q.H., Haywood, J.R. & Toney, G.M., 2003. Sympathoexcitation by PVN-Injected Bicuculline Requires Activation of Excitatory Amino Acid Receptors. *Hypertension*, 42(4), pp.725–731. Available at: http://www.ncbi.nlm.nih.gov/pubmed/12900439.
Chen, R. et al., 2008. Strong resetting of the mammalian clock by constant light followed by constant darkness. *The Journal of neuroscience : the official journal of the Society for Neuroscience*, 28(46), pp.11839–47. Available at: http://www.ncbi.nlm.nih.gov/pubmed/19005049.
Chen, S.-T. et al., 2005. Deregulated expression of the PER1 , PER2 and PER3 genes in breast cancers. *Carcinogenesis*, 26(7), pp.1241–1246. Available at: http://academic.oup.com/carcin/article/26/7/1241/2390900/Deregulated-expression-of-the-PER1-PER2-and-PER3.
Cheon, S. et al., 2013. Glucocorticoid-mediated Period2 induction delays the phase of circadian rhythm. *Nucleic Acids Research*, 41(12), pp.6161–6174. Available at: http://academic.oup.com/nar/article/41/12/6161/1028125/Glucocorticoidmediated-Period2-induction-delays.
CHILDS, G. V., WESTLUND, K.N. & UNABIA, G., 1989. Characterization of Anterior Pituitary Target Cells for Arginine Vasopressin: Including Cells that Store Adrenocorticotropin, Thyrotropin-β, and Both Hormones*. *Endocrinology*, 125(1), pp.554–559. Available at: http://www.ncbi.nlm.nih.gov/pubmed/2544413.
Cho, H. et al., 2012. Regulation of circadian behaviour and metabolism by REV-ERB-α and REV-ERB-β. *Nature*, 485(7396), pp.123–127. Available at: http://www.nature.com/articles/nature11048.
Christiansen, S. et al., 2016. Altered Expression Pattern of Clock Genes in a Rat Model of Depression. *International Journal of Neuropsychopharmacology*, 19(11), p.pyw061. Available at: https://academic.oup.com/ijnp/article-lookup/doi/10.1093/ijnp/pyw061.
Chu, J.W. et al., 2001. Successful Long-Term Treatment of Refractory Cushing's Disease with High-Dose Mifepristone (RU 486). *The Journal of Clinical Endocrinology & Metabolism*, 86(8), pp.3568–3573. Available at: https://academic.oup.com/jcem/article-lookup/doi/10.1210/jcem.86.8.7740.
Collingridge, G.L., Kehl, S.J. & McLennan, H., 1983. Excitatory amino acids in synaptic transmission in the Schaffer collateral-commissural pathway of the rat hippocampus.

The Journal of physiology, 334, pp.33–46. Available at: http://www.ncbi.nlm.nih.gov/pubmed/6306230.
Coluccia, D. et al., 2008. Glucocorticoid therapy-induced memory deficits: acute versus chronic effects. *The Journal of neuroscience : the official journal of the Society for Neuroscience*, 28(13), pp.3474–3478.
Conn, D.L., 2001. Resolved: Low-dose prednisone is indicated as a standard treatment in patients with rheumatoid arthritis. *Arthritis and rheumatism*, 45(5), pp.462–7. Available at: http://www.ncbi.nlm.nih.gov/pubmed/11642646.
Conrad, C. et al., 2004. Influence of chronic corticosterone and glucocorticoid receptor antagonism in the amygdala on fear conditioning. *Neurobiology of Learning and Memory*, 81(3), pp.185–199. Available at: http://www.ncbi.nlm.nih.gov/pubmed/15082020 [Accessed July 14, 2018].
Conrad, C.D. et al., 1996. Chronic stress impairs rat spatial memory on the Y maze, and this effect is blocked by tianeptine pretreatment. *Behavioral neuroscience*, 110(6), pp.1321–34. Available at: http://www.ncbi.nlm.nih.gov/pubmed/8986335.
Conrad, C.D. et al., 1999. Repeated restraint stress facilitates fear conditioning independently of causing hippocampal CA3 dendritic atrophy. *Behavioral neuroscience*, 113(5), pp.902–13. Available at: http://www.ncbi.nlm.nih.gov/pubmed/10571474.
Conway-Campbell, B.L. et al., 2010. Glucocorticoid ultradian rhythmicity directs cyclical gene pulsing of the clock gene period 1 in rat hippocampus. *Journal of neuroendocrinology*, 22(10), pp.1093–100. Available at: http://www.ncbi.nlm.nih.gov/pubmed/20649850.
Conway-Campbell, B.L. et al., 2012. Molecular dynamics of ultradian glucocorticoid receptor action. *Molecular and Cellular Endocrinology*, 348(2), pp.383–393. Available at: http://www.ncbi.nlm.nih.gov/pubmed/21872640.
Coomans, C.P. et al., 2013. The suprachiasmatic nucleus controls circadian energy metabolism and hepatic insulin sensitivity. *Diabetes*, 62(4), pp.1102–8. Available at: http://www.ncbi.nlm.nih.gov/pubmed/23274903.
Cornu, M. et al., 2014. Hepatic mTORC1 controls locomotor activity, body temperature, and lipid metabolism through FGF21. *Proceedings of the National Academy of Sciences*, 111(32), pp.11592–11599. Available at: http://www.ncbi.nlm.nih.gov/pubmed/25082895.
Crumbley, C. & Burris, T.P., 2011. Direct Regulation of CLOCK Expression by REV-ERB I. Hansen, ed. *PLoS ONE*, 6(3), p.e17290. Available at: http://www.ncbi.nlm.nih.gov/pubmed/21479263.
Cui, Z., Gerfen, C.R. & Young, W.S., 2013. Hypothalamic and other connections with dorsal CA2 area of the mouse hippocampus. *Journal of Comparative Neurology*, 521(8), pp.1844–1866. Available at: http://www.ncbi.nlm.nih.gov/pubmed/23172108.
Cunningham, E.T., Bohn, M.C. & Sawchenko, P.E., 1990. Organization of adrenergic inputs to the paraventricular and supraoptic nuclei of the hypothalamus in the rat. *The Journal of Comparative Neurology*, 292(4), pp.651–667. Available at: http://doi.wiley.com/10.1002/cne.902920413.
Damiola, F. et al., 2000. Restricted feeding uncouples circadian oscillators in peripheral tissues from the central pacemaker in the suprachiasmatic nucleus. *Genes & development*, 14(23), pp.2950–61. Available at: http://www.ncbi.nlm.nih.gov/pubmed/11114885.
Davidson, A.J. et al., 2003. Is the food-entrainable circadian oscillator in the digestive system? *Genes, Brain and Behavior*, 2(1), pp.32–39. Available at:

http://doi.wiley.com/10.1034/j.1601-183X.2003.00005.x.
Dayas, C. V., Buller, K.M. & Day, T.A., 1999. Neuroendocrine responses to an emotional stressor: evidence for involvement of the medial but not the central amygdala. *European Journal of Neuroscience*, 11(7), pp.2312–2322. Available at: http://doi.wiley.com/10.1046/j.1460-9568.1999.00645.x.
DeBruyne, J.P. et al., 2006. A Clock Shock: Mouse CLOCK Is Not Required for Circadian Oscillator Function. *Neuron*, 50(3), pp.465–477. Available at: https://www.sciencedirect.com/science/article/pii/S0896627306002674?via%3Dihub.
DeBruyne, J.P., Weaver, D.R. & Reppert, S.M., 2007. CLOCK and NPAS2 have overlapping roles in the suprachiasmatic circadian clock. *Nature Neuroscience*, 10(5), pp.543–545. Available at: http://www.ncbi.nlm.nih.gov/pubmed/17417633.
DeFronzo, R.A. & Tripathy, D., 2009. Skeletal muscle insulin resistance is the primary defect in type 2 diabetes. *Diabetes care*, 32 Suppl 2(suppl 2), pp.S157-63. Available at: http://www.ncbi.nlm.nih.gov/pubmed/19875544.
Delerive, P., Chin, W.W. & Suen, C.S., 2002. Identification of Reverbα as a Novel RORα Target Gene. *Journal of Biological Chemistry*, 277(38), pp.35013–35018. Available at: http://www.ncbi.nlm.nih.gov/pubmed/12114512.
Demski-Allen, R., 2014. *Characterisation of the Molecular and Cognitive Effects of synthetic glucocorticoid treatment*.
Diamond, D.M. et al., 1992. Inverted-U relationship between the level of peripheral corticosterone and the magnitude of hippocampal primed burst potentiation. *Hippocampus*, 2(4), pp.421–430. Available at: http://www.ncbi.nlm.nih.gov/pubmed/1308198.
Díaz-Muñoz, M. et al., 2000. Anticipatory changes in liver metabolism and entrainment of insulin, glucagon, and corticosterone in food-restricted rats. *American Journal of Physiology-Regulatory, Integrative and Comparative Physiology*, 279(6), pp.R2048–R2056. Available at: http://www.physiology.org/doi/10.1152/ajpregu.2000.279.6.R2048.
Diorio, D., Viau, V. & Meaney, M.J., 1993. The role of the medial prefrontal cortex (cingulate gyrus) in the regulation of hypothalamic-pituitary-adrenal responses to stress. *The Journal of neuroscience : the official journal of the Society for Neuroscience*, 13(9), pp.3839–47. Available at: http://www.ncbi.nlm.nih.gov/pubmed/8396170.
Doi, M., Hirayama, J. & Sassone-Corsi, P., 2006. Circadian Regulator CLOCK Is a Histone Acetyltransferase. *Cell*, 125(3), pp.497–508. Available at: https://www.sciencedirect.com/science/article/pii/S0092867406004442.
Drevets, W.C. et al., 1992. A functional anatomical study of unipolar depression. *The Journal of neuroscience : the official journal of the Society for Neuroscience*, 12(9), pp.3628–41. Available at: http://www.ncbi.nlm.nih.gov/pubmed/1527602.
Dubrovsky, Y. V., Samsa, W.E. & Kondratov, R. V., 2010. Deficiency of circadian protein CLOCK reduces lifespan and increases age-related cataract development in mice. *Aging*, 2(12), pp.936–944. Available at: http://www.ncbi.nlm.nih.gov/pubmed/21149897.
Dudley, T.E., Dinardo, L.A. & Glass, J.D., 1999. In Vivo Assessment of the Midbrain Raphe Nuclear Regulation of Serotonin Release in the Hamster Suprachiasmatic Nucleus. *Journal of Neurophysiology*, 81(4), pp.1469–1477. Available at: http://www.physiology.org/doi/10.1152/jn.1999.81.4.1469.
Dumont, J.R. et al., 2012. Anterior thalamic nuclei lesions in rats disrupt markers of neural plasticity in distal limbic brain regions. *Neuroscience*, 224, pp.81–101.

Available at: http://www.ncbi.nlm.nih.gov/pubmed/22917615.
Dyar, K.A. et al., 2014. Muscle insulin sensitivity and glucose metabolism are controlled by the intrinsic muscle clock. *Molecular Metabolism*, 3(1), pp.29–41. Available at: http://www.ncbi.nlm.nih.gov/pubmed/24567902.
Earl, E. et al., 2018. Characterisation of glucocorticoid receptor activation profiles in rat brain and pituitary during treatment with the synthetic glucocorticoids methylprednisolone and dexamethasone. *Journal of Psychopharmacology*, (In review.
Earl, E., Stubbs, F.. & Conway-Campbell, B.L., 2018. Dynamics of endogenous and synthetic glucocorticoid binding. *In review*.
Eastman, C. & Rechtschaffen, A., 1983. Circadian temperature and wake rhythms of rats exposed to prolonged continuous illumination. *Physiology & behavior*, 31(4), pp.417–27. Available at: http://www.ncbi.nlm.nih.gov/pubmed/6657763.
Eastman, C.I., Mistlberger, R.E. & Rechtschaffen, A., 1984. Suprachiasmatic nuclei lesions eliminate circadian temperature and sleep rhythms in the rat. *Physiology & Behavior*, 32(3), pp.357–368. Available at: https://www.sciencedirect.com/science/article/pii/0031938484902488.
Ebling, F.J.P. et al., 1992. Circadian and Photoperiodic Time Measurement in Male Syrian Hamsters Following Lesions of the Melatonin-Binding Sites of the Paraventricular Thalamus. *Journal of Biological Rhythms*, 7(3), pp.241–254. Available at: http://www.ncbi.nlm.nih.gov/pubmed/1330085.
Eckel-Mahan, K.L. et al., 2008. Circadian oscillation of hippocampal MAPK activity and cAmp: implications for memory persistence. *Nature neuroscience*, 11(9), pp.1074–82. Available at: http://www.ncbi.nlm.nih.gov/pubmed/19160506.
Edelstein, K. & Amir, S., 1999. The role of the intergeniculate leaflet in entrainment of circadian rhythms to a skeleton photoperiod. *The Journal of neuroscience : the official journal of the Society for Neuroscience*, 19(1), pp.372–80. Available at: http://www.ncbi.nlm.nih.gov/pubmed/9870966.
Edmonds, S.C. & Adler, N.T., 1977. Food and light as entrainers of circadian running activity in the rat. *Physiology & Behavior*, 18(5), pp.915–919. Available at: https://www.sciencedirect.com/science/article/pii/0031938477902013.
Edwards, C.R.W. et al., 1988. LOCALISATION OF 11β-HYDROXYSTEROID DEHYDROGENASE—TISSUE SPECIFIC PROTECTOR OF THE MINERALOCORTICOID RECEPTOR. *The Lancet*, 332(8618), pp.986–989. Available at: https://www.sciencedirect.com/science/article/pii/S0140673688907428.
Van Eekelen, J.A.M. et al., 1988. Distribution of the mineralocorticoid and the glucocorticoid receptor mRNAs in the rat hippocampus. *Journal of Neuroscience Research*, 21(1), pp.88–94. Available at: http://doi.wiley.com/10.1002/jnr.490210113.
Ehlers, C.L., Reed, T.K. & Henriksen, S.J., 1986. Effects of corticotropin-releasing factor and growth hormone-releasing factor on sleep and activity in rats. *Neuroendocrinology*, 42(6), pp.467–74. Available at: http://www.ncbi.nlm.nih.gov/pubmed/3084988.
Eliava, M. et al., 2016. A New Population of Parvocellular Oxytocin Neurons Controlling Magnocellular Neuron Activity and Inflammatory Pain Processing. *Neuron*, 89(6), pp.1291–1304. Available at: http://www.ncbi.nlm.nih.gov/pubmed/26948889.
Emery, P. et al., 1998. CRY, a Drosophila clock and light-regulated cryptochrome, is a major contributor to circadian rhythm resetting and photosensitivity. *Cell*, 95(5), pp.669–79. Available at: http://www.ncbi.nlm.nih.gov/pubmed/9845369.

Erkut, Z.A., Pool, C. & Swaab, D.F., 1998. Glucocorticoids Suppress Corticotropin-Releasing Hormone and Vasopressin Expression in Human Hypothalamic Neurons. *The Journal of Clinical Endocrinology & Metabolism*, 83(6), pp.2066–2073. Available at: http://press.endocrine.org/doi/10.1210/jcem.83.6.4881.

Eschenko, O. et al., 2008. Sustained increase in hippocampal sharp-wave ripple activity during slow-wave sleep after learning. *Learning & memory (Cold Spring Harbor, N.Y.)*, 15(4), pp.222–8. Available at: http://www.ncbi.nlm.nih.gov/pubmed/18385477.

Etchegaray, J.-P. et al., 2009. Casein kinase 1 delta regulates the pace of the mammalian circadian clock. *Molecular and cellular biology*, 29(14), pp.3853–66. Available at: http://www.ncbi.nlm.nih.gov/pubmed/19414593.

Etchegaray, J.-P. et al., 2003. Rhythmic histone acetylation underlies transcription in the mammalian circadian clock. *Nature*, 421(6919), pp.177–182. Available at: http://www.ncbi.nlm.nih.gov/pubmed/12483227.

Eun, B. et al., 2011. Induction of Per1 expression following an experimentally induced epilepsy in the mouse hippocampus. *Neuroscience Letters*, 498(2), pp.110–113. Available at: http://www.ncbi.nlm.nih.gov/pubmed/21420468.

Fang, H. & Gough, J., 2014. SupraHex: An R/Bioconductor package for tabular omics data analysis using a supra-hexagonal map. *Biochemical and Biophysical Research Communications*, 443(1), pp.285–289.

Fanselow, M.S. & LeDoux, J.E., 1999. Why we think plasticity underlying Pavlovian fear conditioning occurs in the basolateral amygdala. *Neuron*, 23(2), pp.229–32. Available at: http://www.ncbi.nlm.nih.gov/pubmed/10399930.

Feillet, C.A. et al., 2008. Forebrain oscillators ticking with different clock hands. *Molecular and Cellular Neuroscience*, 37(2), pp.209–221. Available at: https://www.sciencedirect.com/science/article/pii/S1044743107002217.

Feldman, S., Conforti, N. & Saphier, D., 1990. The preoptic area and bed nucleus of the stria terminalis are involved in the effects of the amygdala on adrenocortical secretion. *Neuroscience*, 37(3), pp.775–779. Available at: https://www.sciencedirect.com/science/article/pii/030645229090107F.

FENDLER, K., KARMOS, G. & TELEGDY, G., 1961. The effect of hippocampal lesion on pituitary-adrenal function. *Acta physiologica Academiae Scientiarum Hungaricae*, 20, pp.293–7. Available at: http://www.ncbi.nlm.nih.gov/pubmed/13892267.

Field, M.D. et al., 2000. Analysis of clock proteins in mouse SCN demonstrates phylogenetic divergence of the circadian clockwork and resetting mechanisms. *Neuron*, 25(2), pp.437–47. Available at: http://www.ncbi.nlm.nih.gov/pubmed/10719897 [Accessed July 12, 2018].

Fields, H.L. et al., 2007. Ventral Tegmental Area Neurons in Learned Appetitive Behavior and Positive Reinforcement. *Annual Review of Neuroscience*, 30(1), pp.289–316. Available at: http://www.ncbi.nlm.nih.gov/pubmed/17376009.

Filiano, A.N. et al., 2013. Chronic Ethanol Consumption Disrupts the Core Molecular Clock and Diurnal Rhythms of Metabolic Genes in the Liver without Affecting the Suprachiasmatic Nucleus W. Schwartz, ed. *PLoS ONE*, 8(8), p.e71684. Available at: http://www.ncbi.nlm.nih.gov/pubmed/23951220.

Fischette, C.T. et al., 1980. Differential fornix ablations and the circadian rhythmicity of adrenal corticosteroid secretion. *Brain Research*, 195(2), pp.373–387. Available at: https://www.sciencedirect.com/science/article/pii/0006899380900736.

Foster, R.G. & Hankins, M.W., 2007. Circadian vision. *Current Biology*, 17(17), pp.R746–R751. Available at: http://www.ncbi.nlm.nih.gov/pubmed/17803920.

Frank, L.M., Brown, E.N. & Wilson, M., 2000. Trajectory Encoding in the Hippocampus and Entorhinal Cortex. *Neuron*, 27(1), pp.169–178. Available at: https://www.sciencedirect.com/science/article/pii/S0896627300000180.

Frédéric, F. et al., 2006. Enhanced endocrine response to novel environment stress and lack of corticosterone circadian rhythm instaggerer (Rora sg/sg) mutant mice. *Journal of Neuroscience Research*, 83(8), pp.1525–1532. Available at: http://doi.wiley.com/10.1002/jnr.20843.

Frey, S., Bergado, J.. & Frey, J.., 2003. Modulation of late phases of long-term potentiation in rat dentate gyrus by stimulation of the medial septum. *Neuroscience*, 118(4), pp.1055–1062. Available at: https://www.sciencedirect.com/science/article/pii/S0306452203000290.

Frodl, T. et al., 2012. Reduced expression of glucocorticoid-inducible genes GILZ and SGK-1: high IL-6 levels are associated with reduced hippocampal volumes in major depressive disorder. *Translational Psychiatry*, 2(3), pp.e88–e88. Available at: http://www.nature.com/articles/tp201214.

Frotscher, M., 1985. Mossy fibres form synapses with identified pyramidal basket cells in the CA3 region of the guinea-pig hippocampus: a combined Golgi-electron microscope study. *Journal of Neurocytology*, 14(2), pp.245–259. Available at: http://link.springer.com/10.1007/BF01258450.

Fuhrmann, F. et al., 2015. Locomotion, Theta Oscillations, and the Speed-Correlated Firing of Hippocampal Neurons Are Controlled by a Medial Septal Glutamatergic Circuit. *Neuron*, 86(5), pp.1253–1264. Available at: https://www.sciencedirect.com/science/article/pii/S0896627315004080.

Gagne, D., Pons, M. & Philibert, D., 1985. RU 38486: a potent antiglucocorticoid in vitro and in vivo. *Journal of steroid biochemistry*, 23(3), pp.247–51. Available at: http://www.ncbi.nlm.nih.gov/pubmed/2864478.

Gais, S. et al., 2002. Learning-dependent increases in sleep spindle density. *The Journal of neuroscience : the official journal of the Society for Neuroscience*, 22(15), pp.6830–4. Available at: http://www.ncbi.nlm.nih.gov/pubmed/12151563.

Gais, S. et al., 2007. Sleep transforms the cerebral trace of declarative memories. *Proceedings of the National Academy of Sciences*, 104(47), pp.18778–18783. Available at: http://www.ncbi.nlm.nih.gov/pubmed/18000060.

Gallina, D., Zelinka, C. & Fischer, A.J., 2014. Glucocorticoid receptors in the retina, Muller glia and the formation of Muller glia-derived progenitors. *Development*, 141(17), pp.3340–3351. Available at: http://www.ncbi.nlm.nih.gov/pubmed/25085975.

Gamble, K.L. et al., 2007. Gastrin-Releasing Peptide Mediates Light-Like Resetting of the Suprachiasmatic Nucleus Circadian Pacemaker through cAMP Response Element-Binding Protein and Per1 Activation. *Journal of Neuroscience*, 27(44), pp.12078–12087. Available at: http://www.ncbi.nlm.nih.gov/pubmed/17978049.

Garfinkel, D. et al., 1995. Improvement of sleep quality in elderly people by controlled-release melatonin. *The Lancet*, 346(8974), pp.541–544. Available at: https://www.sciencedirect.com/science/article/pii/S0140673695913823.

Gatfield, D. & Schibler, U., 2008. Circadian glucose homeostasis requires compensatory interference between brain and liver clocks. *Proceedings of the National Academy of Sciences of the United States of America*, 105(39), pp.14753–4. Available at: http://www.ncbi.nlm.nih.gov/pubmed/18812506.

Gekakis, N. et al., 1998. Role of the CLOCK protein in the mammalian circadian mechanism. *Science (New York, N.Y.)*, 280(5369), pp.1564–9. Available at: http://www.ncbi.nlm.nih.gov/pubmed/9616112.

George, C.L. et al., 2017. Ultradian glucocorticoid exposure directs gene-dependent and tissue-specific mRNA expression patterns in vivo. *Molecular and cellular endocrinology*, 439, pp.46–53. Available at: http://www.ncbi.nlm.nih.gov/pubmed/27769714.

Giguere, V. et al., 1986. Functional Domains of the Human Glucocorticoid Receptor. *Cell*, 46, pp.645–652.

Gilhooley, M.J., Pinnock, S.B. & Herbert, J., 2011. Rhythmic expression of per1 in the dentate gyrus is suppressed by corticosterone: Implications for neurogenesis. *Neuroscience Letters*, 489(3), pp.177–181. Available at: https://www.sciencedirect.com/science/article/pii/S0304394010015454.

Gillette, M.U. & Tischkau, S.A., 1999. Suprachiasmatic nucleus: the brain's circadian clock. *Recent progress in hormone research*, 54, pp.33-58; discussion 58–9. Available at: http://www.ncbi.nlm.nih.gov/pubmed/10548871.

Girardeau, G. et al., 2009. Selective suppression of hippocampal ripples impairs spatial memory. *Nature Neuroscience*, 12(10), pp.1222–1223. Available at: http://www.nature.com/articles/nn.2384.

Gomez, F. et al., 1997. Arginine vasopressin (AVP) depletion in neurons of the suprachiasmatic nuclei affects the AVP content of the paraventricular neurons and stimulates adrenocorticotrophic hormone release. *Journal of Neuroscience Research*, 50(4), pp.565–574. Available at: http://www.ncbi.nlm.nih.gov/pubmed/9404718.

Goto, S.G. & Denlinger, D.L., 2002. Short-day and long-day expression patterns of genes involved in the flesh fly clock mechanism: period, timeless,cycle and cryptochrome. *Journal of Insect Physiology*, 48(8), pp.803–816. Available at: https://www.sciencedirect.com/science/article/pii/S0022191002001087.

Gottlieb, D.I. & Cowan, W.M., 1973. Autoradiographic studies of the commissural and ipsilateral association connections of the hippocampus and dentate gyrus. I. The commissural connections. *The Journal of Comparative Neurology*, 149(4), pp.393–421. Available at: http://doi.wiley.com/10.1002/cne.901490402.

Granados-Fuentes, D. et al., 2004. Olfactory bulb neurons express functional, entrainable circadian rhythms. *The European journal of neuroscience*, 19(4), pp.898–906. Available at: http://www.ncbi.nlm.nih.gov/pubmed/15009137.

Granados-Fuentes, D., Tseng, A. & Herzog, E.D., 2006. A Circadian Clock in the Olfactory Bulb Controls Olfactory Responsivity. *Journal of Neuroscience*, 26(47), pp.12219–12225. Available at: http://www.ncbi.nlm.nih.gov/pubmed/17122046.

Graves, L.A. et al., 2003. Sleep deprivation selectively impairs memory consolidation for contextual fear conditioning. *Learning & memory (Cold Spring Harbor, N.Y.)*, 10(3), pp.168–76. Available at: http://www.ncbi.nlm.nih.gov/pubmed/12773581.

Gray, T.S., Carney, M.E. & Magnuson, D.J., 1989. Direct Projections from the Central Amygdaloid Nucleus to the Hypothalamic Paraventricular Nucleus: Possible Role in Stress-Induced Adrenocorticotropin Release. *Neuroendocrinology*, 50(4), pp.433–446. Available at: http://www.ncbi.nlm.nih.gov/pubmed/2554178.

Grol, M.J. et al., 2006. Cerebral changes during performance of overlearned arbitrary visuomotor associations. *The Journal of neuroscience : the official journal of the Society for Neuroscience*, 26(1), pp.117–25. Available at: http://www.ncbi.nlm.nih.gov/pubmed/16399678.

Grønli, J. et al., 2006. Chronic mild stress inhibits BDNF protein expression and CREB activation in the dentate gyrus but not in the hippocampus proper. *Pharmacology Biochemistry and Behavior*, 85(4), pp.842–849. Available at: https://www.sciencedirect.com/science/article/pii/S009130570600387X.

Gruart, A., Muñoz, M.D. & Delgado-García, J.M., 2006. Involvement of the CA3-CA1

Synapse in the Acquisition of Associative Learning in Behaving Mice. *Journal of Neuroscience*, 26(4), pp.1077–1087. Available at: http://www.ncbi.nlm.nih.gov/pubmed/16436593.
Guillaumond, F. et al., 2005. Differential Control of Bmal1 Circadian Transcription by REV-ERB and ROR Nuclear Receptors. *Journal of Biological Rhythms*, 20(5), pp.391–403. Available at: http://www.ncbi.nlm.nih.gov/pubmed/16267379.
Guo, H. et al., 2005. Differential control of peripheral circadian rhythms by suprachiasmatic-dependent neural signals. *Proceedings of the National Academy of Sciences of the United States of America*, 102(8), pp.3111–6. Available at: http://www.ncbi.nlm.nih.gov/pubmed/15710878.
Habib, K.E., Gold, P.W. & Chrousos, G.P., 2001. Neuroendocrinology of stress. *Endocrinology and metabolism clinics of North America*, 30(3), p.695–728; vii–viii. Available at: http://www.ncbi.nlm.nih.gov/pubmed/11571937.
Hall, J.C., 1983. Complex brain and behavioral functions disrupted by mutations in Drosophila. *Developmental Genetics*, 4(4), pp.355–378. Available at: http://doi.wiley.com/10.1002/dvg.1020040411.
Hamani, C. et al., 2011. The Subcallosal Cingulate Gyrus in the Context of Major Depression. *Biological Psychiatry*, 69(4), pp.301–308. Available at: https://www.sciencedirect.com/science/article/pii/S0006322310010036.
Han, F. et al., 2005. Colocalization of mineralocorticoid receptor and glucocorticoid receptor in the hippocampus and hypothalamus. *Neuroscience research*, 51(4), pp.371–81. Available at: http://www.ncbi.nlm.nih.gov/pubmed/15740800.
Hara, R. et al., 2001. Restricted feeding entrains liver clock without participation of the suprachiasmatic nucleus. *Genes to cells : devoted to molecular & cellular mechanisms*, 6(3), pp.269–78. Available at: http://www.ncbi.nlm.nih.gov/pubmed/11260270.
Hargreaves, E.L. et al., 2005. Major Dissociation Between Medial and Lateral Entorhinal Input to Dorsal Hippocampus. *Science*, 308(5729), pp.1792–1794. Available at: http://www.ncbi.nlm.nih.gov/pubmed/15961670.
Harper, R.M., Woo, M.A. & Alger, J.R., 2000. Visualization of sleep influences on cerebellar and brainstem cardiac and respiratory control mechanisms. *Brain Research Bulletin*, 53(1), pp.125–131. Available at: https://www.sciencedirect.com/science/article/pii/S0361923000003178.
Harrington, M.E., 1997. The ventral lateral geniculate nucleus and the intergeniculate leaflet: interrelated structures in the visual and circadian systems. *Neuroscience and biobehavioral reviews*, 21(5), pp.705–27. Available at: http://www.ncbi.nlm.nih.gov/pubmed/9353800.
Harrington, M.E., Nance, D.M. & Rusak, B., 1987. Double-labeling of neuropeptide Y-immunoreactive neurons which project from the geniculate to the suprachiasmatic nuclei. *Brain research*, 410(2), pp.275–82. Available at: http://www.ncbi.nlm.nih.gov/pubmed/2439175.
Hasan, S. et al., 2011. Altered sleep and behavioral activity phenotypes in PER3-deficient mice. *American Journal of Physiology-Regulatory, Integrative and Comparative Physiology*, 301(6), pp.R1821–R1830. Available at: http://www.ncbi.nlm.nih.gov/pubmed/21957163.
Hattar, S. et al., 2002. Melanopsin-containing retinal ganglion cells: architecture, projections, and intrinsic photosensitivity. *Science (New York, N.Y.)*, 295(5557), pp.1065–70. Available at: http://www.sciencemag.org/cgi/doi/10.1126/science.1069609.
Hayreh, S.S. & Zimmerman, B., 2003. Visual deterioration in giant cell arteritis patients

while on high doses of corticosteroid therapy. *Ophthalmology*, 110(6), pp.1204–1215. Available at: https://www.sciencedirect.com/science/article/pii/S0161642003002288.

Heath, R.G. et al., 1978. Cerebellar stimulation: effects on septal region, hippocampus, and amygdala of cats and rats. *Biological psychiatry*, 13(5), pp.501–29. Available at: http://www.ncbi.nlm.nih.gov/pubmed/728506.

Heath, R.G. & Harper, J.W., 1974. Ascending projections of the cerebellar fastigial nucleus to the hippocampus, amygdala, and other temporal lobe sites: Evoked potential and histological studies in monkeys and cats. *Experimental Neurology*, 45(2), pp.268–287. Available at: https://www.sciencedirect.com/science/article/pii/0014488674901186.

Henley, D.E. et al., 2009. Development of an automated blood sampling system for use in humans. *Journal of Medical Engineering & TechnologyOnline) Journal Journal of Medical Engineering & Technology*, 333, pp.309–1902. Available at: http://www.tandfonline.com/action/journalInformation?journalCode=ijmt20.

Hensler, J.G., 2006. Serotonergic modulation of the limbic system. *Neuroscience & Biobehavioral Reviews*, 30(2), pp.203–214. Available at: https://www.sciencedirect.com/science/article/pii/S0149763405001181.

Herman, J.P. et al., 2003. Central mechanisms of stress integration: hierarchical circuitry controlling hypothalamo–pituitary–adrenocortical responsiveness. *Frontiers in Neuroendocrinology*, 24(3), pp.151–180. Available at: https://www.sciencedirect.com/science/article/pii/S0091302203000293.

Herman, J.P. et al., 1995. Contribution of the Ventral Subiculum to Inhibitory Regulation of the Hypothalamo-Pituitary-Adrenocortical Axis. *Journal of Neuroendocrinology*, 7(6), pp.475–482. Available at: http://doi.wiley.com/10.1111/j.1365-2826.1995.tb00784.x.

Herman, J.P. et al., 1993. Diurnal Regulation of Glucocorticoid Receptor and Mineralocorticoid Receptor mRNAs in Rat Hippocampus. *Molecular and Cellular Neuroscience*, 4(2), pp.181–190. Available at: https://www.sciencedirect.com/science/article/pii/S1044743183710225?via%3Dihub.

Herman, J.P. et al., 1989. Evidence for hippocampal regulation of neuroendocrine neurons of the hypothalamo-pituitary-adrenocortical axis. *The Journal of neuroscience : the official journal of the Society for Neuroscience*, 9(9), pp.3072–82. Available at: http://www.ncbi.nlm.nih.gov/pubmed/2795152.

Herman, J.P. et al., 2016. Regulation of the Hypothalamic-Pituitary-Adrenocortical Stress Response. In *Comprehensive Physiology*. Hoboken, NJ, USA: John Wiley & Sons, Inc., pp. 603–621. Available at: http://www.ncbi.nlm.nih.gov/pubmed/27065163.

Herman, J.P. & Cullinan, W.E., 1997. Neurocircuitry of stress: central control of the hypothalamo–pituitary–adrenocortical axis. *Trends in Neurosciences*, 20(2), pp.78–84. Available at: https://www.sciencedirect.com/science/article/pii/S0166223696100692.

Herman, J.P. & Spencer, R., 1998. Regulation of hippocampal glucocorticoid receptor gene transcription and protein expression in vivo. *The Journal of neuroscience : the official journal of the Society for Neuroscience*, 18(18), pp.7462–73. Available at: http://www.ncbi.nlm.nih.gov/pubmed/9736665.

Hida, A. et al., 2015. Screening of Clock Gene Polymorphisms Demonstrates Association of a PER3 Polymorphism with Morningness–Eveningness Preference and Circadian Rhythm Sleep Disorder. *Scientific Reports*, 4(1), p.6309. Available at: http://www.nature.com/articles/srep06309.

Hirayama, J. et al., 2007. CLOCK-mediated acetylation of BMAL1 controls circadian function. *Nature*, 450(7172), pp.1086–1090. Available at: http://www.ncbi.nlm.nih.gov/pubmed/18075593.

Hirose, T., Smith, R.J. & Jetten, A.M., 1994. ROR-γ: The Third Member of ROR/RZR Orphan Receptor Subfamily That Is Highly Expressed in Skeletal Muscle. *Biochemical and Biophysical Research Communications*, 205(3), pp.1976–1983. Available at: http://www.ncbi.nlm.nih.gov/pubmed/7811290.

Hitti, F.L. & Siegelbaum, S.A., 2014. The hippocampal CA2 region is essential for social memory. *Nature*, 508(7494), pp.88–92. Available at: http://www.ncbi.nlm.nih.gov/pubmed/24572357.

Hoang Dang, V., 2014. Wavelet-based spectral analysis. *Analytical Chemistry*, 62, pp.144–153.

Hocke, K., 1998. Phase estimation with the Lomb-Scargle periodogram method. *Geophysicis*, 16, pp.356–358. Available at: https://www.researchgate.net/publication/283359043.

Hodge, B.A. et al., 2015. The endogenous molecular clock orchestrates the temporal separation of substrate metabolism in skeletal muscle. *Skeletal Muscle*, 5(1), p.17. Available at: http://www.skeletalmusclejournal.com/content/5/1/17.

Hofstetter, J.R., Grahame, N.J. & Mayeda, A.R., 2003. Circadian activity rhythms in high-alcohol-preferring and low-alcohol-preferring mice. *Alcohol*, 30(1), pp.81–85. Available at: https://www.sciencedirect.com/science/article/pii/S0741832903000958#FIG1.

Hogenesch, J.B. et al., 1997. Characterization of a subset of the basic-helix-loop-helix-PAS superfamily that interacts with components of the dioxin signaling pathway. *The Journal of biological chemistry*, 272(13), pp.8581–93. Available at: http://www.ncbi.nlm.nih.gov/pubmed/9079689.

Holsboer, F., von Bardeleben, U. & Steiger, A., 1988. Effects of Intravenous Corticotropin-Releasing Hormone upon Sleep-Related Growth Hormone Surge and Sleep EEG in Man. *Neuroendocrinology*, 48(1), pp.32–38. Available at: http://www.ncbi.nlm.nih.gov/pubmed/3262835.

Honma, S. et al., 1988. Rhythms in behaviors, body temperature and plasma corticosterone in SCN lesioned rats given methamphetamine. *Physiology & Behavior*, 44(2), pp.247–255. Available at: https://www.sciencedirect.com/science/article/pii/0031938488901461.

Ter Horst, G.J. et al., 1991. Projections from the rostral parvocellular reticular formation to pontine and medullary nuclei in the rat: Involvement in autonomic regulation and orofacial motor control. *Neuroscience*, 40(3), pp.735–758. Available at: https://www.sciencedirect.com/science/article/pii/030645229190009D.

Horst, G.T.J. van der et al., 1999. Mammalian Cry1 and Cry2 are essential for maintenance of circadian rhythms. *Nature*, 398(6728), pp.627–630. Available at: http://www.nature.com/articles/19323.

Hosp, J.A. et al., 2011. Dopaminergic projections from midbrain to primary motor cortex mediate motor skill learning. *The Journal of neuroscience : the official journal of the Society for Neuroscience*, 31(7), pp.2481–7. Available at: http://www.ncbi.nlm.nih.gov/pubmed/21325515.

Huang, D.W., Sherman, B.T. & Lempicki, R.A., 2009. Bioinformatics enrichment tools: paths toward the comprehensive functional analysis of large gene lists. *Nucleic Acids Research*, 37(1), pp.1–13. Available at: http://www.ncbi.nlm.nih.gov/pubmed/19033363.

Huang, D.W., Sherman, B.T. & Lempicki, R.A., 2009. Systematic and integrative

analysis of large gene lists using DAVID bioinformatics resources. *Nature Protocols*, 4(1), pp.44–57. Available at: http://www.ncbi.nlm.nih.gov/pubmed/19131956.
Huang, W. et al., 2011. Circadian rhythms, sleep, and metabolism. *The Journal of clinical investigation*, 121(6), pp.2133–41. Available at: http://www.ncbi.nlm.nih.gov/pubmed/21633182.
Hui, G.K. et al., 2004. Memory enhancement of classical fear conditioning by post-training injections of corticosterone in rats. *Neurobiology of Learning and Memory*, 81(1), pp.67–74. Available at: https://www.sciencedirect.com/science/article/pii/S1074742703001126.
Huikuri, H. V. et al., 1992. Circadian rhythm of heart rate variability in survivors of cardiac arrest. *The American Journal of Cardiology*, 70(6), pp.610–615. Available at: https://www.sciencedirect.com/science/article/pii/000291499290200I.
Hurlbert, R.J., 2000. Methylprednisolone for acute spinal cord injury: an inappropriate standard of care. *Journal of Neurosurgery: Spine*, 93(1), pp.1–7. Available at: http://thejns.org/doi/10.3171/spi.2000.93.1.0001.
Hurley, K.M. et al., 1991. Efferent projections of the infralimbic cortex of the rat. *The Journal of Comparative Neurology*, 308(2), pp.249–276. Available at: http://www.ncbi.nlm.nih.gov/pubmed/1716270.
Husse, J. et al., 2012. Circadian Clock Genes Per1 and Per2 Regulate the Response of Metabolism-Associated Transcripts to Sleep Disruption K. L. Gamble, ed. *PLoS ONE*, 7(12), p.e52983. Available at: http://www.ncbi.nlm.nih.gov/pubmed/23285241.
Ibata, Y. et al., 1989. Vasoactive intestinal peptide (VIP)-like immunoreactive neurons located in the rat suprachiasmatic nucleus receive a direct retinal projection. *Neuroscience Letters*, 97(1–2), pp.1–5. Available at: https://www.sciencedirect.com/science/article/pii/0304394089901298.
Ibuka, N. & Kawamura, H., 1975. Loss of circadian rhythm in sleep-wakefulness cycle in the rat by suprachiasmatic nucleus lesions. *Brain Research*, 96(1), pp.76–81. Available at: https://www.sciencedirect.com/science/article/pii/0006899375905740.
Ikeda, M. & Nomura, M., 1997. cDNA Cloning and Tissue-Specific Expression of a Novel Basic Helix–Loop–Helix/PAS Protein (BMAL1) and Identification of Alternatively Spliced Variants with Alternative Translation Initiation Site Usage. *Biochemical and Biophysical Research Communications*, 233(1), pp.258–264. Available at: http://www.ncbi.nlm.nih.gov/pubmed/9144434.
Inagaki, N. et al., 1988. Organization of histaminergic fibers in the rat brain. *The Journal of Comparative Neurology*, 273(3), pp.283–300. Available at: http://www.ncbi.nlm.nih.gov/pubmed/3062046.
Inoue, H. et al., 2004. Role of STAT-3 in regulation of hepatic gluconeogenic genes and carbohydrate metabolism in vivo. *Nature Medicine*, 10(2), pp.168–174. Available at: http://www.nature.com/articles/nm980.
Inouye, S.T. & Kawamura, H., 1982. Characteristics of a circadian pacemaker in the suprachiasmatic nucleus. *Journal of Comparative Physiology ? A*, 146(2), pp.153–160. Available at: http://link.springer.com/10.1007/BF00610233.
Ishizuka, N., Weber, J. & Amaral, D.G., 1990. Organization of intrahippocampal projections originating from CA3 pyramidal cells in the rat. *The Journal of Comparative Neurology*, 295(4), pp.580–623. Available at: http://doi.wiley.com/10.1002/cne.902950407.
Itowi, N. et al., 1990. Effects of histamine and alpha-fluoromethylhistidine injections on circadian phase of free-running rhythms. *Physiology & behavior*, 47(3), pp.549–54.

Available at: http://www.ncbi.nlm.nih.gov/pubmed/2359768.
Ivry, R.B., Keele, S.W. & Diener, H.C., 1988. Dissociation of the lateral and medial cerebellum in movement timing and movement execution. *Experimental Brain Research*, 73(1), pp.167–180. Available at: http://link.springer.com/10.1007/BF00279670.
Jagannath, A., Peirson, S.N. & Foster, R.G., 2013. Sleep and circadian rhythm disruption in neuropsychiatric illness. *Current Opinion in Neurobiology*, 23(5), pp.888–894. Available at: https://www.sciencedirect.com/science/article/pii/S0959438813000858.
Jiang, C. & Salton, S., 2013. The role of neurotrophins in major depressive disorder. *Translational Neuroscience*, 4(1), pp.46–58. Available at: http://www.ncbi.nlm.nih.gov/pubmed/23691270.
Jilg, A. et al., 2009. Temporal dynamics of mouse hippocampal clock gene expression support memory processing. *Hippocampus*, 20(3), p.NA-NA. Available at: http://doi.wiley.com/10.1002/hipo.20637.
Jin, X. et al., 1999. A Molecular Mechanism Regulating Rhythmic Output from the Suprachiasmatic Circadian Clock. *Cell*, 96(1), pp.57–68. Available at: https://www.sciencedirect.com/science/article/pii/S0092867400809599.
Joëls, M., Fernandez, G. & Roozendaal, B., 2011. Stress and emotional memory: a matter of timing. *Trends in Cognitive Sciences*, 15(6), pp.280–288. Available at: https://www.sciencedirect.com/science/article/pii/S136466131100074X.
Jones, C.R. et al., 1999. Familial advanced sleep-phase syndrome: A short-period circadian rhythm variant in humans. *Nature Medicine*, 5(9), pp.1062–1065. Available at: http://www.ncbi.nlm.nih.gov/pubmed/10470086.
Jones, M.W. & Wilson, M.A., 2005. Theta Rhythms Coordinate Hippocampal–Prefrontal Interactions in a Spatial Memory Task R. Morris, ed. *PLoS Biology*, 3(12), p.e402. Available at: http://dx.plos.org/10.1371/journal.pbio.0030402.
Judd, L.L. et al., 2014. Adverse Consequences of Glucocorticoid Medication: Psychological, Cognitive, and Behavioral Effects. *American Journal of Psychiatry*, 171(10), pp.1045–1051. Available at: http://psychiatryonline.org/doi/abs/10.1176/appi.ajp.2014.13091264.
Kajiyama, Y. et al., 2010. Prednisolone causes anxiety- and depression-like behaviors and altered expression of apoptotic genes in mice hippocampus. *Progress in Neuro-Psychopharmacology and Biological Psychiatry*, 34(1), pp.159–165. Available at: https://www.sciencedirect.com/science/article/pii/S0278584609003765#fig2.
Kalin, N., 2018. HPA and Amygdala CRH Alterations Associated With Primate Anxiety. *Biological Psychiatry*, 83(9), p.S53. Available at: https://www.sciencedirect.com/science/article/pii/S000632231830249X.
Kalsbeek, A. et al., 2008. Circadian Control of the Daily Plasma Glucose Rhythm: An Interplay of GABA and Glutamate J. A. L. Calbet, ed. *PLoS ONE*, 3(9), p.e3194. Available at: http://dx.plos.org/10.1371/journal.pone.0003194.
Kalsbeek, A. et al., 1999. GABA release from suprachiasmatic nucleus terminals is necessary for the light-induced inhibition of nocturnal melatonin release in the rat. *Neuroscience*, 91(2), pp.453–61. Available at: http://www.ncbi.nlm.nih.gov/pubmed/10366002.
Kalsbeek, A. & Buijs, R.M., 2002. Output pathways of the mammalian suprachiasmatic nucleus: coding circadian time by transmitter selection and specific targeting. *Cell and Tissue Research*, 309(1), pp.109–118. Available at: http://www.ncbi.nlm.nih.gov/pubmed/12111541.
Kamphuis, W. et al., 2005. Circadian expression of clock genes and clock-controlled

genes in the rat retina. *Biochemical and Biophysical Research Communications*, 330(1), pp.18–26. Available at: https://www.sciencedirect.com/science/article/pii/S0006291X05003943#fig3.
Kaneko, K. et al., 2009. Obesity alters circadian expressions of molecular clock genes in the brainstem. *Brain Research*, 1263, pp.58–68. Available at: https://www.sciencedirect.com/science/article/pii/S0006899309000031.
Kang, D. et al., 2015. Theta-rhythmic drive between medial septum and hippocampus in slow-wave sleep and microarousal: a Granger causality analysis. *Journal of Neurophysiology*, 114(5), pp.2797–2803. Available at: http://www.physiology.org/doi/10.1152/jn.00542.2015.
van de Kar, L.D. & Lorens, S.A., 1979. Differential serotonergic innervation of individual hypothalamic nuclei and other forebrain regions by the dorsal and median midbrain raphe nuclei. *Brain research*, 162(1), pp.45–54. Available at: http://www.ncbi.nlm.nih.gov/pubmed/761086.
Karolczak, M. et al., 2004. Clock gene mRNA and protein rhythms in the pineal gland of mice. *European Journal of Neuroscience*, 19(12), pp.3382–3388. Available at: http://www.ncbi.nlm.nih.gov/pubmed/15217395.
Katada, S. & Sassone-Corsi, P., 2010. The histone methyltransferase MLL1 permits the oscillation of circadian gene expression. *Nature Structural & Molecular Biology*, 17(12), pp.1414–1421. Available at: http://www.ncbi.nlm.nih.gov/pubmed/21113167.
Kawano, H. & Daikoku, S., 1981. Immunohistochemical demonstration of LHRH neurons and their pathways in the rat hypothalamus. *Neuroendocrinology*, 32(3), pp.179–86. Available at: https://www.karger.com/Article/FullText/123153.
Keenan, P. et al., 1996. The effect on memory of chronic prednisone treatment in patients with systemic disease. *American Academy of Neurology*, 47, pp.1396–1402.
Kelemen, E. et al., 2014. Hippocampal corticosterone impairs memory consolidation during sleep but improves consolidation in the wake state. *Hippocampus*, 24(5), pp.510–5. Available at: http://www.ncbi.nlm.nih.gov/pubmed/24596244.
Khan, S.H., Ling, J. & Kumar, R., 2011. TBP Binding-Induced Folding of the Glucocorticoid Receptor AF1 Domain Facilitates Its Interaction with Steroid Receptor Coactivator-1 A. J. Cooney, ed. *PLoS ONE*, 6(7), p.e21939. Available at: http://www.ncbi.nlm.nih.gov/pubmed/21760925.
Kida, S. & Serita, T., 2014. Functional roles of CREB as a positive regulator in the formation and enhancement of memory. *Brain Research Bulletin*, 105, pp.17–24. Available at: https://www.sciencedirect.com/science/article/pii/S0361923014000653.
King, D.P. et al., 1997. Positional cloning of the mouse circadian clock gene. *Cell*, 89(4), pp.641–53. Available at: http://www.ncbi.nlm.nih.gov/pubmed/9160755.
Kiss, J. et al., 2008. Synaptic contacts of vesicular glutamate transporter 2 fibres on chemically identified neurons of the hypothalamic suprachiasmatic nucleus of the rat. *European Journal of Neuroscience*, 28(9), pp.1760–1774. Available at: http://doi.wiley.com/10.1111/j.1460-9568.2008.06463.x.
Kitchener, P. et al., 2004. Differences between brain structures in nuclear translocation and DNA binding of the glucocorticoid receptor during stress and the circadian cycle. *The European journal of neuroscience*, 19(7), pp.1837–46. Available at: http://www.ncbi.nlm.nih.gov/pubmed/15078557.
de Kloet, E.R., Oitzl, M.S. & Joëls, M., 1999. Stress and cognition: are corticosteroids good or bad guys? *Trends in Neurosciences*, 22(10), pp.422–426. Available at: https://www.sciencedirect.com/science/article/pii/S0166223699014381#bib0225.

Knierim, J.J., Neunuebel, J.P. & Deshmukh, S.S., 2014. Functional correlates of the lateral and medial entorhinal cortex: objects, path integration and local-global reference frames. *Philosophical transactions of the Royal Society of London. Series B, Biological sciences*, 369(1635), p.20130369. Available at: http://www.ncbi.nlm.nih.gov/pubmed/24366146.

Knigge, K.M., 1961. Adrenocortical Response to Stress in Rats with Lesions in Hippocampus and Amygdala. *Experimental Biology and Medicine*, 108(1), pp.18–21. Available at: http://ebm.sagepub.com/lookup/doi/10.3181/00379727-108-26832.

Knutson, K.L., 2007. Impact of sleep and sleep loss on glucose homeostasis and appetite regulation. *Sleep medicine clinics*, 2(2), pp.187–197. Available at: http://www.ncbi.nlm.nih.gov/pubmed/18516218.

Ko, C.H. & Takahashi, J.S., 2006. Molecular components of the mammalian circadian clock. *Human Molecular Genetics*, 15(suppl_2), pp.R271–R277. Available at: http://academic.oup.com/hmg/article/15/suppl_2/R271/624758/Molecular-components-of-the-mammalian-circadian.

Köhler, C., 1990. Subicular projections to the hypothalamus and brainstem: some novel aspects revealed in the rat by the anterogradePhaseolus vulgaris leukoagglutinin (PHA-L) tracing method. *Progress in Brain Research*, 83, pp.59–69. Available at: https://www.sciencedirect.com/science/article/pii/S0079612308612418.

Koike, N. et al., 2012. Transcriptional Architecture and Chromatin Landscape of the Core Circadian Clock in Mammals. *Science*, 338(6105), pp.349–354. Available at: http://www.ncbi.nlm.nih.gov/pubmed/22936566.

Kondratov, R. V et al., 2006. Early aging and age-related pathologies in mice deficient in BMAL1, the core componentof the circadian clock. *Genes & development*, 20(14), pp.1868–73. Available at: http://www.ncbi.nlm.nih.gov/pubmed/16847346.

Kondratova, A.A. et al., 2010. Circadian clock proteins control adaptation to novel environment and memory formation. *Aging*, 2(5), pp.285–97. Available at: http://www.ncbi.nlm.nih.gov/pubmed/20519775.

Koyanagi, S. et al., 2006. Chronic Treatment with Prednisolone Represses the Circadian Oscillation of Clock Gene Expression in Mouse Peripheral Tissues. *Molecular Endocrinology*, 20(3), pp.573–583.

Kramer, A. et al., 2005. A Screen for Secreted Factors of the Suprachiasmatic Nucleus. In *Methods in enzymology*. pp. 645–663. Available at: http://www.ncbi.nlm.nih.gov/pubmed/15817317.

KRIEGER, D.T., 1980. Ventromedial Hypothalamic Lesions Abolish Food-Shifted Circadian Adrenal and Temperature Rhythinicity*. *Endocrinology*, 106(3), pp.649–654. Available at: https://academic.oup.com/endo/article-lookup/doi/10.1210/endo-106-3-649.

Kriegsfeld, L.J., Korets, R. & Silver, R., 2003. Expression of the circadian clock gene Period 1 in neuroendocrine cells: an investigation using mice with a Per1::GFP transgene. *The European journal of neuroscience*, 17(2), pp.212–20. Available at: http://www.ncbi.nlm.nih.gov/pubmed/12542657.

Kruisbrink, J. et al., 1987. Effects of enhanced cerebrospinal fluid levels of vasopressin, vasopressin antagonist or vasoactive intestinal polypeptide on circadian sleep-wake rhythm in the rat. *Brain research*, 419(1–2), pp.76–86. Available at: http://www.ncbi.nlm.nih.gov/pubmed/3676743.

Kuhn, H.G., Dickinson-Anson, H. & Gage, F.H., 1996. Neurogenesis in the dentate gyrus of the adult rat: age-related decrease of neuronal progenitor proliferation. *The Journal of neuroscience : the official journal of the Society for Neuroscience*, 16(6), pp.2027–33. Available at: http://www.ncbi.nlm.nih.gov/pubmed/8604047.

Kumar, R. & Thompson, E.B., 2005. Gene regulation by the glucocorticoid receptor: structure:function relationship. *The Journal of steroid biochemistry and molecular biology*, 94, pp.383–394.
Kumar, R. & Thompson, E.B., 1999. The structure of the nuclear hormone receptors. *Steroids*, 64(5), pp.310–9. Available at: http://www.ncbi.nlm.nih.gov/pubmed/10406480.
Kume, K. et al., 1999. mCRY1 and mCRY2 Are Essential Components of the Negative Limb of the Circadian Clock Feedback Loop. *Cell*, 98(2), pp.193–205. Available at: https://www.sciencedirect.com/science/article/pii/S0092867400810144.
Kupersmith, M.J. et al., 1994. Megadose corticosteroids in multiple sclerosis. *Neurology*, 44(1), pp.1–4. Available at: http://www.ncbi.nlm.nih.gov/pubmed/8290041.
Kuruvilla, M. V & Ainge, J.A., 2017. Lateral Entorhinal Cortex Lesions Impair Local Spatial Frameworks. *Frontiers in systems neuroscience*, 11, p.30. Available at: http://www.ncbi.nlm.nih.gov/pubmed/28567006.
de la Iglesia, H.O., Meyer, J. & Schwartz, W.J., 2003. Lateralization of circadian pacemaker output: Activation of left- and right-sided luteinizing hormone-releasing hormone neurons involves a neural rather than a humoral pathway. *The Journal of neuroscience : the official journal of the Society for Neuroscience*, 23(19), pp.7412–4. Available at: http://www.ncbi.nlm.nih.gov/pubmed/12917377.
Lacaille, J.C. et al., 1987. Local circuit interactions between oriens/alveus interneurons and CA1 pyramidal cells in hippocampal slices: electrophysiology and morphology. *The Journal of neuroscience : the official journal of the Society for Neuroscience*, 7(7), pp.1979–93. Available at: http://www.ncbi.nlm.nih.gov/pubmed/3612227.
Lamacz, M. et al., 1991. [The intermediate lobe of the pituitary, model of neuroendocrine communication]. *Archives internationales de physiologie, de biochimie et de biophysique*, 99(3), pp.205–19. Available at: http://www.ncbi.nlm.nih.gov/pubmed/1717055.
Lamia, K.A. et al., 2011. Cryptochromes mediate rhythmic repression of the glucocorticoid receptor. *Nature*, 480.
Lammel, S. et al., 2012. Input-specific control of reward and aversion in the ventral tegmental area. *Nature*, 491(7423), pp.212–217. Available at: http://www.nature.com/articles/nature11527.
Lamont, E.W. et al., 2005. The central and basolateral nuclei of the amygdala exhibit opposite diurnal rhythms of expression of the clock protein Period2. *Proceedings of the National Academy of Sciences*, 102(11), pp.4180–4184. Available at: http://www.ncbi.nlm.nih.gov/pubmed/15746242.
Landgraf, D. et al., 2016. NPAS2 Compensates for Loss of CLOCK in Peripheral Circadian Oscillators A. Kramer, ed. *PLOS Genetics*, 12(2), p.e1005882. Available at: http://dx.plos.org/10.1371/journal.pgen.1005882.
Landolt, H.-P. et al., 1996. Effect of age on the sleep EEG: slow-wave activity and spindle frequency activity in young and middle-aged men. *Brain Research*, 738(2), pp.205–212. Available at: https://www.sciencedirect.com/science/article/pii/S0006899396007706.
Lang, F. et al., 2010. Significance of SGK1 in the regulation of neuronal function. *The Journal of Physiology*, 588(18), pp.3349–3354. Available at: http://doi.wiley.com/10.1113/jphysiol.2010.190926 [Accessed July 12, 2018].
Laposky, A. et al., 2005. Deletion of the mammalian circadian clock gene BMAL1/Mop3 alters baseline sleep architecture and the response to sleep deprivation. *Sleep*, 28(4), pp.395–409. Available at: http://www.ncbi.nlm.nih.gov/pubmed/16171284.
Lee, H. et al., 2011. The period of the circadian oscillator is primarily determined by the

balance between casein kinase 1 and protein phosphatase 1. *Proceedings of the National Academy of Sciences of the United States of America*, 108(39), pp.16451–6. Available at: http://www.ncbi.nlm.nih.gov/pubmed/21930935.
Lee, I. & Kesner, R.P., 2004. Encoding versus retrieval of spatial memory: Double dissociation between the dentate gyrus and the perforant path inputs into CA3 in the dorsal hippocampus. *Hippocampus*, 14(1), pp.66–76. Available at: http://doi.wiley.com/10.1002/hipo.10167.
Lee, J. et al., 2008. Dual Modification of BMAL1 by SUMO2/3 and Ubiquitin Promotes Circadian Activation of the CLOCK/BMAL1 Complex. *Molecular and Cellular Biology*, 28(19), pp.6056–6065. Available at: http://www.ncbi.nlm.nih.gov/pubmed/18644859.
LeGates, T.A., Fernandez, D.C. & Hattar, S., 2014. Light as a central modulator of circadian rhythms, sleep and affect. *Nature Reviews Neuroscience*, 15(7).
Lei, S. & McBain, C.J., 2004. Two Loci of Expression for Long-Term Depression at Hippocampal Mossy Fiber-Interneuron Synapses. *Journal of Neuroscience*, 24(9), pp.2112–2121. Available at: http://www.ncbi.nlm.nih.gov/pubmed/14999062.
Leise, T.L., 2013. Wavelet analysis of circadian and ultradian behavioral rhythms. *Journal of Circadian Rhythms*, 11(1), p.5. Available at: http://www.jcircadianrhythms.com/content/11/1/5.
Leise, T.L. et al., 2013. Wavelet Meets Actogram. *Journal of Biological Rhythms*, 28(1), pp.62–68. Available at: http://journals.sagepub.com/doi/10.1177/0748730412468693.
Leutgeb, S. et al., 2005. Independent Codes for Spatial and Episodic Memory in Hippocampal Neuronal Ensembles. *Science*, 309(5734), pp.619–623. Available at: http://www.ncbi.nlm.nih.gov/pubmed/16040709.
Levine, J.D. et al., 1986. Circadian activity rhythms in rats with midbrain raphe lesions. *Brain Research*, 384(2), pp.240–249. Available at: https://www.sciencedirect.com/science/article/pii/0006899386911601.
Lévy, B. et al., 2003. [Topical methylprednisolone vs lidocaïne for the prevention of postoperative sore throat]. *Annales francaises d'anesthesie et de reanimation*, 22(7), pp.595–9. Available at: http://www.ncbi.nlm.nih.gov/pubmed/12946491.
Levy, O. et al., 2007. Light-responsive cryptochromes from a simple multicellular animal, the coral Acropora millepora. *Science (New York, N.Y.)*, 318(5849), pp.467–70. Available at: http://www.ncbi.nlm.nih.gov/pubmed/17947585.
Li, X.-G. et al., 1994. The hippocampal CA3 network: An in vivo intracellular labeling study. *Journal of Comparative Neurology*, 339(2), pp.181–208. Available at: http://doi.wiley.com/10.1002/cne.903390204.
Lightman, S.L. & Conway-Campbell, B.L., 2010. The crucial role of pulsatile activity of the HPA axis for continuous dynamic equilibration. *Nat Rev Neurosci*, 11(10), pp.710–718. Available at: http://www.ncbi.nlm.nih.gov/entrez/query.fcgi?cmd=Retrieve&db=PubMed&dopt=Citation&list_uids=20842176%5Cnhttp://www.ncbi.nlm.nih.gov/pubmed/20842176.
Lim, H.-W. et al., 2015. Genomic redistribution of GR monomers and dimers mediates transcriptional response to exogenous glucocorticoid in vivo. *Genome research*, 25(6), pp.836–44. Available at: http://www.ncbi.nlm.nih.gov/pubmed/25957148.
Di Lorenzo, F. et al., 2016. Long-term potentiation-like cortical plasticity is disrupted in Alzheimer's disease patients independently from age of onset. *Annals of Neurology*, 80(2), pp.202–210. Available at: http://www.ncbi.nlm.nih.gov/pubmed/27255833.
Loving, R.T., Kripke, D.F. & Glazner, L.K., 1996. Circadian rhythms in the human pupil

and eyelid. *American Journal of Physiology-Regulatory, Integrative and Comparative Physiology*, 271(2), pp.R320–R324. Available at: http://www.ncbi.nlm.nih.gov/pubmed/8770129.

Lu, J. et al., 2001. Contrasting effects of ibotenate lesions of the paraventricular nucleus and subparaventricular zone on sleep-wake cycle and temperature regulation. *The Journal of neuroscience : the official journal of the Society for Neuroscience*, 21(13), pp.4864–74. Available at: http://www.ncbi.nlm.nih.gov/pubmed/11425913.

Lu, J. et al., 2000. Effect of lesions of the ventrolateral preoptic nucleus on NREM and REM sleep. *The Journal of neuroscience : the official journal of the Society for Neuroscience*, 20(10), pp.3830–42. Available at: http://www.ncbi.nlm.nih.gov/pubmed/10804223.

Lu, J. et al., 2002. Selective activation of the extended ventrolateral preoptic nucleus during rapid eye movement sleep. *The Journal of neuroscience : the official journal of the Society for Neuroscience*, 22(11), pp.4568–76. Available at: http://www.ncbi.nlm.nih.gov/pubmed/12040064.

Lupien, S.J. & Lepage, M., 2001. Stress, memory, and the hippocampus: can't live with it, can't live without it. *Behavioural brain research*, 127(1–2), pp.137–58. Available at: http://www.ncbi.nlm.nih.gov/pubmed/11718889.

Malek, Z.S. et al., 2007. Daily Rhythm of Tryptophan Hydroxylase-2 Messenger Ribonucleic Acid within Raphe Neurons Is Induced by Corticoid Daily Surge and Modulated by Enhanced Locomotor Activity. *Endocrinology*, 148(11), pp.5165–5172. Available at: http://www.ncbi.nlm.nih.gov/pubmed/17595225.

Mallat, S., 2009. A Wavelet Tour of Signal Processing: The Sparse Way. *Academic Press, San Diego*.

Mander, B.A. et al., 2013. Prefrontal atrophy, disrupted NREM slow waves and impaired hippocampal-dependent memory in aging. *Nature Neuroscience*, 16(3), pp.357–364. Available at: http://www.nature.com/articles/nn.3324.

Marchal, C. & Mulle, C., 2004. Postnatal maturation of mossy fibre excitatory transmission in mouse CA3 pyramidal cells: a potential role for kainate receptors. *The Journal of Physiology*, 561(1), pp.27–37. Available at: http://doi.wiley.com/10.1113/jphysiol.2004.069922.

Marcheva, B. et al., 2010. Disruption of the clock components CLOCK and BMAL1 leads to hypoinsulinaemia and diabetes. *Nature*, 466(7306), pp.627–631. Available at: http://www.nature.com/articles/nature09253.

Markus, E.J. et al., 1995. Interactions between location and task affect the spatial and directional firing of hippocampal neurons. *The Journal of neuroscience : the official journal of the Society for Neuroscience*, 15(11), pp.7079–94. Available at: http://www.ncbi.nlm.nih.gov/pubmed/7472463.

Marrosu, F. et al., 1990. Corticotropin-releasing factor (CRF) increases paradoxical sleep (PS) rebound in PS-deprived rats. *Brain Research*, 515(1–2), pp.315–318. Available at: https://www.sciencedirect.com/science/article/pii/000689939090614H.

Marshall, L. et al., 2006. Boosting slow oscillations during sleep potentiates memory. *Nature*, 444(7119), pp.610–613. Available at: http://www.nature.com/articles/nature05278.

Le Martelot, G. et al., 2012. Genome-Wide RNA Polymerase II Profiles and RNA Accumulation Reveal Kinetics of Transcription and Associated Epigenetic Changes During Diurnal Cycles A. Kramer, ed. *PLoS Biology*, 10(11), p.e1001442. Available at: http://www.ncbi.nlm.nih.gov/pubmed/23209382.

Martin, R.A., Handel, S.F. & Aldama, A.E., 1991. Inability to sneeze as a manifestation of medullary neoplasm. *Neurology*, 41(10), pp.1675–6. Available at:

http://www.ncbi.nlm.nih.gov/pubmed/1922817.
Massin, M.M. et al., 2000. Circadian rhythm of heart rate and heart rate variability. *Archives of disease in childhood*, 83(2), pp.179–82. Available at: http://www.ncbi.nlm.nih.gov/pubmed/10906034.
Mayberg, H.S. et al., 2000. Regional metabolic effects of fluoxetine in major depression: serial changes and relationship to clinical response. *Biological psychiatry*, 48(8), pp.830–43. Available at: http://www.ncbi.nlm.nih.gov/pubmed/11063978.
Maywood, E.S. et al., 1999. Rapid down-regulation of mammalian period genes during behavioral resetting of the circadian clock. *Proceedings of the National Academy of Sciences of the United States of America*, 96(26), pp.15211–6. Available at: http://www.ncbi.nlm.nih.gov/pubmed/10611364.
Mcarthur, A.J. et al., 2000. Gastrin-Releasing Peptide Phase-Shifts Suprachiasmatic Nuclei Neuronal Rhythms In Vitro. *Neuroscience*, 20(14), pp.5496–5502. Available at: https://pdfs.semanticscholar.org/d520/2daddc8eeab08c8b81d77fa43cdfaa793d86.pdf.
McGrath, R.E. & Yahia, M., 1993. Preliminary data on seasonally related alcohol dependence. *The Journal of clinical psychiatry*, 54(7), pp.260–2. Available at: http://www.ncbi.nlm.nih.gov/pubmed/8335652.
McKinley, M.J. et al., 2015. The median preoptic nucleus: front and centre for the regulation of body fluid, sodium, temperature, sleep and cardiovascular homeostasis. *Acta Physiologica*, 214(1), pp.8–32. Available at: http://doi.wiley.com/10.1111/apha.12487.
McLay, R.N., Freeman, S.M. & Zadina, J.E., 1998. Chronic Corticosterone Impairs Memory Performance in the Barnes Maze. *Physiology & Behavior*, 63(5), pp.933–937. Available at: https://www.sciencedirect.com/science/article/pii/S0031938497005295.
Medvedev, A. et al., 1996. Cloning of a cDNA encoding the murine orphan receptor RZR/ROR gamma and characterization of its response element. *Gene*, 181(1–2), pp.199–206. Available at: http://www.ncbi.nlm.nih.gov/pubmed/8973331.
Megías, M. et al., 2001. Total number and distribution of inhibitory and excitatory synapses on hippocampal CA1 pyramidal cells. *Neuroscience*, 102(3), pp.527–40. Available at: http://www.ncbi.nlm.nih.gov/pubmed/11226691.
Meijer, J.H. & De Vries, M.J., 1995. Light-Induced Phase Shifts in Onset and Offset of Running-Wheel Activity in the Syrian Hamster. *Journal of Biological Rhythms*, 10(1), pp.4–16. Available at: http://journals.sagepub.com/doi/10.1177/074873049501000101.
Menet, J.S., Pescatore, S. & Rosbash, M., 2014. CLOCK:BMAL1 is a pioneer-like transcription factor. *Genes & development*, 28(1), pp.8–13. Available at: http://www.ncbi.nlm.nih.gov/pubmed/24395244.
Meng, N.H., Wang, T.G. & Lien, I.N., 2000. Dysphagia in patients with brainstem stroke: incidence and outcome. *American journal of physical medicine & rehabilitation*, 79(2), pp.170–5. Available at: http://www.ncbi.nlm.nih.gov/pubmed/10744192.
Meng, Q.-J. et al., 2008. Setting Clock Speed in Mammals: The CK1ε tau Mutation in Mice Accelerates Circadian Pacemakers by Selectively Destabilizing PERIOD Proteins. *Neuron*, 58(1), pp.78–88. Available at: https://www.sciencedirect.com/science/article/pii/S0896627308001049.
Merzenich, M.M. & Reid, M.D., 1974. Representation of the cochlea within the inferior colliculus of the cat. *Brain Research*, 77(3), pp.397–415. Available at: https://www.sciencedirect.com/science/article/pii/0006899374906301.

Meyer-Bernstein, E.L. & Morin, L.P., 1996. Differential serotonergic innervation of the suprachiasmatic nucleus and the intergeniculate leaflet and its role in circadian rhythm modulation. *The Journal of neuroscience : the official journal of the Society for Neuroscience*, 16(6), pp.2097–111. Available at: http://www.ncbi.nlm.nih.gov/pubmed/8604054.

Meyer-Bernstein, E.L. & Morin, L.P., 1999. Electrical stimulation of the median or dorsal raphe nuclei reduces light-induced FOS protein in the suprachiasmatic nucleus and causes circadian activity rhythm phase shifts. *Neuroscience*, 92(1), pp.267–79. Available at: http://www.ncbi.nlm.nih.gov/pubmed/10392849.

Mieda, M. et al., 2015. Cellular Clocks in AVP Neurons of the SCN Are Critical for Interneuronal Coupling Regulating Circadian Behavior Rhythm. *Neuron*, 85(5), pp.1103–1116. Available at: http://www.ncbi.nlm.nih.gov/pubmed/25741730.

Mieda, M. & Sakurai, T., 2011. Bmal1 in the nervous system is essential for normal adaptation of circadian locomotor activity and food intake to periodic feeding. *The Journal of neuroscience : the official journal of the Society for Neuroscience*, 31(43), pp.15391–6. Available at: http://www.ncbi.nlm.nih.gov/pubmed/22031885.

Mifsud, K.R. & Reul, J.M.H.M., 2016. Acute stress enhances heterodimerization and binding of corticosteroid receptors at glucocorticoid target genes in the hippocampus. *Proceedings of the National Academy of Sciences of the United States of America*, 113(40), pp.11336–11341. Available at: http://www.ncbi.nlm.nih.gov/pubmed/27655894.

Mikkelsen, J.D., 1990. Projections from the lateral geniculate nucleus to the hypothalamus of the mongolian gerbil (Meriones unguiculatus): An anterograde and retrograde tracing study. *The Journal of Comparative Neurology*, 299(4), pp.493–508. Available at: http://www.ncbi.nlm.nih.gov/pubmed/1700802.

Mikkelsen, J.D. & Vrang, N., 1994. A direct pretectosuprachiasmatic projection in the rat. *Neuroscience*, 62(2), pp.497–505. Available at: https://www.sciencedirect.com/science/article/pii/0306452294903824.

Miles, R. et al., 1996. Differences between Somatic and Dendritic Inhibition in the Hippocampus. *Neuron*, 16(4), pp.815–823. Available at: https://www.sciencedirect.com/science/article/pii/S0896627300801014.

Miller, B.H. et al., 2007. Circadian and CLOCK-controlled regulation of the mouse transcriptome and cell proliferation. *Proceedings of the National Academy of Sciences*, 104(9), pp.3342–3347. Available at: http://www.ncbi.nlm.nih.gov/pubmed/17360649.

Miller, M.A. et al., 2015. Photoperiod is associated with hippocampal volume in a large community sample. *Hippocampus*, 25(4), pp.534–43. Available at: http://www.ncbi.nlm.nih.gov/pubmed/25394737.

Mirescu, C. et al., 2006. Sleep deprivation inhibits adult neurogenesis in the hippocampus by elevating glucocorticoids. *Proceedings of the National Academy of Sciences of the United States of America*, 103(50), pp.19170–5. Available at: http://www.ncbi.nlm.nih.gov/pubmed/17135354.

Mitra, R., Ferguson, D. & Sapolsky, R.M., 2009. Mineralocorticoid Receptor Overexpression in Basolateral Amygdala Reduces Corticosterone Secretion and Anxiety. *Biological Psychiatry*, 66(7), pp.686–690. Available at: https://www.sciencedirect.com/science/article/pii/S0006322309004570.

Moga, M.M. & Moore, R.Y., 1997. Organization of neural inputs to the suprachiasmatic nucleus in the rat. *The Journal of comparative neurology*, 389(3), pp.508–34. Available at: http://www.ncbi.nlm.nih.gov/pubmed/9414010.

Moga, M.M. & Saper, C.B., 1994. Neuropeptide-immunoreactive neurons projecting to

the paraventricular hypothalamic nucleus in the rat. *The Journal of Comparative Neurology*, 346(1), pp.137–150. Available at: http://doi.wiley.com/10.1002/cne.903460110.

Moga, M.M., Weis, R.P. & Moore, R.Y., 1995. Efferent projections of the paraventricular thalamic nucleus in the rat. *The Journal of Comparative Neurology*, 359(2), pp.221–238. Available at: http://www.ncbi.nlm.nih.gov/pubmed/7499526.

Moore, R.Y., 1995. Neural control of the pineal gland. *Behavioural Brain Research*, 73(1–2), pp.125–130. Available at: https://www.sciencedirect.com/science/article/pii/0166432896000836.

Moore, R.Y. & Eichler, V.B., 1972. Loss of a circadian adrenal corticosterone rhythm following suprachiasmatic lesions in the rat. *Brain research*, 42(1), pp.201–6. Available at: http://www.ncbi.nlm.nih.gov/pubmed/5047187.

Moore, R.Y. & Klein, D.C., 1974. Visual pathways and the central neural control of a circadian rhythm in pineal serotonin N-acetyltransferase activity. *Brain research*, 71(1), pp.17–33. Available at: http://www.ncbi.nlm.nih.gov/pubmed/4595289.

Moore, R.Y., Speh, J.C. & Leak, R.K., 2002. Suprachiasmatic nucleus organization. *Cell and Tissue Research*, 309(1), pp.89–98. Available at: http://link.springer.com/10.1007/s00441-002-0575-2.

Moriya, S. et al., 2014. Effect of quetiapine on Per1, Per2, and Bmal1 clock gene expression in the mouse amygdala and hippocampus. *Journal of pharmacological sciences*, 125(3), pp.329–32. Available at: http://www.ncbi.nlm.nih.gov/pubmed/24965164.

Morris, K.A. & Gold, P.E., 2012. Age-related impairments in memory and in CREB and pCREB expression in hippocampus and amygdala following inhibitory avoidance training. *Mechanisms of Ageing and Development*, 133(5), pp.291–299. Available at: https://www.sciencedirect.com/science/article/pii/S0047637412000395.

Morris, R., 2008. Morris water maze. *Scholarpedia*, 3(8), p.6315. Available at: http://www.scholarpedia.org/article/Morris_water_maze.

Morris, R.G.M. et al., 1982. Place navigation impaired in rats with hippocampal lesions. *Nature*, 297(5868), pp.681–683. Available at: http://www.nature.com/articles/297681a0.

Muller, D. et al., 2002. LTP, Memory and Structural Plasticity. *Current Molecular Medicine*, 2(7), pp.605–611. Available at: http://www.eurekaselect.com/openurl/content.php?genre=article&issn=1566-5240&volume=2&issue=7&spage=605.

Murakami, N. et al., 1991. Long-term cultured neurons from rat suprachiasmatic nucleus retain the capacity for circadian oscillation of vasopressin release. *Brain research*, 545(1–2), pp.347–50. Available at: http://www.ncbi.nlm.nih.gov/pubmed/1860057.

Mure, L.S. et al., 2018. Diurnal transcriptome atlas of a primate across major neural and peripheral tissues. *Science*, 359(6381), p.eaao0318. Available at: http://www.ncbi.nlm.nih.gov/pubmed/29439024.

Muzyk, A.J. & Holt, S., 2010. Corticosteroid psychosis: Stop therapy or add psychotropics? *Current Psychiatry*, 9(1). Available at: http://currentpsychiatry..

Naber, D., Sand, P. & Heigl, B., 1996. Psychopathological and neuropsychological effects of 8-days' corticosteroid treatment. A prospective study. *Psychoneuroendocrinology*, 21(1), pp.25–31. Available at: http://www.ncbi.nlm.nih.gov/pubmed/8778901.

Nakahata, Y. et al., 2008. The NAD+-Dependent Deacetylase SIRT1 Modulates CLOCK-Mediated Chromatin Remodeling and Circadian Control. *Cell*, 134(2), pp.329–340. Available at: http://www.ncbi.nlm.nih.gov/pubmed/18662547.

Nakamura, W. et al., 2005. Cellular/Molecular Differential Response of Period 1 Expression within the Suprachiasmatic Nucleus. *Neuroscience*, 25(23), pp.5481–5487. Available at: http://www.jneurosci.org/content/jneuro/25/23/5481.full.pdf.

Nasca, C. et al., 2015. Mind the gap: glucocorticoids modulate hippocampal glutamate tone underlying individual differences in stress susceptibility. *Molecular psychiatry*, 20(6), pp.755–63. Available at: http://www.ncbi.nlm.nih.gov/pubmed/25178162.

Naylor, E. et al., 2000. The circadian clock mutation alters sleep homeostasis in the mouse. *The Journal of neuroscience : the official journal of the Society for Neuroscience*, 20(21), pp.8138–43. Available at: http://www.ncbi.nlm.nih.gov/pubmed/11050136.

Neunuebel, J.P. et al., 2013. Conflicts between Local and Global Spatial Frameworks Dissociate Neural Representations of the Lateral and Medial Entorhinal Cortex. *Journal of Neuroscience*, 33(22), pp.9246–9258. Available at: http://www.ncbi.nlm.nih.gov/pubmed/23719794.

Newell-Price, J. et al., 2006. Cushing's syndrome Epidemiology and prognosis. *www.thelancet.com*, 367.

Nieman, L.K. et al., 2008. The Diagnosis of Cushing's Syndrome: An Endocrine Society Clinical Practice Guideline. *The Journal of Clinical Endocrinology & Metabolism*, 93(5), pp.1526–1540. Available at: http://press.endocrine.org/doi/abs/10.1210/jc.2008-0125.

De Novellis, V. et al., 1995. Hypothalamic sites mediating cardiovascular effects of microinjected bicuculline and EAAs in rats. *American Journal of Physiology-Regulatory, Integrative and Comparative Physiology*, 269(1), pp.R131–R140. Available at: http://www.ncbi.nlm.nih.gov/pubmed/7631885.

O'Callaghan, E.K. et al., 2012. Long-lasting effects of sepsis on circadian rhythms in the mouse. *PloS one*, 7(10), p.e47087. Available at: http://www.ncbi.nlm.nih.gov/pubmed/23071720.

O'Keefe, J. & Speakman, A., 1987. Single unit activity in the rat hippocampus during a spatial memory task. *Experimental Brain Research*, 68(1), pp.1–27. Available at: http://link.springer.com/10.1007/BF00255230.

Ohta, H., Yamazaki, S. & Mcmahon, D.G., 2005. Constant light desynchronizes mammalian clock neurons. *NATURE NEUROSCIENCE*, 8(3). Available at: https://search.proquest.com/openview/44f63cf4c808d84ebc2d5f70bc59eaf3/1?pq-origsite=gscholar&cbl=44706.

Oishi, K. et al., 1998a. Antiphase Circadian Expression betweenBMAL1andperiodHomologue mRNA in the Suprachiasmatic Nucleus and Peripheral Tissues of Rats. *Biochemical and Biophysical Research Communications*, 253(2), pp.199–203. Available at: http://www.ncbi.nlm.nih.gov/pubmed/9878515.

Oishi, K. et al., 2003. Genome-wide expression analysis of mouse liver reveals CLOCK-regulated circadian output genes. *The Journal of biological chemistry*, 278(42), pp.41519–27. Available at: http://www.ncbi.nlm.nih.gov/pubmed/12865428.

Oishi, K. et al., 1998b. Humoral signals mediate the circadian expression of rat period homologue (rPer2) mRNA in peripheral tissues. *Neuroscience Letters*, 256(2), pp.117–119. Available at: http://linkinghub.elsevier.com/retrieve/pii/S0304394098007654.

Oitzl, M.S. & de Kloet, E.R., 1992. Selective corticosteroid antagonists modulate specific aspects of spatial orientation learning. *Behavioral neuroscience*, 106(1), pp.62–71. Available at: http://www.ncbi.nlm.nih.gov/pubmed/1313244.

Okabe, T. et al., 2016. REV-ERBα influences the stability and nuclear localization of the glucocorticoid receptor. *Journal of cell science*, 129(21), pp.4143–4154. Available

at: http://www.ncbi.nlm.nih.gov/pubmed/27686098.
Oliva, D. et al., 1982. VIP stimulates ACTH release and adenylate cyclase in human ACTH-secreting pituitary adenomas. *European Journal of Pharmacology*, 83(1–2), pp.101–105. Available at: https://www.sciencedirect.com/science/article/pii/0014299982902916.
Oliveri, R.L. et al., 1998. Pulsed methylprednisolone induces a reversible impairment of memory in patients with relapsing-remitting multiple sclerosis. *Acta neurologica Scandinavica*, 97(6), pp.366–369.
Olsen, L., Knigge, U. & Warberg, J., 1992. Gastrin-releasing peptide stimulation of corticotropin secretion in male rats. *Endocrinology*, 130(5), pp.2710–2716. Available at: https://academic.oup.com/endo/article-lookup/doi/10.1210/en.130.5.2710.
Ono, D., Honma, K. & Honma, S., 2015. Circadian and ultradian rhythms of clock gene expression in the suprachiasmatic nucleus of freely moving mice. *Scientific Reports*, 5(1), p.12310. Available at: http://www.nature.com/articles/srep12310.
Overman, R.A., Yeh, J.-Y. & Deal, C.L., 2013. Prevalence of Oral Glucocorticoid Usage in the United States: A General Population Perspective. *Arthritis Care & Research*, 65(2), pp.294–298. Available at: http://onlinelibrary.wiley.com/store/10.1002/acr.21796/asset/21796_ftp.pdf?v=1&t=j6hzb2ei&s=e130ea85cb69ea590f5223cecac8dfa9d4fb6d1f.
PALCHYKOVA, S. et al., 2006. Sleep deprivation impairs object recognition in mice. *Neurobiology of Learning and Memory*, 85(3), pp.263–271. Available at: http://www.ncbi.nlm.nih.gov/pubmed/16423541.
Pan, W.-X. & McNaughton, N., 2002. The role of the medial supramammillary nucleus in the control of hippocampal theta activity and behaviour in rats. *European Journal of Neuroscience*, 16(9), pp.1797–1809. Available at: http://doi.wiley.com/10.1046/j.1460-9568.2002.02267.x.
Pan, W.-X. & McNaughton, N., 2004. The supramammillary area: its organization, functions and relationship to the hippocampus. *Progress in Neurobiology*, 74(3), pp.127–166. Available at: https://www.sciencedirect.com/science/article/pii/S0301008204001613.
Panda, S. et al., 2002. Melanopsin (Opn4) Requirement for Normal Light-Induced Circadian Phase Shifting. *Science*, 298(5601), pp.2213–2216. Available at: http://www.ncbi.nlm.nih.gov/pubmed/12481141.
Panula, P. et al., 1989. Histamine-immunoreactive nerve fibers in the rat brain. *Neuroscience*, 28(3), pp.585–610. Available at: http://www.ncbi.nlm.nih.gov/pubmed/2710333.
Partonen, T. et al., 2007. Three circadian clock genes Per2, Arntl, and Npas2 contribute to winter depression. *Annals of Medicine*, 39(3), pp.229–238. Available at: http://www.tandfonline.com/doi/full/10.1080/07853890701278795.
Paskitti, M.., McCreary, B.. & Herman, J.., 2000. Stress regulation of adrenocorticosteroid receptor gene transcription and mRNA expression in rat hippocampus: time-course analysis. *Molecular Brain Research*, 80(2), pp.142–152. Available at: https://www.sciencedirect.com/science/article/pii/S0169328X00001212.
Patel, S.A. et al., 2016. Calorie restriction regulates circadian clock gene expression through BMAL1 dependent and independent mechanisms. *Scientific Reports*, 6(1), p.25970. Available at: http://www.nature.com/articles/srep25970.
Patke, A. et al., 2017. Mutation of the Human Circadian Clock Gene CRY1 in Familial Delayed Sleep Phase Disorder. *Cell*, 169(2), p.203–215.e13. Available at:

https://www.sciencedirect.com/science/article/pii/S009286741730346X.
Pavlides, C. et al., 1996. Role of adrenal steroid mineralocorticoid and glucocorticoid receptors in long-term potentiation in the CA1 field of hippocampal slices. *Brain research*, 738(2), pp.229–35. Available at: http://www.ncbi.nlm.nih.gov/pubmed/8955517.
Paxinos, G. & Watson, C.R., 2007. The Rat Brain in Stereotaxic Coordinates. *Academic Press, San Diego*, 3rd.
Peek, C.B. et al., 2017. Circadian Clock Interaction with HIF1α Mediates Oxygenic Metabolism and Anaerobic Glycolysis in Skeletal Muscle. *Cell Metabolism*, 25(1), pp.86–92. Available at: https://www.sciencedirect.com/science/article/pii/S1550413116304909#fig1.
Peirson, S.N. et al., 2006. Comparison of clock gene expression in SCN, retina, heart, and liver of mice. *Biochemical and Biophysical Research Communications*, 351(4), pp.800–807. Available at: http://www.sciencedirect.com/science/article/pii/S0006291X06023035.
Pereira, A.M., Tiemensma, J. & Romijn, J.A., 2010. Neuropsychiatric disorders in Cushing's syndrome. *Neuroendocrinology*, 92 Suppl 1(Suppl. 1), pp.65–70. Available at: http://www.ncbi.nlm.nih.gov/pubmed/20829621.
Perreau-Lenz, S. et al., 2003. Suprachiasmatic control of melatonin synthesis in rats: inhibitory and stimulatory mechanisms. *The European journal of neuroscience*, 17(2), pp.221–8. Available at: http://www.ncbi.nlm.nih.gov/pubmed/12542658.
Peters, A., 1971. Stellate cells of the rat parietal cortex. *The Journal of Comparative Neurology*, 141(3), pp.345–373. Available at: http://doi.wiley.com/10.1002/cne.901410306.
Phan, T.H. et al., 2011. The Diurnal Oscillation of MAP (Mitogen-Activated Protein) Kinase and Adenylyl Cyclase Activities in the Hippocampus Depends on the Suprachiasmatic Nucleus. *Journal of Neuroscience*, 31(29), pp.10640–10647. Available at: http://www.ncbi.nlm.nih.gov/pubmed/21775607.
Pinnock, S.B. et al., 2009. Synergistic effects of dehydroepiandrosterone and fluoxetine on proliferation of progenitor cells in the dentate gyrus of the adult male rat. *Neuroscience*, 158(4), pp.1644–1651. Available at: http://www.ncbi.nlm.nih.gov/pubmed/19068226.
Pivonello, R. et al., 2015. Neuropsychiatric disorders in Cushing's syndrome. *Frontiers in Neuroscience*, 9, p.129. Available at: http://journal.frontiersin.org/article/10.3389/fnins.2015.00129/abstract.
Plihal, W. & Born, J., 1997. Effects of Early and Late Nocturnal Sleep on Declarative and Procedural Memory. *Journal of Cognitive Neuroscience*, 9(4), pp.534–547. Available at: http://www.ncbi.nlm.nih.gov/pubmed/23968216.
Plihal, W. & Born, J., 1999a. Effects of early and late nocturnal sleep on priming and spatial memory. *Psychophysiology*, 36(5), pp.571–82. Available at: http://www.ncbi.nlm.nih.gov/pubmed/10442025.
Plihal, W. & Born, J., 1999b. Memory consolidation in human sleep depends on inhibition of glucocorticoid release. *Neuroreport*, 10(13), pp.2741–7. Available at: http://www.ncbi.nlm.nih.gov/pubmed/10511433.
Van den Pol, A.N., 1980. The hypothalamic suprachiasmatic nucleus of rat: intrinsic anatomy. *The Journal of comparative neurology*, 191(4), pp.661–702. Available at: http://doi.wiley.com/10.1002/cne.901910410.
Pooley, J.R., 2015. Interaction of the MR and GR in the Nucleus and at DNA.
Preitner, N. et al., 2002. The orphan nuclear receptor REV-ERBalpha controls circadian transcription within the positive limb of the mammalian circadian oscillator. *Cell*,

110(2), pp.251–60. Available at: http://www.ncbi.nlm.nih.gov/pubmed/12150932.
Prewitt, C.M. & Herman, J.P., 1998. Anatomical interactions between the central amygdaloid nucleus and the hypothalamic paraventricular nucleus of the rat: a dual tract-tracing analysis. *Journal of chemical neuroanatomy*, 15(3), pp.173–85. Available at: http://www.ncbi.nlm.nih.gov/pubmed/9797074.
Price, T.S. et al., 2008. WAVECLOCK: wavelet analysis of circadian oscillation. *Bioinformatics (Oxford, England)*, 24(23), pp.2794–5. Available at: http://www.ncbi.nlm.nih.gov/pubmed/18931366.
Qian, X. et al., 2012. Circadian and Ultradian Rhythms of Free Glucocorticoid Hormone Are Highly Synchronized between the Blood, the Subcutaneous Tissue, and the Brain. *Endocrinology*, 153(9), pp.4346–4353. Available at: https://academic.oup.com/endo/article-lookup/doi/10.1210/en.2012-1484.
Quirk, G.J., Armony, J.L. & LeDoux, J.E., 1997. Fear Conditioning Enhances Different Temporal Components of Tone-Evoked Spike Trains in Auditory Cortex and Lateral Amygdala. *Neuron*, 19(3), pp.613–624. Available at: https://www.sciencedirect.com/science/article/pii/S089662730080375X.
Rakai, B.D. et al., 2014. Survival of Adult Generated Hippocampal Neurons Is Altered in Circadian Arrhythmic Mice N. Cermakian, ed. *PLoS ONE*, 9(6), p.e99527. Available at: http://dx.plos.org/10.1371/journal.pone.0099527.
Rasch, B. et al., 2007. Odor Cues During Slow-Wave Sleep Prompt Declarative Memory Consolidation. *Science*, 315(5817), pp.1426–1429. Available at: http://www.ncbi.nlm.nih.gov/pubmed/17347444.
Rasch, B. & Born, J., 2013. About sleep's role in memory. *Physiological reviews*, 93(2), pp.681–766. Available at: http://www.ncbi.nlm.nih.gov/pubmed/23589831.
Raspé, E. et al., 2002. Identification of Rev-erbalpha as a physiological repressor of apoC-III gene transcription. *Journal of lipid research*, 43(12), pp.2172–9. Available at: http://www.ncbi.nlm.nih.gov/pubmed/12454280.
Rath, M.F., Rovsing, L. & Møller, M., 2014. Circadian oscillators in the mouse brain: molecular clock components in the neocortex and cerebellar cortex. *Cell and Tissue Research*, 357(3), pp.743–755. Available at: http://www.ncbi.nlm.nih.gov/pubmed/24842045.
Rawashdeh, O. et al., 2014a. PERIOD1 coordinates hippocampal rhythms and memory processing with daytime. *Hippocampus*, 24(6), pp.712–723. Available at: http://www.ncbi.nlm.nih.gov/pubmed/24550127.
Rawashdeh, O. et al., 2014b. PERIOD1 coordinates hippocampal rhythms and memory processing with daytime. *Hippocampus*, 24(6), pp.712–723. Available at: http://doi.wiley.com/10.1002/hipo.22262.
Rawashdeh, O. et al., 2016. Period1 gates the circadian modulation of memory-relevant signaling in mouse hippocampus by regulating the nuclear shuttling of the CREB kinase pP90RSK. *Journal of neurochemistry*. Available at: http://www.ncbi.nlm.nih.gov/pubmed/27246400.
Rea, M.A., Buckley, B. & Lutton, L.M., 1993. Local administration of EAA antagonists blocks light-induced phase shifts and c-fos expression in hamster SCN. *The American journal of physiology*, 265(5 Pt 2), pp.R1191-8. Available at: http://www.ncbi.nlm.nih.gov/pubmed/7902017.
Rea, M.A., Glass, J.D. & Colwell, C.S., 1994. Serotonin Modulates Photic Responses in the Hamster Suprachiasmatic Nuclei. *The Journal of Neuroscience*, 74(6), pp.3635–3642. Available at: http://www.jneurosci.org/content/jneuro/14/6/3635.full.pdf.
Rebuffé-Scrive, M. et al., 1992. Effect of chronic stress and exogenous glucocorticoids on regional fat distribution and metabolism. *Physiology & Behavior*, 52(3), pp.583–

590. Available at: https://www.sciencedirect.com/science/article/pii/0031938492903512.
Reddy, A.B. et al., 2007. Glucocorticoid signaling synchronizes the liver circadian transcriptome. *Hepatology*, 45(6), pp.1478–1488. Available at: http://www.ncbi.nlm.nih.gov/pubmed/17538967.
Reddy, T.E. et al., 2012. The hypersensitive glucocorticoid response specifically regulates period 1 and expression of circadian genes. *Molecular and cellular biology*, 32(18), pp.3756–67. Available at: http://www.ncbi.nlm.nih.gov/pubmed/22801371.
Reebs, S.G. & Mrosovsky, N., 1989. Effects of Induced Wheel Running on the Circadian Activity Rhythms of Syrian Hamsters: Entrainment and Phase Response Curve. *Journal of Biological Rhythms*, 4(1), pp.39–48. Available at: http://journals.sagepub.com/doi/10.1177/074873048900400103.
Reeth, O. Van & Turek, F.W., 1989. Stimulated activity mediates phase shifts in the hamster circadian clock induced by dark pulses or benzodiazepines. *Nature*, 339(6219), pp.49–51. Available at: http://www.nature.com/doifinder/10.1038/339049a0.
Refinetti, R., Kaufman, C.M. & Menaker, M., 1994. Complete suprachiasmatic lesions eliminate circadian rhythmicity of body temperature and locomotor activity in golden hamsters. *Journal of Comparative Physiology A*, 175(2), pp.223–232. Available at: http://link.springer.com/10.1007/BF00215118.
Refinetti, R. & Menaker, M., 1992. The circadian rhythm of body temperature. *Physiology & Behavior*, 51(3), pp.613–637. Available at: https://www.sciencedirect.com/science/article/pii/0031938492901888.
Rekers, N. V. et al., 2016. Mechanisms and risk assessment of steroid resistance in acute kidney transplant rejection. *Transplant Immunology*, 38, pp.3–14. Available at: http://www.ncbi.nlm.nih.gov/pubmed/27480047.
Relles, D. et al., 2013. Circadian Gene Expression and Clinicopathologic Correlates in Pancreatic Cancer. *Journal of Gastrointestinal Surgery*, 17(3), pp.443–450. Available at: http://link.springer.com/10.1007/s11605-012-2112-2.
Reppert, S.M. & Weaver, D.R., 2002. Coordination of circadian timing in mammals. *Nature*, 418(6901), pp.935–941. Available at: http://www.nature.com/articles/nature00965.
Reul, J.M. & de Kloet, E.R., 1986. Anatomical resolution of two types of corticosterone receptor sites in rat brain with in vitro autoradiography and computerized image analysis. *Journal of steroid biochemistry*, 24(1), pp.269–72. Available at: http://www.ncbi.nlm.nih.gov/pubmed/3702410.
Reul, J.M.H.M. & Kloet, E.R. DE, 1985. Two Receptor Systems for Corticosterone in Rat Brain: Microdistribution and Differential Occupation. *Endocrinology*, 117(6), pp.2505–2511. Available at: http://press.endocrine.org/doi/abs/10.1210/endo-117-6-2505.
Rey, M. et al., 1994. Corticosterone Effects on Long-Term Potentiation in Mouse Hippocampal Slices. *Neuroendocrinology*, 60(1), pp.36–41. Available at: http://www.ncbi.nlm.nih.gov/pubmed/8090280.
Riccio, A.P. & Goldman, B.D., 2000. Circadian rhythms of locomotor activity in naked mole-rats (Heterocephalus glaber). *Physiology & Behavior*, 71(1–2), pp.1–13. Available at: https://www.sciencedirect.com/science/article/pii/S003193840000281X.
Ripperger, J.A. et al., 2000. CLOCK, an essential pacemaker component, controls expression of the circadian transcription factor DBP. *Genes & development*, 14(6),

pp.679–89. Available at: http://www.ncbi.nlm.nih.gov/pubmed/10733528.
Ripperger, J.A. & Merrow, M., 2011. Perfect timing: Epigenetic regulation of the circadian clock. *FEBS Letters*, 585(10), pp.1406–1411. Available at: http://www.ncbi.nlm.nih.gov/pubmed/21536041.
Ripperger, J.A. & Schibler, U., 2006. Rhythmic CLOCK-BMAL1 binding to multiple E-box motifs drives circadian Dbp transcription and chromatin transitions. *Nature Genetics*, 38(3), pp.369–374. Available at: http://www.nature.com/articles/ng1738.
Risold, P.. & Swanson, L.., 1997. Connections of the rat lateral septal complex. *Brain Research Reviews*, 24(2–3), pp.115–195. Available at: https://www.sciencedirect.com/science/article/pii/S016501739700009X.
Roelink, H., 2000. Hippocampus formation: An intriguing collaboration. *Current Biology*, 10(7), pp.R279–R281. Available at: https://www.sciencedirect.com/science/article/pii/S0960982200004073.
Roozendaal, B., de Quervain, D.J.-F. & McGaugh, J.L., 1998. Stress and glucocorticoids impair retrieval of long-term spatial memory. *Nature*, 394(6695), pp.787–790. Available at: http://www.nature.com/doifinder/10.1038/29542.
Rosbash, M. & Hall, J.C., 1985. Biological Clocks in Drosophila: Finding the Molecules That Make Them Tick. *Cell*, 43(0), pp.3–4. Available at: http://www.bio.brandeis.edu/rosbash-lab/PublishedPapers/1982-1986/Rosbash.Cell.1985.pdf.
Rosenwasser, A.M. et al., 2005. Circadian activity rhythms in selectively bred ethanol-preferring and nonpreferring rats. *Alcohol*, 36(2), pp.69–81. Available at: http://www.ncbi.nlm.nih.gov/pubmed/16396740.
Rozwaha, T., 2017. *Circadian rhythmicity in Hippocampus and Perirhinal Cortex is Dysregulated during chronic Methyl-Prednisolone treatment*.
Ruby, N.F. et al., 2008. Hippocampal-dependent learning requires a functional circadian system. *Proceedings of the National Academy of Sciences*, 105(40), pp.15593–15598. Available at: http://www.ncbi.nlm.nih.gov/pubmed/18832172.
Ruby, N.F. et al., 2002. The suprachiasmatic nucleus is essential for circadian body temperature rhythms in hibernating ground squirrels. *The Journal of neuroscience : the official journal of the Society for Neuroscience*, 22(1), pp.357–64. Available at: http://www.ncbi.nlm.nih.gov/pubmed/11756519.
Rudic, R.D. et al., 2004. BMAL1 and CLOCK, Two Essential Components of the Circadian Clock, Are Involved in Glucose Homeostasis Steve O'Rahilly, ed. *PLoS Biology*, 2(11), p.e377. Available at: http://dx.plos.org/10.1371/journal.pbio.0020377.
Rudolf Thal, D. et al., 2000. Alzheimer-Related τ-Pathology in the Perforant Path Target Zone and in the Hippocampal Stratum Oriens and Radiatum Correlates with Onset and Degree of Dementia. *Experimental Neurology*, 163(1), pp.98–110. Available at: https://ac.els-cdn.com/S0014488600973801/1-s2.0-S0014488600973801-main.pdf?_tid=0e44ee36-ceea-4439-b4dd-83a9d1dfa81d&acdnat=1530453021_12540c0252a25054e46ba1e5a68805e4.
Ruf, T., 1999. The Lomb-Scargle Periodogram in Biological Rhythm Research: Analysis of Incomplete and Unequally Spaced Time-Series. *Biological Rhythm Research*, 30(2), pp.178–201. Available at: https://www.tandfonline.com/doi/full/10.1076/brhm.30.2.178.1422.
Rupprecht, R. et al., 1993. Pharmacological and functional characterization of human mineralocorticoid and glucocorticoid receptor ligands. *European Journal of Pharmacology: Molecular Pharmacology*, 247(2), pp.145–154. Available at: https://www.sciencedirect.com/science/article/pii/092241069390072H.

Rushworth, M.F.S. et al., 2011. Frontal Cortex and Reward-Guided Learning and Decision-Making. *Neuron*, 70(6), pp.1054–1069. Available at: https://www.sciencedirect.com/science/article/pii/S0896627311003953.
Sabbar, M. et al., 2017. Circadian Clock Protein Content and Daily Rhythm of Locomotor Activity Are Altered after Chronic Exposure to Lead in Rat. *Frontiers in Behavioral Neuroscience*, 11, p.178. Available at: http://journal.frontiersin.org/article/10.3389/fnbeh.2017.00178/full.
Sage, D. et al., 2004. Influence of the Corticosterone Rhythm on Photic Entrainment of Locomotor Activity in Rats. *Journal of Biological Rhythms*, 19(2), pp.144–156. Available at: http://journals.sagepub.com/doi/10.1177/0748730403261894.
Sainio, E.-L., Lehtola, T. & Roininen, P., 1988. Radioimmunoassay of total and free corticosterone in rat plasma: Measurement of the effect of different doses of corticosterone. *Steroids*, 51(5–6), pp.609–622. Available at: https://www.sciencedirect.com/science/article/pii/0039128X88900566?via%3Dihub.
Sakai, T. et al., 2004. A clock gene, period, plays a key role in long-term memory formation in Drosophila. *National Acad Sciences*. Available at: http://www.pnas.org/content/101/45/16058.short.
Sancar, A., 2004. Regulation of the mammalian circadian clock by cryptochrome. *The Journal of biological chemistry*, 279(33), pp.34079–82. Available at: http://www.ncbi.nlm.nih.gov/pubmed/15123698.
Sandborn, W.J. et al., 2012. Adalimumab Induces and Maintains Clinical Remission in Patients With Moderate-to-Severe Ulcerative Colitis. *Gastroenterology*, 142(2), p.257–265.e3. Available at: https://www.sciencedirect.com/science/article/pii/S001650851101506X.
Sandi, C., Loscertales, M. & Guaza, C., 1997. Experience-dependent Facilitating Effect of Corticosterone on Spatial Memory Formation in the Water Maze. *European Journal of Neuroscience*, 9(4), pp.637–642. Available at: http://doi.wiley.com/10.1111/j.1460-9568.1997.tb01412.x.
Saper, C.B. et al., 2005. The hypothalamic integrator for circadian rhythms. *Trends in Neurosciences*, 28(3), pp.152–157. Available at: http://www.sciencedirect.com/science/article/pii/S0166223604003959.
Sato, T.K. et al., 2004. A Functional Genomics Strategy Reveals Rora as a Component of the Mammalian Circadian Clock. *Neuron*, 43(4), pp.527–537. Available at: https://www.sciencedirect.com/science/article/pii/S089662730400460X.
Sawchenko, P.E., Arias, C.A. & Mortrud, M.T., 1993. Local Tetrodotoxin Blocks Chronic Stress Effects on Corticotropin-Releasing Factor and Vasopressin Messenger Ribonucleic Acids in Hypophysiotropic Neurons. *Journal of Neuroendocrinology*, 5(4), pp.341–348. Available at: http://doi.wiley.com/10.1111/j.1365-2826.1993.tb00493.x.
Schaaf, M.J.M., De Kloet, E.R. & Vreugdenhil, E., 2000. Corticosterone Effects on BDNF Expression in the Hippocampus Implications for Memory Formation. *Stress*, 3(3), pp.201–208. Available at: http://www.tandfonline.com/doi/full/10.3109/10253890009001124.
Scharfman, H.E., Goodman, J.H. & Sollas, A.L., 2000. Granule-like neurons at the hilar/CA3 border after status epilepticus and their synchrony with area CA3 pyramidal cells: functional implications of seizure-induced neurogenesis. *The Journal of neuroscience : the official journal of the Society for Neuroscience*, 20(16), pp.6144–58. Available at: http://www.ncbi.nlm.nih.gov/pubmed/10934264.
Schibler, U. & Sassone-Corsi, P., 2002. A Web of Circadian Pacemakers. *Cell*, 111(7), pp.919–922. Available at:

http://www.sciencedirect.com/science/article/pii/S0092867402012254.
Schlessinger, A.R., Cowan, W.M. & Gottlieb, D.I., 1975. An autoradiographic study of the time of origin and the pattern of granule cell migration in the dentate gyrus of the rat. *The Journal of Comparative Neurology*, 159(2), pp.149–175. Available at: http://doi.wiley.com/10.1002/cne.901590202.
Schmahmann, J.D., 1991. An emerging concept. The cerebellar contribution to higher function. *Archives of neurology*, 48(11), pp.1178–87. Available at: http://www.ncbi.nlm.nih.gov/pubmed/1953406.
Schmahmann, J.D., 2004. Disorders of the Cerebellum: Ataxia, Dysmetria of Thought, and the Cerebellar Cognitive Affective Syndrome. *The Journal of Neuropsychiatry and Clinical Neurosciences*, 16(3), pp.367–378. Available at: http://www.ncbi.nlm.nih.gov/pubmed/15377747.
Schmutz, I., Albrecht, U. & Ripperger, J.A., 2012. The role of clock genes and rhythmicity in the liver. *Molecular and Cellular Endocrinology*, 349(1), pp.38–44. Available at: http://www.ncbi.nlm.nih.gov/pubmed/21664421.
Schroeder, A. et al., 2011. Circadian regulation of cardiovascular function: a role for vasoactive intestinal peptide. *American Journal of Physiology-Heart and Circulatory Physiology*, 300(1), pp.H241–H250. Available at: http://www.physiology.org/doi/10.1152/ajpheart.00190.2010.
Schultz, C. & Engelhardt, M., 2014. Anatomy of the hippocampal formation. *Frontiers of neurology and neuroscience*, 34, pp.6–17. Available at: http://www.ncbi.nlm.nih.gov/pubmed/24777126.
Schwartz, W.J. et al., 2011. Distinct patterns of Period gene expression in the suprachiasmatic nucleus underlie circadian clock photoentrainment by advances or delays. *Proceedings of the National Academy of Sciences of the United States of America*, 108(41), pp.17219–24. Available at: http://www.ncbi.nlm.nih.gov/pubmed/21969555.
Schwartz, W.J. et al., 1983. In vivo metabolic activity of the suprachiasmatic nuclei: a comparative study. *Brain Research*, 274(1), pp.184–187. Available at: https://www.sciencedirect.com/science/article/pii/0006899383905383.
Segall, L.A. et al., 2006. Glucocorticoid rhythms control the rhythm of expression of the clock protein, Period2, in oval nucleus of the bed nucleus of the stria terminalis and central nucleus of the amygdala in rats. *Neuroscience*, 140(3), pp.753–757. Available at: https://www.sciencedirect.com/science/article/pii/S0306452206004076.
Segall, L.A. & Amir, S., 2010. Glucocorticoid Regulation of Clock Gene Expression in the Mammalian Limbic Forebrain. *Journal of Molecular Neuroscience*, 42(2), pp.168–175. Available at: http://link.springer.com/10.1007/s12031-010-9341-1.
Senft, R.A. et al., 2016. Distribution and Abundance of Glucocorticoid and Mineralocorticoid Receptors throughout the Brain of the Great Tit (Parus major) M. J. Coleman, ed. *PLOS ONE*, 11(2), p.e0148516. Available at: http://dx.plos.org/10.1371/journal.pone.0148516.
Sequeira, A. et al., 2012. Gene Expression Changes in the Prefrontal Cortex, Anterior Cingulate Cortex and Nucleus Accumbens of Mood Disorders Subjects That Committed Suicide B. J. Harrison, ed. *PLoS ONE*, 7(4), p.e35367. Available at: http://www.ncbi.nlm.nih.gov/pubmed/22558144.
Sherin, J.E. et al., 1996. Activation of ventrolateral preoptic neurons during sleep. *Science (New York, N.Y.)*, 271(5246), pp.216–9. Available at: http://www.ncbi.nlm.nih.gov/pubmed/8539624.
SHIBLEY, H.L., MALCOLM, R.J. & VEATCH, L.M., 2008. Adolescents with Insomnia

and Substance Abuse: Consequences and Comorbidities. *Journal of Psychiatric Practice*, 14(3), pp.146–153. Available at: https://insights.ovid.com/crossref?an=00131746-200805000-00003.
Shieh, K.-R., 2003. Distribution of the rhythm-related genes rPERIOD1, rPERIOD2, and rCLOCK, in the rat brain. *Neuroscience*, 118(3), pp.831–843. Available at: https://www.sciencedirect.com/science/article/pii/S0306452203000046.
Shinohara, K. et al., 1994. Circadian rhythms in the release of vasoactive intestinal polypeptide and arginine-vasopressin in organotypic slice culture of rat suprachiasmatic nucleus. *Neuroscience letters*, 170(1), pp.183–6. Available at: http://www.ncbi.nlm.nih.gov/pubmed/8041503.
Short, D., El Masry, W. & Jones, P., 2000. High dose methylprednisolone in the management of acute spinal cord injury – a systematic review from a clinical perspective. *Spinal Cord*, 38(5), pp.273–286. Available at: http://www.nature.com/articles/3100986.
Siegel, J.M., 2001. The REM sleep-memory consolidation hypothesis. *Science (New York, N.Y.)*, 294(5544), pp.1058–63. Available at: http://www.ncbi.nlm.nih.gov/pubmed/11691984.
Silver, R. et al., 1996. A diffusible coupling signal from the transplanted suprachiasmatic nucleus controlling circadian locomotor rhythms. *Nature*, 382(6594), pp.810–813. Available at: http://www.nature.com/doifinder/10.1038/382810a0.
Simasko, S.M. & Mukherjee, S., 2009. Novel analysis of sleep patterns in rats separates periods of vigilance cycling from long-duration wake events. *Behavioural brain research*, 196(2), pp.228–36. Available at: http://www.ncbi.nlm.nih.gov/pubmed/18835301.
Skaggs, W.E. & McNaughton, B.L., 1996. Replay of neuronal firing sequences in rat hippocampus during sleep following spatial experience. *Science (New York, N.Y.)*, 271(5257), pp.1870–3. Available at: http://www.ncbi.nlm.nih.gov/pubmed/8596957.
Slusher, M., 1966. Effects of cortisol implants in the brainstem and ventral hippocampus on diurnal corticosteroid levels. *Experimental Brain Research*, 1(2), pp.184–194. Available at: http://link.springer.com/10.1007/BF00236870.
Smith, S.M. & Vale, W.W., 2006. The role of the hypothalamic-pituitary-adrenal axis in neuroendocrine responses to stress. *Dialogues in clinical neuroscience*, 8(4), pp.383–95. Available at: http://www.ncbi.nlm.nih.gov/pubmed/17290797.
Sonino, N. & Fava, G., 2001. Psychiatric disorders associated with Cushing's syndrome. *CNS drugs*, 15(5), pp.361–373. Available at: http://link.springer.com/10.2165/00023210-200115050-00003.
Soria, V. et al., 2010. Differential Association of Circadian Genes with Mood Disorders: CRY1 and NPAS2 are Associated with Unipolar Major Depression and CLOCK and VIP with Bipolar Disorder. *Neuropsychopharmacology*, 35(6), pp.1279–1289. Available at: http://www.nature.com/articles/npp2009230.
Soták, M. et al., 2016. Peripheral circadian clocks are diversely affected by adrenalectomy. *Chronobiology International*, 0528(April).
Spanagel, R. et al., 2005. The clock gene Per2 influences the glutamatergic system and modulates alcohol consumption. *Nature Medicine*, 11(1), pp.35–42. Available at: http://www.nature.com/articles/nm1163.
Spiga, F. et al., 2011. ACTH-dependent ultradian rhythm of corticosterone secretion. *Endocrinology*, 152(4), pp.1448–57. Available at: http://www.ncbi.nlm.nih.gov/pubmed/21303945.
Sprague, J.M., 1966. Interaction of cortex and superior colliculus in mediation of visually guided behavior in the cat. *Science (New York, N.Y.)*, 153(3743), pp.1544–7.

Available at: http://www.ncbi.nlm.nih.gov/pubmed/5917786.
van Staa, T.P. et al., 2000. Use of oral corticosteroids in the United Kingdom. *QJM : monthly journal of the Association of Physicians*, 93(2), pp.105–11. Available at: http://www.ncbi.nlm.nih.gov/pubmed/10700481.
Stanewsky, R. et al., 1998. The cryb mutation identifies cryptochrome as a circadian photoreceptor in Drosophila. *Cell*, 95(5), pp.681–92. Available at: http://www.ncbi.nlm.nih.gov/pubmed/9845370.
Starkman, M.N. et al., 1992. Hippocampal Formation Volume, Memory Dysfunction, and Cortisoi Levels in Patients with Cushing's Syndrome. *BIOL PSYCHIATRY*, 32, pp.756–765.
Stenvers, D.J. et al., 2016. Dim light at night disturbs the daily sleep-wake cycle in the rat. *Scientific Reports*, 6(1), p.35662. Available at: http://www.nature.com/articles/srep35662.
Stephan, F.K., Swann, J.M. & Sisk, C.L., 1979. Entrainment of circadian rhythms by feeding schedules in rats with suprachiasmatic lesions. *Behavioral and Neural Biology*, 25(4), pp.545–554. Available at: https://www.sciencedirect.com/science/article/pii/S0163104779903327.
Stephan, F.K. & Zucker, I., 1972. Circadian rhythms in drinking behavior and locomotor activity of rats are eliminated by hypothalamic lesions. *Proceedings of the National Academy of Sciences of the United States of America*, 69(6), pp.1583–6. Available at: http://www.ncbi.nlm.nih.gov/pubmed/4556464.
Steriade, M. & McCarley, R.W., 1990. *Brainstem Control of Wakefulness and Sleep*, Springer US. Available at: https://books.google.co.uk/books?hl=en&lr=&id=X5juBwAAQBAJ&oi=fnd&pg=PA1&dq=brainstem+sleep&ots=XPaxFhG7eT&sig=jSNHlXOMVqyjjEDzvxQto1u5czw#v=onepage&q=brainstem sleep&f=false.
Stevens, C.F., 1998. A million dollar question: does LTP = memory? *Neuron*, 20(1), pp.1–2. Available at: http://www.ncbi.nlm.nih.gov/pubmed/9459434.
Steward, O., 1976. Topographic organization of the projections from the entorhinal area to the hippocampal formation of the rat. *The Journal of Comparative Neurology*, 167(3), pp.285–314. Available at: http://www.ncbi.nlm.nih.gov/pubmed/1270625.
Stickgold, R., 2005. Sleep-dependent memory consolidation. *Nature*, 437(7063), pp.1272–1278. Available at: http://www.nature.com/doifinder/10.1038/nature04286.
Stickgold, R., James, L. & Hobson, J.A., 2000. Visual discrimination learning requires sleep after training. *Nature Neuroscience*, 3(12), pp.1237–1238. Available at: http://www.nature.com/articles/nn1200_1237.
Stojkovic, K., Wing, S.S. & Cermakian, N., 2014. A central role for ubiquitination within a circadian clock protein modification code. *Frontiers in molecular neuroscience*, 7, p.69. Available at: http://www.ncbi.nlm.nih.gov/pubmed/25147498.
Stokkan, K.-A. et al., 2001. Entrainment of the Circadian Clock in the Liver by Feeding. *Science*, 291(5503), pp.490–493. Available at: http://www.sciencemag.org/cgi/doi/10.1126/science.291.5503.490.
Suh, J. et al., 2011. Entorhinal Cortex Layer III Input to the Hippocampus Is Crucial for Temporal Association Memory. *Science*, 334(6061), pp.1415–1420. Available at: http://www.ncbi.nlm.nih.gov/pubmed/22052975.
Sukhotinsky, I. et al., 2005. Movement suppression during anesthesia: Neural projections from the mesopontine tegmentum to areas involved in motor control. *The Journal of Comparative Neurology*, 489(4), pp.425–448. Available at: http://doi.wiley.com/10.1002/cne.20636.
Summa, K.C. et al., 2015. Chronic Alcohol Exposure and the Circadian *Clock* Mutation

Exert Tissue-Specific Effects on Gene Expression in Mouse Hippocampus, Liver, and Proximal Colon. *Alcoholism: Clinical and Experimental Research*, 39(10), pp.1917–1929. Available at: http://doi.wiley.com/10.1111/acer.12834.

Swanson, L.W. & Petrovich, G.D., 1998. What is the amygdala? *Trends in Neurosciences*, 21(8), pp.323–331. Available at: https://www.sciencedirect.com/science/article/pii/S016622369801265X.

Takahashi, H. & Magee, J.C., 2009. Pathway Interactions and Synaptic Plasticity in the Dendritic Tuft Regions of CA1 Pyramidal Neurons. *Neuron*, 62(1), pp.102–111. Available at: http://www.ncbi.nlm.nih.gov/pubmed/19376070.

Takekida, S. et al., 2000. Differential adrenergic regulation of the circadian expression of the clock genes *Period1* and *Period2* in the rat pineal gland. *European Journal of Neuroscience*, 12(12), pp.4557–4561. Available at: http://doi.wiley.com/10.1046/j.0953-816X.2000.01324.x.

Tam, S.K.E. et al., 2017. Constant Light Desynchronizes Olfactory versus Object and Visuospatial Recognition Memory Performance. *The Journal of neuroscience : the official journal of the Society for Neuroscience*, 37(13), pp.3555–3567. Available at: http://www.ncbi.nlm.nih.gov/pubmed/28264977.

Tambe, K. et al., 2010. The Role of Intravenous Methylprednisolone Immunosuppression in the Management of Active Thyroid Eye Disease. *Orbit*, 29(5), pp.227–231. Available at: http://www.tandfonline.com/doi/full/10.3109/01676831003660663.

Tatomir, A., Micu, C. & Crivii, C., 2014. The impact of stress and glucocorticoids on memory. *Clujul medical (1957)*, 87(1), pp.3–6. Available at: http://www.ncbi.nlm.nih.gov/pubmed/26527987.

Terazono, H. et al., 2003. Adrenergic regulation of clock gene expression in mouse liver. *Proceedings of the National Academy of Sciences*, 100(11), pp.6795–6800. Available at: http://www.ncbi.nlm.nih.gov/pubmed/12754374.

Thompson, C.L. et al., 2003. Expression of the Blue-Light Receptor Cryptochrome in the Human Retina. *Investigative Opthalmology & Visual Science*, 44(10), p.4515. Available at: http://iovs.arvojournals.org/article.aspx?doi=10.1167/iovs.03-0303.

Thompson, R.H., Canteras, N.S. & Swanson, L.W., 1996. Organization of projections from the dorsomedial nucleus of the hypothalamus: a PHA-L study in the rat. *The Journal of comparative neurology*, 376(1), pp.143–73. Available at: http://www.ncbi.nlm.nih.gov/pubmed/8946289.

Toh, K.L. et al., 2001. An hPer2 phosphorylation site mutation in familial advanced sleep phase syndrome. *Science (New York, N.Y.)*, 291(5506), pp.1040–3. Available at: http://www.ncbi.nlm.nih.gov/pubmed/11232563.

Tong, X. & Yin, L., 2013. Circadian Rhythms in Liver Physiology and Liver Diseases. In *Comprehensive Physiology*. Hoboken, NJ, USA: John Wiley & Sons, Inc., pp. 917–40. Available at: http://www.ncbi.nlm.nih.gov/pubmed/23720334.

Turek, F.W. et al., 2005. Obesity and Metabolic Syndrome in Circadian Clock Mutant Mice. *Science*, 308(5724), pp.1043–1045. Available at: http://www.ncbi.nlm.nih.gov/pubmed/15845877.

Udoh, U. et al., 2015. The Molecular Circadian Clock and Alcohol-Induced Liver Injury. *Biomolecules*, 5(4), pp.2504–2537. Available at: http://www.mdpi.com/2218-273X/5/4/2504.

Ueda, H.R. et al., 2002. A transcription factor response element for gene expression during circadian night. *Nature*, 418(6897), pp.534–539. Available at: http://www.ncbi.nlm.nih.gov/pubmed/12152080.

Uhl, A. et al., 2002. Pharmacokinetics and pharmacodynamics of methylprednisolone after one bolus dose compared with two dose fractions. *Journal of clinical pharmacy*

and therapeutics, 27(4), pp.281–7. Available at: http://www.ncbi.nlm.nih.gov/pubmed/12174030.
Ulrich-Lai, Y.M., Arnhold, M.M. & Engeland, W.C., 2006. Adrenal splanchnic innervation contributes to the diurnal rhythm of plasma corticosterone in rats by modulating adrenal sensitivity to ACTH. *American Journal of Physiology-Regulatory, Integrative and Comparative Physiology*, 290(4), pp.R1128–R1135. Available at: http://www.physiology.org/doi/10.1152/ajpregu.00042.2003.
Ulrich-Lai, Y.M. & Herman, J.P., 2009. Neural regulation of endocrine and autonomic stress responses. *Nature Reviews Neuroscience*, 10(6), pp.397–409. Available at: http://www.ncbi.nlm.nih.gov/pubmed/19469025.
Uz, T. et al., 2005. Effect of fluoxetine and cocaine on the expression of clock genes in the mouse hippocampus and striatum. *Neuroscience*, 134(4), pp.1309–1316. Available at: https://www.sciencedirect.com/science/article/pii/S0306452205005166.
Valekunja, U.K. et al., 2013. Histone methyltransferase MLL3 contributes to genome-scale circadian transcription. *Proceedings of the National Academy of Sciences*, 110(4), pp.1554–1559. Available at: http://www.ncbi.nlm.nih.gov/pubmed/23297224.
Vanselow, K. et al., 2006. Differential effects of PER2 phosphorylation: molecular basis for the human familial advanced sleep phase syndrome (FASPS). *Genes & development*, 20(19), pp.2660–72. Available at: http://www.ncbi.nlm.nih.gov/pubmed/16983144.
Vázquez-Palacios, G. et al., 2001. Further definition of the effect of corticosterone on the sleep-wake pattern in the male rat. *Pharmacology, biochemistry, and behavior*, 70(2–3), pp.305–10. Available at: http://www.ncbi.nlm.nih.gov/pubmed/11701201.
Verner, T.A., Goodchild, A.K. & Pilowsky, P.M., 2004. A mapping study of cardiorespiratory responses to chemical stimulation of the midline medulla oblongata in ventilated and freely breathing rats. *American Journal of Physiology-Regulatory, Integrative and Comparative Physiology*, 287(2), pp.R411–R421. Available at: http://www.physiology.org/doi/10.1152/ajpregu.00019.2004.
Verwey, M., Robinson, B. & Amir, S., 2013. Recording and analysis of circadian rhythms in running-wheel activity in rodents. *Journal of visualized experiments : JoVE*, (71). Available at: http://www.ncbi.nlm.nih.gov/pubmed/23380887.
Vinson, G.P., 2016. Functional Zonation of the Adult Mammalian Adrenal Cortex. *Frontiers in Neuroscience*, 10, p.238. Available at: http://journal.frontiersin.org/Article/10.3389/fnins.2016.00238/abstract.
Wagner, U. & Born, J., 2008. Memory consolidation during sleep: Interactive effects of sleep stages and HPA regulation. *Stress*, 11(1), pp.28–41. Available at: http://www.tandfonline.com/doi/full/10.1080/10253890701408822.
Waite, E.J. et al., 2012. Ultradian corticosterone secretion is maintained in the absence of circadian cues. *European Journal of Neuroscience*, 36(8), pp.3142–3150. Available at: http://doi.wiley.com/10.1111/j.1460-9568.2012.08213.x.
Walker, M.P. & Stickgold, R., 2004. Sleep-dependent learning and memory consolidation. *Neuron*, 44(1), pp.121–33. Available at: http://www.sciencedirect.com/science/article/pii/S0896627304005409.
Wang, L.M.-C. et al., 2009. Expression of the Circadian Clock Gene *Period2* in the Hippocampus: Possible Implications for Synaptic Plasticity and Learned Behaviour. *ASN Neuro*, 1(3), p.AN20090020. Available at: http://journals.sagepub.com/doi/10.1042/AN20090020.
Wang, Z., Gerstein, M. & Snyder, M., 2009. RNA-Seq: a revolutionary tool for

transcriptomics. *Nature reviews. Genetics*, 10(1), pp.57–63. Available at: http://www.ncbi.nlm.nih.gov/pubmed/19015660.

Watanabe, K. et al., 1993. Circadian rhythms of vasopressin release in primary cultures of rat suprachiasmatic nucleus. *Brain research*, 624(1–2), pp.115–20. Available at: http://www.ncbi.nlm.nih.gov/pubmed/8252382.

Watts, A.G. & Swanson, L.W., 1987. Efferent projections of the suprachiasmatic nucleus: II. Studies using retrograde transport of fluorescent dyes and simultaneous peptide immunohistochemistry in the rat. *The Journal of comparative neurology*, 258(2), pp.230–52. Available at: http://doi.wiley.com/10.1002/cne.902580205.

Weger, M. et al., 2013. Real-time in vivo monitoring of circadian E-box enhancer activity: A robust and sensitive zebrafish reporter line for developmental, chemical and neural biology of the circadian clock. *Developmental Biology*, 380(2), pp.259–273. Available at: https://www.sciencedirect.com/science/article/pii/S0012160613002303#f0005.

Weitzman, E.D., 1976. Circadian rhythms and Episodic memory hormone secretion in man. Available at: https://www.annualreviews.org/doi/pdf/10.1146/annurev.me.27.020176.001301.

WEITZMAN, E.D. et al., 1983. Cortisol Secretion Is Inhibited during Sleep in Normal Man*. *The Journal of Clinical Endocrinology & Metabolism*, 56(2), pp.352–358. Available at: https://academic.oup.com/jcem/article-lookup/doi/10.1210/jcem-56-2-352.

WEITZMAN, E.D. et al., 1971. Twenty-four Hour Pattern of the Episodic Secretion of Cortisol in Normal Subjects. *The Journal of Clinical Endocrinology & Metabolism*, 33(1), pp.14–22. Available at: http://www.ncbi.nlm.nih.gov/pubmed/4326799.

Welsh, D.K. et al., 1995. Individual neurons dissociated from rat suprachiasmatic nucleus express independently phased circadian firing rhythms. *Neuron*, 14(4), pp.697–706. Available at: http://www.ncbi.nlm.nih.gov/pubmed/7718233.

Welsh, D.K., Richardson, G.S. & Dement, W.C., 1985. A circadian rhythm of hippocampal theta activity in the mouse. *Physiology & Behavior*, 35(4), pp.533–538. Available at: https://www.sciencedirect.com/science/article/pii/0031938485901362.

Whitnall, M.H., Kiss, A. & Aguilera, G., 1993. Contrasting effects of central alpha-1-adrenoreceptor activation on stress-responsive and stress-nonresponsive subpopulations of corticotropin-releasing hormone neurosecretory cells in the rat. *Neuroendocrinology*, 58(1), pp.42–8. Available at: http://www.ncbi.nlm.nih.gov/pubmed/8264854.

Wilhelm, I. et al., 2011. Sleep Selectively Enhances Memory Expected to Be of Future Relevance. *Journal of Neuroscience*, 31(5), pp.1563–1569. Available at: http://www.ncbi.nlm.nih.gov/pubmed/21289163.

Williams, C.M. et al., 2008. Blueberry-induced changes in spatial working memory correlate with changes in hippocampal CREB phosphorylation and brain-derived neurotrophic factor (BDNF) levels. *Free Radical Biology and Medicine*, 45(3), pp.295–305. Available at: https://www.sciencedirect.com/science/article/pii/S0891584908002098.

Wilson, M.A. & McNaughton, B.L., 1994. Reactivation of hippocampal ensemble memories during sleep. *Science (New York, N.Y.)*, 265(5172), pp.676–9. Available at: http://www.ncbi.nlm.nih.gov/pubmed/8036517.

Windle, R.J. et al., 1997. Central Oxytocin Administration Reduces Stress-Induced Corticosterone Release and Anxiety Behavior in Rats [1]. *Endocrinology*, 138(7), pp.2829–2834. Available at: https://academic.oup.com/endo/article-lookup/doi/10.1210/endo.138.7.5255.

Wisor, J.P. et al., 2002. A role for cryptochromes in sleep regulation. *BMC neuroscience*, 3, p.20. Available at: http://www.ncbi.nlm.nih.gov/pubmed/12495442.

Witkovsky, P. et al., 2003. Cellular location and circadian rhythm of expression of the biological clock gene Period 1 in the mouse retina. *The Journal of neuroscience : the official journal of the Society for Neuroscience*, 23(20), pp.7670–6. Available at: http://www.ncbi.nlm.nih.gov/pubmed/12930806.

Witter, M.P. et al., 2000. Cortico-hippocampal communication by way of parallel parahippocampal-subicular pathways. *Hippocampus*, 10(4), pp.398–410. Available at: http://doi.wiley.com/10.1002/1098-1063%282000%2910%3A4%3C398%3A%3AAID-HIPO6%3E3.0.CO%3B2-K.

Witter, M.P., 2007. The perforant path: projections from the entorhinal cortex to the dentate gyrus. *Progress in Brain Research*, 163, pp.43–61. Available at: https://www.sciencedirect.com/science/article/pii/S0079612307630039.

Wood, C.M. et al., 2017. Prevalence and influence of cys407* Grm2 mutation in Hannover-derived Wistar rats: mGlu2 receptor loss links to alcohol intake, risk taking and emotional behaviour. *Neuropharmacology*, 115, pp.128–138. Available at: https://www.sciencedirect.com/science/article/pii/S0028390816300922.

Wood, E.R. et al., 2000. Hippocampal Neurons Encode Information about Different Types of Memory Episodes Occurring in the Same Location. *Neuron*, 27(3), pp.623–633. Available at: https://www.sciencedirect.com/science/article/pii/S0896627300000714.

Woon, P.Y. et al., 2007. Aryl hydrocarbon receptor nuclear translocator-like (BMAL1) is associated with susceptibility to hypertension and type 2 diabetes. *Proceedings of the National Academy of Sciences*, 104(36), pp.14412–14417. Available at: http://www.ncbi.nlm.nih.gov/pubmed/17728404.

Xie, M. et al., 2015. Short-term sleep deprivation impairs spatial working memory and modulates expression levels of ionotropic glutamate receptor subunits in hippocampus. *Behavioural Brain Research*, 286, pp.64–70. Available at: https://www.sciencedirect.com/science/article/pii/S0166432815001199.

Xiong, W. et al., 2016. BMAL1 regulates transcription initiation and activates circadian clock gene expression in mammals. *Biochemical and Biophysical Research Communications*, 473(4), pp.1019–1025. Available at: http://www.ncbi.nlm.nih.gov/pubmed/27055591.

Xu, Y. et al., 2007. Modeling of a Human Circadian Mutation Yields Insights into Clock Regulation by PER2. *Cell*, 128(1), pp.59–70. Available at: http://www.ncbi.nlm.nih.gov/pubmed/17218255.

Yabaluri, N. & Bashyam, M.D., 2010. Hormonal regulation of gluconeogenic gene transcription in the liver. *Journal of biosciences*, 35(3), pp.473–84. Available at: http://www.ncbi.nlm.nih.gov/pubmed/20826956.

Yamaguchi, S. et al., 2000. Role of DBP in the circadian oscillatory mechanism. *Molecular and cellular biology*, 20(13), pp.4773–81. Available at: http://www.ncbi.nlm.nih.gov/pubmed/10848603.

Yamaguchi, S. et al., 2003. Synchronization of Cellular Clocks in the Suprachiasmatic Nucleus. *Science*, 302(5649). Available at: http://science.sciencemag.org/content/302/5649/1408/tab-pdf.

Yamamoto, S. et al., 2001. Expression of thePer1 gene in the hamster: Brain atlas and circadian characteristics in the suprachiasmatic nucleus. *The Journal of Comparative Neurology*, 430(4), pp.518–532. Available at: http://doi.wiley.com/10.1002/1096-9861%2820010219%29430%3A4%3C518%3A%3AAID-CNE1047%3E3.0.CO%3B2-H.

Yang, G. et al., 2016. Timing of expression of the core clock gene *Bmal1* influences its effects on aging and survival. *Science Translational Medicine*, 8(324), p.324ra16-324ra16. Available at: http://www.ncbi.nlm.nih.gov/pubmed/26843191.

Yang, X. et al., 2006. Nuclear Receptor Expression Links the Circadian Clock to Metabolism. *Cell*, 126(4), pp.801–810. Available at: https://www.sciencedirect.com/science/article/pii/S0092867406009780.

Yang, X. et al., 2009. THE CIRCADIAN CLOCK GENE *PER1* SUPPRESSES CANCER CELL PROLIFERATION AND TUMOR GROWTH AT SPECIFIC TIMES OF DAY. *Chronobiology International*, 26(7), pp.1323–1339. Available at: http://www.ncbi.nlm.nih.gov/pubmed/19916834.

Ye, L. et al., 2014. Blocking the Mineralocorticoid Receptor Improves Effectiveness of Steroid Treatment for Low Back Pain in Rats. *Anesthesiology*, 121(3), pp.632–643. Available at: http://anesthesiology.pubs.asahq.org/Article.aspx?doi=10.1097/ALN.0000000000000277.

Yeh, K.-T. et al., 2005. Abnormal expression of period 1 (PER1) in endometrial carcinoma. *The Journal of Pathology*, 206(1), pp.111–120. Available at: http://doi.wiley.com/10.1002/path.1756.

Yoshitane, H. et al., 2009. Roles of CLOCK phosphorylation in suppression of E-box-dependent transcription. *Molecular and cellular biology*, 29(13), pp.3675–86. Available at: http://www.ncbi.nlm.nih.gov/pubmed/19414601.

Young, M.E., Razeghi, P. & Taegtmeyer, H., 2001. Clock genes in the heart: characterization and attenuation with hypertrophy. *Circulation research*, 88(11), pp.1142–50. Available at: http://www.ncbi.nlm.nih.gov/pubmed/11397780.

Young, M.W. et al., 1985. A biological clock in Drosophila. *Cold Spring Harbor symposia on quantitative biology*, 50, pp.865–75. Available at: http://www.ncbi.nlm.nih.gov/pubmed/3868509.

Zhang, R. et al., 2014. A circadian gene expression atlas in mammals: implications for biology and medicine. *Proceedings of the National Academy of Sciences of the United States of America*, 111(45).

Zhang, S., Jonklaas, J. & Danielsen, M., 2007. The glucocorticoid agonist activities of mifepristone (RU486) and progesterone are dependent on glucocorticoid receptor levels but not on EC50 values. *Steroids*, 72(6–7), pp.600–608. Available at: http://www.ncbi.nlm.nih.gov/pubmed/17509631.

Zhao, M. et al., 2010. The neuroretina is a novel mineralocorticoid target: aldosterone up-regulates ion and water channels in Müller glial cells. *The FASEB Journal*, 24(9), pp.3405–3415. Available at: http://www.ncbi.nlm.nih.gov/pubmed/20466875.

Zhao, Q. et al., 2016. The clock gene PER1 plays an important role in regulating the clock gene network in human oral squamous cell carcinoma cells. *Oncotarget*, 7(43), pp.70290–70302. Available at: http://www.ncbi.nlm.nih.gov/pubmed/27602964.

Zhao, Z.-D. et al., 2017. A hypothalamic circuit that controls body temperature. *Proceedings of the National Academy of Sciences of the United States of America*, 114(8), pp.2042–2047. Available at: http://www.ncbi.nlm.nih.gov/pubmed/28053227.

Zheng, B. et al., 2001. Nonredundant roles of the mPer1 and mPer2 genes in the mammalian circadian clock. *Cell*, 105(5), pp.683–94. Available at: http://www.ncbi.nlm.nih.gov/pubmed/11389837.

Zheng, X. et al., 2014. Casein Kinase 1 Promotes Synchrony of the Circadian Clock Network. *Molecular and Cellular Biology*, 34(14), pp.2682–2694. Available at: http://www.ncbi.nlm.nih.gov/pubmed/24820422.

Zhou, Q.-Y. & Cheng, M.Y., 2005. Prokineticin 2 and circadian clock output. *FEBS Journal*, 272(22), pp.5703–5709. Available at: http://www.ncbi.nlm.nih.gov/pubmed/16279936.

Zhou, Y.D. et al., 1997. Molecular characterization of two mammalian bHLH-PAS domain proteins selectively expressed in the central nervous system. *Proceedings of the National Academy of Sciences of the United States of America*, 94(2), pp.713–8. Available at: http://www.ncbi.nlm.nih.gov/pubmed/9012850.

Zhou, Z., Chadt, A. & Al-Hasani, H., 2014. Tuning in to the rhythm of clock genes in skeletal muscle. *Molecular metabolism*, 3(1), pp.1–2. Available at: http://www.ncbi.nlm.nih.gov/pubmed/24567898.

Zmrzljak, U.P. et al., 2013. Inducible cAMP early repressor regulates the Period 1 gene of the hepatic and adrenal clocks. *The Journal of biological chemistry*, 288(15), pp.10318–27. Available at: http://www.ncbi.nlm.nih.gov/pubmed/23443664.

Zola-Morgan, S., Squire, L.R. & Amaral, D.G., 1986. Human amnesia and the medial temporal region: enduring memory impairment following a bilateral lesion limited to field CA1 of the hippocampus. *The Journal of neuroscience : the official journal of the Society for Neuroscience*, 6(10), pp.2950–67. Available at: http://www.ncbi.nlm.nih.gov/pubmed/3760943.

Zorzon, M. et al., 2005. Long-term effects of intravenous high dose methylprednisolone pulses on bone mineral density in patients with multiple sclerosis. *European Journal of Neurology*, 12(7), pp.550–556. Available at: http://doi.wiley.com/10.1111/j.1468-1331.2005.00988.